

RAPID ESTIMATION OF LIVES OF DEFICIENT SUPERPAVE MIXES AND
LABORATORY-BASED ACCELERATED MIX TESTING MODELS

by

CHANDRA BAHADUR MANANDHAR

B. Eng., Tribhuvan University, 1994
M. Eng., Asian Institute of Technology, 1998

AN ABSTRACT OF A DISSERTATION

submitted in partial fulfillment of the requirements for the degree

DOCTOR OF PHILOSOPHY

Department of Civil Engineering
College of Engineering

KANSAS STATE UNIVERSITY
Manhattan, Kansas

2010

Abstract

The engineers from the Kansas Department of Transportation (KDOT) often have to decide whether or not to accept non-conforming Superpave mixtures during construction. The first part of this study focused on estimating lives of deficient Superpave pavements incorporating nonconforming Superpave mixtures. These criteria were based on the Hamburg Wheel-Tracking Device (HWTD) test results and analysis. The second part of this study focused on developing accelerated mix testing models to considerably reduce test duration.

To accomplish the first objective, nine fine-graded Superpave mixes of 12.5-mm nominal maximum aggregate size (NMAS) with asphalt grade PG 64-22 from six administrative districts of KDOT were selected. Specimens were prepared at three different target air void levels @ N_{design} gyrations and four target simulated in-place density levels with the Superpave gyratory compactor. Average number of wheel passes to 20-mm rut depth, creep slope, stripping slope, and stripping inflection point in HWTD tests were recorded and then used in the statistical analysis. Results showed that, in general, higher simulated in-place density up to a certain limit of 91% to 93%, results in a higher number of wheel passes until 20-mm rut depth in HWTD tests. A Superpave mixture with very low air voids @ N_{design} (2%) level performed very poorly in the HWTD test.

HWTD tests were also performed on six 12.5-mm NMAS mixtures with air voids @ N_{design} of 4% for six projects, simulated in-place density of 93%, two temperature levels and five load levels with binder grades of PG 64-22, PG 64-28, and PG 70-22.

Field cores of 150-mm in diameter from three projects in three KDOT districts with 12.5-mm NMAS and asphalt grade of PG 64-22 were also obtained and tested in HWTD for model evaluation. HWTD test results indicated as expected. Statistical analysis was performed and accelerated mix testing models were developed to determine the effect of increased temperature and load on the duration of the HWTD test. Good consistency between predicted and observed test results was obtained when higher temperature and standard load level were used. Test duration of the HWTD can thus be reduced to two hours or less using accelerated mix testing (statistical) models.

RAPID ESTIMATION OF LIVES OF DEFICIENT SUPERPAVE MIXES AND
LABORATORY-BASED ACCELERATED MIX TESTING MODELS

by

CHANDRA BAHADUR MANANDHAR

B. Eng., Tribhuvan University, 1994
M. Eng., Asian Institute of Technology, 1998

A DISSERTATION

submitted in partial fulfillment of the requirements for the degree

DOCTOR OF PHILOSOPHY

Department of Civil Engineering
College of Engineering

KANSAS STATE UNIVERSITY
Manhattan, Kansas

2010

Approved by:

Major Professor
Dr. Mustaque Hossain

Copyright

CHANDRA BAHADUR MANANDHAR

2010

Abstract

The engineers from the Kansas Department of Transportation (KDOT) often have to decide whether or not to accept non-conforming Superpave mixtures during construction. The first part of this study focused on estimating lives of deficient Superpave pavements incorporating nonconforming Superpave mixtures. These criteria were based on the Hamburg Wheel-Tracking Device (HWTD) test results and analysis. The second part of this study focused on developing accelerated mix testing models to considerably reduce test duration.

To accomplish the first objective, nine fine-graded Superpave mixes of 12.5-mm nominal maximum aggregate size (NMAS) with asphalt grade PG 64-22 from six administrative districts of KDOT were selected. Specimens were prepared at three different target air void levels @ N_{design} gyrations and four target simulated in-place density levels with the Superpave gyratory compactor. Average number of wheel passes to 20-mm rut depth, creep slope, stripping slope, and stripping inflection point in HWTD tests were recorded and then used in the statistical analysis. Results showed that, in general, higher simulated in-place density up to a certain limit of 91% to 93%, results in a higher number of wheel passes until 20-mm rut depth in HWTD tests. A Superpave mixture with very low air voids @ N_{design} (2%) level performed very poorly in the HWTD test.

HWTD tests were also performed on six 12.5-mm NMAS mixtures with air voids @ N_{design} of 4% for six projects, simulated in-place density of 93%, two temperature levels and five load levels with binder grades of PG 64-22, PG 64-28, and PG 70-22.

Field cores of 150-mm in diameter from three projects in three KDOT districts with 12.5-mm NMAS and asphalt grade of PG 64-22 were also obtained and tested in HWTD for model evaluation. HWTD test results indicated as expected. Statistical analysis was performed and accelerated mix testing models were developed to determine the effect of increased temperature and load on the duration of the HWTD test. Good consistency between predicted and observed test results was obtained when higher temperature and standard load level were used. Test duration of the HWTD can thus be reduced to two hours or less using accelerated mix testing (statistical) models.

Table of Contents

List of Figures	ix
List of Tables	xvi
Acknowledgements	xx
Dedication	xxi
CHAPTER 1 - INTRODUCTION	1
1.1 General	1
1.2 Problem Statement	1
1.3 Objectives of the Study	3
1.4 Dissertation Outline	3
CHAPTER 2 - LITERATURE REVIEW	4
2.1 Superpave System	4
2.2 Asphalt Pavement Distresses	4
2.2.1 Rutting	5
2.2.2 Fatigue Cracking	6
2.2.3 Low-Temperature Cracking	7
2.2.4 Stripping/ Moisture Damage	8
2.2.4.1 Moisture-Related Distresses	10
2.2.4.2 Chemical and Mechanical Processes of Moisture Damage in HMA	14
2.2.4.3 Treatment for Moisture Sensitivity	16
2.2.4.4 Test Methods to Predict Moisture Sensitivity of Hot-Mix Asphalt Mixtures	17
2.2.4.5 Cost Effectiveness	20
2.3 Torture Test Devices	20
2.4 Accelerated Mix Testing and Statistical Analysis	21
2.4.1. Overview	21
2.4.2 Weibull Distribution	22
2.4.3 Survival Analysis	22
2.4.3.1 Survival Function	23
2.4.3.2. Right-Censored Data	24

2.4.4 Cubic Model.....	24
CHAPTER 3 - OBJECTIVE 1: DEVELOPMENT OF CRITERIA FOR OUT-OF-SPECIFICATION PAVEMENTS.....	25
3.1 Experimental Design.....	27
3.2 Test Specimen Preparation	28
3.3 Test Equipment	33
3.3.1 Hamburg Wheel-Tracking Device.....	33
3.3.2 Marshall Stability Tester and KT-56 Test.....	37
3.4 Laboratory Test Results	40
3.4.1 HWTD Test Results	40
3.4.2 KT-56 Test Results	49
3.5 Statistical Analysis.....	49
3.5.1 Influence of Air Voids @ N_{design} and Simulated In-Place Density	49
3.5.2 Development of Life-Prediction Equation.....	53
3.6 Mixtures from the Field	58
3.6.1 Field Coring and Testing	58
3.6.2 HWTD Test Results and Field Verification.....	59
CHAPTER 4 - OBJECTIVE 2: DEVELOPMENT OF LABORATORY-BASED ACCELERATED MIX TESTING MODELS.....	60
4.1 Experimental Design.....	60
4.2 Test Specimen Preparation	62
4.3 Hamburg Wheel-Tracking Device (HWTD)	62
4.4 Laboratory Test Results	63
4.5 Statistical Analysis.....	72
4.5.1 Influence of Temperature and Load.....	72
4.5.2 Development of Accelerated Mix Testing Models Considering Effects of Temperature and Load.....	76
4.5.3 Development of Accelerated Mix Testing Models Considering Effects of Temperature, Load, and Air Voids	90
4.6 Mixtures from the Field	98
4.6.1 Field Coring and Testing	98

4.6.2 HWTD Test Results and Field Verification Considering Effects of Temperature and Load	99
4.6.3 HWTD Test Results and Field Verification Considering Effects of Temperature, Load, and Air Voids	106
CHAPTER 5 - CONCLUSIONS AND RECOMMENDATIONS.....	109
5.1 Conclusions.....	109
5.2 Recommendations.....	110
References.....	111
Appendix A - HWTD, G_{mm} , and G_{mb} Test Results for Development of Criteria for Out-of-Specification Pavements	119
Appendix B - Histogram of HWTD Test Results with Simulated In-Place Densities and Air Voids for Development of Criteria for Out-of-Specification Pavements	132
Appendix C - Comparative Plots of HWTD Test Results for Development of Criteria for Out-of-Specification Pavements	151
Appendix D - Calculation of Lives of Deficient Superpave Pavements	179
Appendix E - HWTD, G_{mm} , G_{mb} , Simulated In-Place Densities and Air Voids Test Results for Development of Laboratory - Based Accelerated Mix Testing Models and Field Cores ...	190
Appendix F - Comparison of Models Predicted with Observed Wheel Passes.....	206
Appendix G - Typical SAS Input Files.....	222

List of Figures

Figure 2.1 Rutting in the Wheel Paths	5
Figure 2.2 Pavement Surface Deformations Due to Traffic Loading (<i>Archilla 2000</i>)	6
Figure 2.3 Fatigue Cracks on Asphalt Pavement.....	7
Figure 2.4 Low-Temperature Crack on Flexible Pavement.....	8
Figure 2.5 Raveling of Asphalt Pavement (Hicks et al. 2003)	10
Figure 2.6 Typical Localized Failure Due to Moisture Damage (Hicks et al. 2003)	11
Figure 2.7 Loss of Fatigue Life Due to Moisture Damage (Hicks et al. 2003)	12
Figure 2.8 Stiffness Loss of HMA Due to Moisture Damage (Hicks et al. 2003).....	12
Figure 2.9 Weibull Survival Functions for $\alpha = 0.5, \lambda = 0.2638$ (_____); $\alpha = 1.0, l = 0.1$ (.....); $\alpha = 3.0, \lambda = 0.00208$ (-----) (Klein and Moeschberger 2003)	23
Figure 3.1 Flow Chart of Research Methodology	26
Figure 3.2 Aggregate Gradation of Mixtures.....	29
Figure 3.3 Project Sites for Estimation of Lives of Deficient Superpave Pavements	30
Figure 3.4 Superpave Gyrotory Compactor	32
Figure 3.5 Hamburg Wheel-Tracking Device	35
Figure 3.6 Interpretation of HWTD Results (Aschenbrener 1994)	36
Figure 3.7 Marshall Stability Tester	38
Figure 3.8 HWTD Wheel Passes Results for K-4 Project with Target Simulated In-Place Densities and Target Air Voids @ N_{design}	44
Figure 3.9 HWTD Creep Slope Results for K-4 Project with Target Simulated In-Place Densities and Target Air Voids @ N_{design}	44
Figure 3.10 HWTD Stripping Slope Results for K-4 Project with Target Simulated In-Place Densities and Target Air Voids @ N_{design}	45
Figure 3.11 HWTD Stripping Inflection Points Results for K-4 Project with Target Simulated In- Place Densities and Target Air Voids @ N_{design}	45
Figure 3.12 Comparative HWTD Test Results of K-4 Project at 2% Target Air	46
Figure 3.13 Comparative HWTD Test Results of K-4 Project at 4% Target Air	47

Figure 3.14 Comparative HWTD Test Results of K-4 Project at 7% Target Air	48
Figure 3.15 Comparison of HWTD Test Results of Laboratory Samples with Field Cores	59
Figure 4.1 Aggregate Gradation Charts for the Mixtures	61
Figure 4.2 HWTD Test Results of K-4 Project in District I	65
Figure 4.3 HWTD Test Results of US-24 Project in District III	66
Figure 4.4 HWTD Test Results of US-50 Project in District V	66
Figure 4.5 HWTD Test Results of US-83 Project in District VI	67
Figure 4.6 HWTD Test Results of CISL-A Project at KSU	67
Figure 4.7 HWTD Test Results of CISL-B Project at KSU	68
Figure 4.8 HWTD Test Results for Route K-4 and US-24	69
Figure 4.9 HWTD Test Results for Route US-50 and US-83	70
Figure 4.10 HWTD Test Results for CISL-A and CISL-B Projects	71
Figure 4.11 HWTD Test Results with Censored and Uncensored Data	74
Figure 4.12 Comparison of HWTD Results of Model Predicted with Observed for All Six Projects	78
Figure 4.13 Comparison of HWTD Results of Model Predicted with Observed for All Five Projects Without CISL-B	79
Figure 4.14 Comparison of HWTD Results of Model Predicted with Observed for All Four Projects Without CISL Projects	80
Figure 4.15 Comparison of Predicted with Observed Wheel Passes for K-4 Project with Interaction	80
Figure 4.16 Comparison of Predicted with Observed Wheel Passes for US-24 Project with Interaction	81
Figure 4.17 Comparison of Predicted with Observed Wheel Passes for US-50 Project with Interaction	81
Figure 4.18 Comparison of Predicted with Observed Wheel Passes for US-83 Project with Interaction	82
Figure 4.19 Comparison of Predicted with Observed Wheel Passes for CISL-A Project with Interaction	82
Figure 4.20 Comparison of Predicted with Observed Wheel Passes for K-4 Project Without Interaction	83

Figure 4.21 Comparison of Predicted with Observed Wheel Passes for US-24 Project Without Interaction	83
Figure 4.22 Comparison of Predicted with Observed Wheel Passes for US-50 Project Without Interaction	84
Figure 4.23 Comparison of Predicted with Observed Wheel Passes for US-83 Project Without Interaction	84
Figure 4.24 Comparison of Predicted with Observed Wheel Passes for CISL-A Project Without Interaction	85
Figure 4.25 Cox-Snell Residuals To Assess the Fit of Weibull Regression Model	86
Figure 4.26 Cox-Snell Residual Weibull Plot with Interaction of Load and Temperature for K-4 Project	88
Figure 4.27 Cox-Snell Residual Weibull Plot Without Interaction of Load and Temperature for K-4 Project	89
Figure 4.28 Comparison of Predicted with Observed Wheel Passes for K-4 Project Without Interaction	93
Figure 4.29 Comparison of Predicted with Observed Wheel Passes for US-24 Project Without Interaction	94
Figure 4.30 Comparison of Predicted with Observed Wheel Passes for US-50 Project Without Interaction	94
Figure 4.31 Comparison of Predicted with Observed Wheel Passes for US-83 Project Without Interaction	95
Figure 4.32 Comparison of Predicted with Observed Wheel Passes for CISL-A Project Without Interaction	95
Figure 4.33 Comparison of Predicted with Observed Wheel Passes for All Projects Without Interaction	96
Figure 4.34 HWTD Test Results of K-4 Cores.....	100
Figure 4.35 HWTD Test Results of K-258 Cores.....	100
Figure 4.36 HWTD Test Results of US-83 Cores	101
Figure 4.37 Comparison of HWTD Test Results of Laboratory Samples with Field Cores for 705 N Load at 50°C	102

Figure 4.38 Comparison of HWTD Test Results of Laboratory Samples with Field Cores for 705 N Load at 60°C	102
Figure 4.39 Comparison of HWTD Test Results of Laboratory Samples with Field Cores for 750 N Load at 50°C	103
Figure 4.40 Comparison of HWTD Test Results of Laboratory Samples with Field Cores for 750 N Load at 60°C	103
Figure 4.41 Comparison of HWTD Test Results of Laboratory Samples with Field Cores for 795 N Load at 50°C	104
Figure 4.42 Comparison of HWTD Test Results of Laboratory Samples with Field Cores for 795 N Load at 60°C	104
Figure 4.43 Comparison of HWTD Results of Statewide Model-Predicted with Observed in Field Cores	106
Figure 4.44 Comparison of Predicted with Observed Wheel Passes for K-4 Cores Without Interaction	107
Figure 4.45 Comparison of Predicted with Observed Wheel Passes for US-24 Cores Without Interaction	108
Figure 4.46 Comparison of Predicted with Observed Wheel Passes for US-83 Cores Without Interaction	108
Figure B.1 HWTD Wheel Passes Results for K-4 Project with Target Simulated In-Place Densities and Target Air Voids @ N_{design}	133
Figure B.2 HWTD Creep Slope Results for K-4 Project with Target Simulated In-Place Densities and Target Air Voids @ N_{design}	133
Figure B.3 HWTD Stripping Slope Results for K-4 Project with Target Simulated In-Place Densities and Target Air Voids @ N_{design}	134
Figure B.4 HWTD Stripping Inflection Points Results for K-4 Project with Target Simulated In- Place Densities and Target Air Voids @ N_{design}	134
Figure B.5 HWTD Wheel Passes Results for K-9 Project with Target Simulated In-Place Densities and Target Air Voids @ N_{design}	135
Figure B.6 HWTD Creep Slope Results for K-9 Project with Target Simulated In-Place Densities and Target Air Voids @ N_{design}	135

Figure B.7 HWTD Stripping Slope Results for K-9 Project with Target Simulated In-Place Densities and Target Air Voids @ N_{design}	136
Figure B.8 HWTD Stripping Inflection Points Results for K-9 Project with Target Simulated In-Place Densities and Target Air Voids @ N_{design}	136
Figure B.9 HWTD Wheel Passes Results for US-24 Project with Target Simulated In-Place Densities and Target Air Voids @ N_{design}	137
Figure B.10 HWTD Creep Slope Results for US-24 Project with Target Simulated In-Place Densities and Target Air Voids @ N_{design}	137
Figure B.11 HWTD Stripping Slope Results for US-24 Project with Target Simulated In-Place Densities and Target Air Voids @ N_{design}	138
Figure B.12 HWTD Stripping Inflection Points Results for US-24 Project with Target Simulated In-Place Densities and Target Air Voids @ N_{design}	138
Figure B.13 HWTD Wheel Passes Results for K-152 Project with Target Simulated In-Place Densities and Target Air Voids @ N_{design}	139
Figure B.14 HWTD Creep Slope Results for K-152 Project with Target Simulated In-Place Densities and Target Air Voids @ N_{design}	139
Figure B.15 HWTD Stripping Slope Results for K-152 Project with Target Simulated In-Place Densities and Target Air Voids @ N_{design}	140
Figure B.16 HWTD Stripping Inflection Points Results for K-152 Project with Target Simulated In-Place Densities and Target Air Voids @ N_{design}	140
Figure B.17 HWTD Wheel Passes Results for K-15 Project with Target Simulated In-Place Densities and Target Air Voids @ N_{design}	141
Figure B.18 HWTD Creep Slope Results for K-15 Project with Target Simulated In-Place Densities and Target Air Voids @ N_{design}	141
Figure B.19 HWTD Stripping Slope Results for K-15 Project with Target Simulated In-Place Densities and Target Air Voids @ N_{design}	142
Figure B.20 HWTD Stripping Inflection Points Results for K-15 Project with Target Simulated In-Place Densities and Target Air Voids @ N_{design}	142
Figure B.21 HWTD Wheel Passes Results for US-83 Project with Target Simulated In-Place Densities and Target Air Voids @ N_{design}	143

Figure B.22 HWTD Creep Slope Results for US-83 Project with Target Simulated In-Place Densities and Target Air Voids @ N_{design}	143
Figure B.23 HWTD Stripping Slope Results for US-83 Project with Target Simulated In-Place Densities and Target Air Voids @ N_{design}	144
Figure B.24 HWTD Stripping Inflection Points Results for US-83 Project with Target Simulated In-Place Densities and Target Air Voids @ N_{design}	144
Figure B.25 HWTD Wheel Passes Results for K-246 Project with Target Simulated In-Place Densities and Target Air Voids @ N_{design}	145
Figure B.26 HWTD Creep Slope Results for K-246 Project with Target Simulated In-Place Densities and Target Air Voids @ N_{design}	145
Figure B.27 HWTD Stripping Slope Results for K-246 Project with Target Simulated In-Place Densities and Target Air Voids @ N_{design}	146
Figure B.28 HWTD Stripping Inflection Points Results for K-246 Project with Target Simulated In-Place Densities and Target Air Voids @ N_{design}	146
Figure B.29 HWTD Wheel Passes Results for US-56 Project with Target Simulated In-Place Densities and Target Air Voids @ N_{design}	147
Figure B.30 HWTD Creep Slope Results for US-56 Project with Target Simulated In-Place Densities and Target Air Voids @ N_{design}	147
Figure B.31 HWTD Stripping Slope Results for US-56 Project with Target Simulated In-Place Densities and Target Air Voids @ N_{design}	148
Figure B.32 HWTD Stripping Inflection Points Results for US-56 Project with Target Simulated In-Place Densities and Target Air Voids @ N_{design}	148
Figure B.33 HWTD Wheel Passes Results for US-50 Project with Simulated In-Place Densities and Target Air Voids @ N_{design}	149
Figure B.34 HWTD Creep Slope Results for US-50 Project with Target Simulated In-Place Densities and Target Air Voids @ N_{design}	149
Figure B.35 HWTD Stripping Slope Results for US-50 Project with Target Simulated In-Place Densities and Target Air Voids @ N_{design}	150
Figure B.36 HWTD Stripping Inflection Points Results for US-50 Project with Target Simulated In-Place Densities and Target Air Voids @ N_{design}	150
Figure C.1 Comparative HWTD Test Results of K-4 Project at 2% Target Air	152

Figure C.2 Comparative HWTD Test Results of K-4 Project at 4% Target Air	153
Figure C.3 Comparative HWTD Test Results of K-4 Project at 7% Target Air	154
Figure C.4 Comparative HWTD Test Results of K-9 Project at 2% Target Air	155
Figure C.5 Comparative HWTD Test Results of K-9 Project at 4% Target Air	156
Figure C.6 Comparative HWTD Test Results of K-9 Project at 7% Target Air	157
Figure C.7 Comparative HWTD Test Results of US-24 Project at 2% Target Air	158
Figure C.8 Comparative HWTD Test Results of US-24 Project at 4% Target Air	159
Figure C.9 Comparative HWTD Test Results of US-24 Project at 7% Target Air	160
Figure C.10 Comparative HWTD Test Results of K-152 Project at 2% Target Air	161
Figure C.11 Comparative HWTD Test Results of K-152 Project at 4% Target Air	162
Figure C.12 Comparative HWTD Test Results of K-152 Project at 7% Target Air	163
Figure C.13 Comparative HWTD Test Results of K-15 Project at 2% Target Air	164
Figure C.14 Comparative HWTD Test Results of K-15 Project at 4% Target Air	165
Figure C.15 Comparative HWTD Test Results of K-15 Project at 7% Target Air	166
Figure C.16 Comparative HWTD Test Results of US-83 Project at 2% Target Air	167
Figure C.17 Comparative HWTD Test Results of US-83 Project at 4% Target Air	168
Figure C.18 Comparative HWTD Test Results of US-83 Project at 7% Target Air	169
Figure C.19 Comparative HWTD Test Results of K-246 Project at 2% Target Air	170
Figure C.20 Comparative HWTD Test Results of K-246 Project at 4% Target Air	171
Figure C.21 Comparative HWTD Test Results of K-246 Project at 7% Target Air	172
Figure C.22 Comparative HWTD Test Results of US-56 Project at 2% Target Air	173
Figure C.23 Comparative HWTD Test Results of US-56 Project at 4% Target Air	174
Figure C.24 Comparative HWTD Test Results of US-56 Project at 7% Target Air	175
Figure C.25 Comparative HWTD Test Results of US-50 Project at 2% Target Air	176
Figure C.26 Comparative HWTD Test Results of US-50 Project at 4% Target Air	177
Figure C.27 Comparative HWTD Test Results of US-50 Project at 7% Target Air	178

List of Tables

Table 2.1 Factors Contributing to Moisture-Related Distresses (Hicks et al. 2003)	9
Table 2.2 Moisture Sensitivity Tests on Loose Samples (Solaimanian et al. 2007).....	19
Table 2.3 Moisture Sensitivity Tests on Compacted Specimens (Solaimanian et al. 2007)	19
Table 3.1 Properties of Superpave Mixes for Life Estimation	28
Table 3.2 Design Single-Point Gradation of Aggregates.....	30
Table 3.3 TxDOT Requirement of HMA for HWTD Test at 50 °C (122 °F)	37
Table 3.4 Summary of Hamburg Wheel-Tracking Device Test Results (Average number of wheel passes to a 20-mm rut depth).....	41
Table 3.5 Summary of Hamburg Wheel-Tracking Device Test Results (Output Parameters).....	42
Table 3.6 Summary of KT-56 Test Results for Estimation of Life of Deficient Pavements.....	49
Table 3.7 Summary of Statistical Analysis for Estimation of Life of Deficient Superpave Pavements	52
Table 3.8 Models Derived for Estimating Life of Deficient Superpave Pavements	54
Table 3.9 Calculation of Life of Deficient Superpave Pavements of K-4 Project.....	57
Table 3.10 Models for Estimating Life of Deficient Superpave Pavements	58
Table 3.11 HWTD Test Results of Laboratory Samples with Field Cores	59
Table 4.1 Properties of Superpave Mixes	61
Table 4.2 Design Single-Point Gradation of Aggregates.....	62
Table 4.3 Summary of Hamburg Wheel Test Results (Average number of wheel passes).....	63
Table 4.4 Summary of Hamburg Wheel Test Results (Output Parameters).....	64
Table 4.5 Summary of Statistical Analysis for Accelerated Mix Testing Models	75
Table 4.6 Summary of Statistical Analysis for Accelerated Mix Testing Models	77
Table 4.7 Comparison of HWTD Results of Model Predicted with Observed Data	78
Table 4.8 Summary of Accelerated Mix Testing Models with Temperature, Load, and Air Voids	91
Table 4.9 Comparison of Model Predicted with Observed Wheel Passes.....	92
Table 4.10 Comparison of HWTD Results and Model-Predicted Wheel Passes for Field Cores	97

Table 4.11 Accelerated Mix Testing Models.....	98
Table 4.12 Summary of Hamburg Wheel Test Results of Cored Samples (Average number of wheel passes)	99
Table 4.13 Comparison of Model-Predicted with Observed in Field Cores Results.....	105
Table A.1 Hamburg Wheel-Tracking Device Test Results (Number of Wheel Passes)	120
Table A.2 Simulated In-Place Densities and Air Voids for K-4 Project in District I.....	121
Table A.3 Simulated In-Place Densities and Air Voids for K-9 Project in District II	123
Table A.4 Simulated In-Place Densities and Air Voids for US-24 Project in District III	124
Table A.5 Simulated In-Place Densities and Air Voids for K-152 Project in District IV	125
Table A.6 Simulated In-Place Densities and Air Voids for K-15 Project in District V	126
Table A.7 Simulated In-Place Densities and Air Voids for US-83 Project in District VI.....	128
Table A.8 Simulated In-Place Densities and Air Voids for K-246 Project in District I.....	129
Table A.9 Simulated In-Place Densities and Air Voids for US-56 Project in District II	130
Table A.10 Simulated In-Place Densities and Air Voids for US-50 Project in District V	131
Table D.1 Lives of Deficient Superpave Pavements for Route K-4.....	180
Table D.2 Lives of Deficient Superpave Pavements for Route K-9.....	181
Table D.3 Lives of Deficient Superpave Pavements for Route US-24.....	182
Table D.4 Lives of Deficient Superpave Pavements for Route K-152.....	183
Table D.5 Lives of Deficient Superpave Pavements for Route K-15.....	184
Table D.6 Lives of Deficient Superpave Pavements for Route US-83.....	185
Table D.7 Lives of Deficient Superpave Pavements for Route K-246.....	186
Table D.8 Lives of Deficient Superpave Pavements for Route US-56.....	187
Table D.9 Lives of Deficient Superpave Pavements for Route US-50.....	188
Table D.10 Lives of Deficient Superpave Pavements for Statewide Project	189
Table E.1 Summary of Hamburg Wheel Test Results for Accelerated Mix Testing Models (Number of wheel passes at left and right wheel paths)	191
Table E.2 Air Voids and Asphalt Content of Hamburg Test Samples for Accelerated Mix Testing Models.....	192
Table E.3 Simulated In-Place Densities and Air Voids for K-4 Project in District I	193
Table E.4 Simulated In-Place Densities and Air Voids for US-24 Project in District III	194
Table E.5 Simulated In-Place Densities and Air Voids for US-24 Project in District III	195

Table E.6 Simulated In-Place Densities and Air Voids for US-50 Project in District V	196
Table E.7 Simulated In-Place Densities and Air Voids for US-50 Project in District V	197
Table E.8 Simulated In-Place Densities and Air Voids for US-83 Project in District VI	198
Table E.9 Simulated In-Place Densities and Air Voids for US-83 Project in District VI	199
Table E.10 Simulated In-Place Densities and Air Voids for CISL-A Project	200
Table E.11 Simulated In-Place Densities and Air Voids for CISL-B Project	201
Table E.12 Summary of Hamburg Wheel Test Results of Field Cores for Accelerated Mix Testing Models (Number of wheel passes at left and right wheel paths)	202
Table E.13 Air Voids of Hamburg Test Samples of Field Cores	202
Table E.14 Simulated In-Place Densities and Air Voids for K-4 Field Cores	203
Table E.15 Simulated In-Place Densities and Air Voids for K-258 Field Cores	204
Table E.16 Simulated In-Place Densities and Air Voids for US-83 Field Cores	205
Table F.1 Comparison of Model Predicted with Observed Wheel Passes for K-4 Project Considering Temperature and Load with Interaction	207
Table F.2 Comparison of Model Predicted With Observed Wheel Passes for US-24 Project Considering Temperature and Load with Interaction	207
Table F.3 Comparison of Model Predicted With Observed Wheel Passes for US-50 Project Considering Temperature and Load with Interaction	208
Table F.4 Comparison of Model Predicted With Observed Wheel Passes for US-83 Project Considering Temperature and Load with Interaction	208
Table F.5 Comparison of Model Predicted With Observed Wheel Passes for CISL-A Project Considering Temperature and Load with Interaction	209
Table F.6 Comparison of Model-Predicted with Observed Wheel Passes for All Projects Without CISL Projects Considering Temperature and Load with Interaction.....	209
Table F.7 Comparison of Model-Predicted with Observed Wheel Passes for All Projects Without CISL-B Considering Temperature and Load with Interaction.....	210
Table F.8 Comparison of Model Predicted With Observed Wheel Passes for All Projects Considering Temperature and Load with Interaction	211
Table F.9 Comparison of Model Predicted with Observed Wheel Passes for K-4 Project Considering Temperature and Load Without Interaction	212

Table F.10 Comparison of Model Predicted With Observed Wheel Passes for US-24 Project Considering Temperature and Load without Interaction	212
Table F.11 Comparison of Model Predicted With Observed Wheel Passes for US-50 Project Considering Temperature and Load without Interaction	213
Table F.12 Comparison of Model Predicted With Observed Wheel Passes for US-83 Project Considering Temperature and Load without Interaction	213
Table F.13 Comparison of Model Predicted With Observed Wheel Passes for CISL-A Project Considering Temperature and Load without Interaction	214
Table F.14 Comparison of Model-Predicted with Observed Wheel Passes for All Without CISL Projects Considering Temperature and Load Without Interaction	214
Table F.15 Comparison of Model-Predicted with Observed Wheel Passes for All Projects Without CISL-B Considering Temperature and Load Without Interaction	215
Table F.16 Comparison of Model Predicted With Observed Wheel Passes for All Projects Considering Temperature and Load without Interaction	215
Table F.17 Comparison of Model Predicted With Observed Wheel Passes for K-4 Project	216
Table F.18 Comparison of Model Predicted With Observed Wheel Passes for US-24 Project .	216
Table F.19 Comparison of Model Predicted With Observed Wheel Passes for US-50 Project .	217
Table F.20 Comparison of Model Predicted With Observed Wheel Passes for US-83 Project .	217
Table F.21 Comparison of Model Predicted With Observed Wheel Passes for CISL-A Project	218
Table F.22 Comparison of Model Predicted With Observed Wheel Passes for All Projects	218
Table F.23 Comparison of Model Predicted With Observed Wheel Passes for All Projects Model Compared With US-24 Project	219
Table F.24 Comparison of Model-Predicted with Observed Wheel Passes for K-4 Model Compared with K-4 Cores	220
Table F.25 Comparison of Model-Predicted with Observed Wheel Passes for US-24 Model Compared with K-258 Cores	220
Table F.26 Comparison of Model-Predicted with Observed Wheel Passes for US-83 Model Compared with US-83 Cores	221

Acknowledgements

I would like to express my deepest gratitude and sincere appreciation to my major professor, Dr. Mustaque Hossain, for his invaluable guidance, constant support, and encouragement; not only to my study and research at Kansas State University, but to creative ideas, independent and critical thinking, achieving goals of my professional career, and much more.

I would also like to thank and express my appreciation to Dr. Stefan Romanoschi for serving on my dissertation committee and providing frequent helps and valuable suggestions in this research. I would also like to thank Dr. Paul Nelson for being my committee member and for his frequent advice during this dissertation work. My sincere gratitude goes to Dr. Sunanda Dissanayake for being my committee member and for her suggestions and encouragement. I owe a great debt to all my committee members for their valuable suggestions and guidance in getting this dissertation into shape.

I gratefully acknowledge the financial support provided by the Kansas Department of Transportation (KDOT) for this study. I also appreciate Mr. Cliff Hobson and Mr. Chuck Espinoza of KDOT for their support on coordination with various project personnel for materials collection and field coring.

I would also like to thank all fellow co-workers, and graduate and undergraduate students who helped me with laboratory sample fabrication and testing.

Finally, I am also grateful to my parents, and brothers and sisters who have always been a constant source of inspiration. I express my special thanks and gratitude to my wife, Nisha, and twin sons, Nripesh and Dipesh, for their unconditional love and support in my life.

Dedication

This dissertation is dedicated to my late father, **Mr. Bhakta Bahadur Manandhar**, and my mother, **Mrs. Nhuchhe Maya Manandhar**, for their endless support.

CHAPTER 1 - INTRODUCTION

1.1 General

Roadways in the United States are key elements of the transportation system. Roadway pavements are mainly classified as flexible or rigid. Flexible pavements (also called asphalt pavements) are constructed of bituminous and granular materials, while rigid pavements are constructed of Portland cement concrete. As of 2008, there were about 4.4 million kilometers (2.73 million miles) of paved roads, of which 94% were asphalt surfaced (FHWA 2008). Composite pavements are the third type identified by the Federal Highway Administration (FHWA). Composite pavements are mostly asphalt layers overlaid on concrete pavements (FHWA 2008). Asphalt-surfaced pavements include bituminous and composite types.

The first asphalt roadway in the United States was constructed in Newark, New Jersey, in 1870. The first hot-mix asphalt pavement, which was a mixture of asphalt cement with clean angular-graded sand and mineral filler, was laid on Pennsylvania Avenue in Washington, D.C. in 1876, using natural asphalt imported from Trinidad Lake (Huang 2004).

About 89% of the state paved-road network in Kansas is asphalt surfaced. Typical design performance period of hot-mix asphalt (HMA) pavement for new construction or reconstruction as per the Kansas Department of Transportation (KDOT) is 10 years. In most cases, some preventive action, such as a slurry seal, is typically needed for these pavements before they reach the end of this performance period. Bituminous and composite pavements are usually overlaid with asphalt concrete for pavement preservation. However, no life is assigned to such an action and average life is about only three years. Frequent failures can be noticed on asphalt pavements in Kansas. The failures can be attributed to some preventable causes such as improper mix design and deficiency in construction density or field density.

1.2 Problem Statement

Three major types of distresses have been observed on asphalt-surfaced pavements in Kansas: rutting, fatigue cracking, and low-temperature cracking. These distresses occur due to high temperatures combined with traffic loading, repeated load applications, aging, moisture damage, and thermal stresses of daily/seasonal temperature cycles. Aging and moisture damage

can be attributed to inadequate mixture design and/or low construction density resulting in a permeable pavement. A permeable pavement will have a shorter life than that of an impermeable pavement. Asphalt mixture will degrade and deteriorate through water and air infiltration, causing subsequent raveling, stripping, and hardening of the binder due to oxidation. Thus, to maximize performance, HMA pavements need to be constructed with adequate field density and should be relatively impermeable. If excessive moisture or water is present in the pavement system, it can strip prematurely (Hicks 1991). Percolation of water and air through the pavement can cause stripping and oxidation of the binder, rutting of the surface layer, and reduction of pavement support. Life of a permeable asphalt pavement would be expected to be less than that of an impermeable pavement (Hicks 1991).

KDOT is increasingly using Superpave mixtures that may be susceptible to moisture damage. Moisture susceptibility is currently evaluated by the Kansas Standard Test Method KT-56, which closely follows the American Association of State Highway and Transportation Officials test method AASHTO T 283, “Resistance of Compacted Bituminous Mixture to Moisture-Induced Damage.” KDOT’s currently specified sampling and testing frequency chart for bituminous construction items for quality control/quality assurance (QC/QA) projects requires that one KT-56 test be performed by the contractor on the first lot (3,000 tons), and then one test per week or per 10,000 tons (Mg). KDOT specifications also require that the bituminous mixture have a minimum tensile strength ratio (TSR) of 80%. Since this test is time consuming, it takes minimum of three days to complete a single test, it often happens that the contractor might have paved a substantial area of the pavement that might contain a mixture that does not satisfy this criterion before the test results are obtained. Acceptance is often left up to the KDOT engineer and as of now, there is no “rational” method available to determine the life reduction of the new asphalt pavement if the defective Superpave mixes are accepted.

For fast and reliable performance testing of asphalt mixes, Hamburg Wheel-Tracking Device (HWTD) was chosen. The HWTD was originally manufactured in the 1970s by Esso, A. G. of Helmut-Wind Inc., Hamburg, Germany. The HWTD test was initially intended for measuring rutting behavior; it was later found to be capable of identifying the mixes with potential moisture resistance. The device was introduced into the United States in the early 1990s by pavement engineers and officials following a European asphalt study tour for technology transfer (European Asphalt Study Tour 1991; Yildirim and Kennedy 2001). This introduction of

the HWTD initiated research to evaluate the capability of the equipment to characterize moisture sensitivity of asphalt mixes and to predict field performance (Lu and Harvey 2006; Liddle and Choi 2007; Lu 2005). The HWTD was found to be sensitive to aggregate quality, asphalt cement stiffness, short-term aging duration, asphalt source or refining processes, antistripping treatments, and compaction temperatures (Aschenbrener 1994; Aschenbrener and Far 1994). The HWTD is gaining popularity for testing rutting and stripping potential of asphalt pavements (Izzo and Tahmoressi 1999).

A single HWTD test takes about six to six and one-half hours. If the test duration can be reduced significantly, HWTD will be an effective tool for QC/QA of HMA.

1.3 Objectives of the Study

The objectives of this study are:

- To develop criteria to accept in-place Superpave mixtures that are out of specification for in-place density and/or air voids @ N_{design} ; and
- To develop accelerated mix testing models for estimating lives of deficient Superpave pavements using the HWTD test results.

1.4 Dissertation Outline

This dissertation is divided into five chapters. The first chapter covers a brief introduction, problem statement, objectives of the study, and dissertation outline. Chapter 2 is a review of the literature. Chapter 3 describes the first objective of the study, to develop criteria for out-of-specification Superpave mixtures. Chapter 4 presents the second objective of the study, to develop laboratory-based accelerated mix testing models. Finally, Chapter 5 presents conclusions and recommendations based on this study.

CHAPTER 2 - LITERATURE REVIEW

This chapter reviews the literature available on the topics of Superpave system, asphalt pavement distresses, torture test devices including Hamburg Wheel-Tracking Device (HWTD), and accelerated mix testing and statistical analysis.

2.1 Superpave System

In 1987, Congress approved the Strategic Highway Research Program (SHRP), a five-year, \$150 million, federal research program to improve performance and durability of United States roads and to make those roads safer for both motorists and highway workers. One third of the SHRP research funds were allocated for development of performance-based asphalt material specifications relating laboratory measurements to field performance. The final product of the SHRP asphalt research program was a new system called Superpave, an abbreviation for superior performing asphalt pavements (Hossain et al. 2008). The Hveem and Marshall methods of mix design have been used since the 1940s. These mix design methods have performed well for many years. As traffic volume and loads increased, a better and more efficient technology was warranted compared to the conventional. Implementation of the Interstate Highway System in 1956 compelled the United States to innovate a new technology to rely on highway transportation for its primary mode of transporting people and goods (Roberts et al. 1996). In addition to traffic loading, climate change has a strong influence on rutting of asphalt concrete pavements (Archilla 2000; Thompson and Nauman 1993).

2.2 Asphalt Pavement Distresses

Asphalt-surfaced pavements in Kansas primarily exhibit three types of distress: rutting, fatigue cracking, and low-temperature cracking.

2.2.1 Rutting

Rutting is a major distress of asphalt pavement. A rut is a surface depression in the wheel path. Uplifting of pavement along the sides of the rut might also occur. Rutting is caused by progressive movement of materials under repeated traffic loads, mainly due to heavy loads, either on asphalt layers or in the subgrade as shown in Figure 2.1. It happens due to consolidation or lateral movement of the materials due to traffic loads. Rutting can be caused by the plastic movement of the asphalt mix as a result of combined effects of traffic loads and elevated temperatures in hot summer, or from inadequate compaction during construction. Significant rutting can lead to structural failures and create a potential for hydroplaning. Excessive asphalt content in the mix is the most common cause for rutting. In this situation, there will be loss of internal friction between aggregate particles, resulting in loads to be carried by asphalt cement instead of aggregate structures. Plastic flow can be minimized using large-size, angular, and rough-textured coarse and fine aggregates, and providing proper compaction during construction (Huang 2004; Roberts et al. 1996). Consolidation is the further compaction of asphalt pavement by traffic after construction, resulting in a reduction of air voids. Typically, asphalt mixtures are designed to have air voids of three to five percent at the design traffic level. During construction of asphalt pavements, air void is maintained at seven to eight percent, expecting the consolidation of pavement to reach the designed air void levels. In some cases, due to poor compaction, initial air voids of the existing pavement can range from 10 to 12 percent (Roberts et al. 1996).



Figure 2.1 Rutting in the Wheel Paths

In addition to traffic loading, climate change has a strong influence on rutting of asphalt pavements (Archilla 2000; Thompson and Nauman 1993).

Rutting happens when the applied stress along the wheel path of traffic loading is high enough to cause shear displacements within the materials. Rutting might be caused due to a single or relatively few excessive loads or tire pressures, causing stresses that approach or exceed the strength of the materials, and in time, heaving alongside of the loaded area. Repeated traffic loadings accumulate deformations over time and become a significant rut if the loadings are channelized in the wheel paths. An illustration of pavement surface deformation is shown in Figure 2.2.

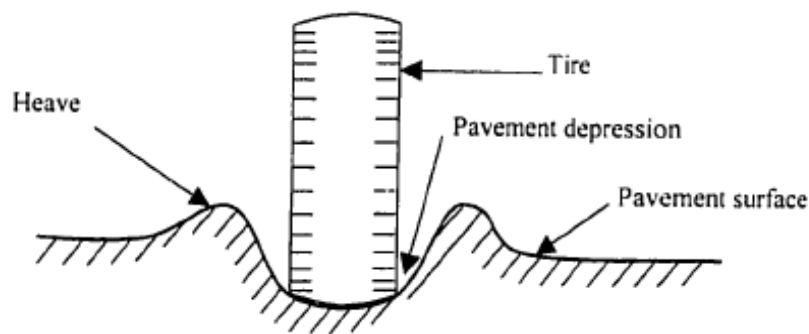


Figure 2.2 Pavement Surface Deformations Due to Traffic Loading (Archilla 2000)

2.2.2 Fatigue Cracking

Fatigue cracking is also called alligator cracking, as the closely spaced crack pattern is similar to that on an alligator's back as shown in Figure 2.3. Fatigue cracking is a series of interconnecting cracks due to fatigue failure of an asphalt pavement under repeated traffic loading. The pieces are usually less than one foot on the longest side. The cracking initiates at the bottom of the asphalt layer, where tensile stress or strain is the highest under a wheel load, and propagates to the surface. It happens due to repetitive axle loads which are too heavy for the pavement structure, or repetitions of a given load that exceed the design number of repetitions. Inadequate pavement drainage worsens the situation of pavements with fatigue cracks. Fatigue cracking also happens due to inadequate pavement thickness or when there has been poor quality control during construction. The advanced stage of fatigue cracking leads to potholes. Major maintenance of fatigue cracking involves removal and replacement. Fatigue cracking is a load-associated failure (Huang 2004; Roberts et al. 1996).



Figure 2.3 Fatigue Cracks on Asphalt Pavement

2.2.3 Low-Temperature Cracking

Low-temperature cracks are transverse cracks, which generally run perpendicular to the centerline of the roadway as shown in Figure 2.4. These transverse cracks are equally spaced and normally occur when the temperature of the pavement surface drops significantly. This produces a thermally induced shrinkage stress that exceeds the tensile strength of the asphalt mixture. Low-temperature cracks normally initiate at the top of the asphalt pavement and propagate down the asphalt layer. These cracks are generally repaired by sealing them with liquid asphalt or other type of sealing materials (ASTM D5078 and D3405). Crack sealing prevents moisture from getting to the base course and subgrade, which reduces the raveling effect and extends the service life of the pavement. Grinding bumps at the cracks is preferred for achieving a smooth ride quality (Roberts et al. 1996; Roberts et al. 2002).



Figure 2.4 Low-Temperature Crack on Flexible Pavement

2.2.4 Stripping/ Moisture Damage

Stripping, a moisture-induced distress, can be defined as the weakening or eventual loss of adhesive bond, between the aggregate surface and the asphalt cement in an HMA pavement or mixture due to the presence of moisture (Roberts et al. 1996). The strength of an asphalt mixture is controlled by the cohesive resistance of binder and grain interlock, and frictional resistance due to the interlock between aggregate grains. Only the good bonding between binder and aggregate can provide cohesive resistance. If the bond is poor, failure occurs at the binder-aggregate interface and results in premature failure of the mixture and the asphalt pavement (Roberts et al. 1996).

Stripping happens due to loss of bond between the aggregates and the asphalt, which typically begins at the bottom of the asphalt layer and progresses upward. Top-down stripping results in raveling, which is the progressive disintegration of an asphalt layer from the surface downwards. Factors affecting asphalt pavements for stripping include inadequate pavement drainage, inadequate compaction, excessive dust coating on aggregates, use of an open-graded

friction course, inadequate drying of aggregates, weak and friable aggregates, overlays on deteriorated pavement, waterproofing membrane and seal coats, and antistripping agents.

Since the late 1970s and early 1980s, it has been increasingly recognized that moisture has a detrimental effect on hot-mix asphalt (HMA) pavements. Moisture-related problems are due to or are accelerated by –

- Adhesive stripping of the asphalt film from the aggregate surface, or
- Cohesion loss of mixture stiffness (Hicks et al. 2003).

These mechanisms can be associated with the aggregates, binder, or interaction between the two constituents. Moisture-related distresses are also accelerated by improper mix design or construction issues, including those given in Table 2.1. Too high or too low binder content and air voids in the mix design contribute moisture related distresses.

Table 2.1 Factors Contributing to Moisture-Related Distresses (Hicks et al. 2003)

MIX DESIGN	<ul style="list-style-type: none"> • Binder and aggregate chemistry • Binder content • Air voids • Additives
PRODUCTION	<ul style="list-style-type: none"> • Percent aggregate coating and quality of passing the no. 200 sieve • Temperature at plant • Excess aggregate moisture content • Presence of clay
CONSTRUCTION	<ul style="list-style-type: none"> • Compaction – high in-place air voids • Permeability – high values • Mix segregation • Changes from mix design to field production (field variability)
CLIMATE	<ul style="list-style-type: none"> • High-rainfall areas • Freeze-thaw cycles • Desert issues (steam stripping)
OTHER FACTORS	<ul style="list-style-type: none"> • Surface drainage • Subsurface drainage • Rehab strategies – chip seals over marginal HMA materials • High truck traffic

2.2.4.1 Moisture-Related Distresses

Moisture-related distress is similar in many ways to distress caused by other factors (materials, design, and construction). Moisture tends to accelerate the extent and severity of the distress. Types of distress that can be related to moisture or other factors are described below.

- **Bleeding, cracking, and rutting:** Presence of a film of asphalt binder on the pavement is called bleeding. It creates a shiny, glass-like reflecting surface and can be quite sticky. Bleeding occurs when asphalt binder fills the aggregate voids during hot weather and expands onto the pavement surface. This can be caused by excessive asphalt binder in the HMA mix and/or low HMA air void content of the mix. These distresses are due to a partial or complete loss of the adhesion bond between the aggregate surface and the asphalt cement. This may be caused by presence of water in the mix due to poor compaction, inadequately dried or dirty aggregates, poor drainage, or poor aggregate-asphalt chemistry. It is aggravated by the presence of traffic and freeze-thaw cycles and can lead to early bleeding, rutting, or fatigue cracking.

- **Raveling:** Progressive loss of surface material by weathering or traffic abrasion, or both, is another manifestation of moisture-related distress as shown in Figure 2.5. It may be caused by poor compaction, inferior aggregates, low asphalt content, high fines content, or moisture-related damage, and it is aggravated by traffic.

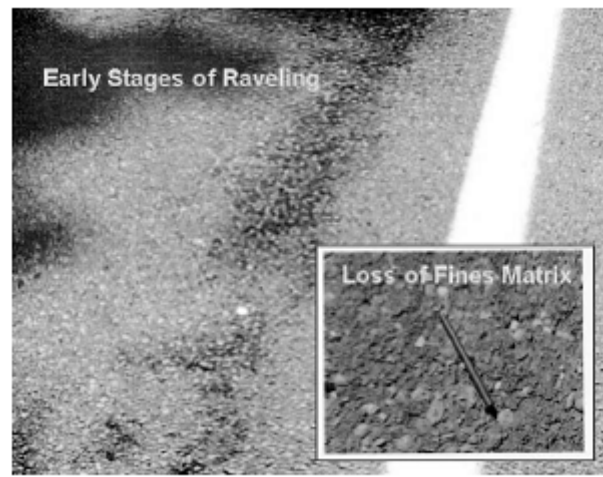


Figure 2.5 Raveling of Asphalt Pavement (Hicks et al. 2003)

- **Localized failures:** This type of distress can be the end result of either of the types discussed above. It is progressive and can be due to loss of adhesion between the binder and the aggregate, or the cohesive strength in the mix itself as shown in Figure 2.6.
- **Structural strength reduction:** This is a result of a cohesive failure causing a loss in stiffness in the mixture.



Figure 2.6 Typical Localized Failure Due to Moisture Damage (Hicks et al. 2003)

Figure 2.7 relates the stress of loss of fatigue life, and Figure 2.8 shows stiffness loss of an asphalt mixture at different stages of moisture conditioning in laboratory-resilient modulus testing.

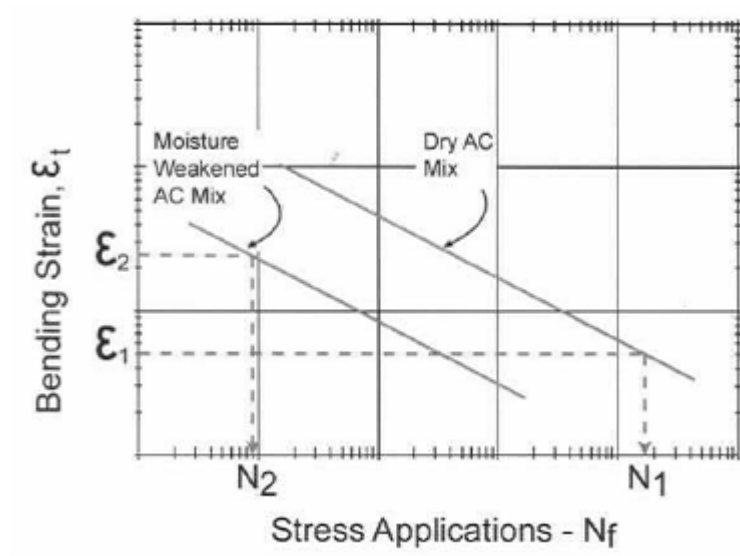


Figure 2.7 Loss of Fatigue Life Due to Moisture Damage (Hicks et al. 2003)

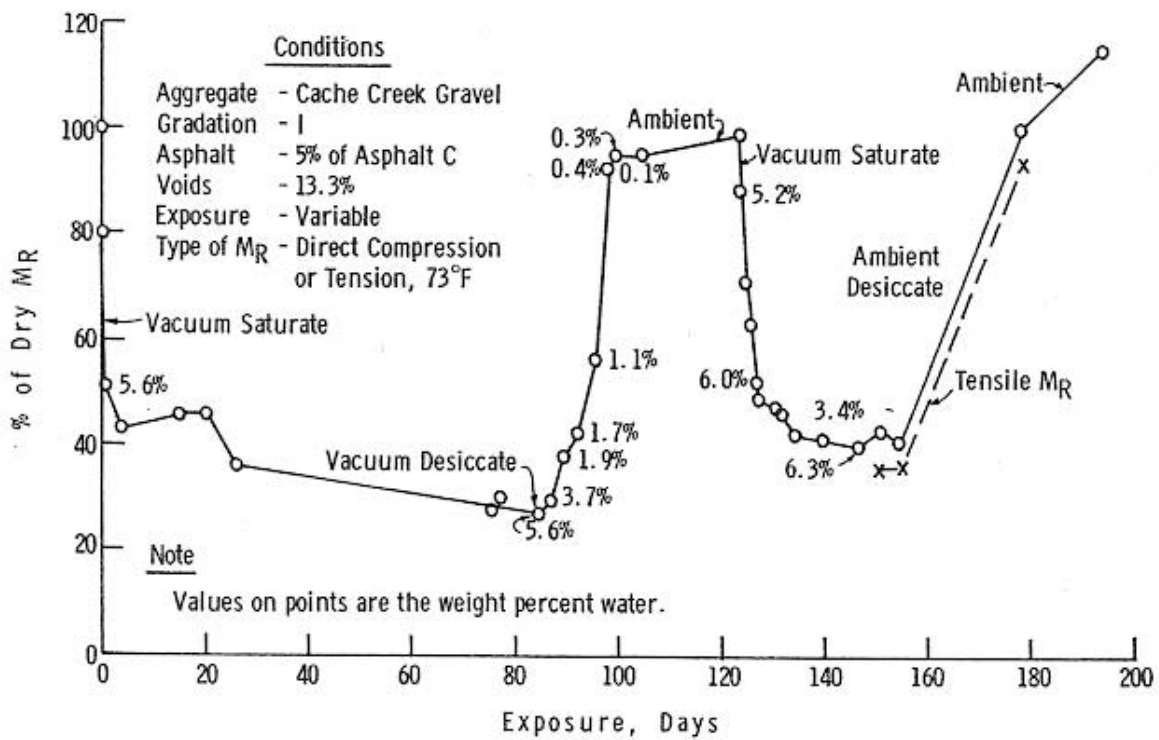


Figure 2.8 Stiffness Loss of HMA Due to Moisture Damage (Hicks et al. 2003)

Loss of adhesion occurs due to water getting in between the asphalt and the aggregate and stripping away the asphalt film. Loss of cohesion is due to a softening of asphalt cement in

the presence of water, which weakens the bond between the asphalt concrete and the aggregate. Severe damage occurs in extreme weather conditions, particularly freeze-thaw action, combined with heavy traffic volume. Quality of compaction and weather condition during pavement construction play a vital role in moisture damage. The most important construction factor is controlling air voids. Using good aggregates and pretreatment of aggregates, and using additives, are some of the methods used to reduce moisture damage, mainly stripping (Hicks 1991; Kandhal 1994). Moisture susceptibility is influenced by aggregate mineralogy, aggregate surface texture, asphalt binder chemistry, and the interaction between asphalt and aggregate. Different aggregate mineralogy and several types of unmodified and modified asphalt binders are being used across the United States, and along with varied environmental conditions, traffic, and construction practices, have made testing to accurately predict HMA moisture susceptibility a difficult task (Solaimanian et al. 2007).

Causes of Moisture-Related Distresses

As listed in Table 2.1, numerous factors can contribute to moisture sensitivity problems in HMA pavements. The following is a brief discussion of these factors.

Moisture-Sensitive Aggregates: Aggregates can greatly influence whether a mixture will be moisture sensitive or not. The aggregate surface chemistry and presence of clay fines are important factors affecting the adhesion between the aggregate and the asphalt binder. Common solutions are use of antistripping agents such as liquids or lime, and elimination of detrimental clay fines through proper processing or specifications (Hicks et al. 2003).

Asphalt Binder Sensitivity to Moisture Damage: The asphalt binder can influence both adhesion between the asphalt and the aggregate and the cohesion of the mastic. Adhesion is influenced by the chemistry of the asphalt as well as by the stiffness of the binder. Cohesive strength of the asphalt matrix in the presence of moisture is also influenced by the chemical nature of the binder and processing techniques (Hicks et al. 2003).

Presence of Water and Traffic: Moisture-related problems do not occur without the presence of water and traffic, which provide the energy to break the adhesive bonds and cause cohesive failures. Repeated freeze-thaw cycles can also accelerate the distresses on the pavement. Moisture can come from the infiltration of precipitation or from beneath the surface by vapor movement and/or capillary rise. Once the moisture is in the pavement, it can affect

either the adhesive bond or cohesive strength. Test methods, which have historically been used to evaluate mixes for moisture sensitivity, have generally examined the effect of moisture on the mix strength or the coating on the aggregates. They have not included the effect of traffic on accelerating moisture-related distresses (Hicks et al. 2003).

Pavement Design Considerations: Pavements with fundamental design flaws trap water or moisture within the structural layers. There must be good drainage design, both surface and subsurface, since water causes moisture-related distress. Application of a surface seals to a moisture-sensitive mix can also be a factor in accelerating moisture damage (Hicks et al. 2003).

Material Production Issues: The method used to refine the binder, particularly the acids and bases of the binder is fundamental to the understanding of moisture-related distresses. Aggregate production issues including cleanliness, moisture content, and hardness are also important. Finally, mix handling, including use of storage silos, may affect the moisture susceptibility of the mixtures (Hicks et al. 2003).

Construction Issues: A number of construction issues can affect the moisture sensitivity of the mix. Weather conditions can affect mix compaction or trap moisture in the mix in some cases. Mix handling techniques (e.g., windrow truck loading) can influence segregation and affect the permeability of the mix. Joint construction techniques can also affect compaction and permeability. The amount of compaction achieved (relative density) has a major effect on the air void content, permeability of the finished pavement, and mix sensitivity to moisture damage. Control (or lack thereof) of required additives can influence long-term performance of the mix. In summary, moisture damage problems in asphalt pavements can be solved using additives, improving mix design and construction practices, and following better specifications (Hicks et al. 2003).

2.2.4.2 Chemical and Mechanical Processes of Moisture Damage in HMA

Various mechanisms have been identified as causes of moisture damage, including detachment, displacement, spontaneous emulsification, pore pressure, hydraulic scour, and effects of the environment on the aggregate-asphalt system (Little and Jones 2003). Moisture damage happens due to a combination of two or more of these causes.

Detachment: Detachment is the separation of an asphalt film from an aggregate surface by a thin film of water without an obvious break in the film. If a three-phase interface consisting of aggregate, asphalt, and water exists, water reduces the free energy of the system more than

asphalt to form a thermodynamically stable condition of minimum surface energy (Little and Jones 2003). Asphalt has relatively low polar activity and the bond between the aggregate and asphalt is mainly due to relatively weak dispersion forces. Water molecules are, on the other hand, highly polar and can replace the asphalt at the asphalt-aggregate interface.

Displacement: Displacement of asphalt at the aggregate surface happens due to a break in the asphalt film. The major source of the break may be an incomplete coating of the aggregate surface (Little and Jones 2003).

Spontaneous Emulsification: Spontaneous emulsification is an inverted emulsion of water droplets in asphalt cement. Organic amines, which are basic nitrogen compounds, can bond strongly to aggregates in the presence of water (Little and Jones 2003).

Pore Pressure: Pore pressure develops under traffic loading when water is entrapped in asphalt concrete. Stresses imparted to the entrapped water from repeated traffic load applications will worsen the damage as the continued buildup in pore pressure disrupts the asphalt film from the aggregate surface or can cause growth of micro-cracks in the asphalt mastic. Little and Jones (2003) indicated that this “strain hardening” differs from classical strain hardening occurring when metals are cold-worked to develop interactive dislocations to prevent slip; instead, strain hardening seen in asphalt concrete is due to the “locking” of the aggregate matrix caused by densification during repeated loading.

Hydraulic Scour: Hydraulic scour happens due to the action of tires on a saturated pavement surface. Water is sucked under the tire into the pavement by the tire action. Osmosis and pullback have been suggested as possible mechanisms of scour (Little and Jones 2003; Taylor and Khosla 1983). According to Cheng et al. (2002), the diffusion of water vapor through asphalt cement itself is considerable and asphalt mastics can hold a large amount of water. They have shown that the amount of water held by asphalt is related to the level of moisture damage that occurs in the mixtures using that asphalt.

pH Instability: Asphalt-aggregate adhesion is strongly influenced by the pH value of the contact water. Researchers investigated the effect of various sources of water on the level of damage that occurred in a boiling test. Stabilization of the pH sensitivity at the asphalt-aggregate interface can minimize the potential for bond breakage, provide strong durable bonds, and reduce stripping (Little and Jones 2003). pH values greater than 10 and lower than four can dislodge

amines from an aggregate surface and can dissolve lime, depending on the type of acid used; these low pH values and high pH values are not found in hot-mix asphalt.

Environmental Effects on the Aggregate-Asphalt System: Several factors such as temperature, air, and water have a tremendous effect on the durability of asphalt concrete mixtures.

2.2.4.3 Treatment for Moisture Sensitivity

Moisture sensitivity problems of HMA are related to the properties of the asphalt binder, properties of the aggregate, hot-mix asphalt characteristics, climate, traffic, construction practices, and pavement design considerations. Mixture designs can be developed with moisture sensitivity as one of the controlling factors. For most projects, an asphalt binder and aggregate are selected and the mixture design is developed.

The mixture is then tested for moisture sensitivity and, if not accepted, a “treatment” of some type is selected based on experience and laboratory testing. HMA is judged to be acceptable if it meets certain laboratory test criteria. Some public agencies require all hot-mix asphalt mixtures to be treated for moisture sensitivity. Other public agencies require that field-produced hot-mix asphalt meets certain laboratory test criteria as part of the test-strip process or during production of hot-mix asphalt for the project, or both (Epps et al. 2003).

Treatments Added to Asphalt Binders: A variety of chemicals are being used to reduce the moisture sensitivity of hot-mix asphalt. Most of the chemicals currently in use are alkyl amines and are sold under a variety of brand names. These chemicals are added directly to the asphalt binder either at the refinery or asphalt terminal, or at the contractor’s asphalt facility during production of the mix with an in-line blending system. These types of chemical additives are generally referred to as “liquid anti-strip agents” or “adhesion agents.” Liquid anti-strip agents are not only used in HMA but are commonly used in cold-applied, asphalt-bound patching materials; in asphalt binders used for chip seals; and in binders used for pre-coating the aggregates in chip seals.

Treatments Applied to Aggregates: Hydrated lime, Portland cement, fly ash, flue dust, and polymers have been added to aggregates to provide resistance to moisture in hot-mix asphalt mixtures. Typically, these materials are added to the aggregate and mixed before the introduction of the asphalt binder in the hot-mix asphalt production process. In some cases, hydrated lime or Portland cement has been added in the drum mixing operation at the point of entry of the asphalt

binder to the heated aggregate. Hydrated lime is currently the most commonly used treatment for aggregates.

2.2.4.4 Test Methods to Predict Moisture Sensitivity of Hot-Mix Asphalt Mixtures

Tests for identifying moisture damage potential of an asphalt-aggregate mixture can be classified into two major categories: those on loose mixtures and those on compacted mixtures. Static immersion and the boil test, both conducted on loose mixtures, were among the first tests introduced to the paving industry. These were followed by the immersion-compression test in the late 1940s. That test was conducted on compacted specimens and was the first test to become an ASTM standard in the mid-1950s. Research in the 1960s brought considerable awareness to asphalt pavement technologists of the significant effects of a laboratory test that currently has the widest acceptance in the paving industry. This test was further modified through the work of Tunicliff and Root (1984).

Wheel-tracking of asphalt mixes submerged under water gained popularity for determination of moisture damage in the 1990s. HWTD and the asphalt pavement analyzer (APA) are among the tests of this type. It was also during this period that the environmental conditioning system (ECS) was introduced to the industry at the completion of the Strategic Highway Research Program (SHRP) in 1993. The Superpave system, the product of SHRP, adopted the standard test method AASHTO T283 as the required test for estimating the risk of moisture damage. This test procedure is similar to the Lottman test procedure with some modifications (AASHTO 2004). With the Superpave system being adopted by most state highway agencies, AASHTO T283 became the most widely used test for moisture damage. The significance of the need for a reliable test was emphasized through the work of researchers such as Johnson (1969), Schmidt and Graf (1972), Jiminez (1974), and Lottman (1978). The work by Jiminez (1974) resulted in a laboratory test simulating the effect of repeated water pressure on the behavior of saturated hot-mix asphalt. Extensive work by Lottman (1978) resulted in use of the procedure within the industry. Some agencies have reported problems with this test in terms of correlation between laboratory results and field observations.

Today, development of a quick, reliable, and practical test procedure for determination of moisture damage remains a challenge for asphalt pavement technologists. An important consideration in developing a test procedure for moisture damage should be calibration of the test to the conditions for which it will be applied. Some tests have been calibrated and

implemented on a local basis (a region within a state). No test has been successfully calibrated and implemented across a wide spectrum of conditions. Consequences for this have been lack of correlation with field performance, lack of good field performance databases, and problems with the tests such as variability and difficulty of execution (Solaimanian et al. 2007).

A general consensus in the industry is that laboratory tests performed on compacted HMA are better than those on a loose asphalt mixture. In NCHRP project 9-34, research was done to develop an improved laboratory test procedure for predicting asphalt concrete susceptibility to moisture damage through integrating the environmental conditioning system (ECS) and Superpave simple performance tests (Solaimanian et al. 2007, Shiwakoti 2007). Superpave simple performance tests include flow time (static creep), flow number (repeated load permanent deformation), and dynamic modulus. The primary conclusion of Phase I of NCHRP Project 9-34 study was that the dynamic modulus test was the most suited of the three simple performance tests for possible use with the ECS in an improved moisture sensitivity test. The duration of water/load conditioning, temperature at the time of conditioning, and magnitude of the conditioning load are the weak points for the ECS/dynamic modulus to be accepted as a routine mix design test. The modulus of the unconditioned specimen, as well as the retained modulus after the ECS/dynamic modulus testing, could be used in the models to determine the impact of moisture damage on developed distresses (rutting and fatigue cracking). Table 2.2 summarizes the tests for moisture sensitivity on loose mixtures. Table 2.3 presents the tests for moisture sensitivity on compacted samples.

Table 2.2 Moisture Sensitivity Tests on Loose Samples (Solaimanian et al. 2007)

Test	ASTM	AASHTO	Other
Methylene blue			Technical Bulletin 145, International Slurry Seal Association
Film stripping			California Test 302
Static immersion	D1664*	T182	
Dynamic immersion			
Chemical immersion			Standard Method TMH1 (Road Research Laboratory 1986, England)
Surface reaction			Ford et al. 1984
Quick bottle			Virginia Transportation Research Council (Maupin 1980)
Boiling	D3625		Tex 530-C Kennedy et al. 1984
Rolling bottle			Isacsson and Jorgenson, Sweden, 1987
Net adsorption			SHRP A-341 (Curtis et al. 1993)
Surface energy			Thelen 1958, HRB Bulletin 192 Cheng et al., AAPT 2002
Pneumatic pull-off			Youtcheff and Aurilio (1997)

* No longer available as ASTM standard.

Table 2.3 Moisture Sensitivity Tests on Compacted Specimens (Solaimanian et al. 2007)

Test	ASTM	AASHTO	Other
Moisture vapor susceptibility			California Test 307 (developed in late 1940s)
Immersion-compression	D 1075	T 165	ASTM STP 252 (Goode 1959)
Marshall immersion			Stuart 1986
Freeze-thaw pedestal test			Kennedy et al. 1982
Original Lottman indirect tension			NCHRP Report 246 (Lottman 1982); Transportation Research Record 515 (1974)
Modified Lottman indirect tension		T 283	NCHRP Report 274 (Tunnicliff and Root 1984), Tex 531-C
Tunnicliff-Root	D 4867		
ECS with resilient modulus			SHRP-A-403 (Al-Swailmi and Terrel 1994)
Hamburg wheel tracking			1993 Tex-242-F
Asphalt pavement analyzer			
ECS/SPT			NCHRP 9-34 2002-03
Multiple freeze thaw			

2.2.4.5 Cost Effectiveness

Material costs of liquid anti-strip agents typically range from \$0.45 to \$0.75 per pound of liquid anti-strip. This equates to a cost of \$6.75 to \$11.25 per ton of asphalt binder for a treatment concentration of 0.75%. Thus, the typical increase in the cost per ton of HMA concrete is from \$0.30 to \$0.70 for the liquid anti-strip agent. The cost for in-line blending equipment installed at the contractor's plant ranges from \$10,000 to \$25,000. Typically, in-line blending equipment is amortized over a five-year period. Total price increase in using a liquid anti-strip agent is typically in the range of \$0.50 to \$0.81 per ton of HMA.

2.3 Torture Test Devices

Torture testing of asphalt specimens has been gaining popularity recently due to its relative ease and simplicity. These tests use a laboratory-prepared asphalt concrete specimen to repeatedly load with steel wheels or rubber tire wheels. Torture tests of this kind are known as loaded wheel testers (LWTs). The primary purpose of LWTs is to perform efficient, effective, and routine laboratory rut-proof testing and field production quality control of Superpave mixtures (Lai 1990). There are many types of LWTs in use today. Europeans have developed the Hamburg Wheel-Tracking Device (HWTD) and the French Pavement Rutting Tester (FPRT). Americans have developed the Georgia Loaded-Wheel Tester (GLWT) (by the Georgia Department of Transportation) and the Evaluator of Rutting and Stripping in Asphalt (ERSA) at the University of Arkansas (Williams 2001). The asphalt pavement analyzer (APA) is a modification of the GLWT (Novak 2007; Williams 2001). Despite the advantages of simplicity and cost effectiveness, there are issues related to LWTs as far as differentiating good and bad mixtures properly (Collins et al. 1995).

In most LWTs, the loading device – in the form of a wheel or a pressurized hose – is tracked back and forth over a testing sample to induce rutting. The load follows the same path in both directions without wander.

The HWTD test performed the best among the Asphalt Pavement Analyzer (APA), French Pavement Rutting Tester (FPRT), and HWTD in research comparing laboratory wheel-tracking test results with the WesTrack test-rut performance (Williams and Prowell 1999). The HWTD test has been gaining acceptance by many state highway agencies (Lu and Harvey 2006).

Studies have shown that the HWTD was capable of evaluating moisture damage as well as rutting.

2.4 Accelerated Mix Testing and Statistical Analysis

2.4.1. Overview

Researchers had named the accelerated tests as the elephant tests, which also include killer tests, design limit tests, design margin tests, design qualification tests, torture tests, and shake and bake (Nelson 1990). If the product survives one of these tests, the responsible engineers have more faith in it. Otherwise, the engineers will redesign or improve the quality to overcome the cause of failure. In this type of test, the specimen may be subjected to a single, severe level of a stress (temperature). It may be subjected to a number of stresses – either simultaneously or sequentially. A good elephant means one that produces the same failures and in the same proportions that will occur in service. Elephant tests provide only qualitative information on whether a product is good or bad (Nelson 1990).

Overstress testing consists of running a product at higher than normal levels of some accelerating stress(es) to shorten product life or to degrade the product faster. Typical accelerating stresses on asphalt mixtures can be temperature, mechanical loads, or traffic loads. Accelerated degradation testing involves overstress testing. Instead of life, product performance is observed as it degrades over time. A model for performance degradation is fitted to such performance data and used to extrapolate performance and time of failure. Thus failure and life can be predicted before any specimens fails (Nelson 1990).

Accelerated degradation is concerned with models and data analyses for degradation of the product over time at overstress and design conditions. Performance degradation data can be analyzed before reaching failure criteria. It accelerates the test by extrapolating performance degradation to estimation time to reach failure criteria. Performance degradation can yield better insight into the degradation process and how to improve it (Nelson 1990). Some of the assumptions of degradation models are as follows:

- Degradation is not reversible.
- Usually a model applies to a single degradation process.
- Degradation of specimen performance before the test is negligible.
- Performance is measured with negligible random error.

2.4.2 Weibull Distribution

Weibull distribution is a very flexible model for survival analysis. As mentioned earlier, the survival function for Weibull distribution is given by $S^x(x) = \exp(-\lambda x^\alpha)$. The hazard rate is expressed as $h^x(x) = \lambda \alpha x^{\alpha-1}$. When the log transform of time is taken, the univariate survival function for $Y = \ln X$ can be expressed as in Equation (2.1).

$$S_y(y) = \exp(-\lambda e^{\alpha y}) \quad (2.1)$$

If we redefine the parameters as $\lambda = \exp(-\mu/\sigma)$ and $\sigma = 1/\alpha$, then Y follows the form of a log linear model as in Equation (2.2).

$$Y = \ln X = \mu + \sigma W \quad (2.2)$$

where W is the extreme value distribution with probability density function as given in Equation (2.3),

$$f_w(w) = \exp(w - e^w); \quad (2.3)$$

and survival function as given in Equation (2.4),

$$S_w(w) = \exp(-e^w). \quad (2.4)$$

2.4.3 Survival Analysis

Survival analysis generally refers to statistical methods for analyzing survival or time-to-event data. The data can be generated from diverse fields such as medicine, biology, public health, epidemiology, engineering, economics, and demography (Klein and Moeschberger 2003). The analysis involves data which get truncated. For example, let X be the time until some specified event. This event may be death, development of some disease, equipment breakdown, conception, cessation of smoking, etc. X is a non-negative random variable. Four functions are used to characterize the distribution of X , namely the *survival function*, which is the probability of survival beyond time x ; the *hazard rate (function)*, which is the chance an individual of age x experiences the event in the next instant; the *probability density (or probability mass) function*, which is the unconditional probability of the event occurring at time x ; and the mean residual probability life at time x , which is the mean time to the event of interest, given that the event has not occurred at x . If any of these parameters is known, then the other three can be uniquely determined (Klein and Moeschberger 2003).

2.4.3.1 Survival Function

The survival function is defined as $S(x) = \Pr(X > x)$. When X is a continuous random variable, the survival function is the complement of the cumulative distribution function, that is, $S(x) = 1 - F(x)$, where $F(x) = \Pr(X \leq x)$. The survival function is the integral of the probability density function, $f(x)$, that is, the survival function for the Weibull distribution is $S(x) = \exp(-\lambda x^\alpha)$, $\lambda > 0$, $\alpha > 0$. Figure 2.9 shows survival curves with a common median of 6.93, but for various α and λ values. These functions are monotone, non-increasing with values equal to one at zero, and zero as the time approaches infinity.

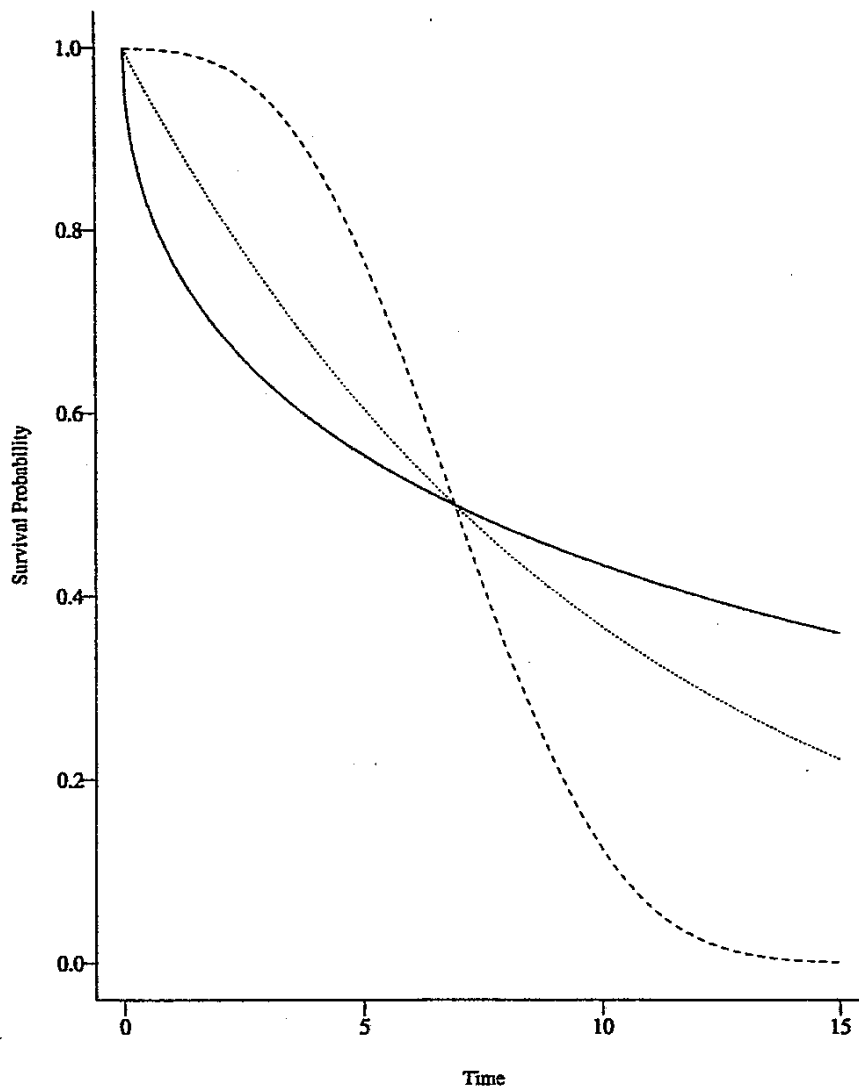


Figure 2.9 Weibull Survival Functions for $\alpha = 0.5$, $\lambda = 0.2638$ (_____); $\alpha = 1.0$, $\lambda = 0.1$ (.....); $\alpha = 3.0$, $\lambda = 0.00208$ (-----) (Klein and Moeschberger 2003)

2.4.3.2. Right-Censored Data

There are two types of right censoring: Type I and Type II. Type I censoring is where the event is observed only if it occurs prior to some pre-specified time. For example, a typical animal study or clinical trial starts with a fixed number of animals or patients to which a treatment (or treatments) is applied (Klein and Moeschberger 2003). Because of time or cost considerations, the investigator will terminate the study or report the results before all subjects realize their events. The second type of right censoring is Type II in which the study continues until the failure of the first r individuals out of n , where r is some predetermined integer. The HWTD test data can be considered as Type I censored since the test is terminated when 20,000 passes or a rut depth of 20 mm (0.8 in.) is reached.

2.4.4 Cubic Model

In an attempt to better capture the curvature of the degradation curves of log (rut) versus log (loadings), in an HWTD test, third-degree polynomials to the degradation paths, called the cubic model, can be fitted.

The following form of equation denotes the cubic model, where Y denotes the log-transformed, rut-depth values and L represents the log-transformed number of load repetitions as shown in Equation (2.5):

$$Y = \beta_0 + \beta_1 L + \beta_2 L^2 + \beta_3 L^3 + e_{ij} \quad (2.5)$$

Parameters β_0 , β_1 , β_2 , and β_3 are coefficients for the intercept, linear, quadratic, and cubic terms, respectively, and e_{ij} is the error term. This cubic model was considered in this study because of its superior residual behavior. Model choice and comparison can be done using the Akaike information criterion (AIC) and the Bayesian (Schwarz') information criterion (BIC). Both criteria utilize the log likelihood of the data, yet punish for the number of parameters in accordance with the parsimony principle. Smaller values of these criteria indicate better models.

CHAPTER 3 - OBJECTIVE 1: DEVELOPMENT OF CRITERIA FOR OUT-OF-SPECIFICATION PAVEMENTS

A flow chart of dissertation study along with modules involved is shown in Figure 3.1. At first, two main research problems were identified for Superpave mixtures. The first was to develop criteria to accept in-place deficient Superpave mixtures and the second was to develop accelerated mix testing models to help QC/QA of asphalt pavement construction. The first part of research will be discussed in this chapter and the second part of the research will be discussed in Chapter 4. To develop criteria to accept in-place deficient Superpave mixtures, nine mixtures were sampled from nine different projects; one project was located in each of KDOT's administrative districts III, IV, and VI; and two projects were located in each of KDOT's administrative districts I, II, and V for developing criteria to accept in-place deficient Superpave mixtures. Replicate cylindrical gyratory-molded test specimens were prepared at three different target air void levels (2%, 4%, and 7%) @ N_{design} gyrations and four simulated in-place density levels (87%, 89%, 91%, and 93%). Thus, the experiment involved a total of 108 set samples (3 air voids @ N_{design} x 4 simulated in-place density levels x 9 projects).

Similarly, for developing accelerated mix testing models, four mixtures were sampled from four different projects, each located in one KDOT administrative district and done by one contractor. Two mixtures with modified binders were selected from the project of the accelerated pavement testing (APT) program at the Civil Infrastructure Systems Laboratory (CISL) of Kansas State University. Samples were tested at two temperatures 50 °C and 60 °C (122 °F and 140 °F), and five load 705, 750, 795, 840, and 885 N (158, 168, 178, 188, and 198 lbs) levels. Thus, the experiment involved a total of 60 sets (6 projects x 2 temperature levels x 5 load levels) of samples.

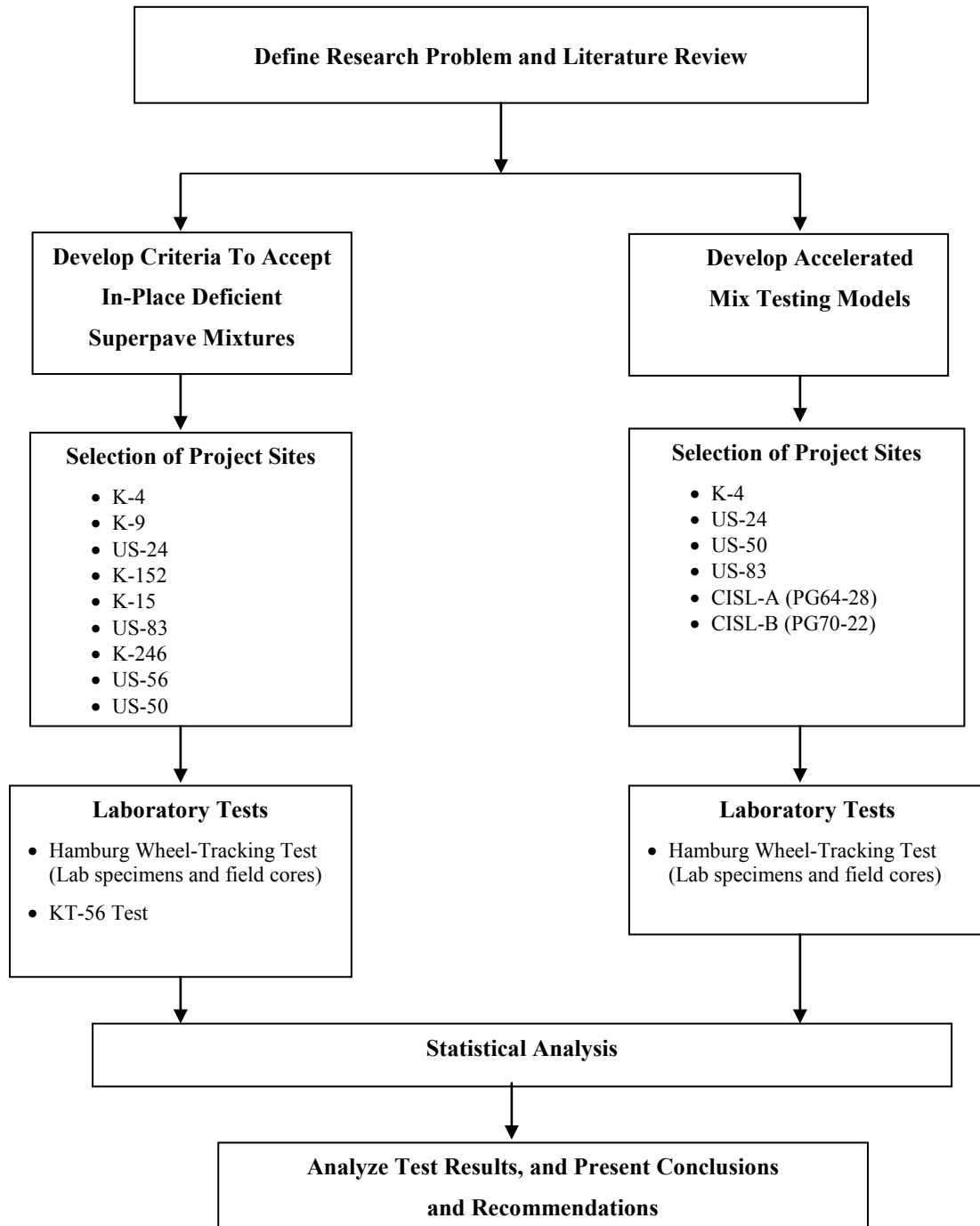


Figure 3.1 Flow Chart of Research Methodology

Laboratory tests were done for both cases using HWTD tests, followed by using field core testing for comparison of laboratory-prepared samples with field cores. Kansas test procedure KT-56 was performed with the laboratory samples for finding out moisture susceptibility. In both cases, statistical analysis was done separately. After analyzing test results, conclusions and recommendations were presented.

The first objective of this research was to develop criteria for out-of-specification Superpave pavement. In this chapter, experimental design, test equipment, laboratory test results, statistical analysis, and mixtures from the field are discussed.

3.1 Experimental Design

To achieve the objective of this study, an experimental design was done based on available KDOT projects with all possible combinations. The statistical experiment was a randomized block design. Fine-graded Superpave mixtures with 12.5-mm (0.5-in.) nominal maximum aggregate size (NMAS) were used in this study. Mixtures were sampled from nine different projects; one project was located in each of KDOT's administrative districts III, IV, and VI; and two projects were located in each of KDOT's administrative districts I, II, and V. Each project was completed by a single contractor. Replicate gyratory-molded test specimens were prepared at three different target air void levels (2%, 4%, and 7%) @ N_{design} gyrations. In Kansas, current quality control specifications for construction require $4 \pm 2\%$ air voids @ N_{design} gyrations for a single sub lot of normally 750 tons. However, according to current KDOT QC/QA percent-within-limits (PWL) specifications for Superpave pavement construction, the lower specification limit (LSL) for air voids is 3% @ N_{design} and the upper specification limit (USL) is 5% @ N_{design} .

Four air void levels (7%, 9%, 11%, and 13%) were also selected and gyratory-molded cylindrical specimens prepared to simulate different compaction levels achieved in Superpave pavement construction corresponding to 93%, 91%, 89%, and 87% of theoretical maximum specific gravity (G_{mm}). According to current KDOT QC/QA PWL specifications for Superpave pavement construction, LSL for simulated in-place density is 91% for a design thickness of 50 mm (2 in.) or less and 92% for a design thickness of greater than 50 mm (2 in.). Thus, the experiment involved a total of 108 sets (3 target air voids @ N_{design} x 4 target simulated in-place density levels x 9 projects). Table 3.1 shows the characteristics of the mixtures obtained from the

projects for this study. The binder grade for all mixtures was PG 64-22. Asphalt content of the base design mixtures (4% air voids @ N_{design}) varied from 4.9% to 6.2%. Mixture properties reported in Table 3.1 were obtained from the mix design data. All properties satisfied Superpave and currently required KDOT criteria. In Figure 3.2, projects K-4 to US-50 are denoted by their routes. It is observed that one mixture (US-24, District III) had a much finer gradation compared to the others. Table 3.2 presents design single-point gradation data of aggregates of all projects. The 0.45 power chart in Figure 3.2 was prepared based on these data.

Table 3.1 Properties of Superpave Mixes for Life Estimation

Route	KDOT District	Design ESALs (millions)	N_{design}	Asphalt Content (%)	Air Voids (%) at N_{design}	VMA (%)	VFA (%)	Dust-Binder Ratio	% G_{mm} at N_{ini}	% G_{mm} at N_{max}
K-4	I	0.4	75	4.90	4.36	13.9	68	0.7	88.8	96.6
K-9	II	0.7	75	5.40	4.08	14.0	72	0.9	89.8	96.8
US-24	III	0.7	75	5.00	3.62	14.1	74	0.9	90.4	97.1
K-152	IV	0.7	75	6.25	4.15	13.7	70	0.8	87.2	97.3
K-15	V	1.2	75	5.30	4.40	14.1	67	1.2	89.5	96.5
US-83	VI	2.2	75	4.90	4.38	13.9	68	1.1	89.7	96.4
K-246	I	0.5	75	5.00	4.02	12.8	67	1.2	87.8	97.2
US-56	II	4.1	100	5.80	4.39	15.0	70	0.8	87.7	96.7
US-50	V	4.5	100	5.40	4.10	14.6	70	0.6	88.4	96.9

NOTES: ESALs = equivalent single-axle loads; VMA = voids in mineral aggregates; VFA = voids filled with asphalt; N_{ini} = initial number of gyrations; N_{max} = maximum number of gyrations.

3.2 Test Specimen Preparation

Target air voids at N_{design} were selected at 4% (base design), 2%, and 7%. Asphalt content corresponding to the target air voids of 4% at N_{design} was chosen from the project's mix design. Asphalt content at other target air voids was initially computed as

$$P_{b,\text{estimated}} = P_{b4\%} - (0.4 \times (V_{\text{req}} - 4\%)) \quad (3.1)$$

where $P_{b,estimated}$ = estimated percent binder (by mass) at target air voids other than 4% (design);

V_{areq} = required air voids; and

$P_{b4\%}$ = percent binder (by mass) corresponding to required 4% air voids.

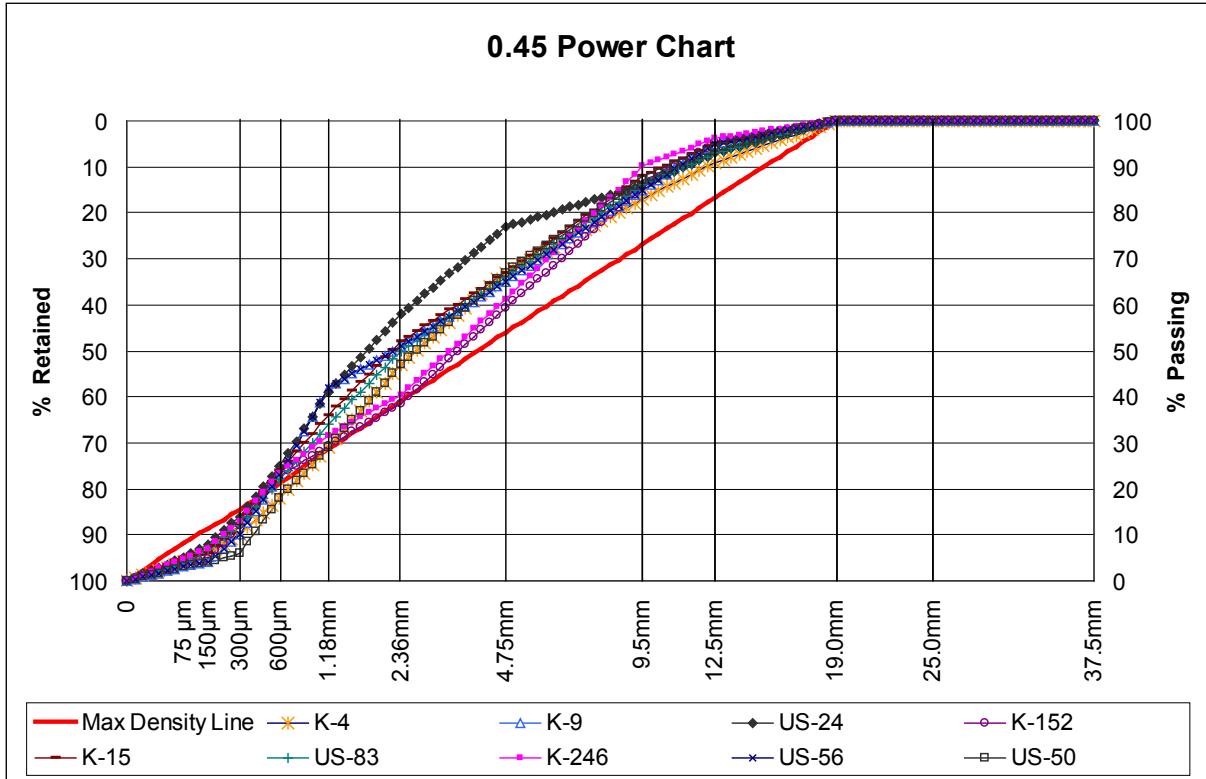


Figure 3.2 Aggregate Gradation of Mixtures

Later a trial mixture with this asphalt content was compacted to N_{design} level and the percent air void @ N_{design} was computed. Figure 3.3 shows project sites considered for estimation of lives of deficient Superpave pavements.

Table 3.2 Design Single-Point Gradation of Aggregates

Route	% Retained Materials on Sieve Size											
	37.5mm (1.5 in.)	25.0mm (1 in.)	19.0mm (3/4 in.)	12.5mm (1/2 in.)	9.5mm (3/8in.)	4.75mm (# 4)	2.36mm (# 8)	1.18mm (# 16)	600µm (# 30)	300µm (# 50)	150µm (#100)	75µm (#200)
Max. Density Line	0	0	0	0	12.1	36.1	52.8	65.4	74.5	81.3	86.4	90.2
K-4	0	0	0	9	17	33	53	71	82	90	94	96.0
K-9	0	0	0	8	13	24	45	64	78	90	94	95.7
US-24	0	0	0	7	14	23	42	59	75	86	92	94.9
K-152	0	0	0	5	14	41	61	71	77	88	95	96.4
K-15	0	0	0	5	12	33	48	64	76	88	94	95.2
US-83	0	0	0	7	14	34	50	66	78	88	93	95.9
K-246	0	0	0	4	10	39	60	68	77	87	93	95.3
US-56	0	0	0	5	15	35	49	58	77	90	96	97.1
US-50	0	0	0	6	13	33	53	71	82	94	96	96.9

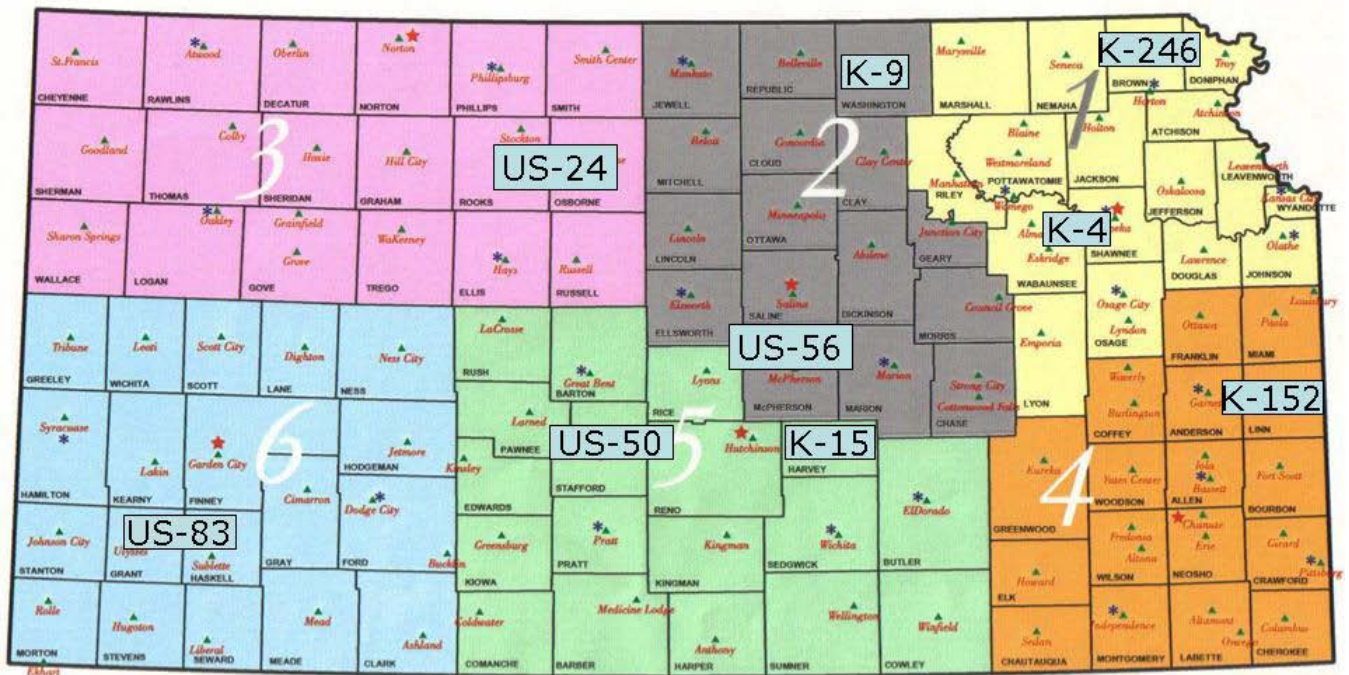


Figure 3.3 Project Sites for Estimation of Lives of Deficient Superpave Pavements

Test specimens were compacted with a Superpave gyratory compactor (SGC) as shown in Figure 3.4. Asphalt content was the only variable changed to get different target air voids @ N_{design} , since any change in gradation would insert another variable into the study and could affect other volumetric parameters. Also, in KDOT's QC/QA program for Superpave mixtures, the job-mix formula (JMF) allows $\pm 0.6\%$ variation in asphalt content.

Four final target air void levels (7%, 9%, 11%, and 13%) were chosen to represent target simulated in-place densities of 93%, 91%, 89%, and 87% of G_{mm} , respectively. These air voids were obtained using the compactive effort in the trial-and-error gyratory compaction of each mixture. Other than the District I mixture on K-4 and the District V mixture on K-15, simulated in-place density of 87% of G_{mm} could not be obtained. The samples would always compact to a level higher than this density.

For each mix, four replicate specimens for HWTD tests were compacted at the same target air void content (or density). Theoretical maximum specific gravity (G_{mm}) of the loose mixtures and bulk specific gravity (G_{mb}) of the compacted specimens were also determined. KDOT standard test methods KT-39 (AASHTO T209) and KT-15 (AASHTO T166) Procedure III were used to determine G_{mm} and G_{mb} , respectively (AASHTO 2001).

The theoretical maximum specific gravity was calculated using Equation (3.2):

$$G_{\text{mm}} = \frac{A}{A - C} \quad (3.2)$$

where

G_{mm} = theoretical maximum specific gravity;

A = mass of dry sample in air, g; and

C = mass of water displaced by sample at 25 °C (77 °F), g.



Figure 3.4 Superpave Gyrotory Compactor

The bulk specific gravity (G_{mb}) of a compacted asphalt mix specimen was determined by computing the ratio of its mass in air to its bulk volume as given in Equation (3.3).

$$G_{mb} = \frac{A}{B - C} \quad (3.3)$$

where

G_{mb} = bulk specific gravity of a compacted specimen;

A = mass of dry specimen in air, g;

B = mass of saturated surface-dry specimen in air, g; and

C = mass of saturated specimen in water, g.

Air voids in the compacted specimens were calculated using Equation (3.4):

$$\% \text{ AirVoids} = \frac{100 \times (G_{mm} - G_{mb})}{G_{mm}} \quad (3.4)$$

The air voids @ N_{design} of the SGC samples were found to vary from 1.0% to 6.0%, 1.0% to 6.8%, and 4.3% to 9.9% for target values of 2%, 4%, and 7%, respectively. These values were computed from the actual gyratory history of the companion plugs that had been compacted to the N_{design} level. Later, air voids were also computed from the extrapolated gyratory history of the samples compacted to the four target densities. The extrapolated air void values varied from 0 to 4.6%, 0 to 6.1%, and 0.3% to 8.6% for target values of 2%, 4%, and 7%, respectively. It is to be noted that both approaches in computation of air voids had limitations, such as accurate determination of bulk density for a specimen with high air voids (% saturation) or compaction of gyratory specimens with high asphalt content (Manandhar et al. 2008).

The simulated average densities obtained were 88% to 92.4%, 88.6% to 97.7%, 89.3% to 97.3%, and 91.1% to 96%, corresponding to target densities of 87%, 89%, 91%, and 93%, respectively. However, the coefficient of variation (COV) of the density of the replicate plugs for a given combination of air voids @ N_{design} and simulated in-place density were remarkably low. For the K-4 mixture in District I, the coefficient of variation varied from 0.19% to 0.46%. Since a few samples had air voids @ N_{design} varying from the target values 2%, 4%, and 7% target values were used in the statistical analysis and blocking was used on the air voids @ N_{design} treatment in the analysis of variance. The largest variation was usually seen for the 2% air voids at samples where very high binder content might have resulted in erratic G_{mb} values. HWTD, G_{mm} , and G_{mb} test results for development of criteria for out-of-specification pavements for each projects are presented in Appendix A.

3.3 Test Equipment

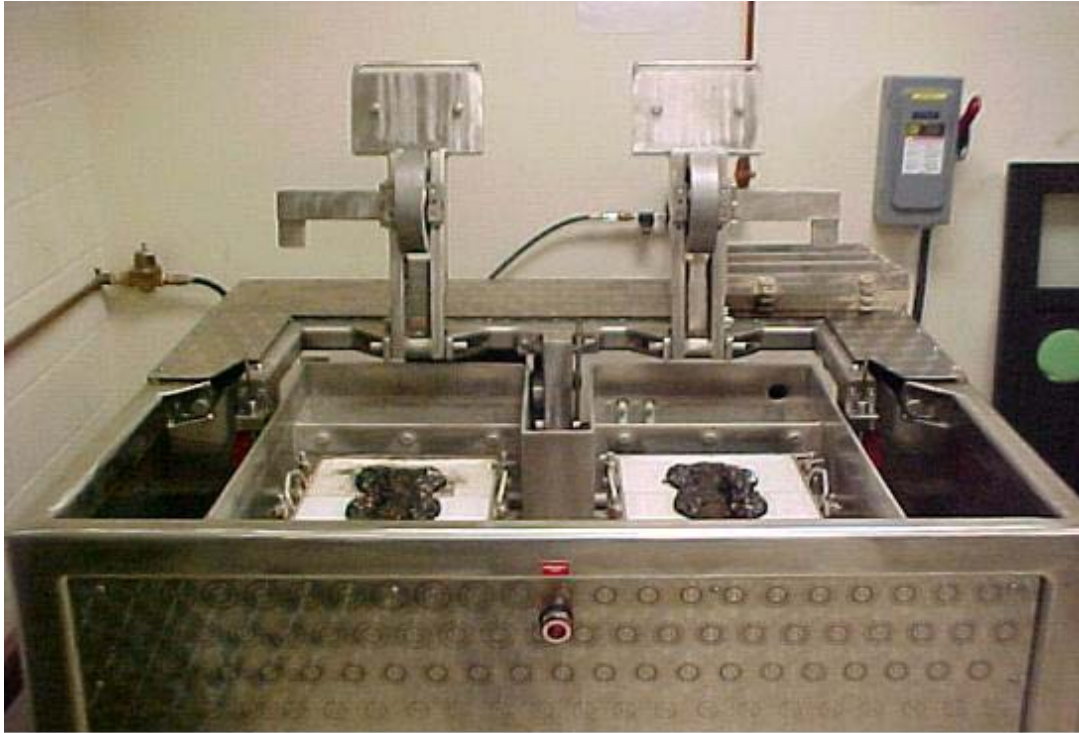
3.3.1 Hamburg Wheel-Tracking Device

As mentioned earlier, many highway agencies have been using loaded-wheel testers for accelerated evaluation of the rutting and stripping potential of designed mixes (Aschenbrener et

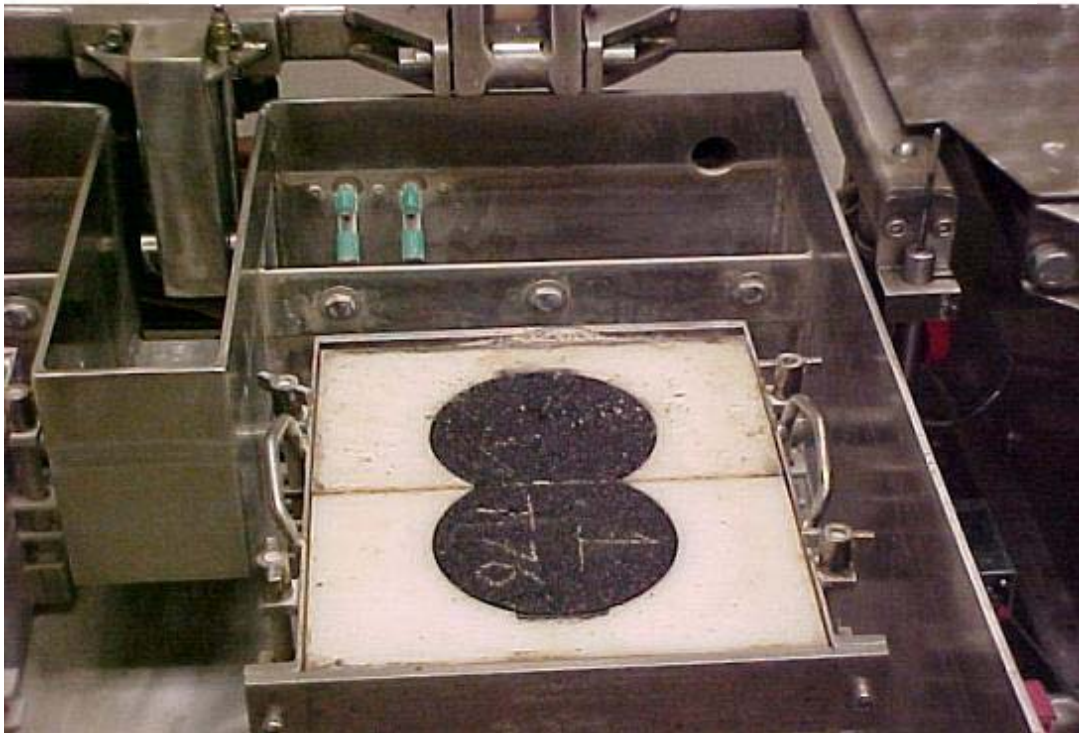
al. 1994; Aschenbrener 1995; Izzo and Tahmoressi 1999). Absence of a mechanical test for the Superpave volumetric mixture has also made this type of test very attractive for evaluating potentially undesirable mixtures. HWTD is one such device that can be used to predict both the rutting and stripping potential of asphalt mixes and has recently been used in a number of studies (Mohammad et al. 2007; Anguiar-Moya et al. 2007; Hrdlicka and Tandon 2007).

HWTD used in this study was manufactured by PMW, Inc. and is capable of testing a pair of samples simultaneously. Figure 3.5 (a) shows the HWTD at Kansas State University. The samples tested were 150-mm-diameter (6-in.-diameter) and 62-mm-tall (2.4-in.-tall) plugs fabricated by the SGC and placed together in special molds as shown in Figure 3.5 (b) following Texas Test Procedure Tex-242-F. The samples were submerged under water at 50°C. Each moving steel wheel of HWTD is 47 mm (1.85 in.) wide and 203.6 mm (8 in.) in diameter. Each wheel applied a load of 705 N (158 lb) and made 52 passes per minute. Each sample was loaded for 20,000 passes or until a 20-mm (0.8 in.) vertical deformation (rut depth) occurred at any point on the sample. Maximum wheel velocity reached was 340 mm/sec (13.4 in./sec), which occurred at the center of the sample. Around six hours were required to test for a maximum of 20,000 passes. Rut depth or deformation was measured at 11 different points along the length of each sample with a linear variable differential transformer (LVDT).

The parameters that can be interpreted from the HWTD test outputs are the number of passes to a 20-mm (0.8-in.) rut depth, creep slope, stripping slope, and stripping inflection point as depicted in Figure 3.6 (Aschenbrener 1995; Yildirim and Kennedy 2002). Creep slope relates to rutting from plastic flow and is the inverse of the rate of deformation in the linear region of the deformation curve, after post-compaction effects have ended and before the onset of stripping. Stripping slope is the inverse of the rate of deformation in the linear region of the deformation curve, after stripping begins and until the end of the test. It is the number of passes required to create a 1-mm (0.04-in.) impression from stripping, and is related to the severity of moisture damage (Aschenbrener and McGennis 1994, Aschenbrener et al. 1994).



(a) Hamburg Wheel-Tracking Device at KSU



(b) Test Samples

Figure 3.5 Hamburg Wheel-Tracking Device

The stripping inflection point is the number of passes at the intersection of the creep slope and the stripping slope, and is related to the resistance of the hot-mix asphalt to moisture damage. An acceptable mix is specified by the city of Hamburg to have less than a 4-mm (0.16-in.) rut depth after 20,000 passes at a 50 °C (122 °F) test temperature (Aschenbrener 1994; 1995; FHWA 2008).

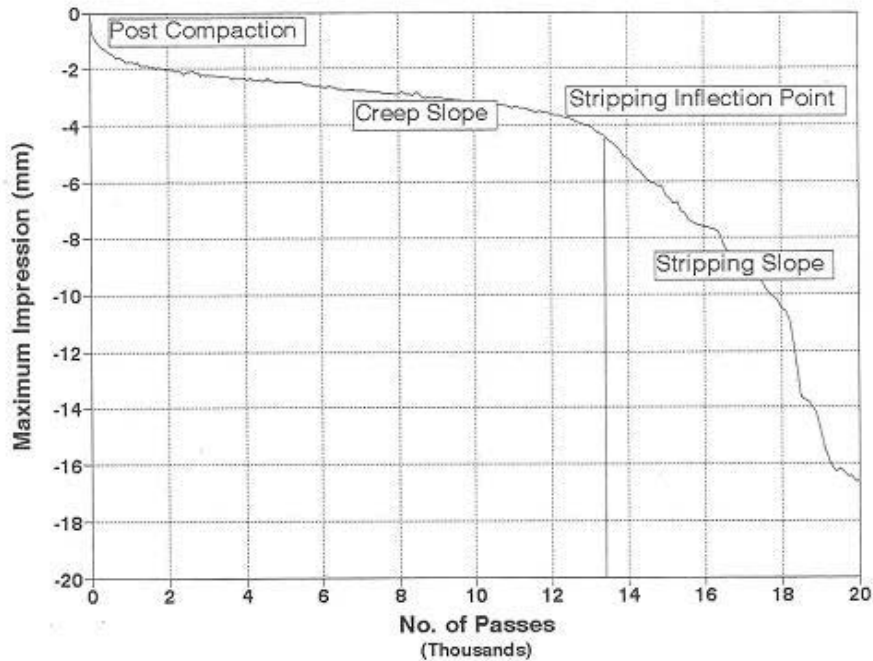


Figure 3.6 Interpretation of HWTD Results (Aschenbrener 1994)

Texas Department of Transportation (TxDOT) has criteria to terminate HWTD tests at a maximum of a 12.5-mm (0.5-in.) rut depth or 20,000 wheel passes, whichever comes first (Button et. al. 2004). TxDOT requirements of HMA for HWTD tests for various binder grades are given in Table 3.3. Colorado Department of Transportation (CDOT) has criteria of loading 20,000 passes or until 20-mm (0.8-in.) rut depth at 50 °C (122 °F).

Table 3.3 TxDOT Requirement of HMA for HWTD Test at 50 °C (122 °F)

High-Temperature Binder Grade	Minimum Number of Passes @ 12.5-mm (0.5-in.) Rut Depth
PG 64-XX	10,000
PG 70-XX	15,000
PG 76-XX or Higher	20,000

3.3.2 Marshall Stability Tester and KT-56 Test

A Marshall stability tester available, manufactured by Gilson Company, was used for testing resistance of a compacted bituminous mixture to moisture-induced damage (AASHTO T283, Kansas Test Method KT-56). This is also known as the modified Lottman test. The tester is a multi-loader frame (HM-386), also called a pro-loader, designed for multiple applications, along with the Marshall stability test component and digital readout unit. Figure 3.7 shows the Marshall stability tester. It has a frame capacity of 44.5 kN (10,000 lbf) and a ¾-hp DC motor to precisely regulate strain rate to $\pm 1\%$ of set point.

Specimen Preparation for KT-56 Test:

- At least six SGC-compacted specimens were prepared for each test with air voids of $(7 \pm 0.5)\%$. The specimens were 150 mm (6 in.) in diameter and approximately (95 ± 5) mm (3.7 ± 0.2) in.) thick.
- After compaction, the specimens were allowed to age at room temperature of 25 ± 3 °C (77 ± 5) °F, for 24 ± 1 hr before continuing the test.
- Theoretical maximum specific gravity of the loose mixture (G_{mm}) using KT-39 and bulk specific gravity of the compacted plugs (G_{mb}), using KT-15 procedure III, were computed. Then, air voids of the specimens were calculated.
- Thickness and diameter of the specimens were measured to the nearest 0.01 mm (0.001 in.).

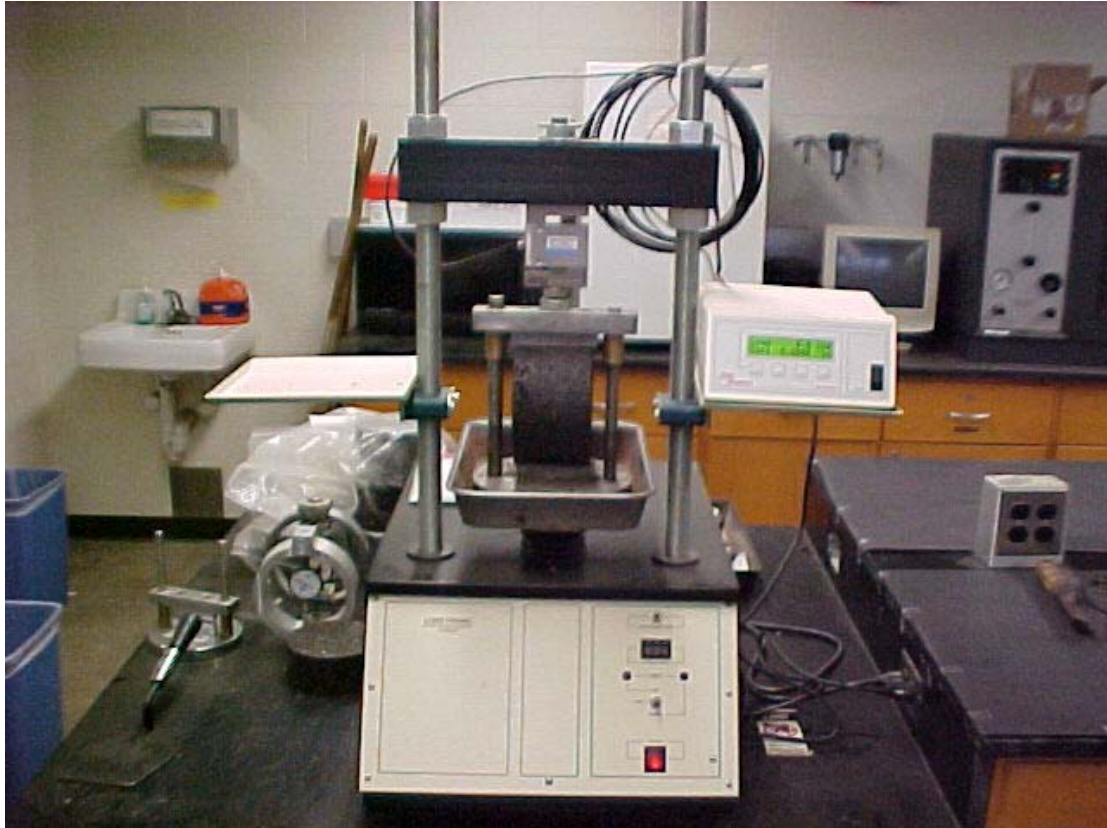


Figure 3.7 Marshall Stability Tester

- Two subsets of three specimens were sorted out, maintaining approximately equal average air voids in each subset.
- The two subsets were the unconditioned subset and the conditioned subset.

Unconditioned subset: Specimens were stored at room temperature; thickness and diameter were measured; on the day of testing, specimens were placed in plastic cylindrical molds and placed in a $25 \pm 0.5^\circ\text{C}$ ($77 \pm 1^\circ\text{F}$) water bath for $2 \text{ hrs} \pm 10 \text{ min}$. The specimens were then ready to be tested with the Marshall stability tester using the indirect tensile test.

Conditioned subset: Specimens were placed in a vacuum container, supported by a perforated base plate filled with potable water to at least 25 mm (1 in.) above the specimen. A partial vacuum was applied for a short time, saturating specimens so that 70-80% of the volume of the air voids was filled with water. The vacuum-saturated specimens were tightly covered with plastic wrap, and each wrapped specimen was placed in a plastic zip-lock bag containing 10 ml of water and sealed. The bags were placed into a freezer at $-18 \pm 3^\circ\text{C}$ ($0 \pm 5^\circ\text{F}$) within two minutes and left for a minimum of 16 hours. They were removed from the freezer, after

removing plastic, frozen samples were placed into a $60 \pm 1 \text{ }^\circ\text{C}$ ($140 \pm 2 \text{ }^\circ\text{F}$) water bath for 24 ± 1 hr. Conditioned specimens were removed one at a time from the water bath and damp-dried quickly.

Saturated surface-dry (SSD) mass was recorded, and they were placed into a $25 \pm 0.5 \text{ }^\circ\text{C}$ ($77 \pm 1 \text{ }^\circ\text{F}$) water bath and weighed in the water; weight was recorded as soon as it stabilized. Final height and diameter of the specimens were determined prior to the indirect tensile test.

- Average tensile strength of the three unconditioned and three conditioned specimens were calculated.
- Tensile strength ratio (%TSR) was computed by dividing the average conditioned strengths by the average of the unconditioned strengths and multiplying by 100%.

Tensile strength can be calculated using Equations (3.5) or (3.6) as shown below:

$$S_t(\text{Metric}) = \frac{2,000(P)}{\pi(t)(D)} \quad (3.5)$$

$$S_t(\text{English}) = \frac{2(P)}{\pi(t)(D)} \quad (3.6)$$

where S_t = tensile strength, kPa (psi);

P = maximum load, N (lbf);

t = specimen thickness, mm (in.); and

D = specimen diameter, mm (in.).

$$\text{Percent Tensile Strength Ratio (\%TSR)} = \frac{100(S_2)}{S_1}$$

where S_1 = average tensile strength of dry subset; and

S_2 = average tensile strength of conditioned subset.

Note that if an anti-stripping agent needed to be used in any mix, it should be mixed with asphalt mixtures for both conditioned and unconditioned subsets of that mix (Hossain et al. 2008; Lottman 1978; 1982).

3.4 Laboratory Test Results

3.4.1 HWTD Test Results

Table 3.4 shows the average number of wheel passes of the HWTD test to reach a 20-mm (0.8-in.) rut depth. The best-performing mixtures were those with 4% and 7% air voids at N_{design} level and final simulated in-place densities of 91% or 93% of G_{mm} . In a number of cases, these mixtures did not reach the failure condition (as indicated by 20,000 passes in Table 3.4 for K-4, K-15, US-50, and US-83). The effect of higher simulated in-place density on better performance up to the certain limit (91-93 %) was evident for almost all mixtures. Percents asphalt content used in each project at various air voids levels are also shown in the same table. High frequency of higher number of wheel passes occurred at simulated in-place density of 91% and 93%. HWTD test results in both (left and right) wheel passes are shown in Appendix A. Similarly, G_{mm} and G_{mb} , simulated in-place densities and air voids for each sample, were tested and computed and are presented in Appendix A.

Table 3.5 shows output parameters (creep slope, stripping slope, and stripping inflection point) of the mixtures under test. Trends in these parameters closely follow those shown by the total number of passes to a 20-mm (0.8-in.) rut depth. Considering all output parameters, the worst-performing mixtures, even when higher in-place densities were obtained, were those with 2% target air voids. It is to be noted that these mixtures had asphalt contents higher than the optimum. Other research has shown similar results. During the first test-track study at the National Center for Asphalt Technology (NCAT), the sections with mixes designed at 0.5% asphalt content above the optimum had the greatest rutting of all 26 tangent test sections (Brown et al. 2002).

Table 3.4 Summary of Hamburg Wheel-Tracking Device Test Results (Average number of wheel passes to a 20-mm rut depth)

Route	KDOT District	% Target Air Voids @ N _{design}														
		2					4					7				
		% Target Simulated In-Place Density				% AC	% Target Simulated In-Place Density				% AC	% Target Simulated In-Place Density				% AC
		87	89	91	93		87	89	91	93		87	89	91	93	
K-4	Dist. I	6,555	10,735	10,350	12,330	5.3	8,855	8,000	20,000	13,700	4.9	9,160	10,755	17,900	15,125	4.1
K-9	Dist. II	N/A	4,900	3,910	4,915	6.0	N/A	6,830	9,435	5,230	5.4	N/A	7,750	8,090	9,990	4.5
US-24	Dist. III	N/A	7,215	12,160	13,065	5.6	N/A	6,800	17,470	17,625	5.0	N/A	10,270	12,660	13,815	4.0
K-152	Dist. IV	N/A	4,870	7,025	8,040	6.75	N/A	3,745	8,300	11,565	6.25	N/A	7,655	14,790	12,460	5.0
K-15	Dist. V	5,850	8,830	7,005	11,585	6.1	6,075	10,810	8,125	19,755	5.3	9,680	18,280	20,000	20,000	4.5
US-83	Dist. VI	N/A	7,480	6,535	11,720	5.5	N/A	15,235	19,200	20,000	4.9	N/A	18,880	18,560	16,335	3.8
K-246	Dist. I	N/A	11,020	4,975	3,895	5.6	N/A	11,460	14,070	7,145	5.0	N/A	17,910	13,200	16,250	4.0
US-56	Dist. II	N/A	3,560	4,185	7,310	6.6	N/A	6,735	14,305	10,400	5.8	N/A	9,150	15,320	18,705	4.6
US-50	Dist. V	N/A	7,270	9,135	20,000	6.2	N/A	11,180	15,400	20,000	5.4	N/A	15,095	20,000	20,000	4.5

NOTES:

Values on the table are the number of wheel passes to a 20-mm (0.8-in.) rut depth;

Failure criteria: 20-mm (0.8-in.) maximum rut depth or 20,000 passes, whichever came first;

A liquid anti-stripping agent (0.25% - 0.5%) was used in Projects K-15, US-83, K-246, and US-83;

% AC means percent asphalt content used; and N/A means not available.

Figures 3.8 to 3.11 illustrate the comparison of the number of wheel passes to reach a 20-mm (0.8-in.) rut depth, creep slope, stripping slope, and stripping inflection point for the three different target air voids at N_{design} level and four different target simulated in-place densities for the K-4 project in District I. Comparative histograms of the number of wheel passes to reach a 20-mm (0.8-in.) rut depth, creep slope, stripping slope, and stripping inflection point for the three different air voids at N_{design} level and four different in-place densities for all projects are shown in Appendix B. It is obvious that the samples with 4% and 7% target air voids @ N_{design} performed similarly for all four parameters studied. These mixtures also performed similarly with respect to the number of wheel passes to reach a maximum 20-mm (0.8-in.) rut depth at almost all simulated in-place density levels.

Table 3.5 Summary of Hamburg Wheel-Tracking Device Test Results (Output Parameters)

Route	Parameter	% Target Air Voids @ N_{design}											
		2				4				7			
		% Target Simulated In-Place Density				% Target Simulated In-Place Density				% Target Simulated In-Place Density			
		87	89	91	93	87	89	91	93	87	89	91	93
K-4	Creep	483	1,010	1,440	1,463	853	1,003	2,360	1,693	1,017	1,322	2,578	1,774
	SIP	3,500	3,550	5,100	5,351	5,150	4,350	10,400	6,950	6,000	6,750	9,301	5,600
	Stripping	296	610	355	477	300	273	799	497	256	293	638	591
K-9	Creep	N/A	677	265	453	N/A	1,440	1,140	674	N/A	1,550	1,781	2,446
	SIP	N/A	2,050	1,450	2,500	N/A	4,400	5,850	2,100	N/A	3,900	4,700	4,800
	Stripping	N/A	244	165	196	N/A	260	188	209	N/A	265	257	332
US-24	Creep	N/A	473	1,440	1,219	N/A	602	2,137	2,795	N/A	1,839	2,432	2,189
	SIP	N/A	981	6,601	8,051	N/A	2,601	10,151	10,601	N/A	6,450	7,001	6,601
	Stripping	N/A	482	444	442	N/A	355	867	793	N/A	390	477	553
K-152	Creep	N/A	254	472	463	N/A	301	287	769	N/A	447	1,304	823
	SIP	N/A	1,050	1,451	1,451	N/A	1,101	981	2,351	N/A	1,951	6,051	5,701
	Stripping	N/A	303	451	573	N/A	313	461	792	N/A	470	572	753
K-15	Creep	450	610	445	692	361	824	610	1,511	906	1,916	3,057	1,995
	SIP	2,200	5,050	2,550	2,550	1,550	6,150	1,750	12,400	3,400	8,250	17,800	4,650
	Stripping	340	512	372	505	386	624	398	1,043	541	1,121	968	8,793
US-83	Creep	N/A	295	231	705	N/A	433	2,658	2,708	N/A	1,677	1,351	2,719
	SIP	N/A	1,451	1,151	5,501	N/A	1,601	10,851	11,401	N/A	11,151	8,751	7,701
	Stripping	N/A	573	421	729	N/A	960	1,067	2,072	N/A	1,244	2,831	896
K-246	Creep	N/A	1,021	321	464	N/A	1,082	1,837	1,012	N/A	2,693	2,818	3,720
	SIP	N/A	6,950	1,450	1,800	N/A	7,600	8,700	3,450	N/A	12,750	9,650	12,400
	Stripping	N/A	390	294	148	N/A	318	405	249	N/A	490	237	233
US-56	Creep	N/A	437	594	1,103	N/A	1,026	1,737	1,773	N/A	1,511	3,238	6,000
	SIP	N/A	1,650	1,800	3,450	N/A	3,300	4,850	5,500	N/A	5,650	7,950	10,500
	Stripping	N/A	179	151	243	N/A	248	564	398	N/A	279	550	783
US-50	Creep	N/A	399	383	3,822	N/A	673	1,261	9,518	N/A	2,067	9,504	9,787
	SIP	N/A	2,550	1,750	4,150	N/A	5,850	9,050	10,550	N/A	7,500	9,600	7,850
	Stripping	N/A	250	337	9,264	N/A	405	349	7,115	N/A	373	11,918	15,062

NOTES: Creep = creep slope; SIP = stripping inflection point; Stripping = stripping slope; and N/A = not available.

However, the samples with 2% air voids @ N_{design} consistently performed the worst. Creep and stripping slopes (passes per mm of rut depth) for the 2% air void samples also indicate that these mixtures are susceptible to both accelerated rutting and stripping failure. Only for 2% air voids @ N_{design} , did the number of wheel passes increase as simulated in-place density increased from 87% to 93%. For 4% and 7% air voids @ N_{design} level, the number of wheel passes increases as simulated in-place density increases from 87% to 91% and decreased at 93% simulated in-place density level. This indicates the optimum, high-performing simulated in-place density falls in between 91% and 93%. KDOT pay factor also considers 92% in-place density as the criteria of full-pay. Contractors will get penalized for in-place density below 92%.

The higher stripping inflection point values for the 4% and 7% air void samples also suggest that these samples are more resistant to moisture damage compared to others at any simulated in-place density levels.

Figures 3.12 to 3.14 show comparative HWTD test result plots for 2%, 4%, and 7% air voids @ N_{design} , respectively. Comparative HWTD test result plots for other projects are presented in Appendix C. In the past, Superpave mixtures compacted to 7% air voids performed better than the mixtures compacted at 9% air voids (Gogula et al. 2003).

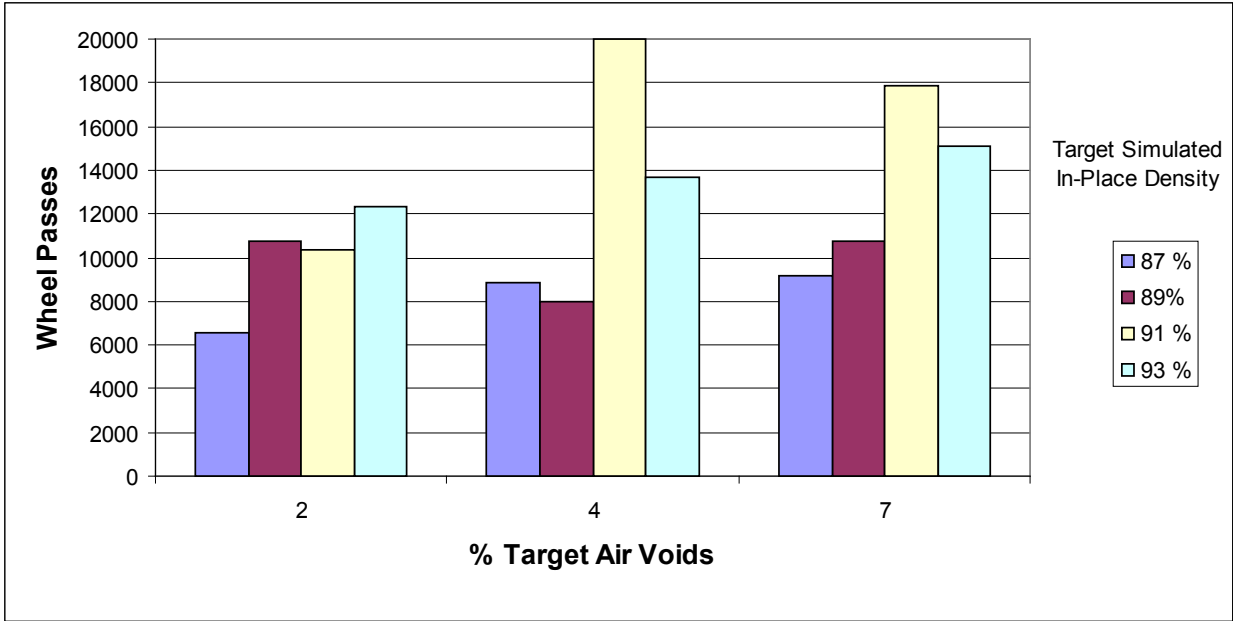


Figure 3.8 HWTD Wheel Passes Results for K-4 Project with Target Simulated In-Place Densities and Target Air Voids @ N_{design}

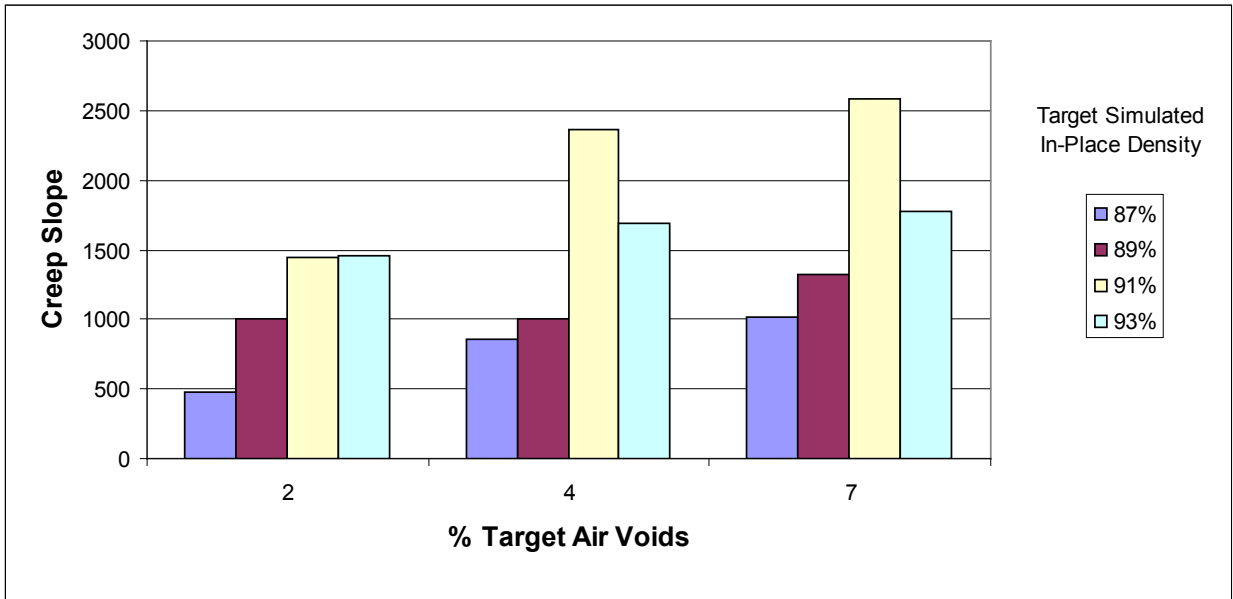


Figure 3.9 HWTD Creep Slope Results for K-4 Project with Target Simulated In-Place Densities and Target Air Voids @ N_{design}

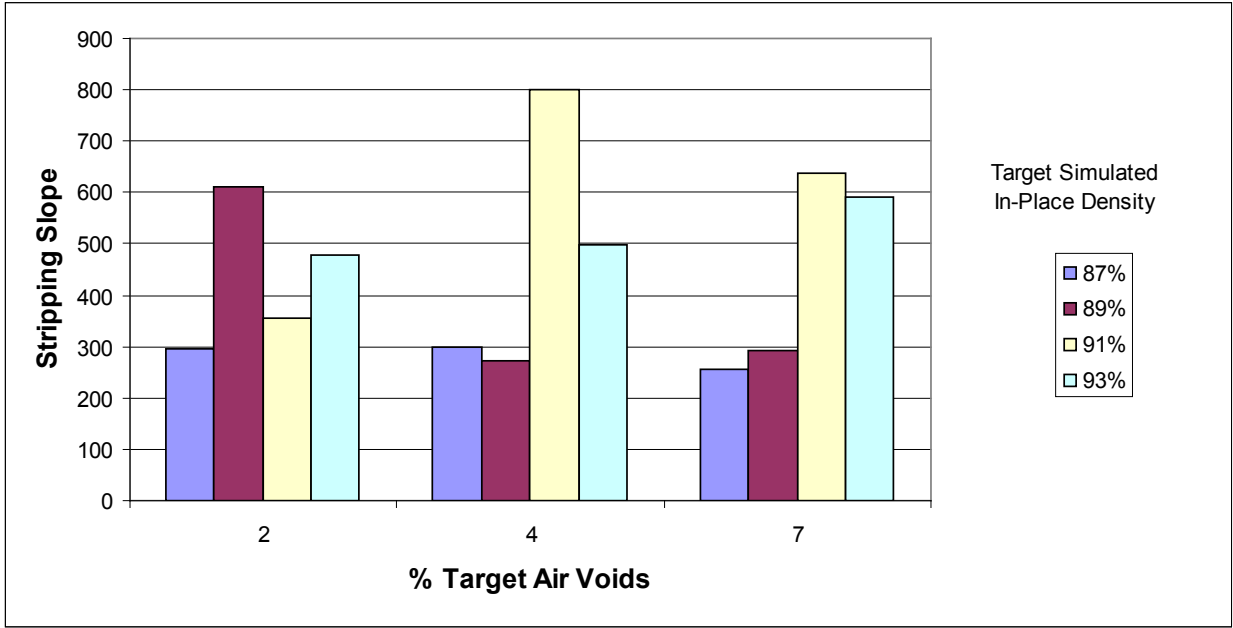


Figure 3.10 HWTD Stripping Slope Results for K-4 Project with Target Simulated In-Place Densities and Target Air Voids @ N_{design}

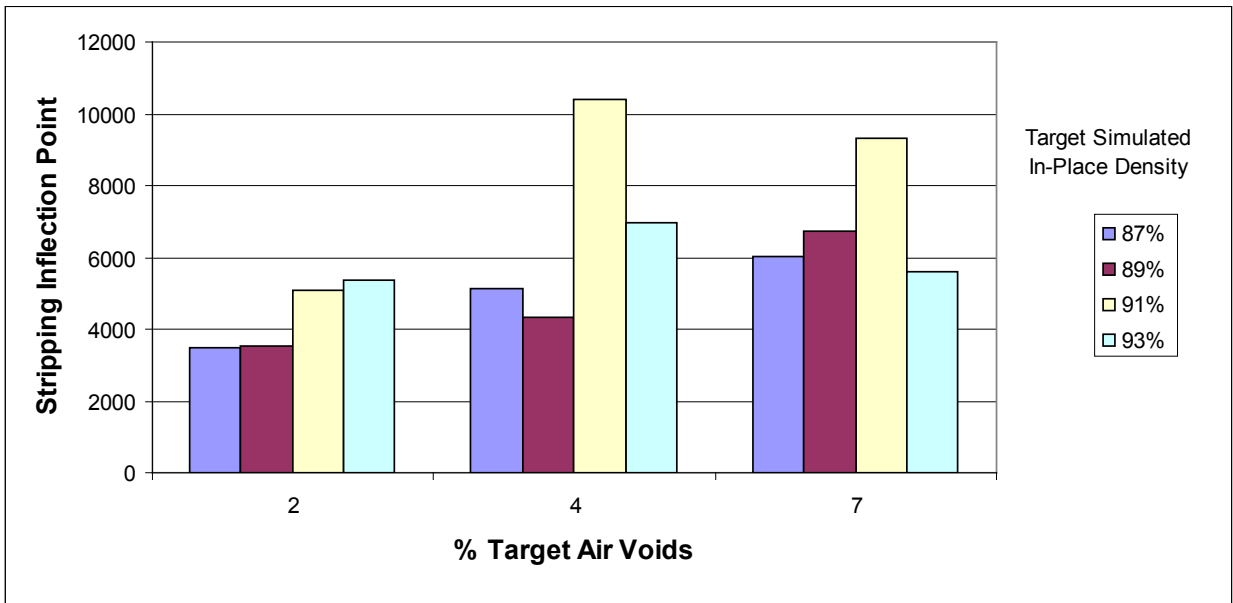


Figure 3.11 HWTD Stripping Inflection Points Results for K-4 Project with Target Simulated In-Place Densities and Target Air Voids @ N_{design}

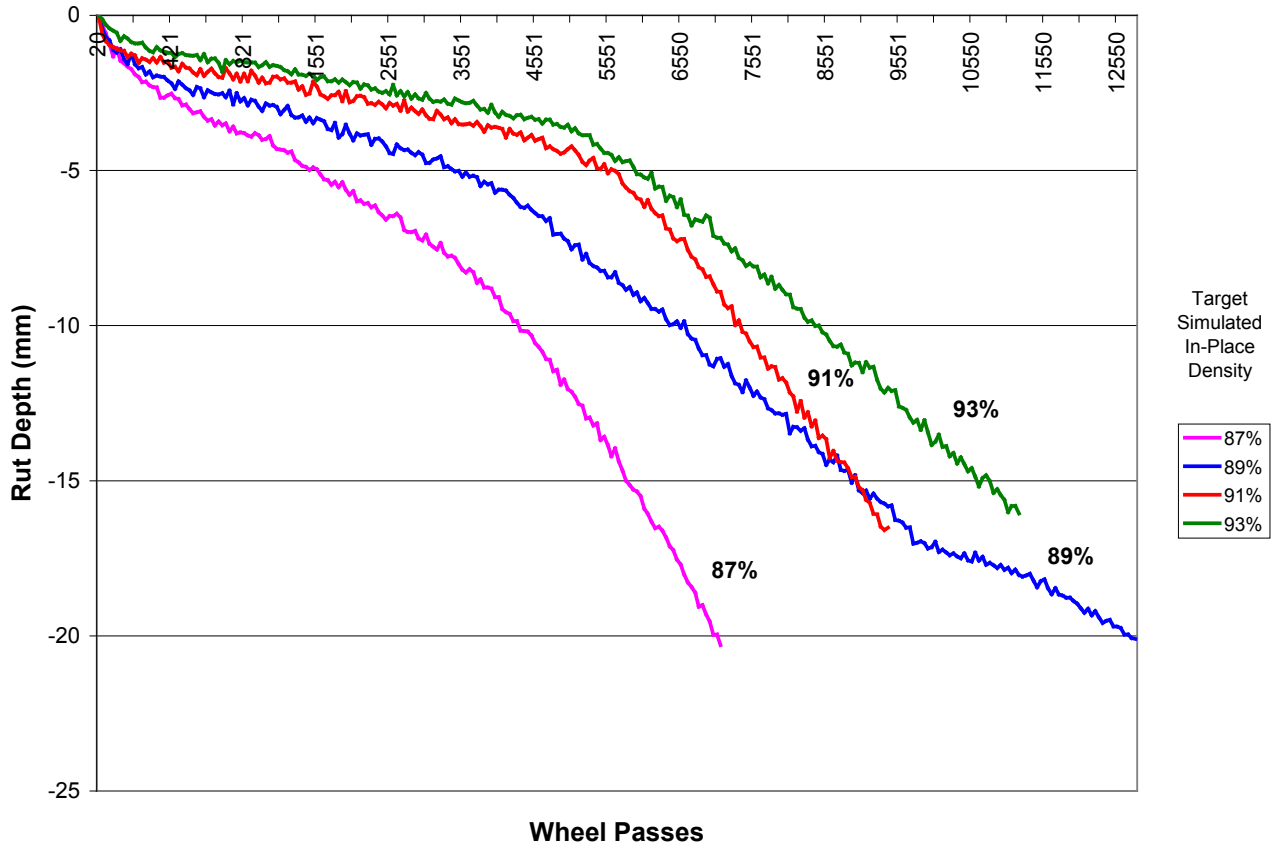


Figure 3.12 Comparative HWTD Test Results of K-4 Project at 2% Target Air Voids @ N_{design}

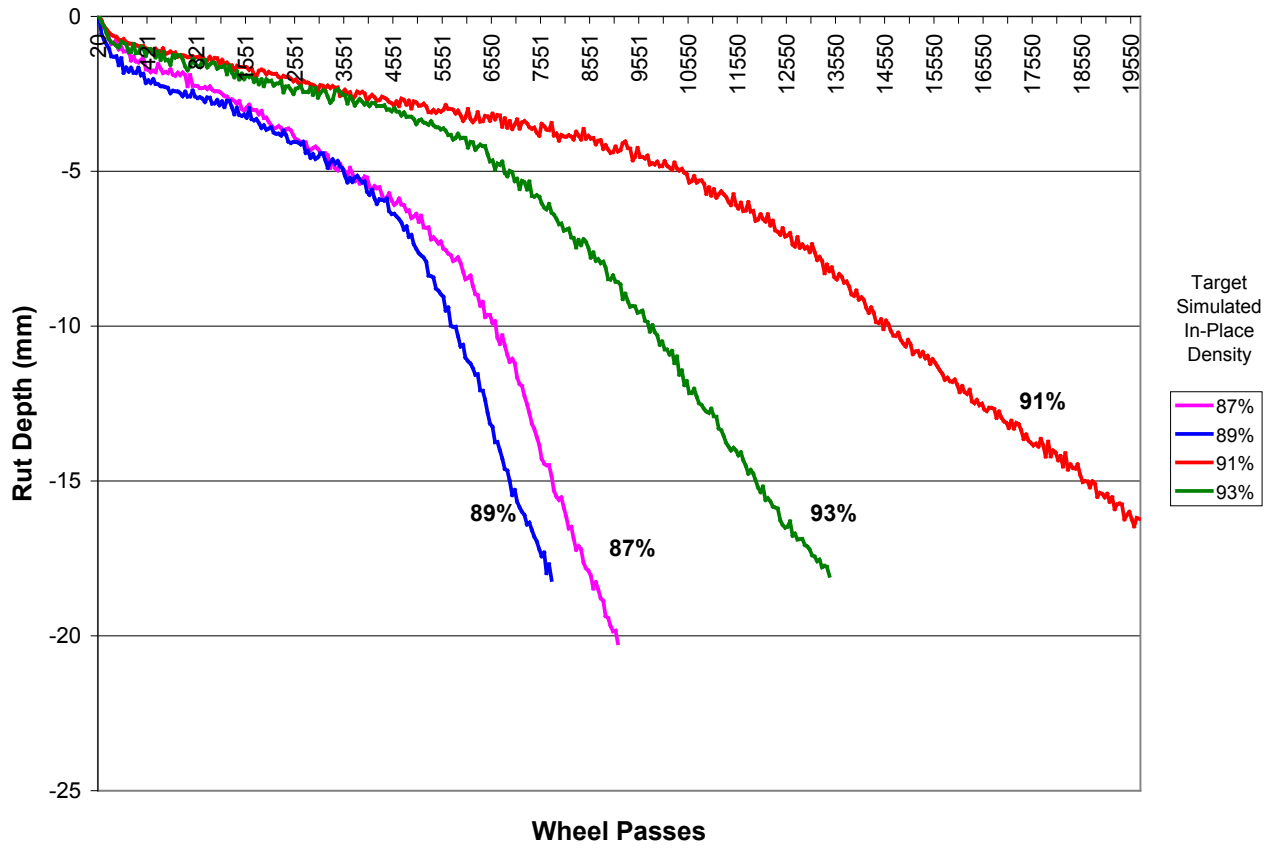


Figure 3.13 Comparative HWTD Test Results of K-4 Project at 4% Target Air Voids @ N_{design}

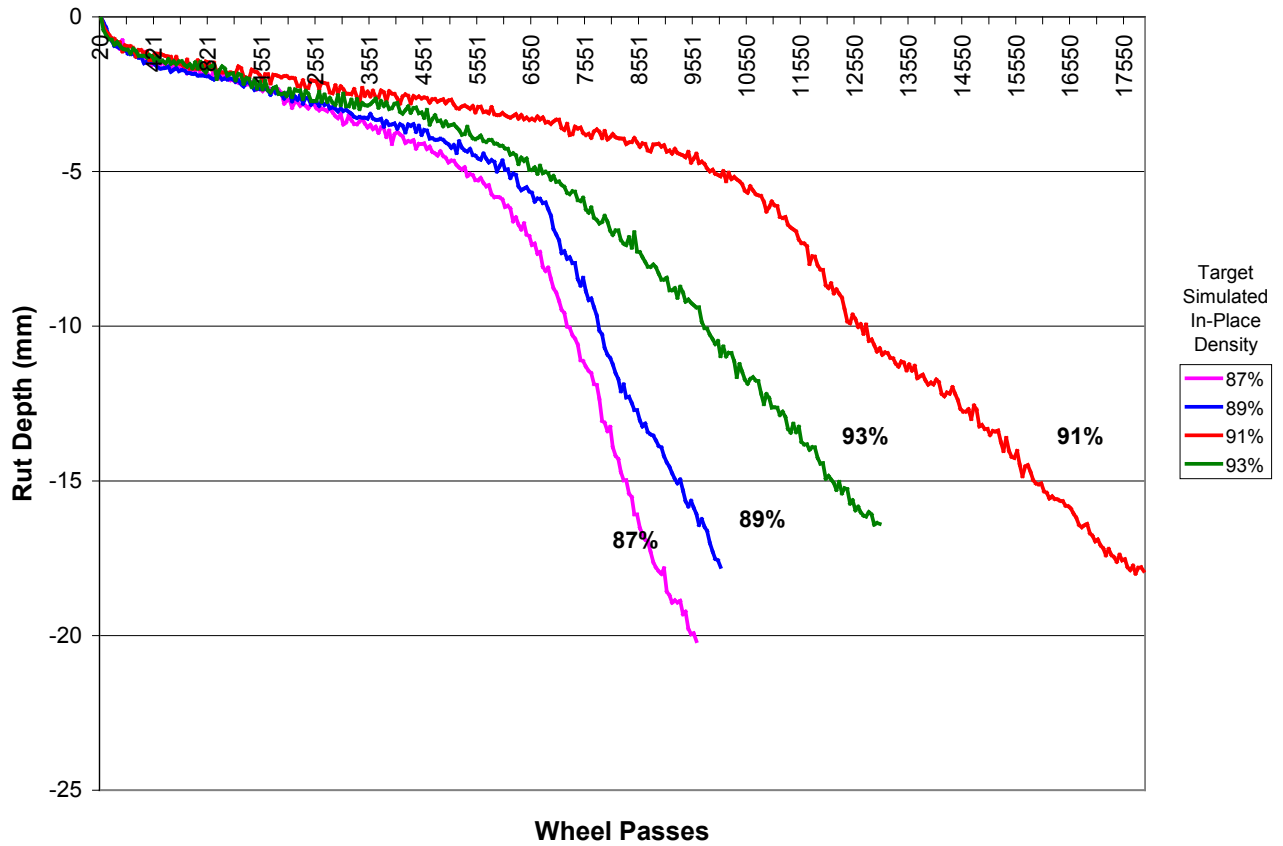


Figure 3.14 Comparative HWTD Test Results of K-4 Project at 7% Target Air Voids @ N_{design}

3.4.2 KT-56 Test Results

KDOT test procedure KT-56 (Lottman) was performed for each mix for 7% air voids @ N_{final} , and design KT-56 test results were taken from the design mix. Table 3.6 shows the results obtained from the KT-56 tests performed in laboratory and presented as actual % tensile strength ratio (TSR). According to current KDOT specifications, acceptable TSR value is 80% or more. Two mixes, K-246 project in District I, and US-50 project in District V, had TSR of less than 80%, which are failing results.

Table 3.6 Summary of KT-56 Test Results for Estimation of Life of Deficient Pavements

Route	KDOT District	Type and % Additive	% Asphalt Content	HWTD		% TSR	
				Left	Right	Design	Actual
K-4	I	None	4.9	20,000	20,000	82.0	86.7
K-9	II	None	5.4	10,240	8,630	85.5	87.7
US-24	III	None	5.0	16,220	18,720	88.8	98.6
K-152	IV	None	6.2	7,000	9,600	84.1	100.0
K-15	V	ARRMAZ HP ⁺ 0.25%	5.3	10,400	5,850	88.4	93.8
US-83	VI	AD-Here, 0.5%	4.9	18,400	20,000	88.2	100.0
K-246	I	ARRMAZ HP ⁺ 0.25%	5.0	13,240	14,900	80.4	74.0
US-56	II	LA-2, 0.3%	5.8	8,610	20,000	81.9	83.0
US-50	V	None	5.4	15,490	15,310	93.2	65.2

3.5 Statistical Analysis

3.5.1 Influence of Air Voids @ N_{design} and Simulated In-Place Density

The effect of mixture air voids @ N_{design} and simulated in-place density on the Superpave mixture performance was studied using the analysis of variance (ANOVA) technique and SAS software (SAS User's Guide). The statistical experiment analyzed was a randomized block experiment with blocking on air voids. This was necessary because of the variations in the air voids @ N_{design} obtained in the experiment. The general linear models (GLM) procedure ANOVA was performed using the least-square means (LSMeans) approach (Kuehl 2000) to test the effect of different factors on the dependent (response) variable.

In this research, four response variables were studied: (a) number of wheel passes to reach a 20-mm (0.8-in.) maximum rut depth, (b) creep slope, (c) stripping slope, and (d) stripping inflection point. The generalized linear model is shown in Equation (3.7):

$$RV = \beta_0 + \beta_1 AirVoid + \beta_2 Density + \beta_3 AirVoid \times Density + \varepsilon \quad (3.7)$$

where RV = various response variables studied;
 $Air Void$ = air voids @ N_{design} ;
 $Density$ = simulated in-place density (as compacted density);
 $Air Void \times Density$ = interaction of air voids and density;
 $\beta_0, \beta_1, \beta_2, \beta_3$ = coefficients; and
 ε = error term.

The analysis was done individually for each district and then by combining data for all districts for statewide model. Since contractors in a given district tend to use aggregates from certain quarries, the district-wise analysis was expected to explain some of the trends in the output. Analysis was also conducted with a slight variation of the model in Equation (3.7), where the interaction term between the air void and density was neglected. It was presumed that this would improve the estimation of the error term used in the analysis.

Table 3.7 shows the summary of statistical analysis for the variables studied with the probability of level of significance at 5 % and 10 %. A p-value is a measure of the extent at which data contradict a given hypothesis, denoted by H_0 . The smaller the p-value, the stronger the evidence provided by the given data against H_0 . It appears that for most mixtures, air voids @ N_{design} and simulated in-place density had a significant effect on the average number of wheel passes to 20-mm (0.8-in.) rut depth. Simulated in-place density and target air voids @ N_{design} have significant effects on average creep slope and average stripping slope. This indicates that these parameters can be treated individually in the specifications like the PWL equations currently used in Kansas.

Results in Table 3.7 indicate that performance parameters, average stripping slope, and average number of wheel passes to a 20-mm rut depth of the US-24 mixture in District III in the HWTD were affected neither by the air voids @ N_{design} nor by the simulated in-place density.

This mixture design was further examined to address this issue. An examination of the composition of the US-24 mix shows that it had 16% crushed limestone, 49% crushed gravel, and 35% natural sand. It also had a negligible amount (0.6%) of fly ash as a mineral filler. The design asphalt (PG 64-22) content was 5%. The crushed gravel, imported from Nebraska, is known to be a very hard aggregate, which is also evident by the strong aggregate structure observed in the gyratory history. Slope of the gyratory graph (% G_{mm} vs. Log No. of gyration) from N_{design} (75) to N_{max} (115) is very flat. This aggregate structure might be the reason for the insensitivity of this mixture toward density and air voids when tested in the HWTD.

Table 3.7 Summary of Statistical Analysis for Estimation of Life of Deficient Superpave Pavements

Route	District	Parameter	Average Creep Slope			Average Stripping Inflection Point			Average Stripping Slope			Average Number of Wheel Passes		
			Estimate	p-value	Significant	Estimate	p-value	Significant	Estimate	p-value	Significant	Estimate	p-value	Significant
K-4	I	A	167.2	0.0244	*	574.0	0.0648	**	14.7	0.5573		-13,496.0	0.3744	
		D	211.0	0.0098	*	379.5	0.2160		50.4	0.0766	**	655.6	0.4094	
		AxD										157.7	0.3420	
K-9	II	A	-10,457.0	0.0455	*	481.7	0.1028	**	-967.5	0.1327		-21,800.3	0.2676	
		D	-586.2	0.0679	**	63.5	0.8907		-57.7	0.1549		-987.4	0.4224	
		AxD	116.5	0.0414	*				10.7	0.1273		245.4	0.2496	
US-24	III	A	360.7	0.0099	*	819.9	0.1783		-2,431.8	0.2888		-7156.1	0.8037	
		D	358.0	0.0313	*	1,394.8	0.0967	**	-63.8	0.5595		480.6	0.7588	
		AxD							26.9	0.2859		83.6	0.7906	
K-152	IV	A	142.7	0.0241	*	866.4	0.0151	*	63.8	0.0373	*	-9,611.4	0.8332	
		D	179.3	0.1129	**	710.3	0.2228		126.0	0.0410	*	1,683.4	0.5190	
		AxD										120.9	0.8068	
K-15	V	A	384.8	0.0013	*	1,588.6	0.0623	**	711.4	0.0866	**	-51,472.9	0.0063	*
		D	210.4	0.0710	**	1,142.0	0.2434		464.5	0.3320		299.0	0.6752	
		AxD										598.2	0.0042	*
US-83	VI	A	529.9	0.0874	**	1,728.7	0.1629		359.5	0.1108	**	-127,505.7	0.0663	**
		D	574.6	0.2800		1,131.8	0.5965		346.1	0.3715		-6,503.3	0.1440	
		AxD										1,381.6	0.0620	**
K-246	I	A	502.1	0.0039	*	-62,359.6	0.0778	**	-18.1	0.4385		-75,241.0	0.0123	*
		D	-0.8	0.9971		-4,984.1	0.0313	*	-68.4	0.1336		-6,089.2	0.0016	*
		AxD				695.3	0.0742	**				836.7	0.0113	*
US-56	II	A	749.5	0.0081	*	1,415.3	0.0002	*	-3,256.1	0.1165	**	-42,919.3	0.2384	
		D	564.8	0.1005	**	910.1	0.0118	*	-88.7	0.3700		-489.7	0.7963	
		AxD							36.5	0.1089	**	493.8	0.2147	
US-50	V	A	1,840.3	0.0023	*	1,233.4	0.0300	*	2,317.2	0.0086	*	71,479.5	0.0061	*
		D	2,541.9	0.0054	*	788.1	0.3127		3,758.8	0.0091	*	6,807.2	0.0002	*
		AxD										-762.3	0.0074	*
Statewide		A	426.0	< .0001	*	967.6	< .0001	*	286.4	0.0437		-11,000.2	0.2710	
		D	152.5	0.2103		261.7	0.2428		157.2	0.3780		223.9	0.6668	
		AxD										136.2	0.2112	

NOTES: * Significant at 5% level of significance; ** Significant at 10% level of significance;
A = Target air voids; D = Simulated-in-place density; and AxD = Interaction of air voids and simulated-in-place density.

3.5.2 Development of Life-Prediction Equation

Table 3.8 lists the equation parameters developed for all projects in this study in ANOVA. Pavement life is expressed in terms of number of repetitions to reach a 20-mm (0.8-in.) rut depth in the HWTD test. Independent variables in the model are simulated in-place density and air voids @ N_{design} . Interaction between these variables was also included, as it was found to increase the coefficient of determination (R^2) of the model and the results were found to be logically acceptable (somewhat gave a better fit by the interaction term). The best equation in terms of the highest R^2 was obtained for the US-50 mixture in District V. A poor fit was obtained for the US-24 mix in District III.

The statewide equation also has a very low R^2 value, indicating that no universal equation can be obtained for the Superpave mixture in terms of its performance in the HWTD test. This also implies that globally, the number of wheel passes of the HWTD to reach a 20-mm (0.8-in.) rut depth for these mixtures can not be explained only by the air voids and/or the simulated in-place density alone. This mixture behavior is also observed in real-life pavements. However, for other pavements, the relationship between laboratory-determined air voids and traffic is well established (Brown and Cross, 1992).

An example of estimation of life of a defective pavement can be illustrated using K-4 mixture data for District I. It was assumed that at 4% air voids @ N_{design} and 92% simulated in-place density (full-pay condition according to current KDOT QC/QA specifications), the number of passes of the HWTD to a 20-mm (0.8-in.) rut depth will be equal to the full life of the pavement. Using the model shown in Table 3.7, the number of passes of the Hamburg Wheel-Tracking Device to a 20-mm (0.8-in.) rut depth can be estimated at other in-place densities and air voids @ N_{design} . Then the percent of lives at those air voids and in-place densities can be computed by taking a ratio with respect to the wheel-load passes at 4% air voids @ N_{design} and 92% simulated in-place density as shown in Table 3.9. The estimated life, obtained this way, cannot be greater than 100%.

For example, the K-4 mixture in District I, 100% life, would correspond to 4% air voids @ N_{design} and 92% simulated in-place density.

Table 3.8 Models Derived for Estimating Life of Deficient Superpave Pavements

Route	District	Parameter	Description	Estimate	p-value	R ²
K-4	I	Intercept	Vertical Intercept	-52,172.1	0.4751	0.48
		A	Target Air Voids	-13,496.0	0.3744	
		D	Simulated In-Place Density	655.6	0.4094	
		A×D	Interaction of Air Voids and Density	157.7	0.3420	
K-9	II	Intercept	Vertical Intercept	94,518.2	0.4079	0.57
		A	Target Air Voids	-21,800.3	0.2676	
		D	Simulated In-Place Density	-987.4	0.4224	
		A×D	Interaction of Air Voids and Density	245.4	0.2496	
US-24	III	Intercept	Vertical Intercept	-33,376.7	0.8165	0.10
		A	Target Air Voids	-7,156.1	0.8037	
		D	Simulated In-Place Density	480.6	0.7588	
		A×D	Interaction of Air Voids and Density	83.6	0.7906	
K-152	IV	Intercept	Vertical Intercept	-153,923.6	0.5248	0.48
		A	Target Air Voids	-9,611.4	0.8332	
		D	Simulated In-Place Density	1,683.4	0.5190	
		A×D	Interaction of Air Voids and Density	120.9	0.8068	
K-15	V	Intercept	Vertical Intercept	-29,365.7	0.6572	0.80
		A	Target Air Voids	-51,472.9	0.0063	
		D	Simulated In-Place Density	299.0	0.6752	
		A×D	Interaction of Air Voids and Density	598.2	0.0042	
US-83	VI	Intercept	Vertical Intercept	618,386.4	0.1414	0.59
		A	Target Air Voids	-127,505.7	0.0663	
		D	Simulated In-Place Density	-6,503.3	0.1440	
		A×D	Interaction of Air Voids and Density	1,381.6	0.0620	
K-246	I	Intercept	Vertical Intercept	563,197.6	0.0015	0.84
		A	Target Air Voids	-75,241.0	0.0123	
		D	Simulated In-Place Density	-6,089.2	0.0016	
		A×D	Interaction of Air Voids and Density	836.7	0.0113	
US-56	II	Intercept	Vertical Intercept	45,013.6	0.7968	0.70
		A	Target Air Voids	-42,919.3	0.2384	
		D	Simulated In-Place Density	-489.7	0.7963	
		A×D	Interaction of Air Voids and Density	493.8	0.2147	
US-50	V	Intercept	Vertical Intercept	-614,106.5	0.0002	0.83
		A	Target Air Voids	71,479.5	0.0061	
		D	Simulated In-Place Density	6,807.2	0.0002	
		A×D	Interaction of Air Voids and Density	-762.3	0.0074	
Statewide		Intercept	Vertical Intercept	-15,475.1	0.7474	0.29
		A	Target Air Voids	-11,000.2	0.2710	
		D	Simulated In-Place Density	223.9	0.6668	
		A×D	Interaction of Air Voids and Density	136.2	0.2112	

The estimated parameters are taken from Table 3.7 as shown below:

$$\text{Vertical intercept } (\beta_0) = -52,172.1$$

$$\text{Target air voids @ } N_{\text{design}} (\beta_1) = -13,496$$

$$\text{Simulated in-place density } (\beta_2) = 655.6$$

$$\text{Interaction of air voids and density } (\beta_3) = 157.7$$

Given

$$\text{Air voids @ } N_{\text{design}} (A) = 4\%, \text{ and}$$

$$\text{Simulated in-place density } (D) = 92\%.$$

The number of Hamburg wheel passes to a 20-mm rut depth is equal to

$$\begin{aligned} \text{WP (A=4\%, D=92\%)} &= \beta_0 + \beta_1 A + \beta_2 D + \beta_3 A \times D \\ &= -52,172.1 - 13,496 \times 4 + 655.6 \times 92 + 157.7 \times 4 \times 92 \\ &= 12,193 \end{aligned}$$

The number of passes corresponding to 2% air voids @ N_{design} and 89% simulated in-place density can be calculated as below:

Given

$$\text{Air voids @ } N_{\text{design}} (A) = 2\%, \text{ and}$$

$$\text{Simulated in-place density } (D) = 89\%.$$

The number of Hamburg wheel passes to a 20-mm rut depth is equal to

$$\begin{aligned} \text{WP (A=2\%, D=89\%)} &= \beta_0 + \beta_1 A + \beta_2 D + \beta_3 A \times D \\ &= -52,172.1 - 13,496 \times 2 + 655.6 \times 89 + 157.7 \times 2 \times 89 \\ &= 7,255 \end{aligned}$$

Thus the life at 2% air voids @ N_{design} and 89% simulated in-place density is given by

$$\begin{aligned} &= (7,255/12,193) \times 100 \\ &= 60\% \end{aligned}$$

Potential loss of life due to the defective pavement = $(100-60)\% = 40\%$.

It is to be noted that the district-wise model was developed due to lack of transferability of the regression equation as found in the combined analysis of data for all districts. Also, as mentioned earlier, contractors in a given district tend to use aggregates from certain quarries. Thus the district-wise analysis should produce a model that may not be universally applicable but is practical for a given geographical area.

The last column in Table 3.9 tabulates the percent of lives that would potentially be lost due to stripping and rutting of the defective Superpave pavements. The results show that low air voids @ N_{design} significantly reduce the life of the Superpave pavement. The results also indicate that if the HWTD test is conducted on a mixture with 4% air voids @ N_{design} and 92% simulated in-place density, the deficient mixture life can be estimated by running HWTD tests on that mixture and taking a simple ratio of the two test results. Estimated life loss can then be calculated and negotiations for pay reduction can be started from that point.

This analysis was repeated with some nonlinear (quadratic) models, i.e. where the response variable, the number of the Hamburg wheel-load repetitions to failure, was a function of the square of the air voids @ N_{design} and/or the density. Although this improved the coefficient of determination (R^2) significantly, the models became extremely sensitive to the input values, and unrealistic values of the loss of life were calculated in some cases. Thus a linear model was chosen for the calculation of life of defective pavements.

Table 3.10 summarizes models derived for estimating life of defective Superpave pavement for all nine individual projects (district-wise) and a statewide model for all projects. The calculation for life of defective pavements based on the parameters developed for all projects and the statewide model are shown in Appendix D.

Table 3.9 Calculation of Life of Deficient Superpave Pavements of K-4 Project

Route	Parameter	Description	Estimate	R ²
K-4	Intercept	Vertical Intercept	-52,172.1	0.48
	A	Target Air Voids @ N _{design}	-13,496.0	
	D	Target Simulated In-Place Density	655.6	
	A×D	Air Voids × Density	157.7	
Wheel Passes = -52,172.1 - 13,496.0 A + 655.6 D + 157.7 A×D				
D	A	Wheel Passes	% Life	% Life Lost
88	2	6,284	52	48
88	4	7,047	58	42
88	7	8,192	67	33
89	2	7,255	60	40
89	4	8,333	68	32
89	7	9,951	82	18
90	2	8,226	67	33
90	4	9,620	79	21
90	7	11,711	96	4
91	2	9,197	75	25
91	4	10,906	89	11
91	7	13,470	100	0
92	2	10,168	83	17
92	4	12,193	100	0
92	7	15,230	100	0
93	2	11,139	91	9
93	4	13,479	100	0
93	7	16,989	100	0

Table 3.10 Models for Estimating Life of Deficient Superpave Pavements

Route	District	Life Models
K-4	I	Wheel Passes = $-52,172.1 - 13,496.0 A + 655.6 D + 157.7 A \times D$
K-9	II	Wheel Passes = $94,518.2 - 21,800.3 A - 987.4 D + 245.4 A \times D$
US-24	III	Wheel Passes = $-33,376.7 - 7,156.1 A + 480.6 D + 83.6 A \times D$
K-152	IV	Wheel Passes = $-153,923.6 - 9,611.4 A + 1,683.4 D + 120.9 A \times D$
K-15	V	Wheel Passes = $-29,365.7 - 51,472.9 A + 299.0 D + 598.2 A \times D$
US-83	VI	Wheel Passes = $618,386.4 - 127,505.7 A - 6,503.3 D + 1,381.6 A \times D$
K-246	I	Wheel Passes = $563,197.6 - 75,241.0 A - 6,089.2 D + 836.7 A \times D$
US-56	II	Wheel Passes = $45,013.6 - 42,919.3 A - 489.7 D + 493.8 A \times D$
US-50	V	Wheel Passes = $-614,106.5 + 71,479.5 A + 6,807.2 D - 762.3 A \times D$
Statewide		Wheel Passes = $-15,475.1 - 11,000.2 A + 223.9 D + 136.2 A \times D$

3.6 Mixtures from the Field

3.6.1 Field Coring and Testing

Field coring was done at three KDOT district projects (District I, III, and VI) with the help of KDOT coring crews. Samples were cored with a six-inch-diameter drilling bit. Cores were cut to make 62-mm (2.4-in.) thick HWTD samples. While coring, some samples were obtained with thickness less than 62 mm (2.4 in.). Plaster of Paris was used to make up the required thicknesses of the HWTD samples prior to testing. Samples from two cores of each project were used to determine maximum theoretical specific gravity (G_{mm}) of the loose asphalt mix. All cores were tested for bulk specific gravity (G_{mb}). Air voids of each sample were computed prior to its testing under HWTD at a standard load of 705 N (158 lbs) and temperature of 50 °C (122 °F). The records of G_{mm} , G_{mb} and air voids for each core are presented on Appendix-E.

3.6.2 HWTD Test Results and Field Verification

Table 3.11 shows the comparison of average number of wheel passes in HWTD tests for Districts I, III, and VI. Figure 3.15 shows the comparison between predicted repetitions at target simulated in-place density of 93% and air void @ N_{design} of 4%, and HWTD test results for samples from field cores. Results indicate that HWTD results of the field cores for ideal construction situations correlates very well with the actual field sample.

Table 3.11 HWTD Test Results of Laboratory Samples with Field Cores

Route	District	No. of Repetitions to 20-mm (0.8-in.) Rut Depth	
		Predicted	Field-Cored Sample
K-4	I	13,479	17,290
K-258	III	13,794	14,270
US-83	VI	17,512	15,210

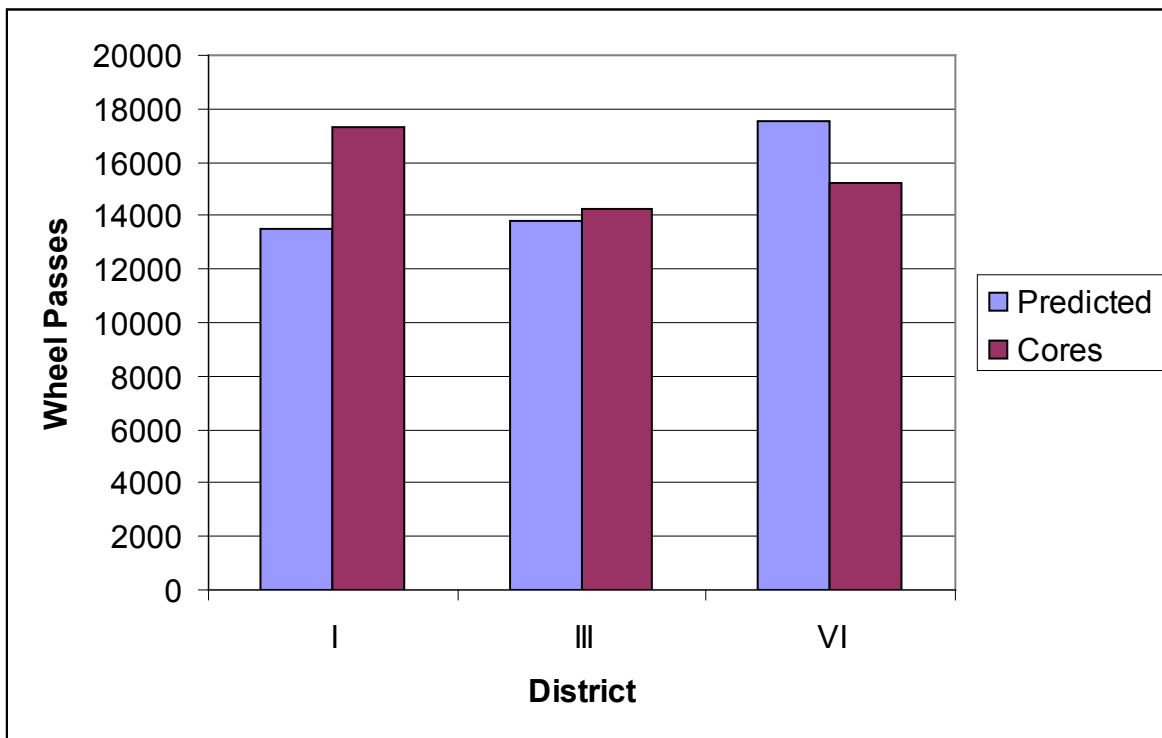


Figure 3.15 Comparison of HWTD Test Results of Laboratory Samples with Field Cores

CHAPTER 4 - OBJECTIVE 2: DEVELOPMENT OF LABORATORY-BASED ACCELERATED MIX TESTING MODELS

The second objective of this research was to develop laboratory-based accelerated mix testing models using Hamburg Wheel-Tracking Device (HWTd) test results. This chapter discusses about experimental design, preparation of test specimens, HWTd, laboratory test results, statistical analysis, and mixtures from the field and their test results.

4.1 Experimental Design

Six fine-graded Superpave mixtures with 12.5-mm (0.5-in.) NMAS were selected for this study. Four mixtures were sampled from four different projects, each located in one KDOT administrative district and done by one contractor. Two mixtures with modified binders were also selected from the pavements of the accelerated pavement testing (APT) program at the Civil Infrastructure Systems Laboratory (CISL) of Kansas State University. Replicate test specimens were prepared at target air void of 4% @ N_{design} gyrations. Simulated in-place density of 93% of the theoretical maximum specific gravity (G_{mm}) was taken (i.e. in-place air voids of 7%) for the Superpave gyratory compactor compacted samples. Samples were tested at two temperature levels (50 °C and 60 °C) or (122 °F and 140 °F) and five load levels (705, 750, 795, 840, and 885 N) or (158, 168, 178, 188, and 198 lbs). Thus, the experiment involved a total of 60 sets (6 projects x 2 temperature levels x 5 load levels) of samples. Table 4.1 shows the characteristics of the mixtures under this study. The binder grade for four mixtures was PG 64-22; one mixture from CISL (denoted as CISL-A) had PG 64-22; and the second mixture from CISL (denoted as CISL-B) had PG 70-22. Asphalt contents of the base design mixtures corresponding to a target 4% air voids @ N_{design} varied from 4.9% to 5.4%.

Table 4.1 Properties of Superpave Mixes

Route	KDOT District	Design ESALs (millions)	N _{design}	PG Binder Grade	Asphalt Content (%)	Air Voids (%) at N _{design}	VMA (%)	VFA (%)	Dust-Binder Ratio	%G _{mm} at N _{ini}	% G _{mm} at N _{max}
K-4	I	0.40	75	PG 64-22	4.90	4.36	13.9	68	0.7	88.8	96.6
US-24	III	0.70	75	PG 64-22	5.00	3.62	14.1	74	0.9	90.4	97.1
US-50	V	4.50	100	PG 64-22	5.40	4.10	14.6	70	0.6	88.4	96.9
US-83	VI	2.20	75	PG 64-22	4.90	4.38	13.9	68	1.1	89.7	96.4
CISL-A	I	2.9	75	PG 64-28	4.90	4.36	14.0	69	0.7	88.8	96.6
CISL-B	N/A	N/A	100	PG 70-22	5.40	4.00	14.5	73	1.1	N/A	N/A

NOTE: N/A means not available.

The mixture properties, reported in Table 4.1, were obtained from the design data. All properties satisfied Superpave and current required KDOT criteria. Figure 4.1 shows the aggregate gradations of the mixes used in this study. It is observed that only one mixture (US-24, District III) had a much finer gradation compared to the others, and one mixture (CISL-B) had much coarser gradation compared to the others.

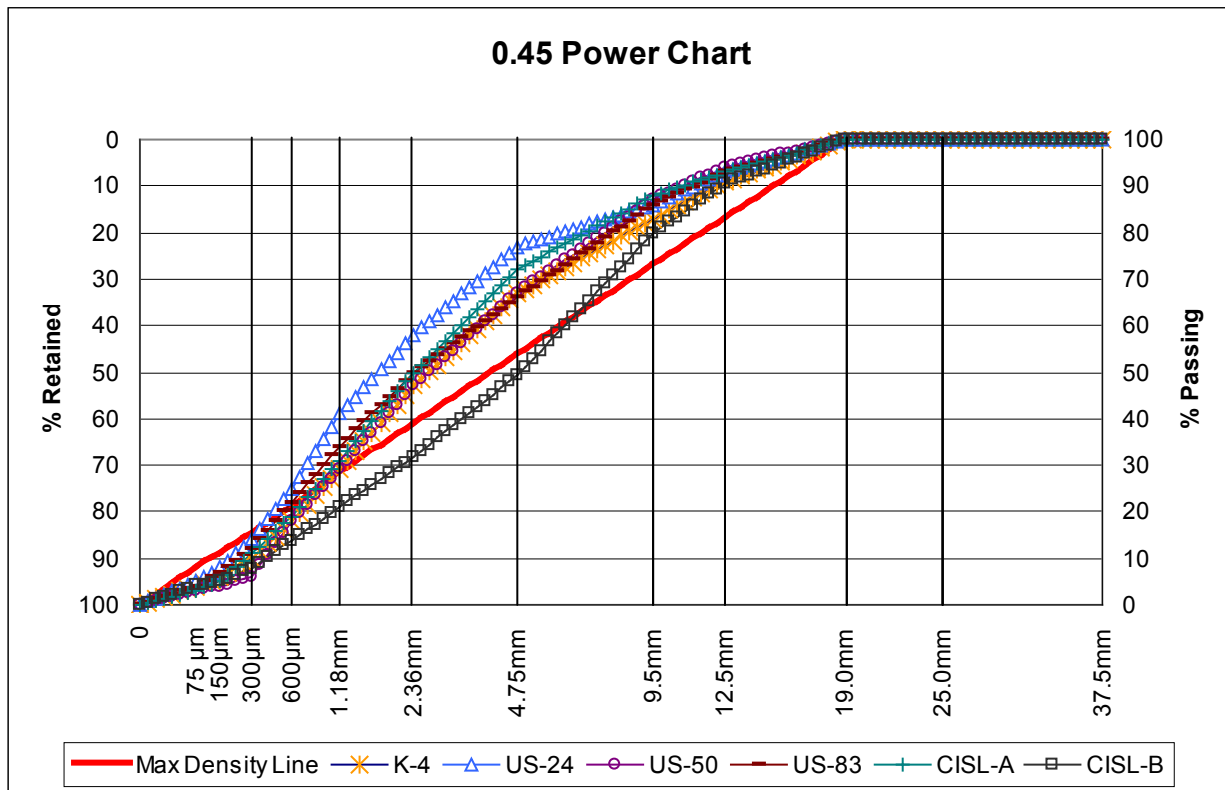


Figure 4.1 Aggregate Gradation Charts for the Mixtures

4.2 Test Specimen Preparation

Test specimens were compacted with a Superpave gyratory compactor. Target air voids at N_{design} of 4% and simulated in-place density of 93% were selected. Ten sets of samples were prepared for testing with air voids of $(7 \pm 1)\%$ for temperature levels of 50 °C (122 °F) and 60 °C (140 °F), and five load levels of 705, 750, 795, 840, and 885 N (158, 168, 178, 188, and 198 lbs). Sample preparation procedures for the HWTD test is the same as described in section 3.2.

For each mix, four replicate specimens for HWTD tests were compacted at the same target air-void content (or density) for each test. Theoretical maximum specific gravity (G_{mm}) of the loose mixtures and bulk specific gravity (G_{mb}) of the compacted specimens were determined in the laboratory, and air voids in the compacted specimens were calculated using Equation (3.2).

Table 4.2 presents the data of design single-point gradation of aggregates of all projects.

Table 4.2 Design Single-Point Gradation of Aggregates

Route	% Retained Materials on Sieve Size											
	37.5mm (1.5 in.)	25.0mm (1 in.)	19.0mm (3/4 in.)	12.5mm (1/2 in.)	9.5mm (3/8in.)	4.75mm (# 4)	2.36mm (# 8)	1.18mm (# 16)	600µm (# 30)	300µm (# 50)	150µm (#100)	75µm (#200)
Max. Density Line	0	0	0	0	12.1	36.1	52.8	65.4	74.5	81.3	86.4	90.2
K-4	0	0	0	9	17	33	53	71	82	90	94	96.0
US-24	0	0	0	7	14	23	42	59	75	86	92	94.9
US-50	0	0	0	6	13	33	53	71	82	94	96	96.9
US-83	0	0	0	7	14	34	50	66	78	88	93	95.9
CISL-A	0	0	0	7	12	28	50	69	81	89	95	96.8
CISL-B	0	0	0	9	20	51	68	79	86	92	95	95.9

4.3 Hamburg Wheel-Tracking Device (HWTD)

The HWTD was used in the laboratory test. The equipment description has been given in section 3.3.1. A wheel-load adjustment kit was used to change the load from 705 N to 750, 795, 840, and 885 N (158 lbs to 168, 178, 188, and 198 lbs). Wheel-load calibration was done each time under changing wheel loads to any desired load levels. HWTD tests with high loads of 840 and 885 N (188 and 198 lbs) were done only for three projects (US-24, US-50, and US-83) to access the effect of higher loads in HWTD tests.

4.4 Laboratory Test Results

Table 4.3 shows HWTD test results in terms of the average number of passes and average air voids. The best performing mixture, in terms of number of passes to reach a 20-mm (0.8 in.) rut depth, is the CISL-B mixture with a binder grade of PG 70-22. This mixture did not reach the failure condition (as indicated by 20,000 passes on the table) under both temperature and load levels. The effect of a modified binder on better performance is quite evident. HWTD test results in both (left and right) wheel passes are shown in Appendix E. Similarly, G_{mm} and G_{mb} , simulated in-place densities and air voids for each sample, were tested and computed and are presented in Appendix E.

Table 4.4 shows other output parameters (creep slope, stripping slope, and stripping inflection point) of the mixtures under test. Trends in these parameters closely follow the trends shown by the total number of passes to a 20-mm (0.8-in) rut depth. From the figures, it is evident that the number of wheel passes in the HWTD test decrease rapidly as temperature increases from 50°C (122 °F) to 60°C (140 °F). But the decrease in the number of wheel passes is not remarkable at the higher load level for the same temperature.

Table 4.3 Summary of Hamburg Wheel Test Results (Average number of wheel passes)

Route	Temp. (°C)	Load (705 N)		Load (750 N)		Load (795 N)		Load (840 N)		Load (885 N)	
		Wheel Passes	% Air Voids								
K-4	50	13,700	6.5	18,730	5.7	15,950	6.3	N/A	N/A	N/A	N/A
	60	7,230	6.7	4,075	6.8	3,995	6.5	N/A	N/A	N/A	N/A
US-24	50	17,625	6.8	17,390	5.5	16,650	5.3	11,210	6.2	13,385	6.3
	60	3,535	5.6	2,565	5.5	3,180	5.5	3,335	6.4	1,400	6.3
US-50	50	20,000	7.5	20,000	6.8	20,000	7.3	8,420	7.4	7,450	7.4
	60	5,355	7.9	9,150	7.1	4,295	7.3	2,640	6.6	2,170	6.3
US-83	50	20,000	6.1	20,000	6.9	20,000	6.0	11,260	5.8	15,770	5.5
	60	7,145	6.1	3,970	5.9	7,025	6.3	3,500	6.0	2,845	6.5
CISL-A	50	20,000	7.1	18,070	7.7	15,055	7.4	N/A	N/A	N/A	N/A
	60	5,390	7.9	4,020	7.6	4,625	7.2	N/A	N/A	N/A	N/A
CISL-B	50	20,000	7.4	20,000	7.5	20,000	7.4	N/A	N/A	N/A	N/A
	60	20,000	7.2	20,000	7.4	20,000	7.2	N/A	N/A	N/A	N/A

NOTES:

Values on the table are the number of wheel passes to 20-mm (0.8-in.) rut depth;
 Failure criteria: 20-mm (0.8-in.) maximum rut depth or 20,000 wheel passes, whichever came first;
 A liquid anti-stripping agent (0.5%) was used only on the US-83 project; and
 N/A means not available.

Table 4.4 Summary of Hamburg Wheel Test Results (Output Parameters)

Route	Parameter	Load Level									
		705 N		750 N		795 N		840 N		885 N	
		Temperature Level		Temperature Level		Temperature Level		Temperature Level		Temperature Level	
		50 (°C)	60 (°C)								
K-4	Creep Slope	2,040	1,370	3,508	830	3,304	700	N/A	N/A	N/A	N/A
	Stripping Inflection Point	7,050	3,800	8,950	2,150	9,350	1,900	N/A	N/A	N/A	N/A
	Stripping Slope	460	613	613	123	440	165	N/A	N/A	N/A	N/A
US-24	Creep Slope	3,615	492	3,012	152	3,266	432	1,778	380	2,980	154
	Stripping Inflection Point	12,650	1,300	12,850	960	9,550	1,700	7,700	1,650	10,550	940
	Stripping Slope	365	135	203	105	430	99	366	107	164	34
US-50	Creep Slope	11,000	1,305	7,281	1,742	13,590	717	1,580	403	1,250	253
	Stripping Inflection Point	14,600	2,900	15,650	3,000	13,850	1,450	5,650	1,450	4,450	1,100
	Stripping Slope	5,778	154	870	300	405	185	180	78	214	70
US-83	Creep Slope	2,563	284	1,516	158	3,084	316	660	214	1,410	170
	Stripping Inflection Point	13,950	1,050	14,900	1,150	NA	1,000	NA	1,000	4,950	1,150
	Stripping Slope	2,017	401	1,000	123	NA	419	N/A	183	718	135
CISL - A	Creep Slope	4,000	475	3,093	530	7,458	764	N/A	N/A	N/A	N/A
	Stripping Inflection Point	13,400	1,400	12,300	1,550	10,700	1,800	N/A	N/A	N/A	N/A
	Stripping Slope	560	200	508	172	271	168	N/A	N/A	N/A	N/A
CISL - B	Creep Slope	19,725	10,211	21,000	5,935	25,358	22,750	N/A	N/A	N/A	N/A
	Stripping Inflection Point	N/A	N/A	N/A	17,750	N/A	N/A	N/A	N/A	N/A	N/A
	Stripping Slope	N/A	N/A	N/A	486	N/A	N/A	N/A	N/A	N/A	N/A

NOTE: N/A means not available.

Figures 4.2 to 4.7 illustrate the comparison of the number of wheel passes to reach a 20-mm (0.8-in.) rut depth at different temperatures and load levels. Figures 4.8 to 4.10 show the trend of rutting in the HWTD tests of projects at various temperatures and load levels. The steeper slope of the plot at 60 °C (140 °F) indicates that temperature change has a more pronounced effect compared to the load change.

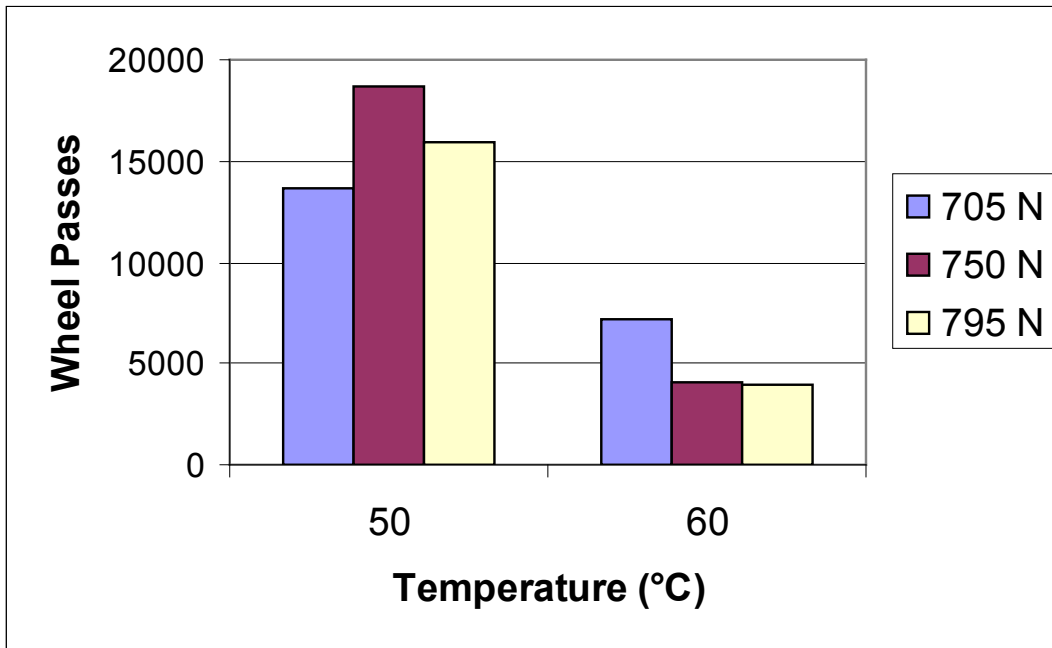


Figure 4.2 HWTD Test Results of K-4 Project in District I

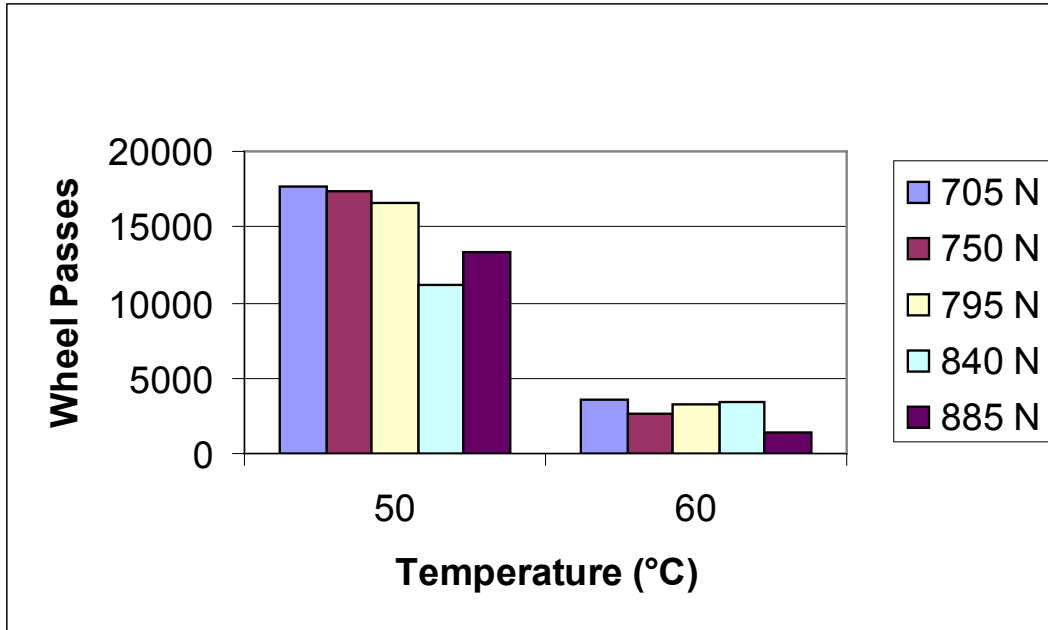


Figure 4.3 HWTD Test Results of US-24 Project in District III

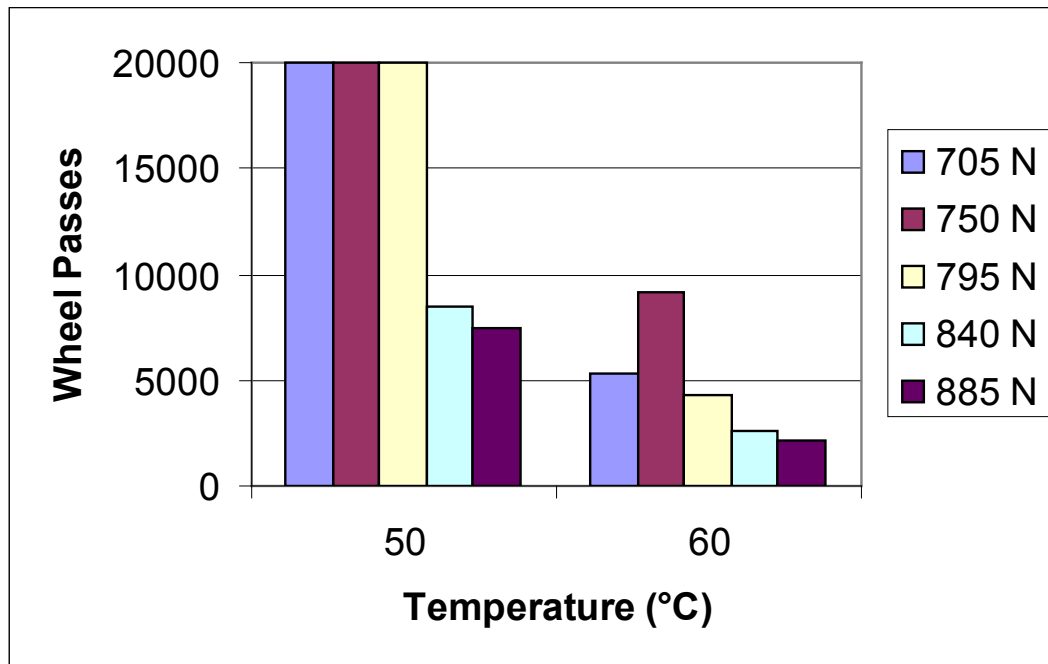


Figure 4.4 HWTD Test Results of US-50 Project in District V

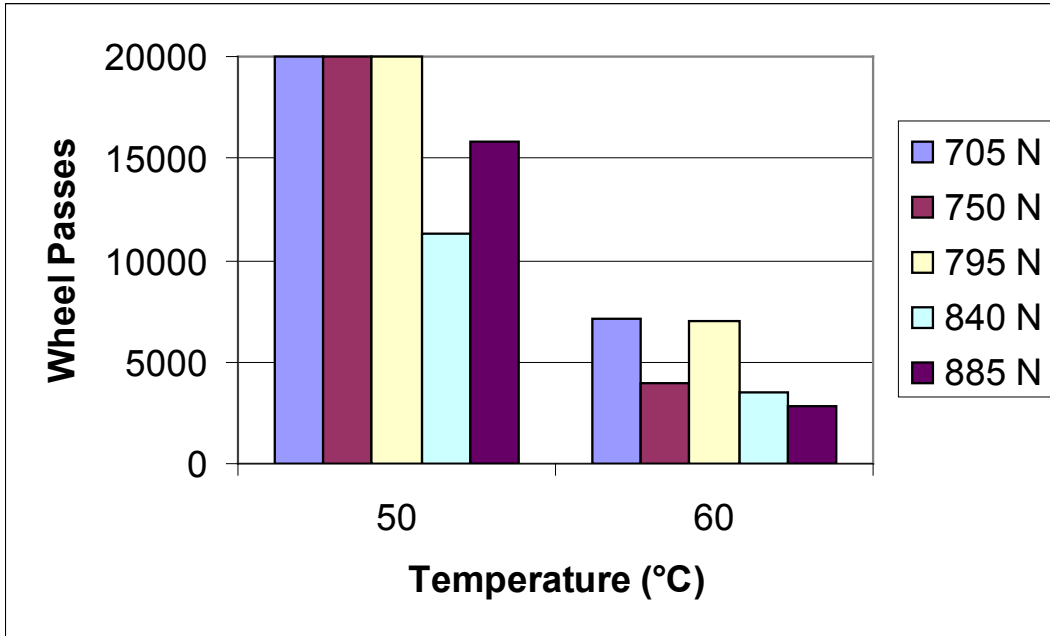


Figure 4.5 HWTD Test Results of US-83 Project in District VI

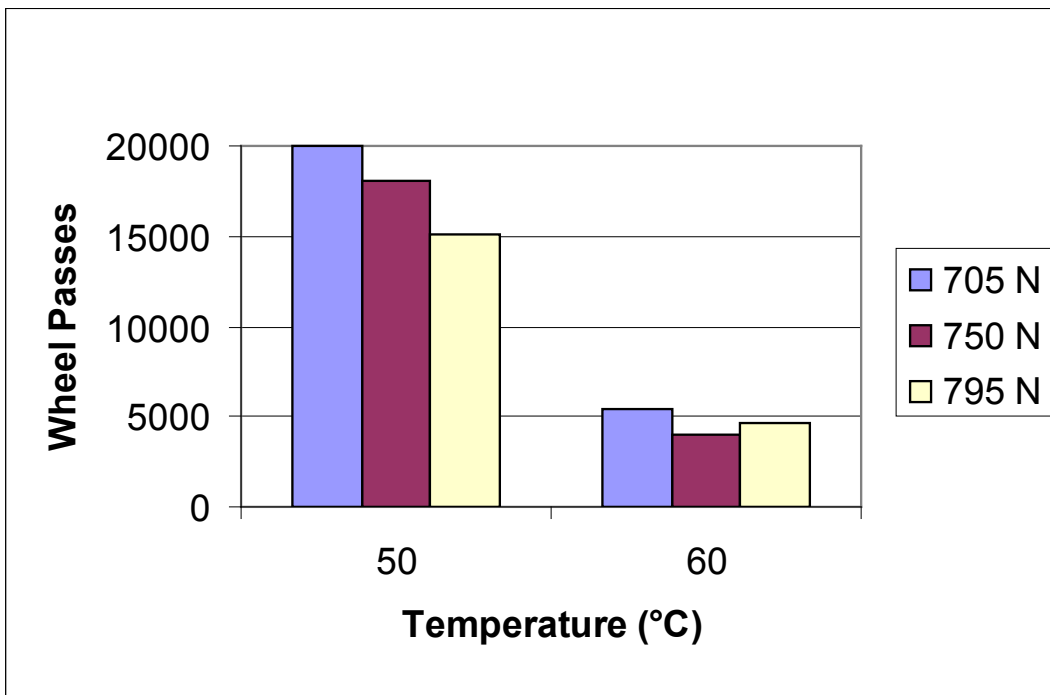


Figure 4.6 HWTD Test Results of CISL-A Project at KSU

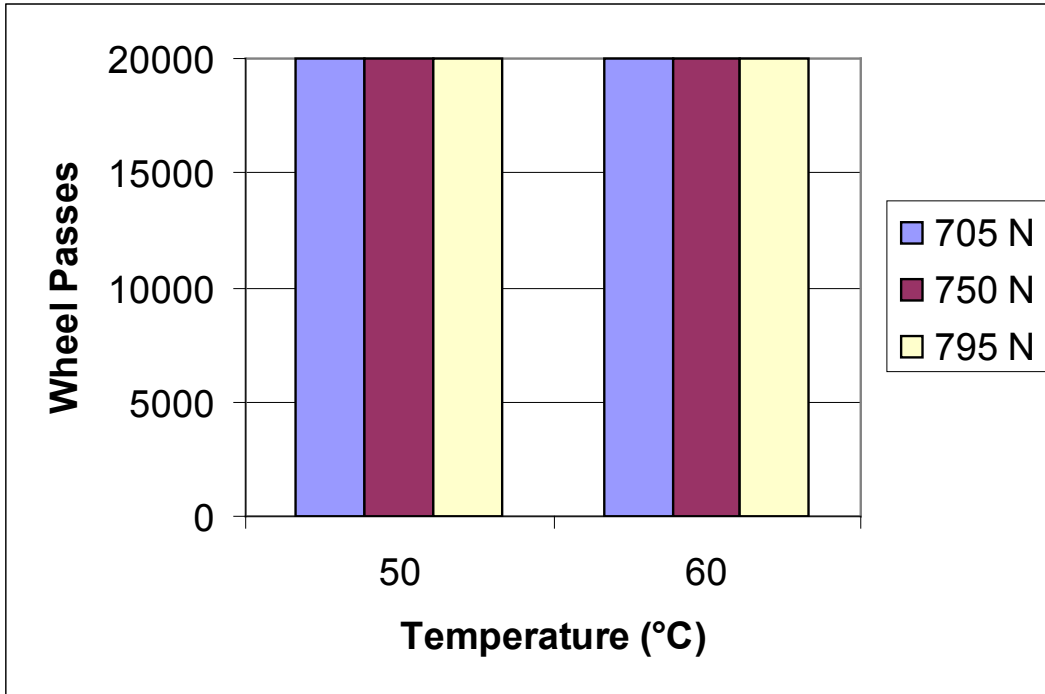
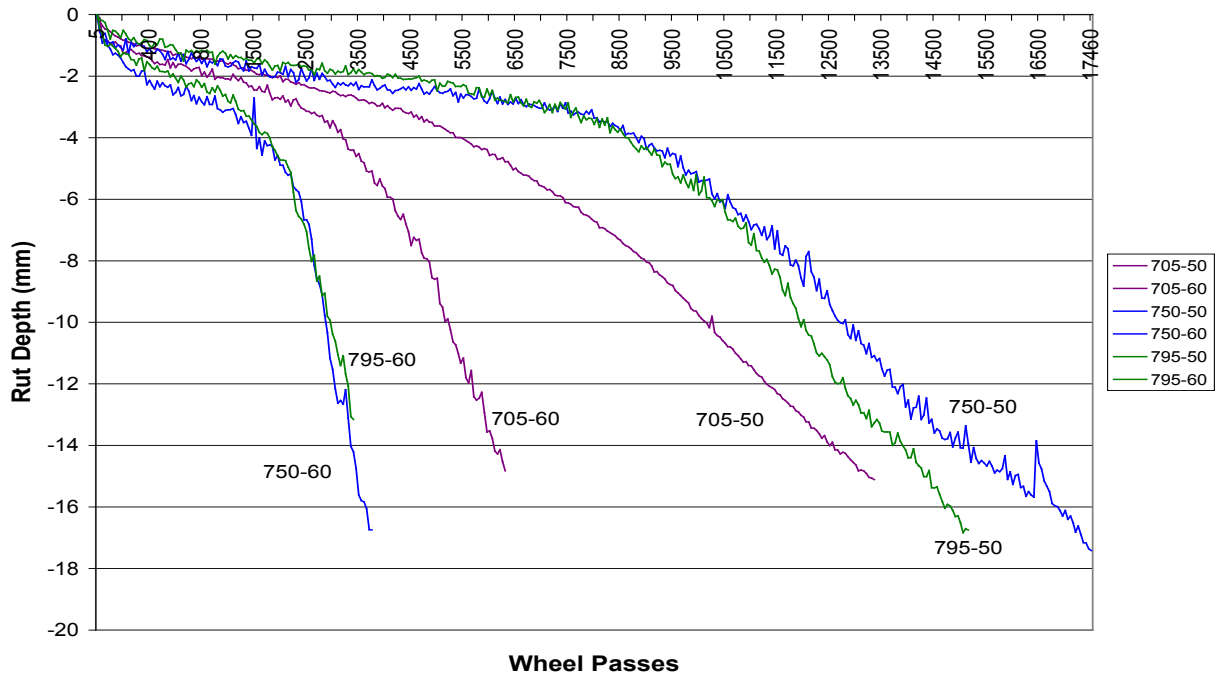
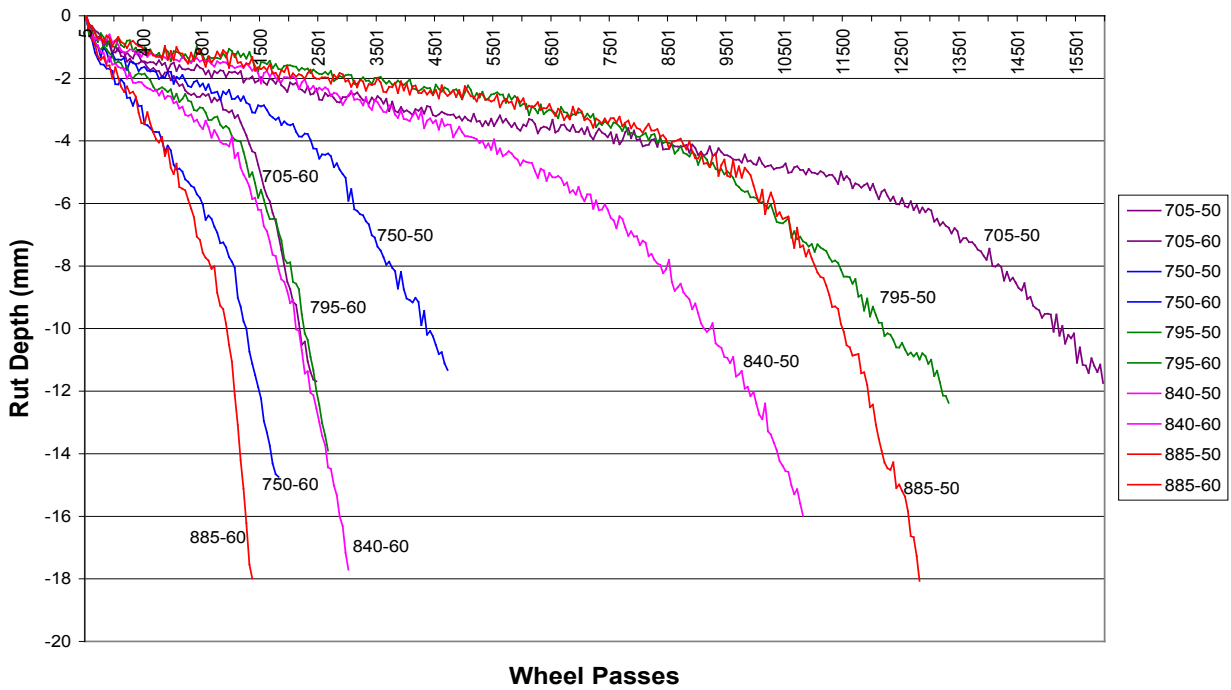


Figure 4.7 HWTD Test Results of CISL-B Project at KSU

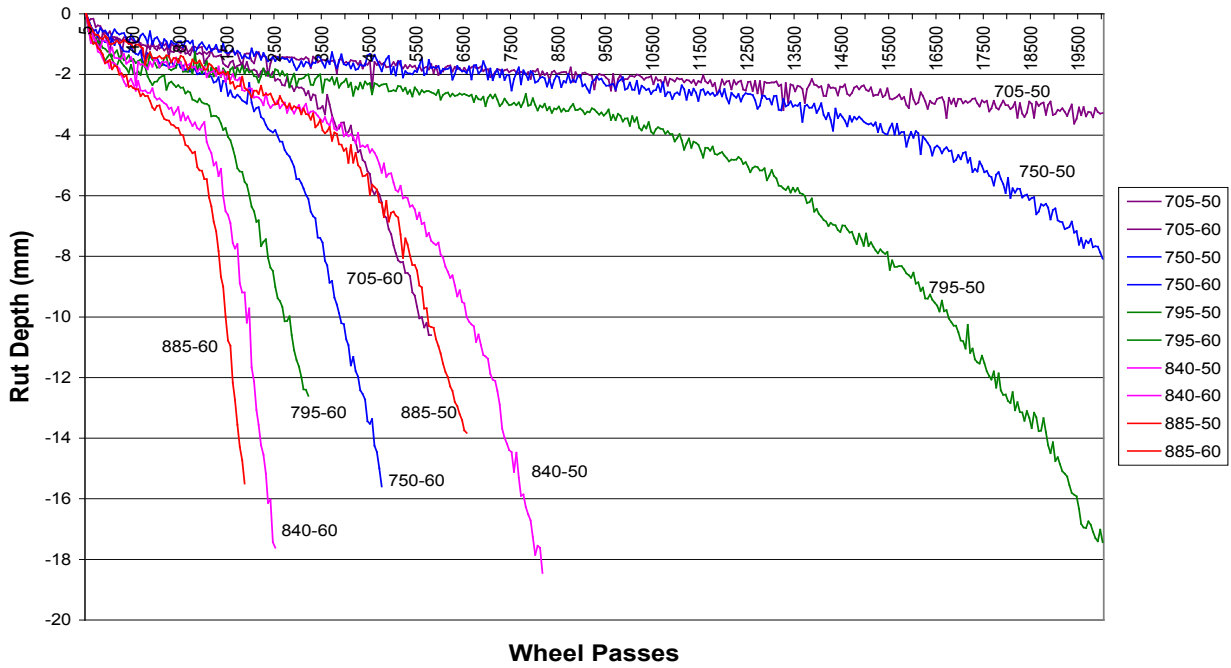


(a) K-4 Route Project

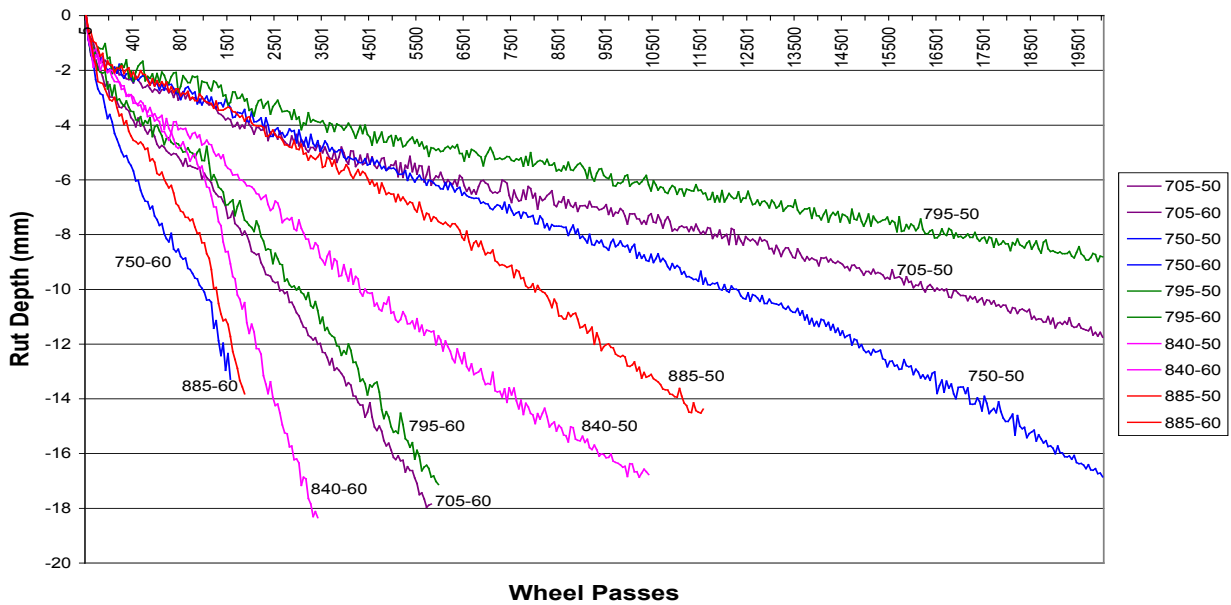


(b) US-24 Route Project

Figure 4.8 HWTD Test Results for Route K-4 and US-24

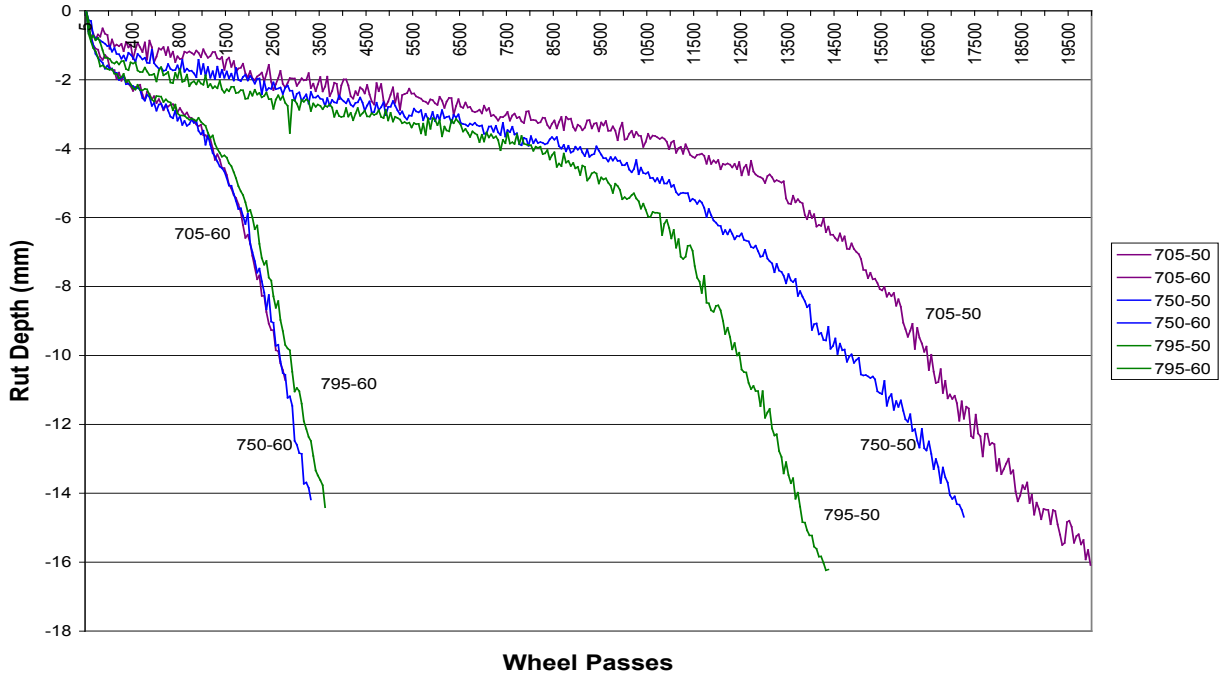


(a) US-50 Route Project

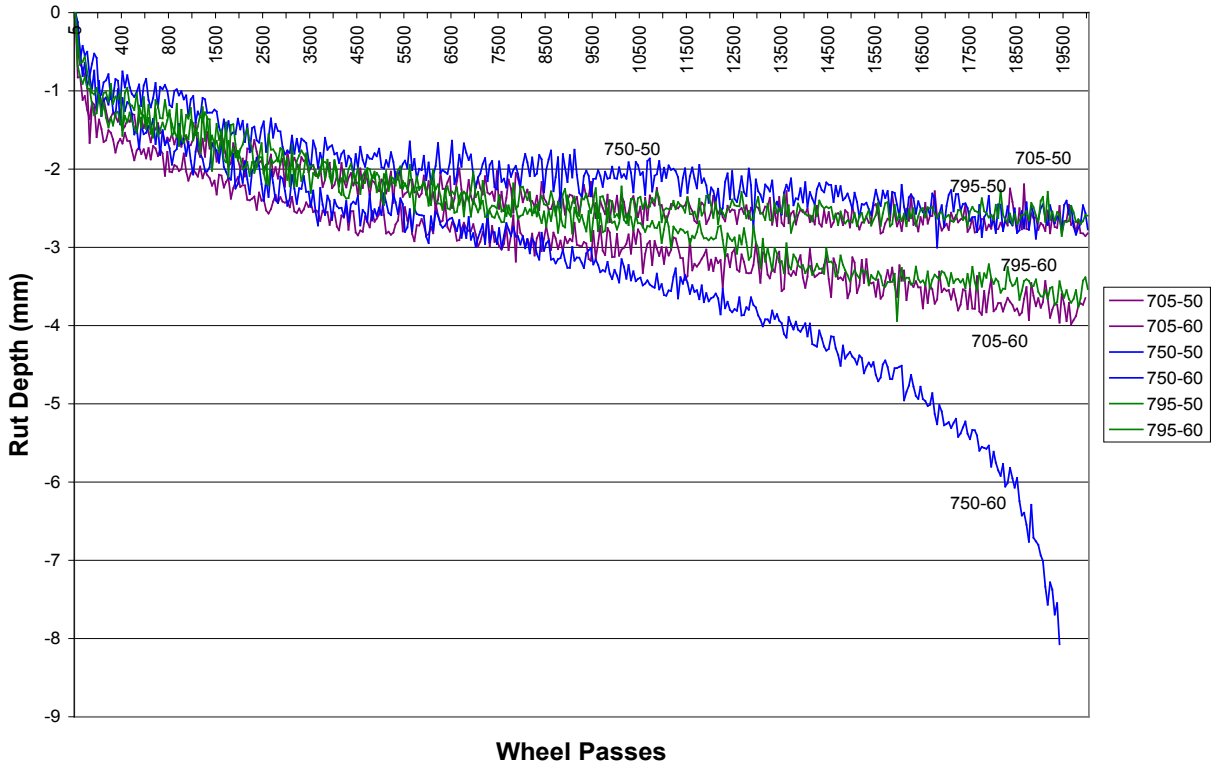


(b) US-83 Route Project

Figure 4.9 HWTD Test Results for Route US-50 and US-83



(a) CISL-A Project



(b) CISL-B Project

Figure 4.10 HWTD Test Results for CISL-A and CISL-B Projects

Figure 4.7 shows that samples from the CISL-B project did not fail at 50 °C (122 °F) and 60 °C (140 °F) at load levels of 705, 750, and 795 N (158, 168, and 178 lbs). Use of a modified binder grade of PG 70-22 and all crushed aggregates in this project are the main reasons. Samples used in CISL-A and CISL-B mixes were plant produced. Samples from other projects were mixed manually in the laboratory. All mixes were subjected to two hours of aging at compaction temperature before fabricating HWTD test samples. Samples from CISL projects were reheated before compaction. Thus, the samples prepared from the CISL projects underwent extra aging prior to compaction, and might have resulted in stiffer samples compared to samples from the other mixes.

4.5 Statistical Analysis

4.5.1 Influence of Temperature and Load

The effect of temperature and load levels on the HWTD test results was studied using the analysis of variance (ANOVA) technique and SAS software (SAS User's Guide 1982). The LIFEREG procedure was performed for development of an accelerated mix testing model to test the effect of different factors on the dependent (response) variable. Models for the response variable consisted of a linear effect composed of the covariates and a random error. The distribution of the random error can be taken from a class of distributions that includes extreme value, normal, logistic, and, by using a log transformation, the exponential, Weibull, lognormal, log logistic, and three-parameter gamma distributions. The PROC LIFEREG procedure fits parametric accelerated failure time models to the survival data that may be left, right, or interval censored (SAS Online Document 2008; Allison 1995; Klein and Moeschberger 2003). The LIFEREG procedure estimates the parameters using a Newton-Raphson algorithm to maximize the log likelihood. The PROC LIFEREG procedure computes the standard errors of the parameter estimates from the inverse of the observed information matrix (SAS Online Document 2008; Lee and Wang 2003). Since some of data are right censored, show a nature of non-normality, and have inconsistent variance, the LIFEREG procedure is the best fit for the statistical analysis.

In this research, four response variables were studied: (a) number of wheel passes to reach a 20-mm maximum rut depth, (b) creep slope, (c) stripping slope, and (d) stripping inflection point.

The Weibull model is shown in Equation (4.1):

$$\ln(RV) = \beta_0 + \beta_1 T + \beta_2 L + \sigma \varepsilon \quad (4.1)$$

where

RV = various response variables studied;

T = temperature (°C);

L = load (N);

$\beta_0, \beta_1, \beta_2$ = coefficients;

σ = scale parameter (1 for exponential model); and

ε = error term.

Analysis was done for each individual project as well as by combining data for all projects, without CISL-A and CISL-B (four projects), and without CISL-B (five projects). Results in Table 4.5 indicate performance parameters, average stripping slope, and average number of wheel passes to a 20-mm (0.8-in.) rut depth. Temperature is a more significant factor affecting outputs than load levels.

Figure 4.11 shows the percentage of HWTD test results which are right censored or reached 20,000 wheel passes before the 20-mm (0.8-in.) rut depth was obtained. Only one project had 100% censored data, two projects had 30% censored data, one project had 17% censored data, and other two projects did not have any censored data.

HWTD Test Results in Percentage

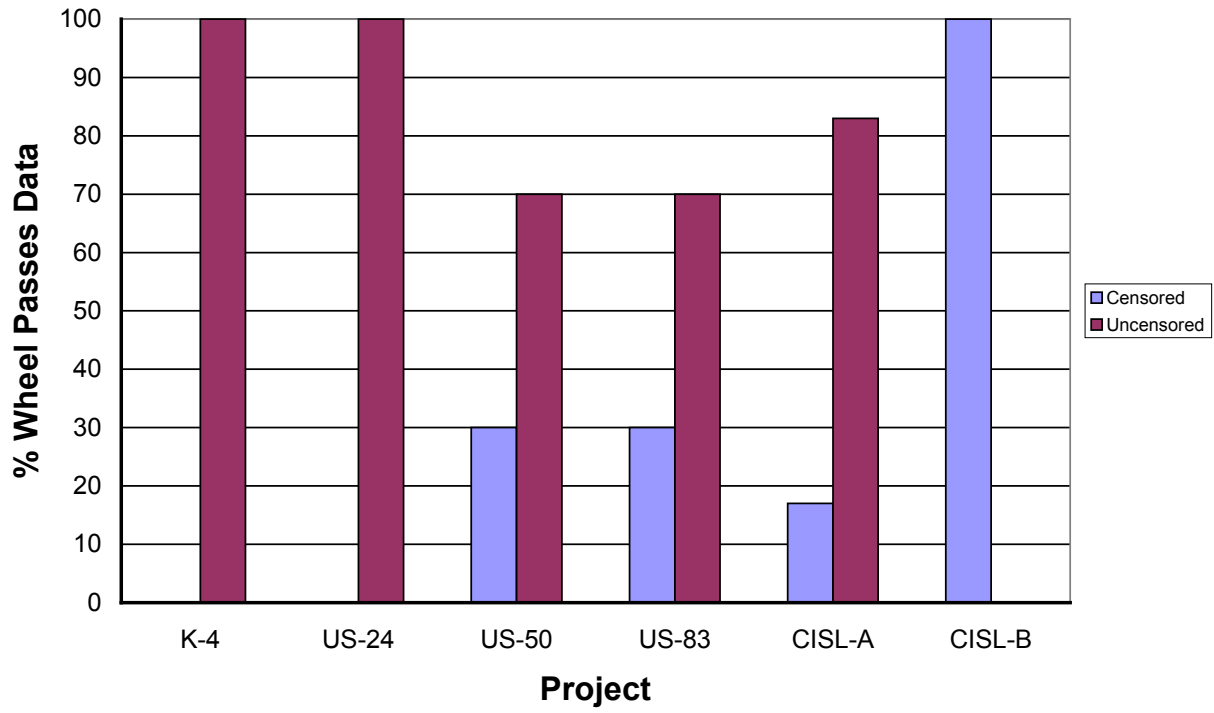


Figure 4.11 HWTD Test Results with Censored and Uncensored Data

Table 4.5 Summary of Statistical Analysis for Accelerated Mix Testing Models

Route	District	Parameter	Average Creep Slope			Average Stripping Inflection Point			Average Stripping Slope			Average Number of Wheel Passes		
			Estimate	p-value	Significant	Estimate	p-value	Significant	Estimate	p-value	Significant	Estimate	p-value	Significant
K-4	I	Intercept	10,395.67	0.2101		-156,550	0.1031	**	-16,142.3	0.4334		19.2288	< 0.0001	*
		T	-198.40	0.0389	*	2,916.67	0.0979	**	336.27	0.3796		-0.1237	< 0.0001	*
		L	3.30	0.6960		258.89	0.0706	**	23.55	0.3982		-0.0043	0.0197	*
		T × L				-4.67	0.0712	**	-0.47	0.3567				
US-24	III	Intercept	18,578.8	0.0001	*	65,695.7	<0.0001	*	1,741.4	0.0056	*	19.6673	< 0.0001	*
		T	-260.82	<0.0001	*	-935.00	<0.0001	*	-20.96	0.0055	*	-0.1623	< 0.0001	*
		L	-3.28	0.2078		-10.42	0.1936		-0.49	0.2798		-0.0023	0.0111	*
		T × L												
US-50	V	Intercept	62,523.4	0.0106	*	86,454.2	0.0006	*	129,975.2	0.0548	*	25.7294	< 0.0001	*
		T	-605.62	0.0269	*	-886.00	0.0015	*	-2,152.15	0.0725	**	-0.1451	< 0.0001	*
		L	-31.83	0.1043	**	-39.39	0.0250	*	-153.24	0.0666	**	-0.0107	< 0.0001	*
		T × L							2.54	0.0865	**			
US-83	VI	Intercept	12,882.6	0.0087	*	322,292	0.0048	*	8,579.98	0.0061	*	23.1491	< 0.0001	*
		T	-161.82	0.0069	*	-5,355.17	0.0064	*	-94.23	0.0136	*	-0.1721	< 0.0001	*
		L	-3.70	0.3078		-333.37	0.0098	*	-3.36	0.1157		-0.0053	0.0031	*
		T × L				5.56	0.0128	*						
CISL-A	I	Intercept	10,541.2	0.5232		216,550	0.0039	*	3,115.5	0.0317	*	19.6677	< 0.0001	*
		T	-426.07	0.0431	*	-3,638.33	0.0045	*	-26.63	0.0324	*	-0.1254	< 0.0001	*
		L	20.82	0.3117		-202.22	0.0079	*	-1.78	0.1597		-0.0047	0.0078	*
		T × L				3.44	0.0089	*						
CISL-B	N/A	Intercept	-8,377.3	0.8805		N/A	N/A		N/A	N/A		N/A	N/A	
		T	-906.23	0.1323		N/A	N/A		N/A	N/A		N/A	N/A	
		L	100.96	0.1914		N/A	N/A		N/A	N/A		N/A	N/A	
		T × L												
All Projects Without CISL		Intercept	28,093.9	0.0002	*	199,853.8	0.0003	*	8,277.7	0.0028	*	21.5924	< 0.0001	*
		T	-318.69	0.0004	*	-3,219.42	0.0011	*	-67.93	0.0369	*	-0.1501	< 0.0001	*
		L	-10.68	0.1064	*	-185.92	0.0059	*	-5.09	0.0461	*	-0.0052	< 0.0001	*
		T × L				2.99	0.0130	*						
All Projects Without CISL-B		Intercept	27,836.1	< 0.0001	*	205,265.5	<0.0001	*	7,344.06	0.0021	*	21.2212	< 0.0001	*
		T	-334.03	< 0.0001	*	-3,322.65	0.0001	*	-61.35	0.0281	*	-0.1470	< 0.0001	*
		L	-9.24	0.1226		-191.97	0.0012	*	-4.44	0.0487	*	-0.0050	< 0.0001	*
		T × L				3.11	0.0033	*						
All Projects		Intercept	41,177.1	0.0077	*	70,468.7	<0.0001	*	7,332.8	0.0019	*	22.8407	< 0.0001	*
		T	-405.56	0.0227	*	-826.27	<0.0001	*	-60.64	0.0261	*	-0.1315	< 0.0001	*
		L	-18.93	0.1986		-23.73	0.0067	*	-4.47	0.0437	*	-0.0078	< 0.0001	*
		T × L												

NOTES: * = significant at 5% level of significance; ** = significant at 10% level of significance;
T = temperature (°C); L = load (N); T × L = interaction of temperature and load; and N/A = not available.

4.5.2 Development of Accelerated Mix Testing Models Considering Effects of Temperature and Load

Table 4.6 lists the equation parameters obtained for all projects in this study using the statistical analysis procedure LIFEREG. Table 4.7 shows the comparison of the predicted and observed wheel passes in the HWTD tests for the projects. In this table, a combined model using data from all six projects and without interaction terms was used. An exponential accelerated life model has been fitted to the data. Results show that good prediction can be made at higher loads and temperatures using models developed from the test results. Results also show that data for only 5,000 repetitions are good enough to fit an exponential accelerated life model. This would translate into approximately two hours of testing time in the HWTD test.

The developed statistical model for overall data without interaction of temperature and load is given in Equation (4.2).

$$WP = e^{(22.8407 - 0.1315T - 0.0078L)} \quad (4.2)$$

where

WP = number of wheel passes;

T = temperature ($^{\circ}\text{C}$); and

L = load (N).

A table comparing the predicted and observed wheel passes in the HWTD tests for individual project is presented in appendix F. Typical SAS input files are shown in Appendix-G.

Table 4.6 Summary of Statistical Analysis for Accelerated Mix Testing Models

Route	District	Parameter	Description	Model With Intersection			Model Without Intersection		
				Estimate	p-value	Significant	Estimate	p-value	Significant
K-4	I	Intercept	Vertical Intercept	-16.3237	0.2520		19.2288	< 0.0001	*
		T	Temperature (°C)	0.4951	0.0440	*	-0.1237	< 0.0001	*
		L	Load (N)	0.0426	0.0248	*	-0.0043	0.0197	*
		T × L	Interaction of Temperature and Load	-0.0008	0.0126	*			
US-24	III	Intercept	Vertical Intercept	17.1197	0.0356	*	19.6673	< 0.0001	*
		T	Temperature (°C)	-0.1159	0.4353		-0.1623	< 0.0001	*
		L	Load (N)	0.0009	0.9322		-0.0023	0.0111	*
		T × L	Interaction of Temperature and Load	-0.0001	0.7534				
US-50	V	Intercept	Vertical Intercept	59.8241	0.0230	*	25.7294	< 0.0001	*
		T	Temperature (°C)	-0.7323	0.1032	**	-0.1451	< 0.0001	*
		L	Load (N)	-0.0512	0.0950	**	-0.0107	< 0.0001	*
		T × L	Interaction of Temperature and Load	0.0007	0.1835				
US-83	VI	Intercept	Vertical Intercept	39.0583	0.1266		23.1491	< 0.0001	*
		T	Temperature (°C)	-0.4465	0.3063		-0.1721	< 0.0001	*
		L	Load (N)	-0.0243	0.4180		-0.0053	0.0031	*
		T × L	Interaction of Temperature and Load	0.0003	0.5240				
CISL-A	I	Intercept	Vertical Intercept	36.5642	0.0630	**	19.6677	< 0.0001	*
		T	Temperature (°C)	-0.4207	0.2162		-0.1254	< 0.0001	*
		L	Load (N)	-0.0268	0.2925		-0.0047	0.0078	*
		T × L	Interaction of Temperature and Load	0.0004	0.3808				
CISL-B	N/A	Intercept	Vertical Intercept	N/A	N/A		N/A	N/A	
		T	Temperature (°C)	N/A	N/A		N/A	N/A	
		L	Load (N)	N/A	N/A		N/A	N/A	
		T × L	Interaction of Temperature and Load	N/A	N/A				
All Projects Without CISL-A and CISL-B		Intercept	Vertical Intercept	15.1836	0.0728	**	21.5924	< 0.0001	*
		T	Temperature (°C)	-0.0355	0.8138		-0.1501	< 0.0001	*
		L	Load (N)	0.0027	0.7961		-0.0052	< 0.0001	*
		T × L	Interaction of Temperature and Load	-0.0001	0.4469				
All Projects Without CISL-B		Intercept	Vertical Intercept	16.1005	0.0329	*	21.2212	< 0.0001	*
		T	Temperature (°C)	-0.0551	0.6829		-0.1470	< 0.0001	*
		L	Load (N)	0.0014	0.8827		-0.0050	< 0.0001	*
		T × L	Interaction of Temperature and Load	-0.0001	0.4952				
All Projects		Intercept	Vertical Intercept	16.6737	0.2164		22.8407	< 0.0001	*
		T	Temperature (°C)	-0.0205	0.9325		-0.1315	< 0.0001	*
		L	Load (N)	0.0000	0.9983		-0.0078	< 0.0001	*
		T × L	Interaction of Temperature and Load	-0.0001	0.6455				

NOTES: * Significant at 5% level of significance; ** Significant at 10% level of significance; and N/A means not available.

Table 4.7 Comparison of HWTD Results of Model Predicted with Observed Data

Temperature (°C)	Load (N)	Model Predicted Wheel Passes	Average Observed Wheel Passes					
			K-4	US-24	US-50	US-83	CISL-A	CISL-B
50	705	47,415	13,700	17,625	20,000	20,000	20,000	20,000
50	750	33,380	18,730	17,390	20,000	20,000	18,070	20,000
50	795	23,499	15,950	16,650	20,000	20,000	15,055	20,000
50	840	16,543	N/A	11,210	8,420	11,260	N/A	N/A
50	885	11,646	N/A	13,385	7,450	15,770	N/A	N/A
60	705	12,730	7,230	3,535	5,355	7,145	5,390	20,000
60	750	8,962	4,075	2,565	9,150	3,970	4,020	20,000
60	795	6,309	3,995	3,180	4,295	7,025	4,625	20,000
60	840	4,441	N/A	3,335	2,640	3,500	N/A	N/A
60	885	3,127	N/A	1,400	2,170	2,845	N/A	N/A

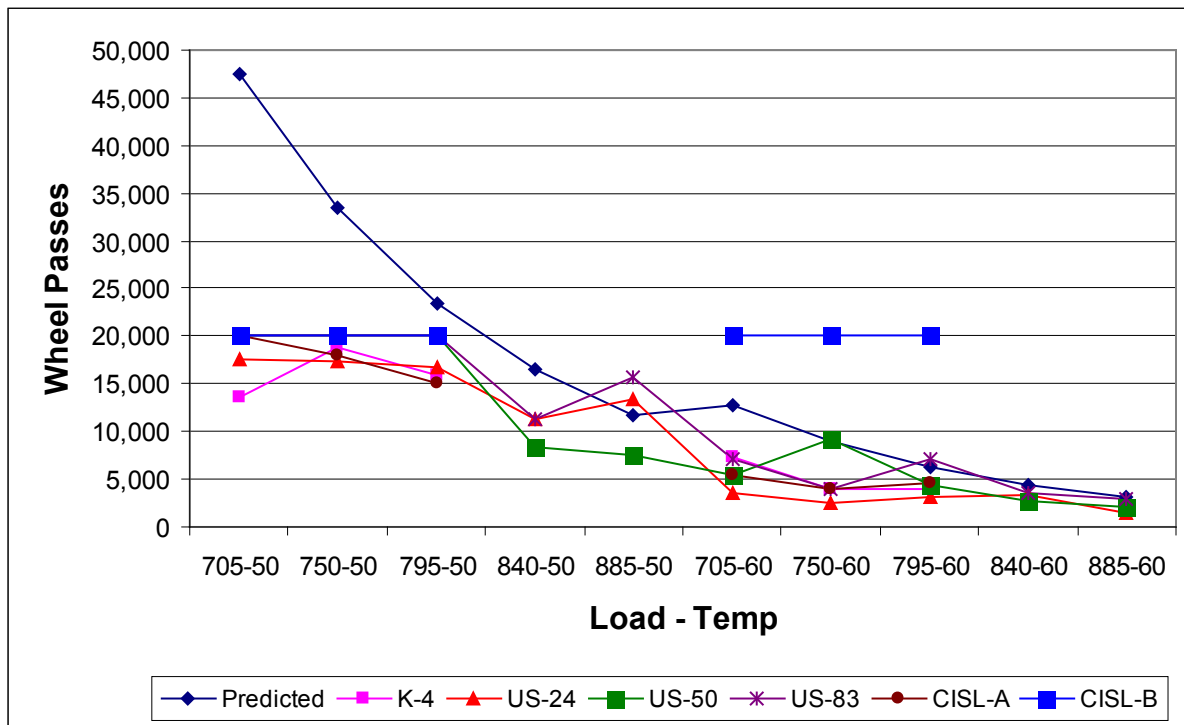


Figure 4.12 Comparison of HWTD Results of Model Predicted with Observed for All Six Projects

Figure 4.12 shows the comparison of HWTD model-predicted results without the interaction term for all six projects and observed results in the laboratory. The comparison of

predicted results for five projects (without CISL-B) and four projects (without CISL-A and CISL-B) with the observed results in laboratory are shown in Figures 4.13 and Figure 4.14, respectively. The predicted results for each individual project and observed results, including the interaction of temperature and load levels, are shown in Figures 4.15 to 4.19. Similarly, predicted results for individual projects and observed results excluding the interaction of temperature and load levels are shown in Figures 4.20 to 4.24. From HWTD test results and statistical analysis, it is observed that the CISL-B project needs to be excluded from this study. CISL-B had the polymer-modified asphalt binder, PG 70-22, which is stiffer than PG 64-22 binder.

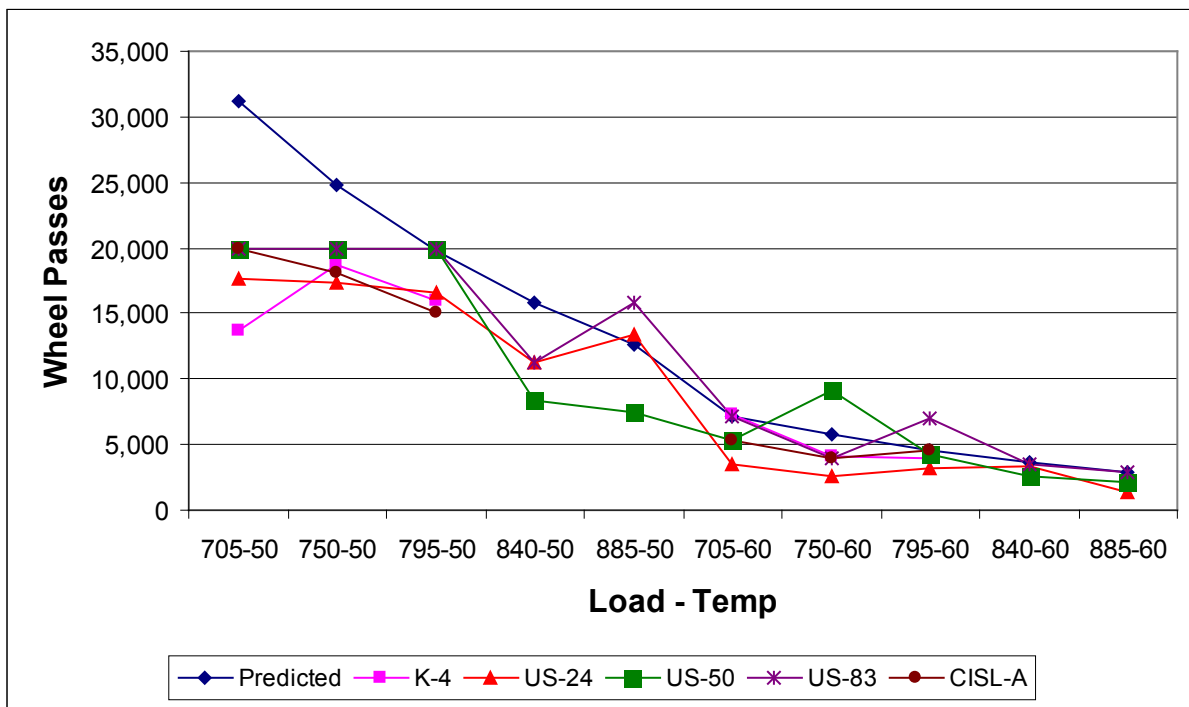


Figure 4.13 Comparison of HWTD Results of Model Predicted with Observed for All Five Projects Without CISL-B

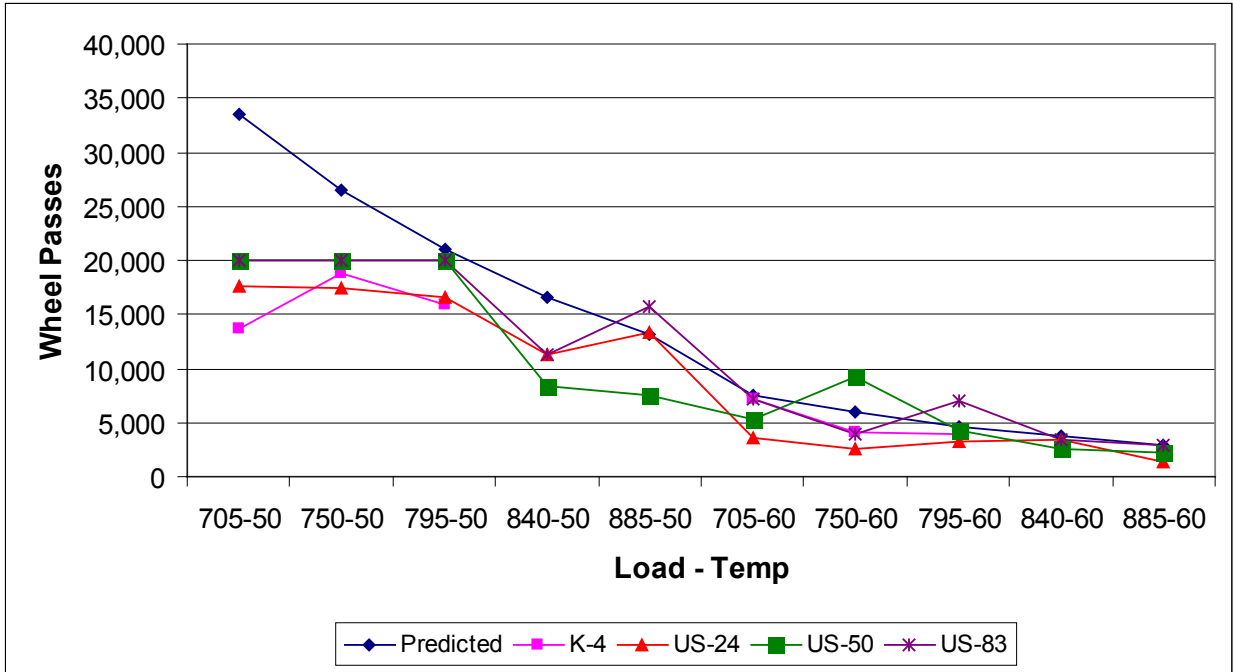


Figure 4.14 Comparison of HWTD Results of Model Predicted with Observed for All Four Projects Without CISL Projects

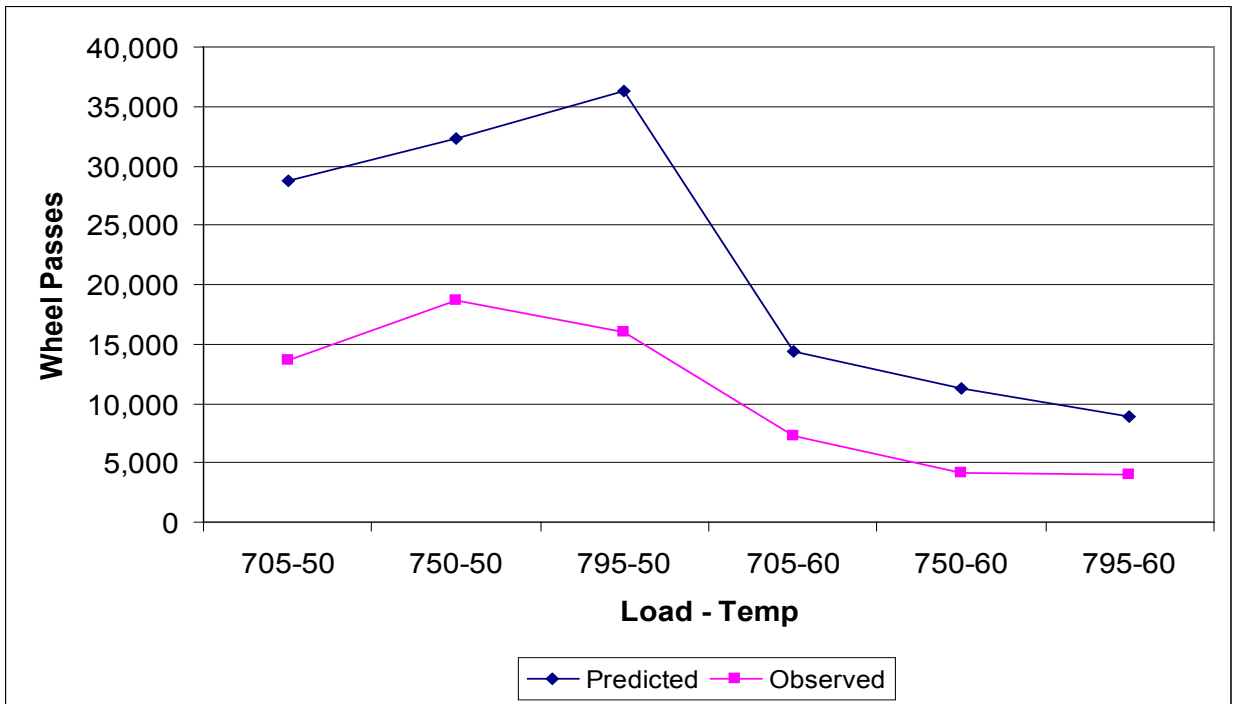


Figure 4.15 Comparison of Predicted with Observed Wheel Passes for K-4 Project with Interaction

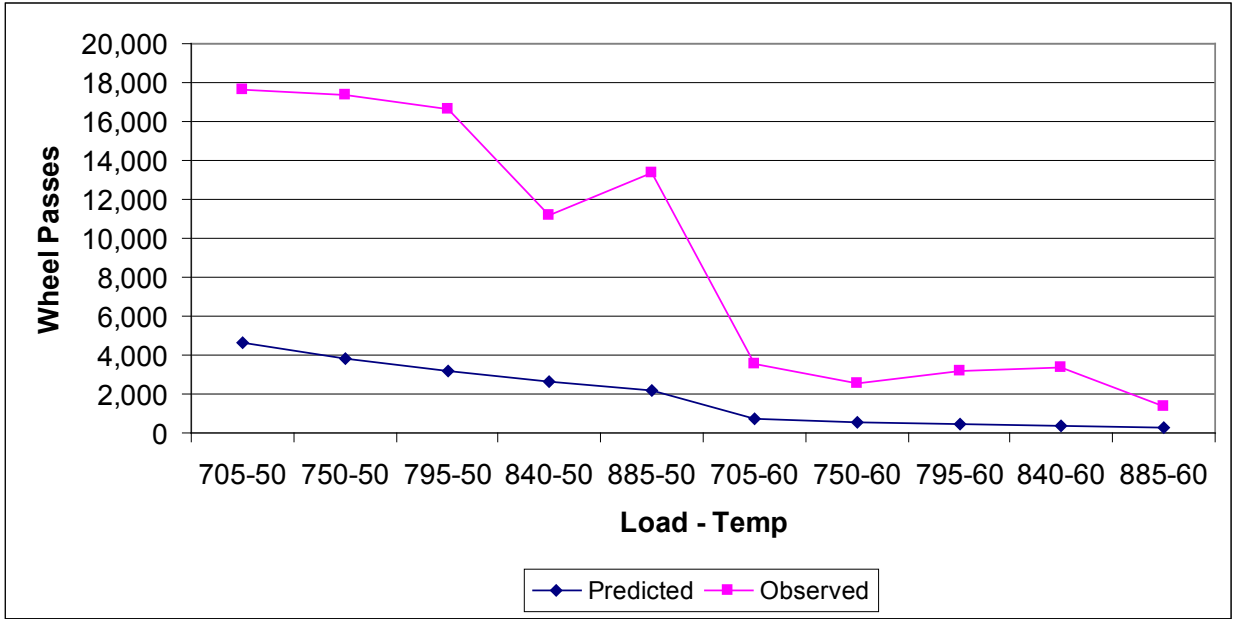


Figure 4.16 Comparison of Predicted with Observed Wheel Passes for US-24 Project with Interaction

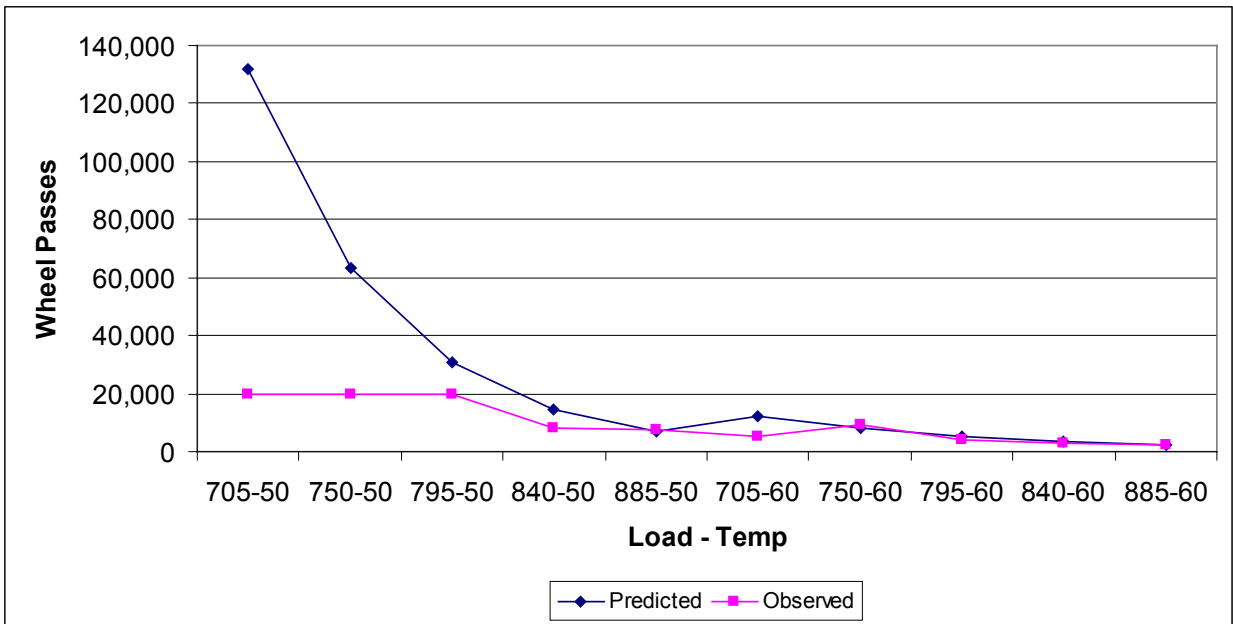


Figure 4.17 Comparison of Predicted with Observed Wheel Passes for US-50 Project with Interaction

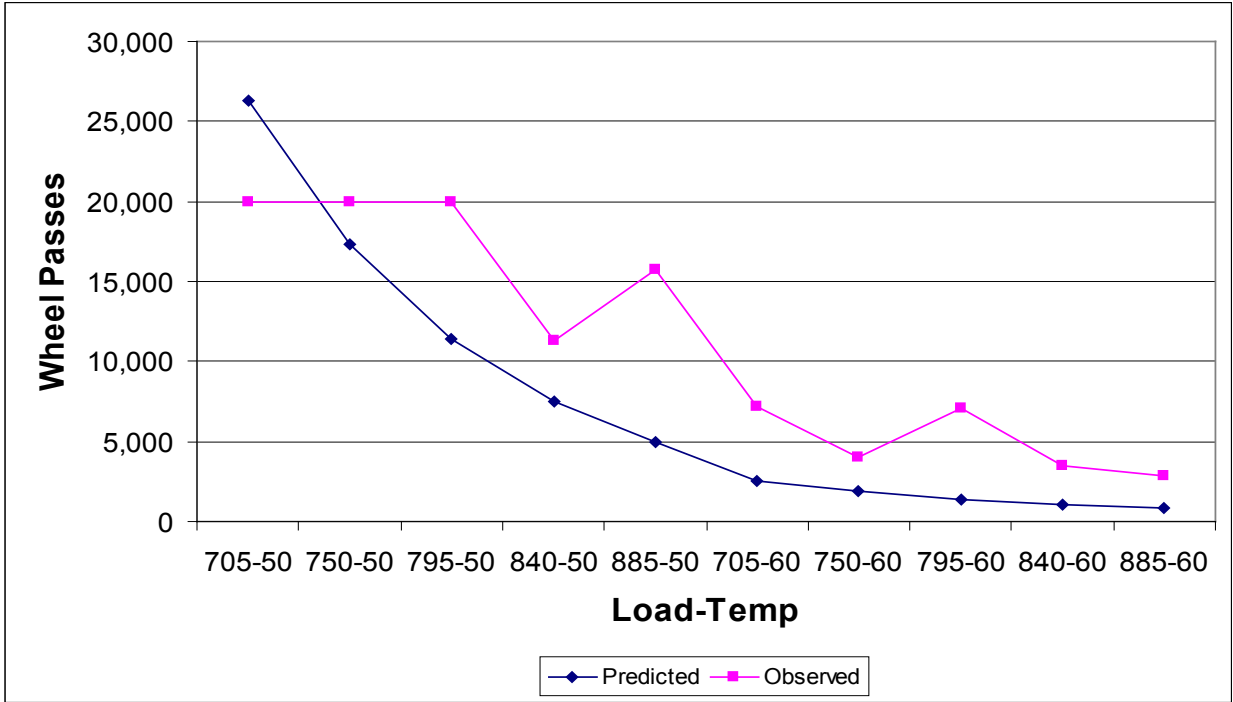


Figure 4.18 Comparison of Predicted with Observed Wheel Passes for US-83 Project with Interaction

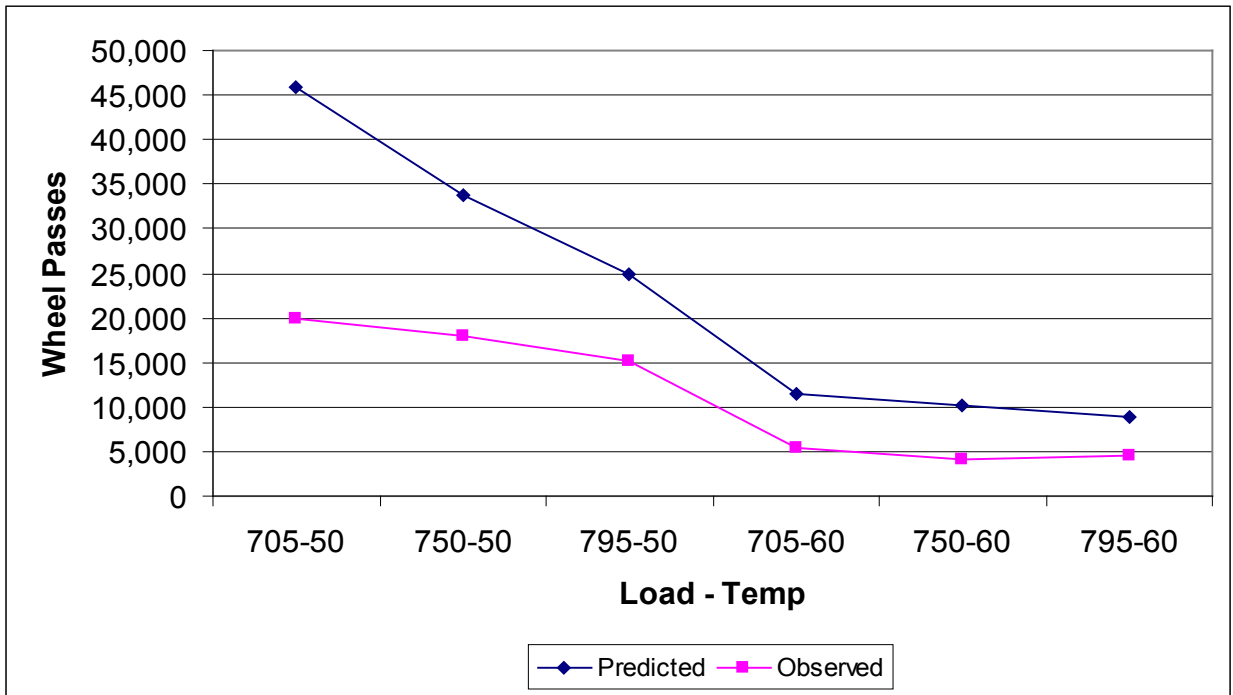


Figure 4.19 Comparison of Predicted with Observed Wheel Passes for CISL-A Project with Interaction

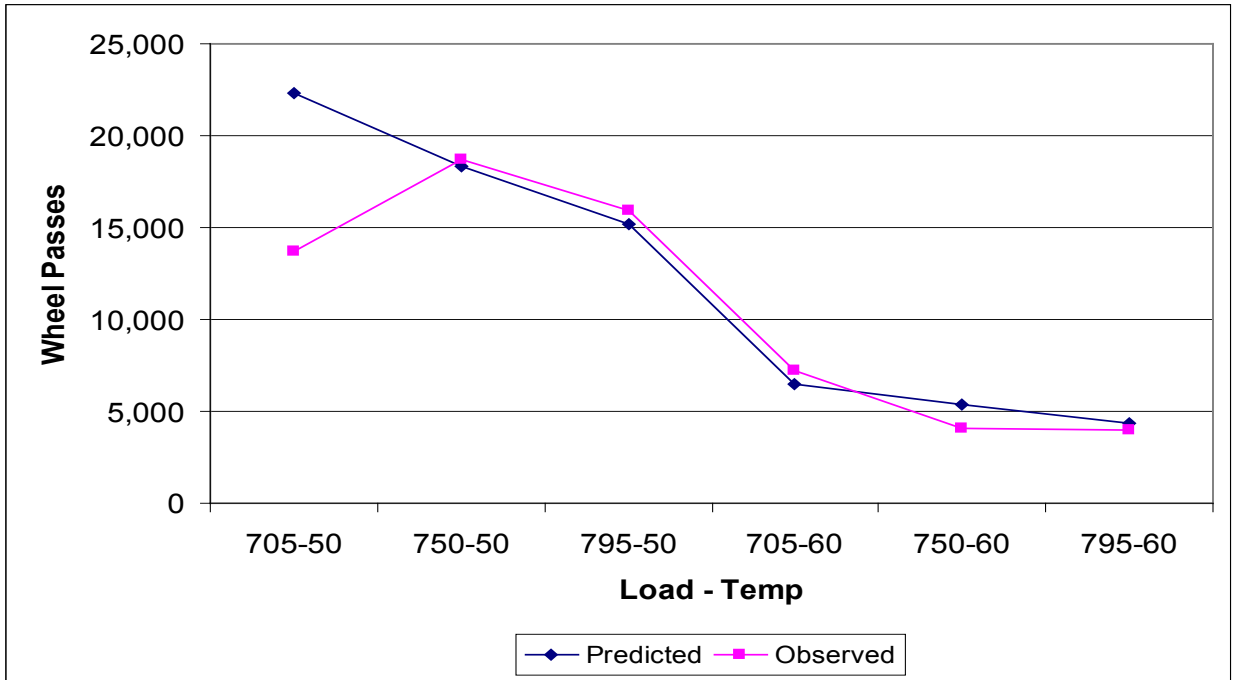


Figure 4.20 Comparison of Predicted with Observed Wheel Passes for K-4 Project Without Interaction

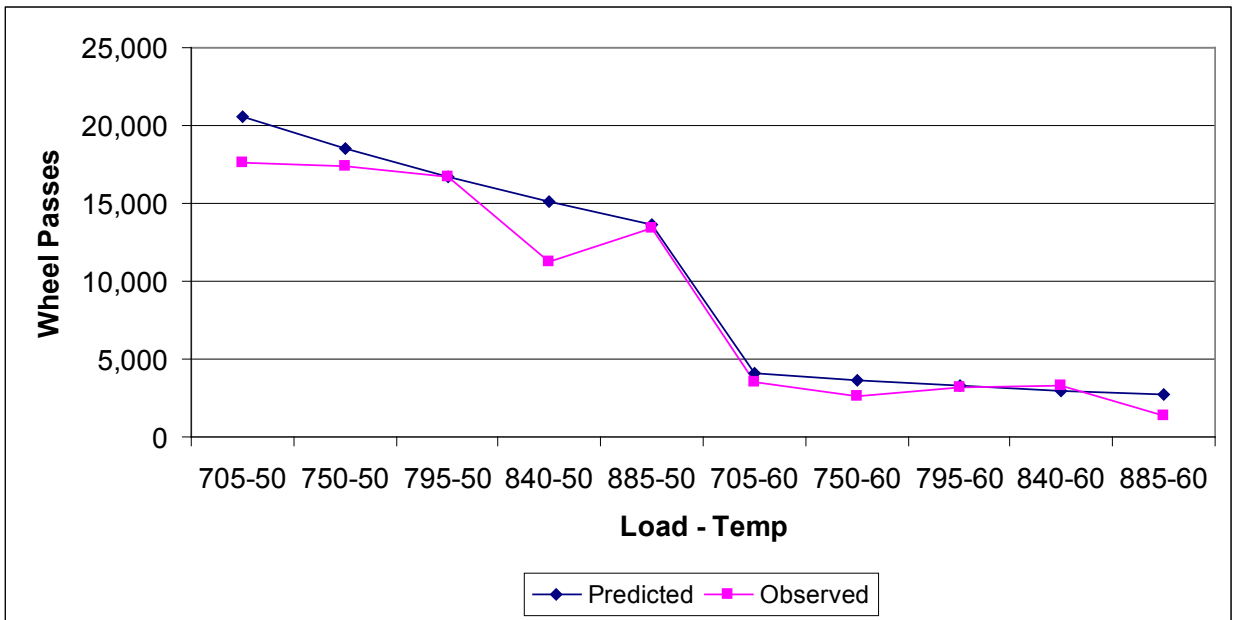


Figure 4.21 Comparison of Predicted with Observed Wheel Passes for US-24 Project Without Interaction

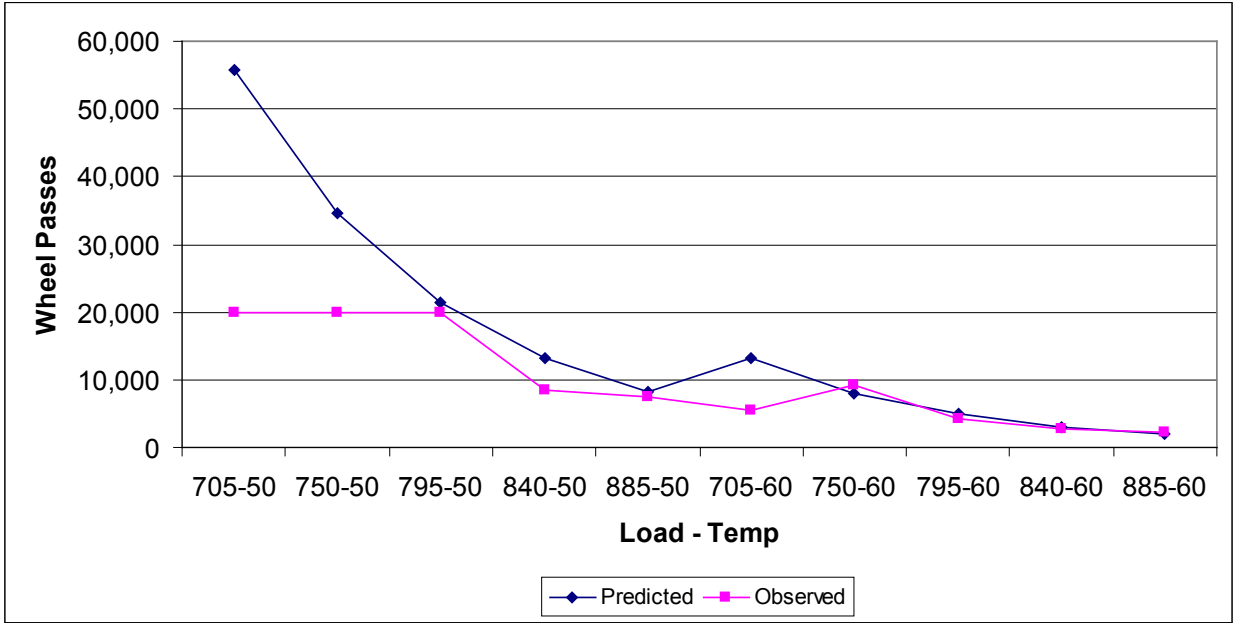


Figure 4.22 Comparison of Predicted with Observed Wheel Passes for US-50 Project Without Interaction

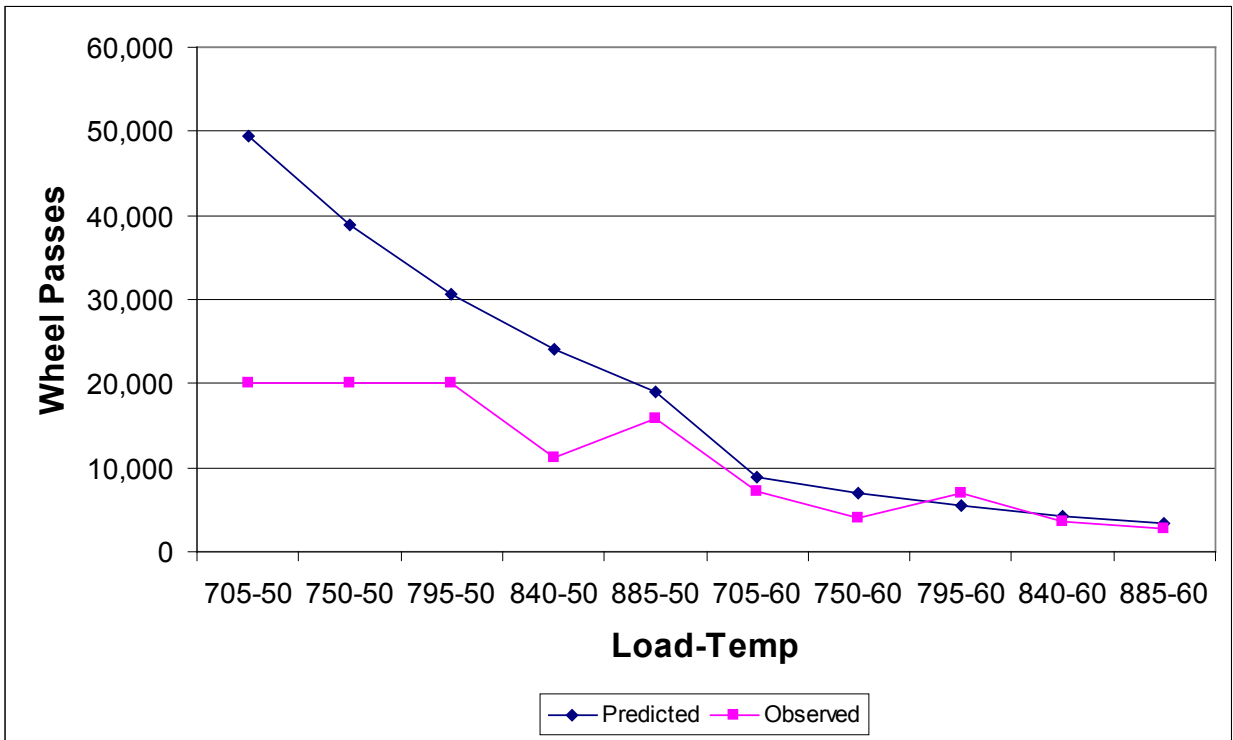


Figure 4.23 Comparison of Predicted with Observed Wheel Passes for US-83 Project Without Interaction

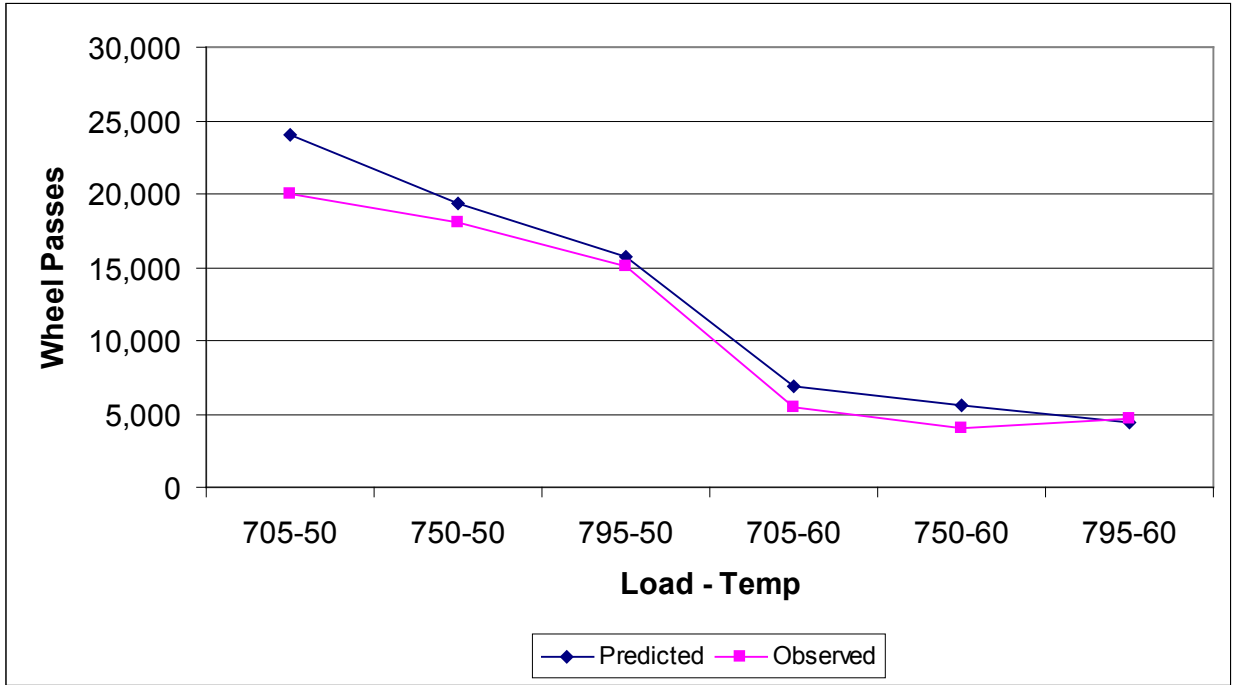
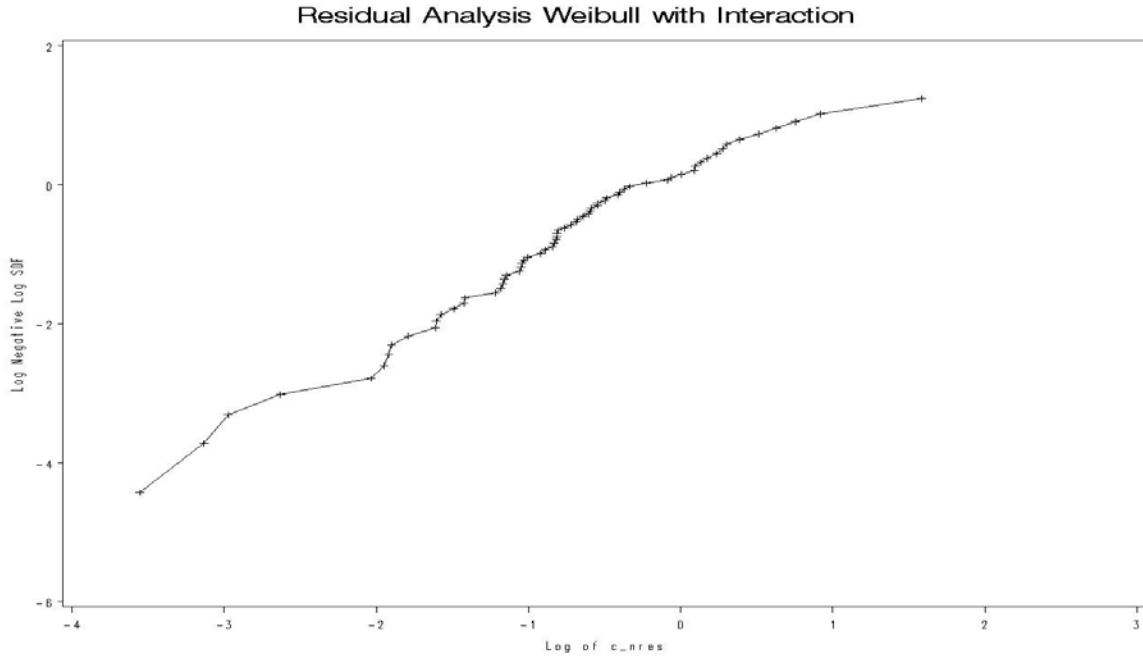
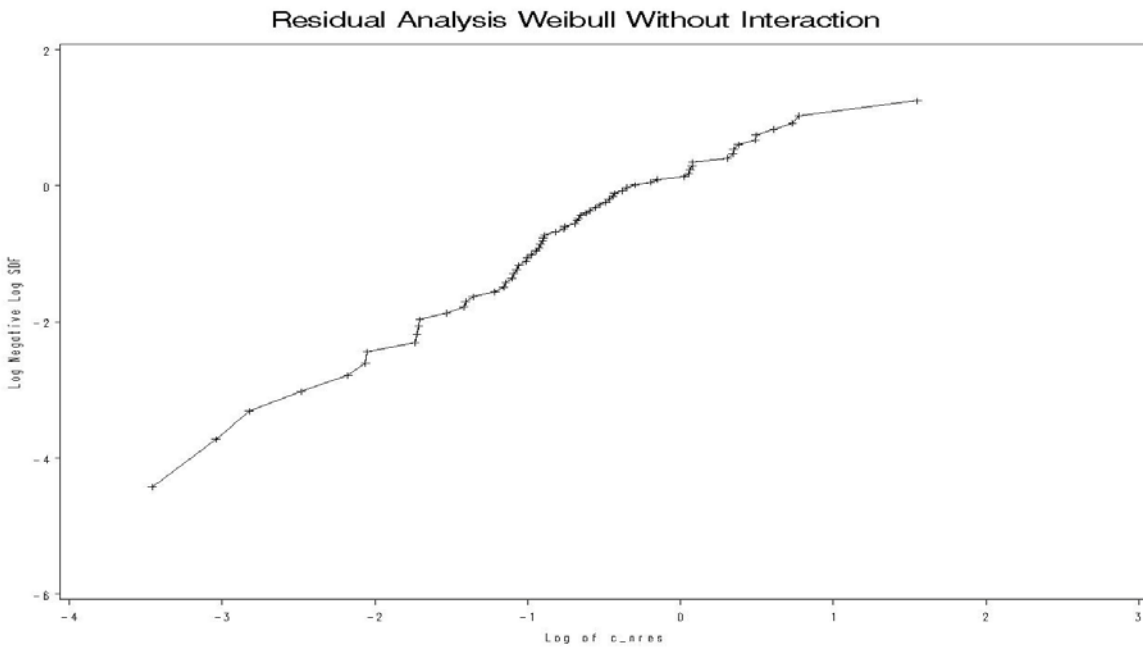


Figure 4.24 Comparison of Predicted with Observed Wheel Passes for CISL-A Project Without Interaction



(a) SAS Plot of Overall Five Projects with Interaction Without CISL-B



(b) SAS Plot of Overall Five Projects Without Interaction Without CISL-B

Figure 4.25 Cox-Snell Residuals To Assess the Fit of Weibull Regression Model

Figure 4.25 (a) shows a plot of residual analysis using the Weibull distribution obtained from SAS for overall data from five projects with interaction between temperature and load levels, excluding CISL-B. Similarly, Figure 4.25 (b) represents similar residual analysis for overall data from five projects excluding CISL-B without interaction terms. Graphical checks are preferred to check the appropriateness rather than formal statistical tests of lack-of-fit, because these tests either tend to have small sample sizes or they always reject a given model for large samples (Klein and Moeschberger 2003). The graphical checks serve as a mean of rejecting clearly inappropriate models (Klein and Moeschberger 2003). Cox-Snell residuals are those which can be used to assess the fit of a parametric accelerated failure time model. Cox-Snell residuals with survival density functions were used for plotting in logarithmic scale as shown in Figure 4.25. In both cases, the plot follows a straight line path at a 45° angle. This plot of residual analysis using the Weibull distribution in Figure 4.25 tells that there is no prominent difference whether taking interaction term between temperature and load levels into the consideration, or not.

Figures 4.26 and 4.27 show the Cox-Snell residual plot analysis of the model for the K-4 project. The “goodness of fit” in this case is indicated by the predicted and observed values falling around the 45° line.

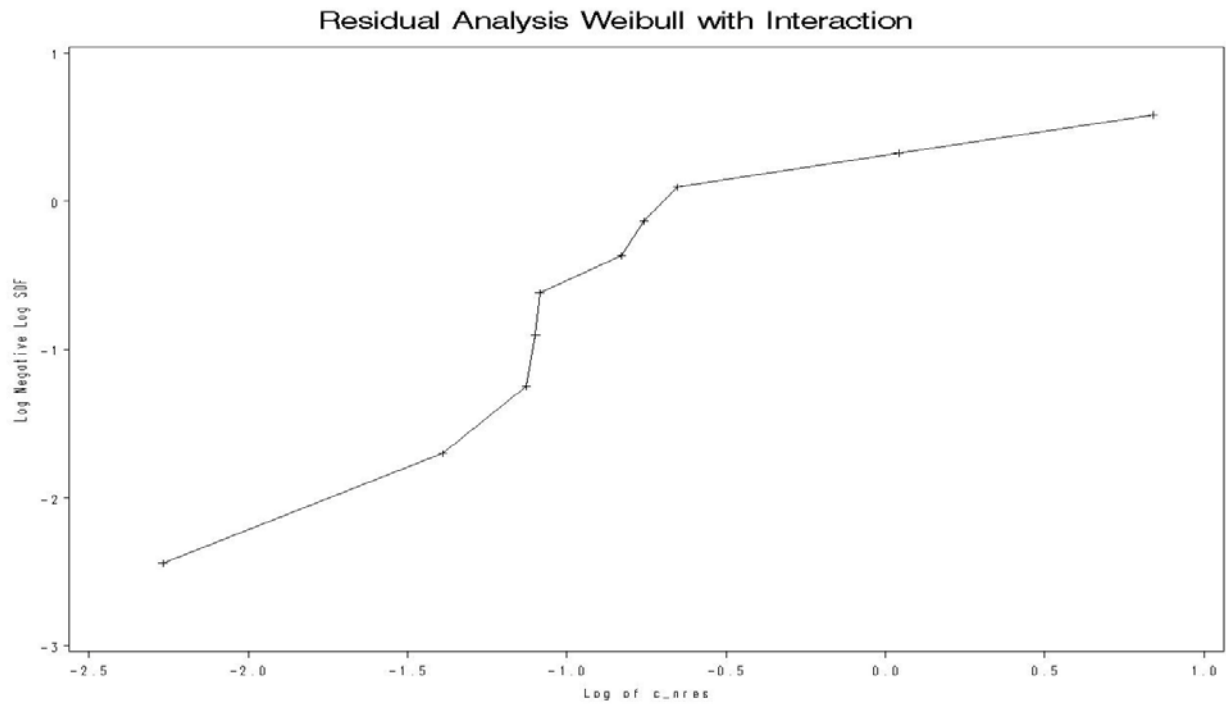


Figure 4.26 Cox-Snell Residual Weibull Plot with Interaction of Load and Temperature for K-4 Project

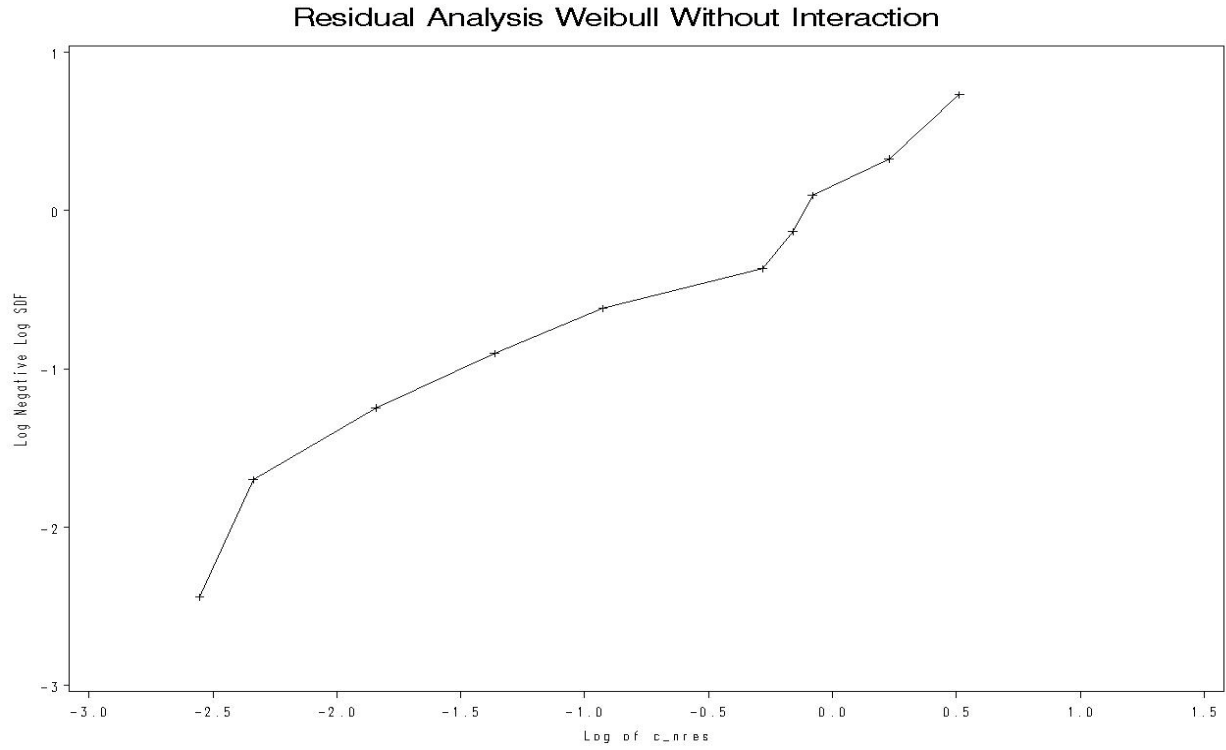


Figure 4.27 Cox-Snell Residual Weibull Plot Without Interaction of Load and Temperature for K-4 Project

4.5.3 Development of Accelerated Mix Testing Models Considering Effects of Temperature, Load, and Air Voids

The air void was added as a mixture characteristic because it varied from 6% to 8% and its effect on HWTD test results is well known for in-place pavements (Gogula et al. 2003). The Weibull residual analysis plots with SAS indicated no significant difference between the models with interaction of temperature and load levels and models without the interaction terms. Thus, no interaction term was included in the model. The analysis was also done individually for each project since the mixture materials (except the binder for four out of six projects) varied from project to project. An example exponential accelerated life model (a special case of Weibull distribution), given in Equation 4.3, has been fitted to the HWTD test data from K-4 project. Since these models are nonlinear, traditional means of examining “goodness” of linear model, like the coefficient of determination (R^2), is not applicable. Thus a residual plot analysis was done. Table 4.8 presents summary of accelerated mix testing models with temperature, load, and air voids. The developed statistical model for K-4 project without interaction terms is given in Equation (4.3).

$$WP = e^{(19.1588 - 0.12T - 0.004L - 0.0504A)} \quad (4.3)$$

where

WP = wheel passes;

T = temperature ($^{\circ}\text{C}$);

L = load (N); and

A = air voids (%).

Table 4.9 shows the comparison of predicted and observed wheel passes in the HWTD tests. Good agreements between predicted and observed values were observed for most mixtures at almost all lower loads 705 and 750 N (158 and 168 lbs) levels and temperature combinations.

Table 4.8 Summary of Accelerated Mix Testing Models with Temperature, Load, and Air Voids

Route	District	Parameter	Description	Model Without Interaction		
				Estimate	p-value	Significant
K-4	I	Intercept	Vertical Intercept	19.1588	< 0.0001	*
		T	Temperature (°C)	- 0.1200	< 0.0001	*
		L	Load (N)	- 0.0040	0.0562	*
		A	Air Voids (%)	- 0.0504	0.8084	
US-24	III	Intercept	Vertical Intercept	19.9521	< 0.0001	*
		T	Temperature (°C)	- 0.1618	< 0.0001	*
		L	Load (N)	- 0.0021	0.0180	*
		A	Air Voids (%)	- 0.0836	0.4521	
US-50	V	Intercept	Vertical Intercept	28.8328	< 0.0001	*
		T	Temperature (°C)	- 0.1560	< 0.0001	*
		L	Load (N)	- 0.0120	< 0.0001	*
		A	Air Voids (%)	-0.1995	0.4941	
US-83	VI	Intercept	Vertical Intercept	24.2580	< 0.0001	*
		T	Temperature (°C)	- 0.1643	< 0.0001	*
		L	Load (N)	- 0.0060	0.0023	*
		A	Air Voids (%)	-0.1675	0.4409	
CISL-A	I	Intercept	Vertical Intercept	33.8756	0.0005	*
		T	Temperature (°C)	- 0.1406	< 0.0001	*
		L	Load (N)	- 0.0122	0.0246	*
		A	Air Voids (%)	- 1.0209	0.1076	**
CISL-B	N/A	Intercept	Vertical Intercept	N/A	N/A	
		T	Temperature (°C)	N/A	N/A	
		L	Load (N)	N/A	N/A	
		A	Air Voids (%)	N/A	N/A	
All Projects		Intercept	Vertical Intercept	20.0357	< 0.0001	*
		T	Temperature (°C)	- 0.1417	< 0.0001	*
		L	Load (N)	- 0.0060	0.0001	*
		A	Air Voids (%)	0.2968	0.0094	*

NOTES: * Significant at 5% level of significance; ** Significant at 10% level of significance; and N/A – not available.

However, greater discrepancy was observed at higher temperature and higher load levels, possibly indicating very accelerated failures of the mixtures under those combinations. The deviation of predicted number of wheel passes from observed HWTD test results is up to 38% for K-4, up to 46% for US-24, up to 69% for US-50, and up to 66 % for US-83, and CISL-A project. For all mixtures, about 7,000 repetitions were needed for failure at this test temperature and load level. This would translate to slightly more than two hours of testing time (about 2 hours 15 minutes) in the HWTD test.

Table 4.9 Comparison of Model Predicted with Observed Wheel Passes

Temp. (°C)	Load (N)	K-4			US-24			US-50			US-83			CISL-A		
		Predicted WP	Observed WP	% Diff.	Predicted WP	Observed WP	% Diff.	Predicted WP	Observed WP	% Diff.	Predicted WP	Observed WP	% Diff.	Predicted WP	Observed WP	% Diff.
50	705	22,275*	13,700	38.5	18,272	17,625	3.5	64,637*	20,000	69.1	59,353*	20,000	66.3	59,648*	20,000	66.5
50	750	19,371	18,730	3.3	18,533	17,390	6.2	43,313*	20,000	53.8	39,626*	20,000	49.5	18,670	18,070	3.2
50	795	15,698	15,950	-1.6	17,146	16,650	2.9	22,844*	20,000	12.5	35,172*	20,000	43.1	14,646	15,055	-2.8
50	840	N/A	N/A	N/A	14,469	11,210	22.5	13,049	8,420	35.5	27,764*	11,260	59.4	N/A	N/A	N/A
50	885	N/A	N/A	N/A	13,055	13,385	-2.5	7,605	7,450	2.0	22,287*	15,770	29.2	N/A	N/A	N/A
60	705	6,642	7,230	-8.9	4,006	3,535	11.7	12,541	5,355	57.3	11,479	7,145	37.8	6,461	5,390	16.6
60	750	5,520	4,075	26.2	3,675	2,565	30.2	8,573	9,150	-6.7	9,061	3,970	56.2	5,068	4,020	20.7
60	795	4,681	3,995	14.6	3,344	3,180	4.9	4,800	4,295	10.5	6,469	7,025	-8.6	4,403	4,625	-5.0
60	840	N/A	N/A	N/A	2,822	3,335	-18.2	3,217	2,640	17.9	5,193	3,500	32.6	N/A	N/A	N/A
60	885	N/A	N/A	N/A	2,589	1,400	45.9	2,155	2,170	-0.7	3,646	2,845	22.0	N/A	N/A	N/A

NOTES: WP – wheel passes; % Diff. – percent difference; * – predicted value exceeding threshold of 20,000 passes in the HWTB test; and N/A – not available.

Figures 4.28 to 4.32 show comparison plots of predicted with observed wheel passes for individual projects without interaction. Similarly, Figure 4.33 shows comparison plots of predicted with observed wheel passes for all six projects without interaction.

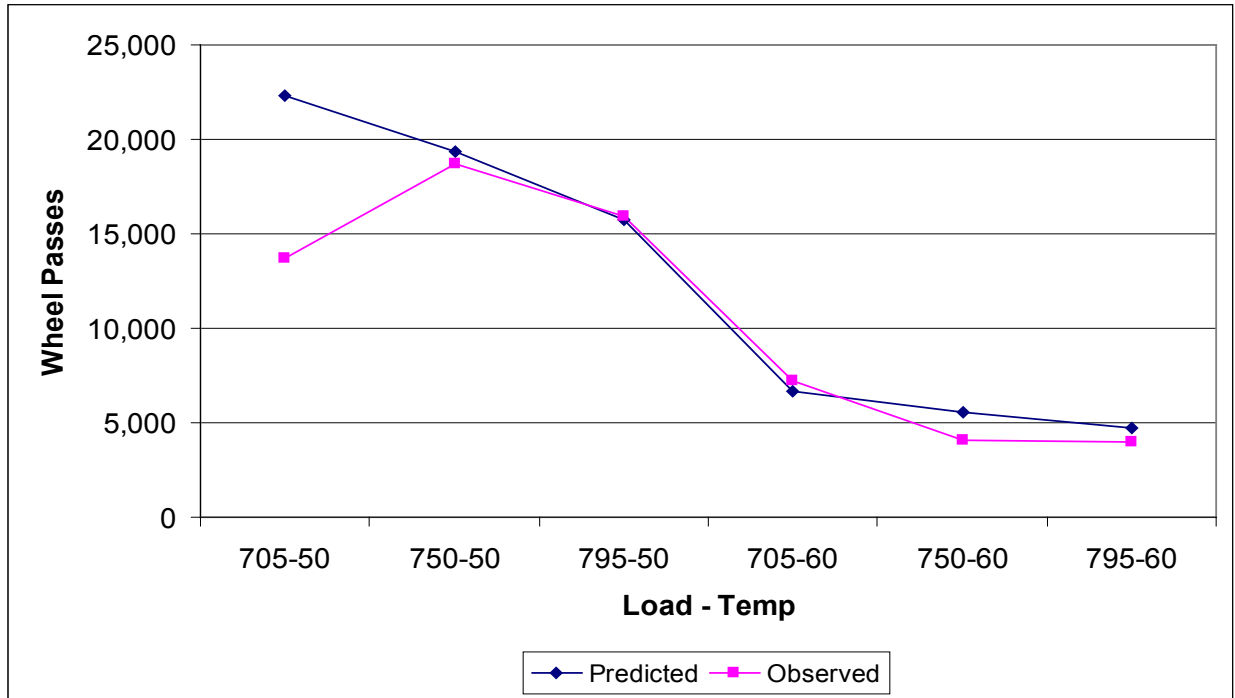


Figure 4.28 Comparison of Predicted with Observed Wheel Passes for K-4 Project Without Interaction

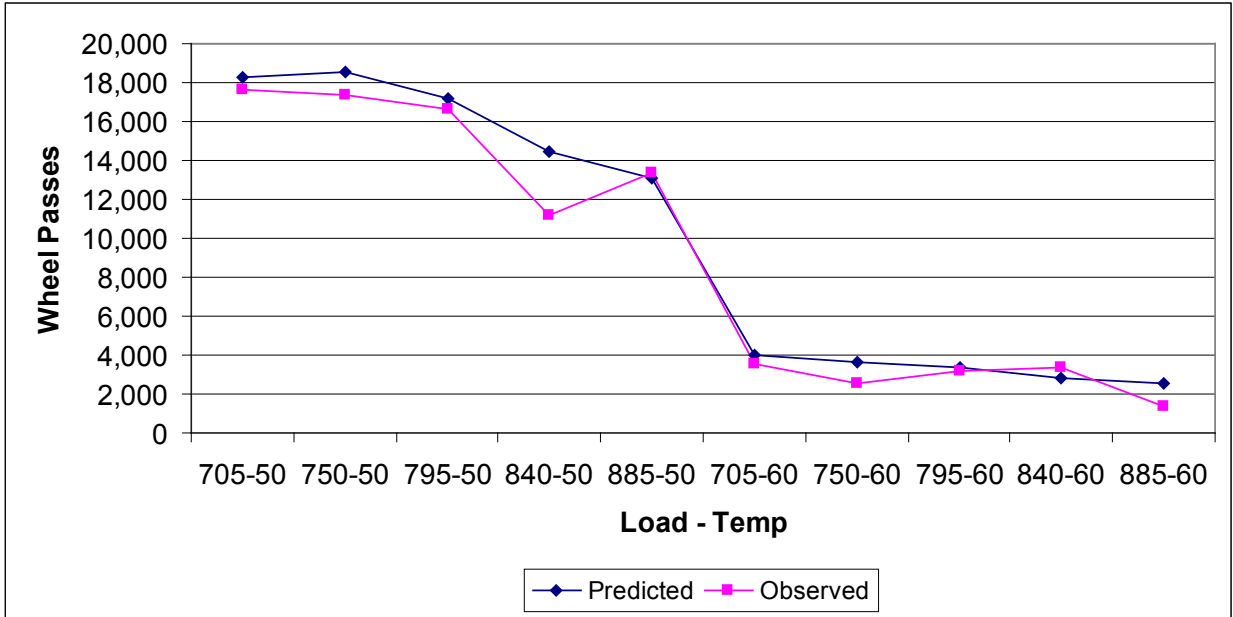


Figure 4.29 Comparison of Predicted with Observed Wheel Passes for US-24 Project Without Interaction

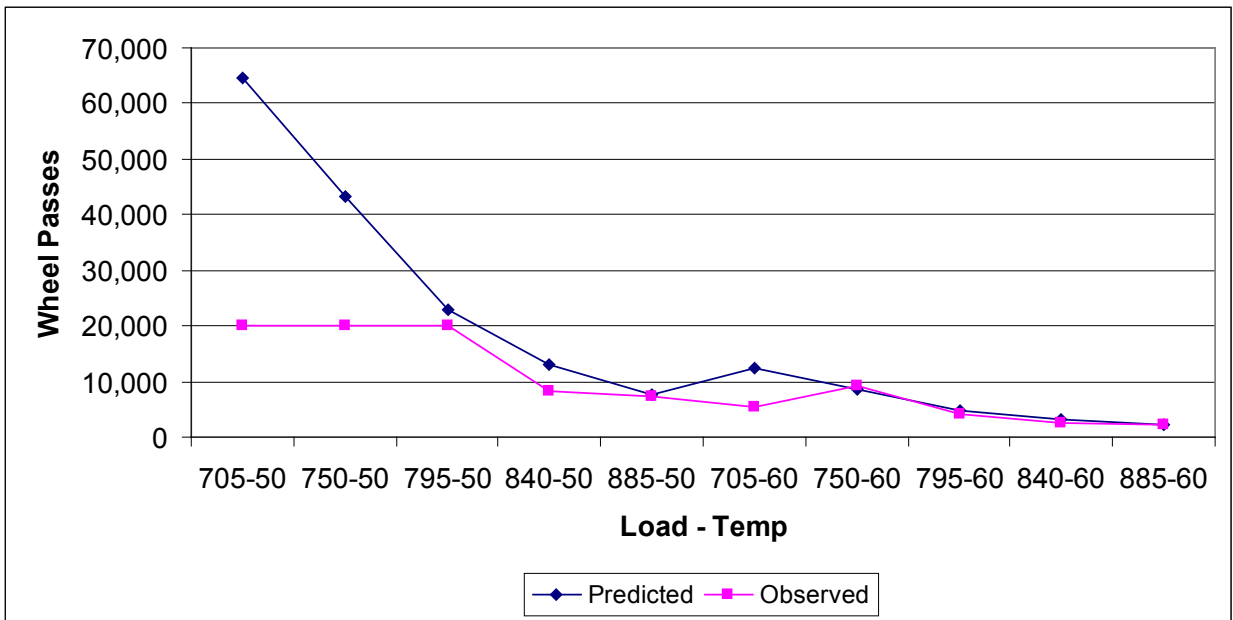


Figure 4.30 Comparison of Predicted with Observed Wheel Passes for US-50 Project Without Interaction

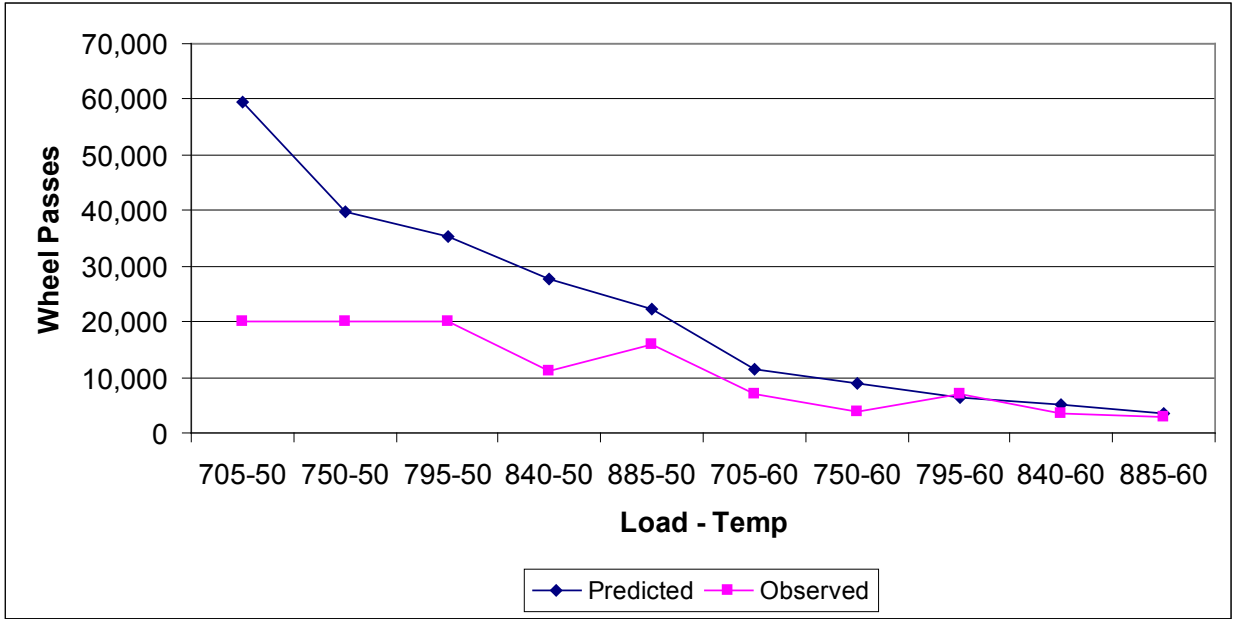


Figure 4.31 Comparison of Predicted with Observed Wheel Passes for US-83 Project Without Interaction

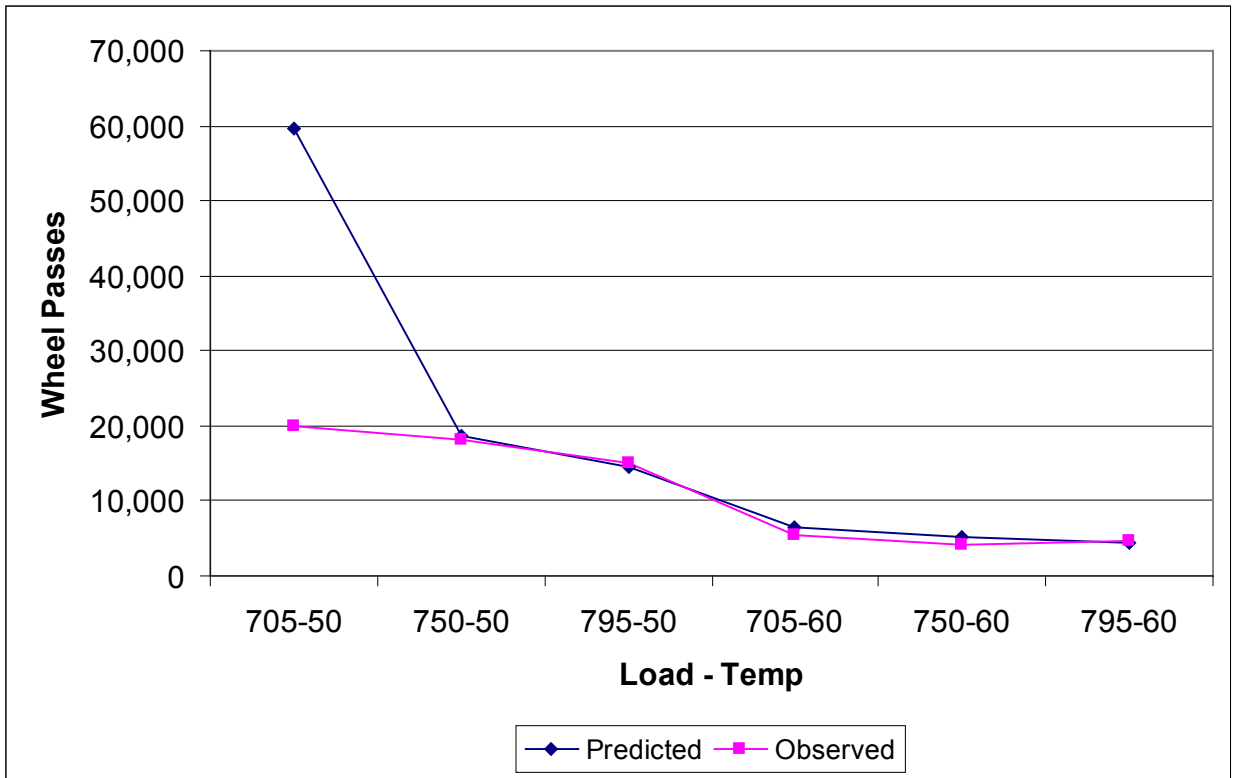


Figure 4.32 Comparison of Predicted with Observed Wheel Passes for CISL-A Project Without Interaction

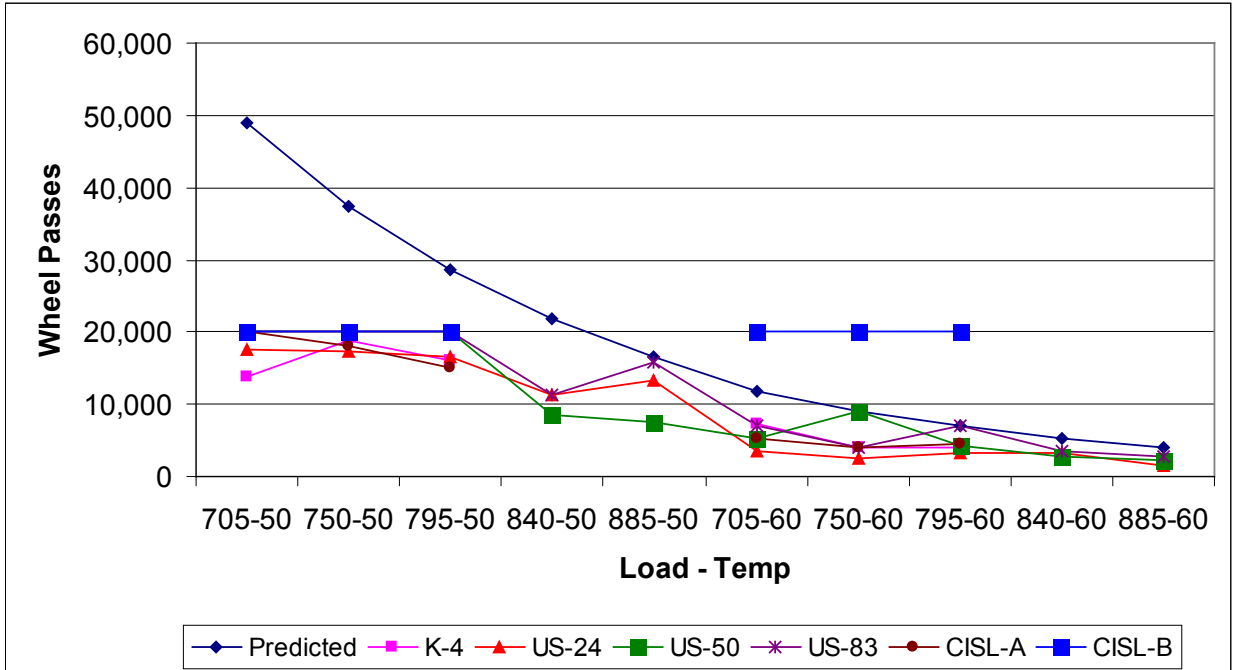


Figure 4.33 Comparison of Predicted with Observed Wheel Passes for All Projects Without Interaction

Table 4.10 shows comparison of HWTD results of the model predicted with observed wheel passes for mixtures from the field without interaction. The individual model developed from laboratory samples of the K-4 project in District I was used for predicting number of wheel passes and compared with observed HWTD test results of K-4 project field cores. The deviation of predicted results in the K-4 project from observed HWTD test results is within 16%, which is reasonable. It indicates the developed accelerated mix testing model can predict performance of the mix very well. Similarly, the model developed from laboratory samples of the US-24 project in District III was used to predict number of wheel passes and compared with HWTD test results of the K-258 project field cores. The mixture used in the K-258 project and the US-24 project was same. In this case, the variation between predicted number of wheel passes and observed number of wheel passes is up to 38%. Similarly, the variation between predicted with observed HWTD test results in the US-83 project field cores is up to 48%.

Table 4.10 Comparison of HWTD Results and Model-Predicted Wheel Passes for Field Cores

Temp. (°C)	Load (N)	K-4				K-258				US-83			
		Air Voids (%)	Predicted WP	Observed WP	% Diff.	Air Voids (%)	Predicted WP	Observed WP	% Diff.	Air Voids (%)	Predicted WP	Observed WP	% Diff.
50	705	9.6	19,053	17,290	9.3	7.9	16,667	14,270	14.4	9.1	29,400*	15,210	48.3
50	750	9.3	16,157	18,020	-11.5	6.8	16,624	15,420	7.2	7.7	28,375*	18,530	34.7
50	795	9.2	13,563	15,130	-11.6	7.4	14,385	10,750	25.3	8.2	19,920	15,070	24.3
60	705	9.4	5,797	4,860	16.2	7.0	3,563	2,870	19.5	9.1	5,686	3,150	44.6
60	750	9.4	4,842	4,590	5.2	9.3	2,675	3,690	-38.0	7.6	5,580	3,310	40.7
60	795	9.6	4,004	3,660	8.6	8.5	2,602	2,450	5.8	8.9	3,426	2,720	20.6

NOTES: WP – wheel passes; % Diff. – percent difference; and * – predicted value exceeding threshold of 20,000 passes in the HWTD test.

Table 4.11 summarizes accelerated mix testing models developed for all five individual projects and a combined model for all projects without interaction between variables, considering effects of temperature, load, and air voids of Superpave asphalt mixture.

Table 4.11 Accelerated Mix Testing Models

Route	District	Accelerated Mix Testing Models
K-4	I	Wheel Passes = exp (19.1588 - 0.1200 T - 0.0040 L - 0.0504 A)
US-24	III	Wheel Passes = exp (19.9521 - 0.1618 T - 0.0021 L - 0.0836 A)
US-50	V	Wheel Passes = exp (28.8328 - 0.1560 T - 0.0120 L - 0.1995 A)
US-83	VI	Wheel Passes = exp (24.2580 - 0.1643 T - 0.0060 L - 0.1675 A)
CISL-A	I	Wheel Passes = exp (33.8756 - 0.1406 T - 0.0122 L - 1.0209 A)
All Projects		Wheel Passes = exp (20.0357 - 0.1417 T - 0.0060 L + 0.2968 A)

4.6 Mixtures from the Field

4.6.1 Field Coring and Testing

Field coring sites were selected in three KDOT district projects (District I, III, and VI). Cored samples were brought to the laboratory and tested in HWTD tests under three load levels 705, 750, and 795 N (158, 168, and 178 lbs) and two temperature levels 50 °C and 60 °C (122 °F and 140 °F). Cores at a project location were usually collected from the right wheel paths, except US-83, where samples were cored from the southbound shoulder since the design asphalt mix was used in the shoulder. Cores were cut to make 62-mm-thick (2.4-in-thick) HWTD samples. If some samples were shorter, Plaster of Paris was used to make 62-mm (2.4-in) samples prior to testing. Two cores from each project were used to test maximum theoretical specific gravity (G_{mm}) of loose asphalt mix. Twenty-four cores (six sets) were used for HWTD tests from each project. All cores also underwent bulk specific gravity (G_{mb}) tests. Air voids for each core were computed prior to testing.

4.6.2 HWTD Test Results and Field Verification Considering Effects of Temperature and Load

Table 4.12 shows the average number of wheel passes in the HWTD tests of the cored samples from District I, III, and VI. Figures 4.34, 4.35, and 4.36 show HWTD test results of field cores from K-4, K-258, and US-83 projects, respectively. More pronounced effect of temperature increment compared to load increment is clearly evident. Figures 4.37 to 4.42 show the comparison of laboratory-prepared samples and field cores at various load and temperature levels. In most cases, the number of wheel passes at a temperature level of 60 °C (140 °F) was less or equal to 5,000, which translates into a test duration of approximately two hours.

Table 4.12 Summary of Hamburg Wheel Test Results of Cored Samples (Average number of wheel passes)

Route	District	% Asphalt Content	Temp. (°C)	HWTD Test Results of Observed Wheel Passes at					
				Load (705 N)		Load (750 N)		Load (795 N)	
				Wheel Passes	% Air Voids	Wheel Passes	% Air Voids	Wheel Passes	% Air Voids
K-4	I	4.9	50	17,290	9.6	18,020	9.3	15,130	9.2
			60	4,860	9.4	4,590	9.4	3,660	9.6
K-258	III	5.0	50	14,270	7.9	15,420	6.8	10,750	7.4
			60	2,870	7.0	3,690	9.3	2,450	8.5
US-83	VI	4.9	50	15,210	9.1	18,530	7.7	15,070	8.2
			60	3,150	9.1	3,310	7.6	2,720	8.9

NOTES:

Wheel Passes – Number of wheel passes to 20-mm (0.8-in.) rut depth;

% Air voids – Actual air voids of Hamburg samples of the field cores; and

Failure criteria: 20-mm (0.8 in.) maximum rut depth or 20,000 wheel passes whichever comes first..

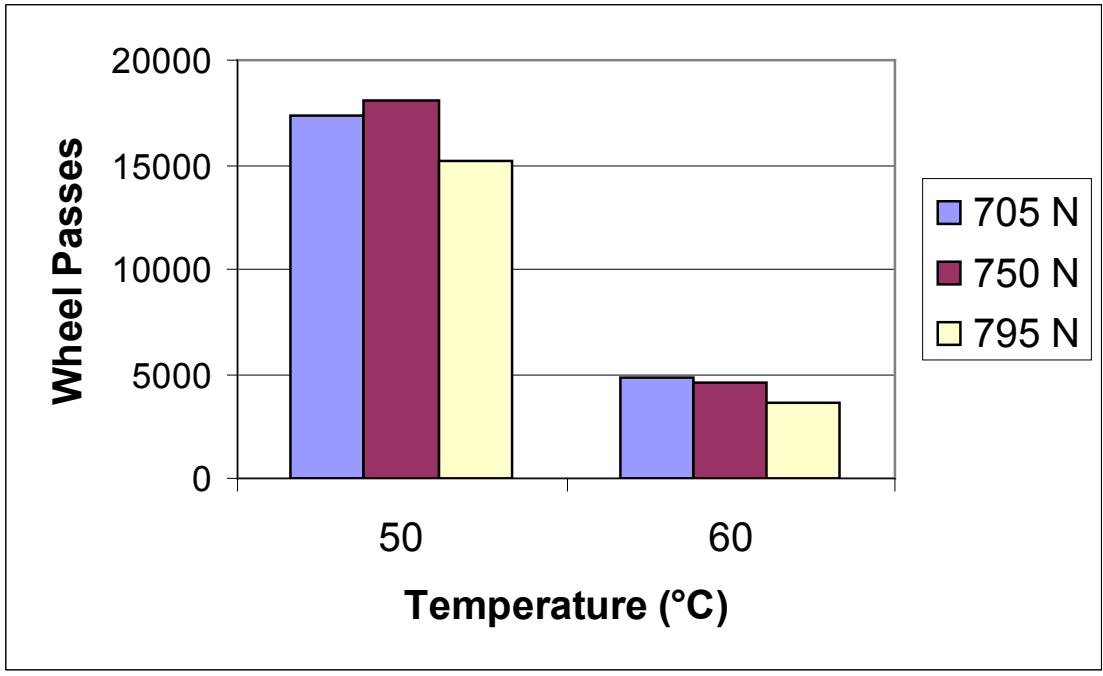


Figure 4.34 HWTD Test Results of K-4 Cores

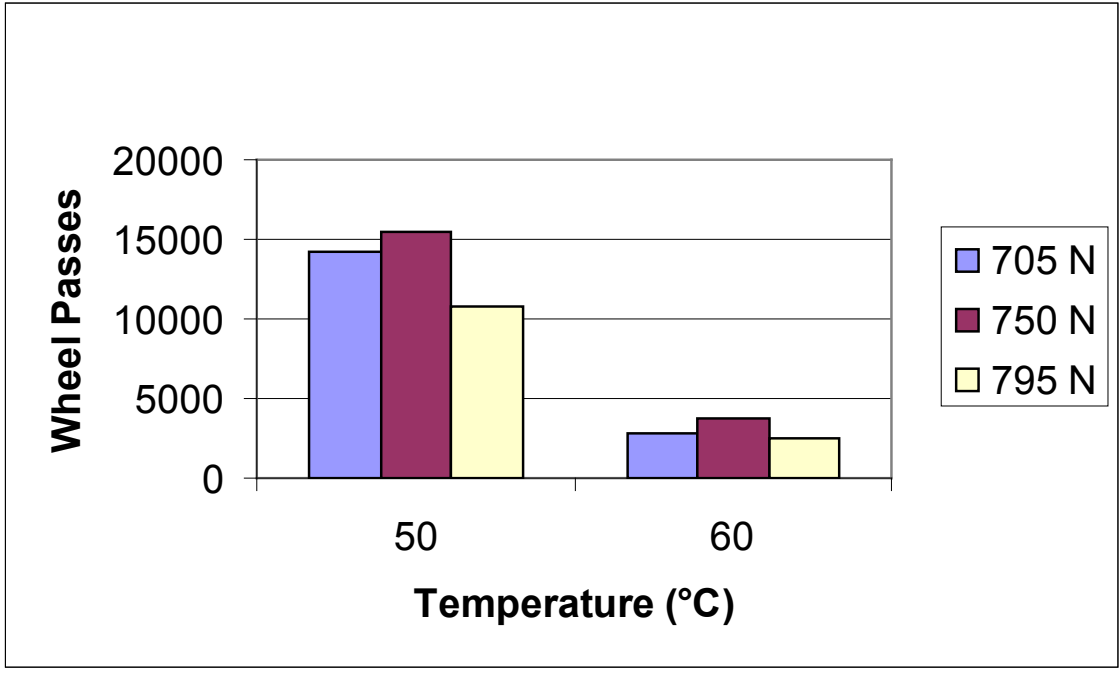


Figure 4.35 HWTD Test Results of K-258 Cores

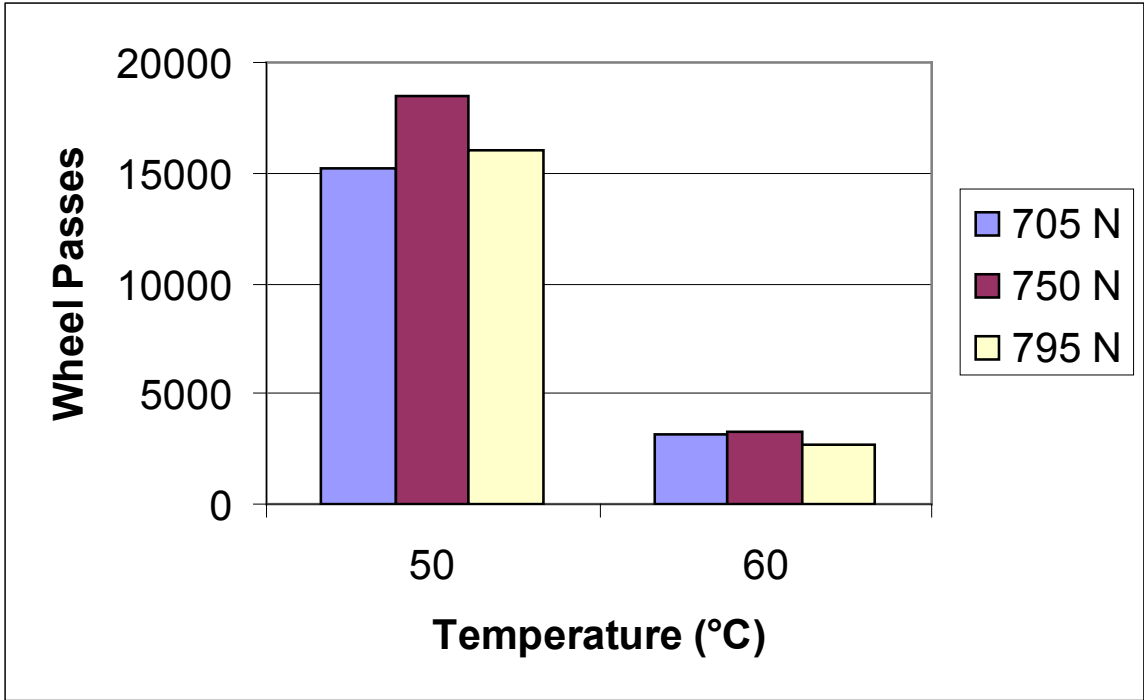


Figure 4.36 HWTD Test Results of US-83 Cores

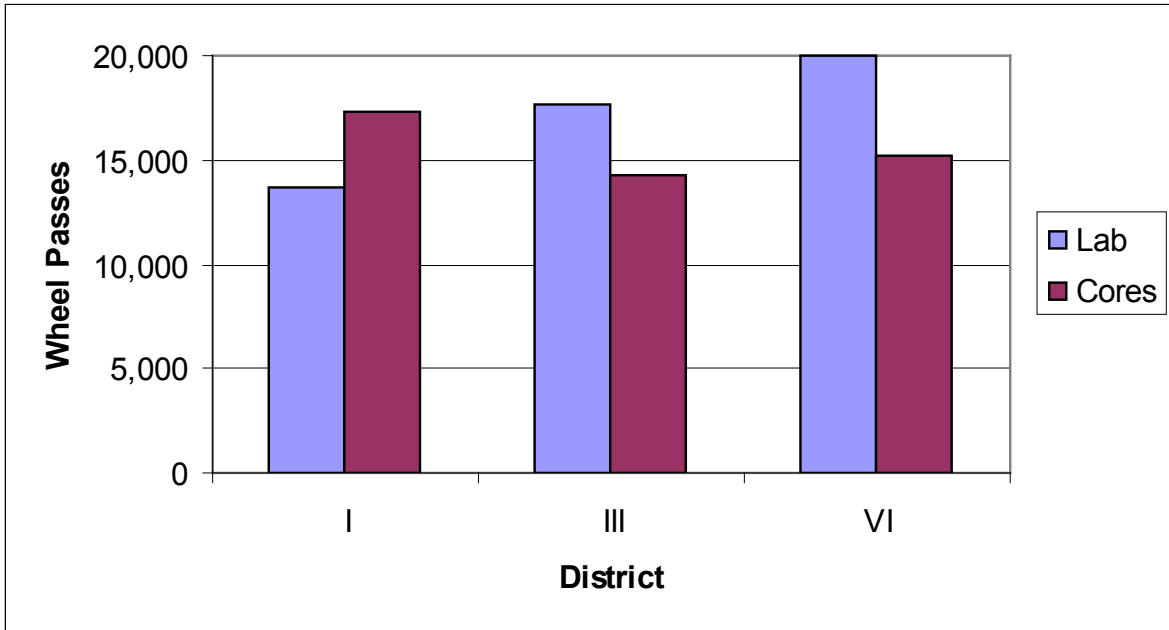


Figure 4.37 Comparison of HWTD Test Results of Laboratory Samples with Field Cores for 705 N Load at 50°C

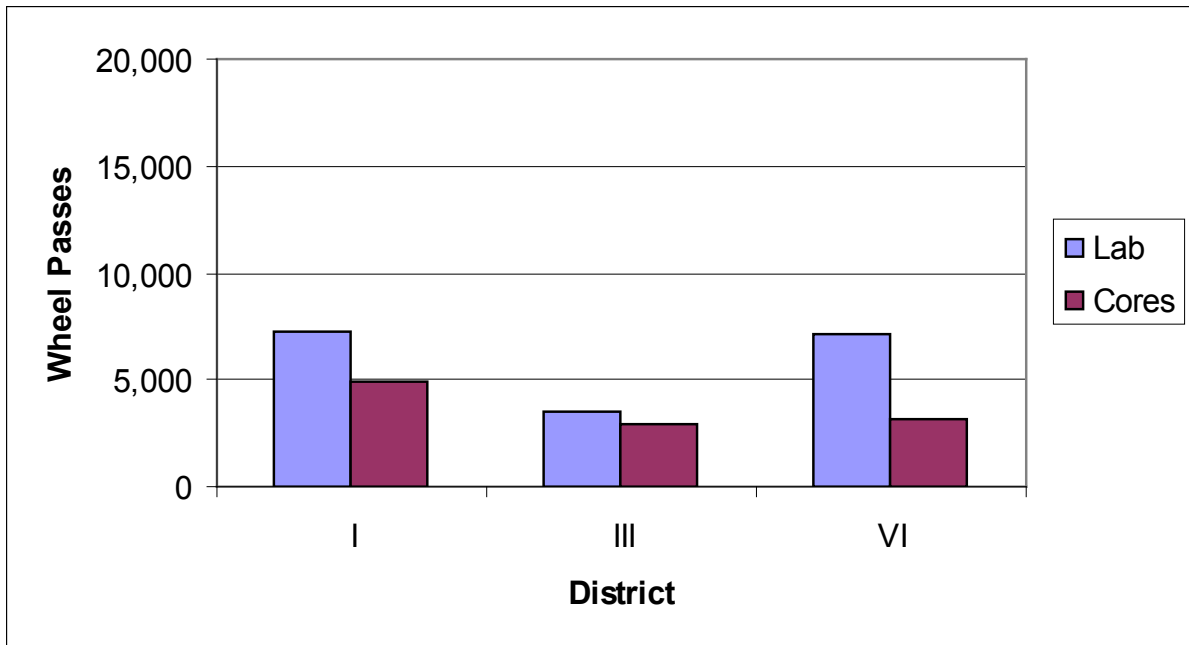


Figure 4.38 Comparison of HWTD Test Results of Laboratory Samples with Field Cores for 705 N Load at 60°C

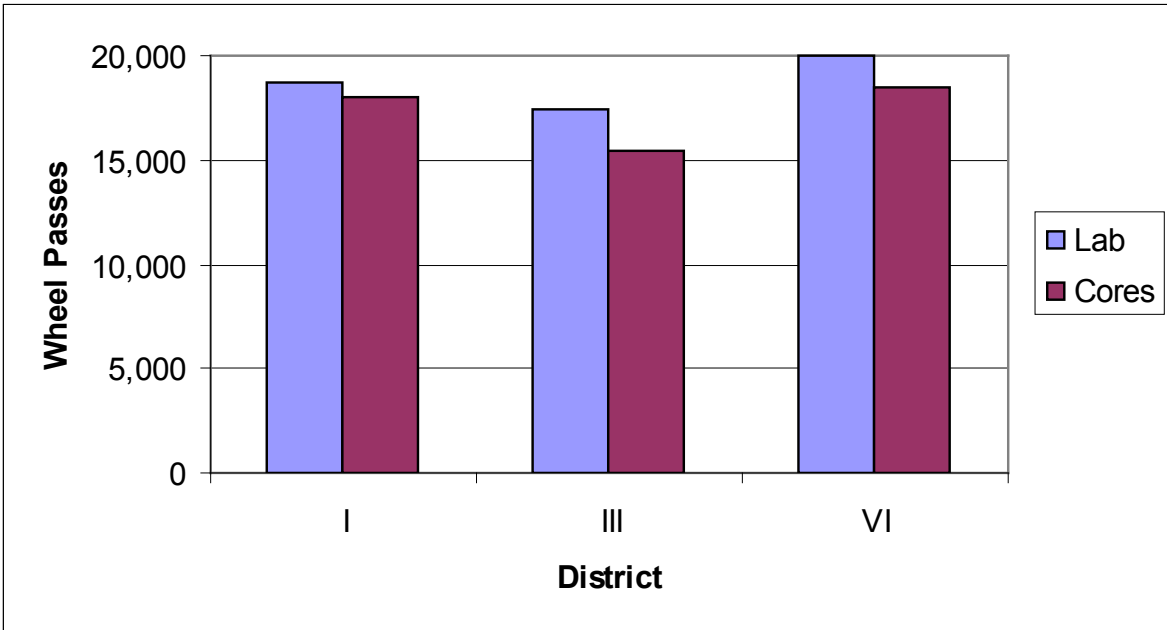


Figure 4.39 Comparison of HWTD Test Results of Laboratory Samples with Field Cores for 750 N Load at 50°C

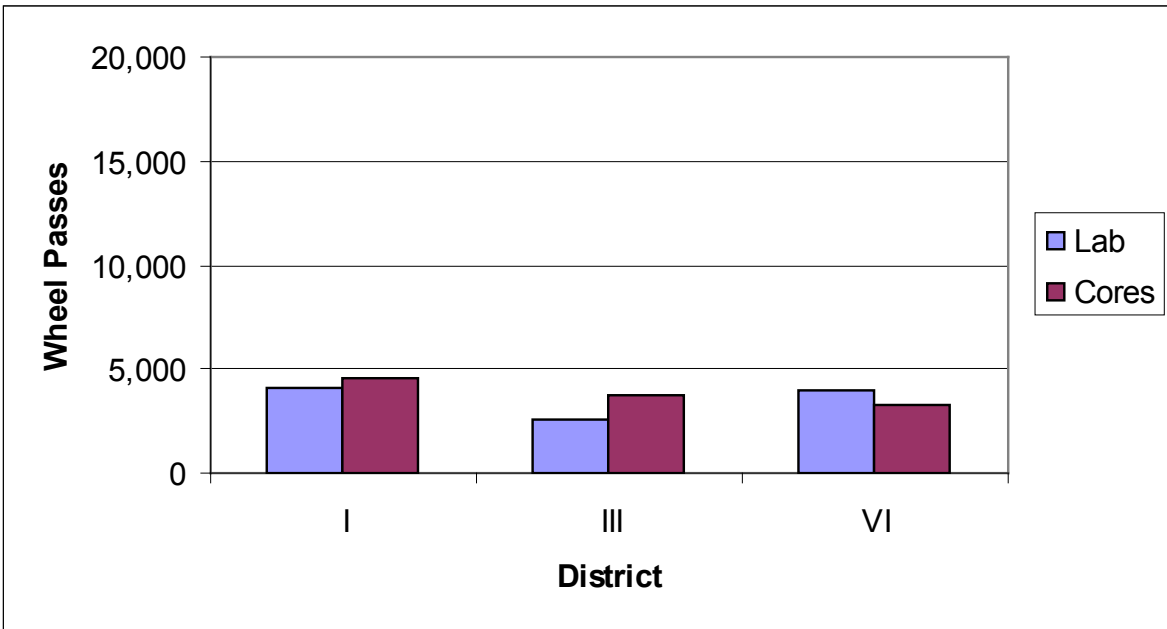


Figure 4.40 Comparison of HWTD Test Results of Laboratory Samples with Field Cores for 750 N Load at 60°C

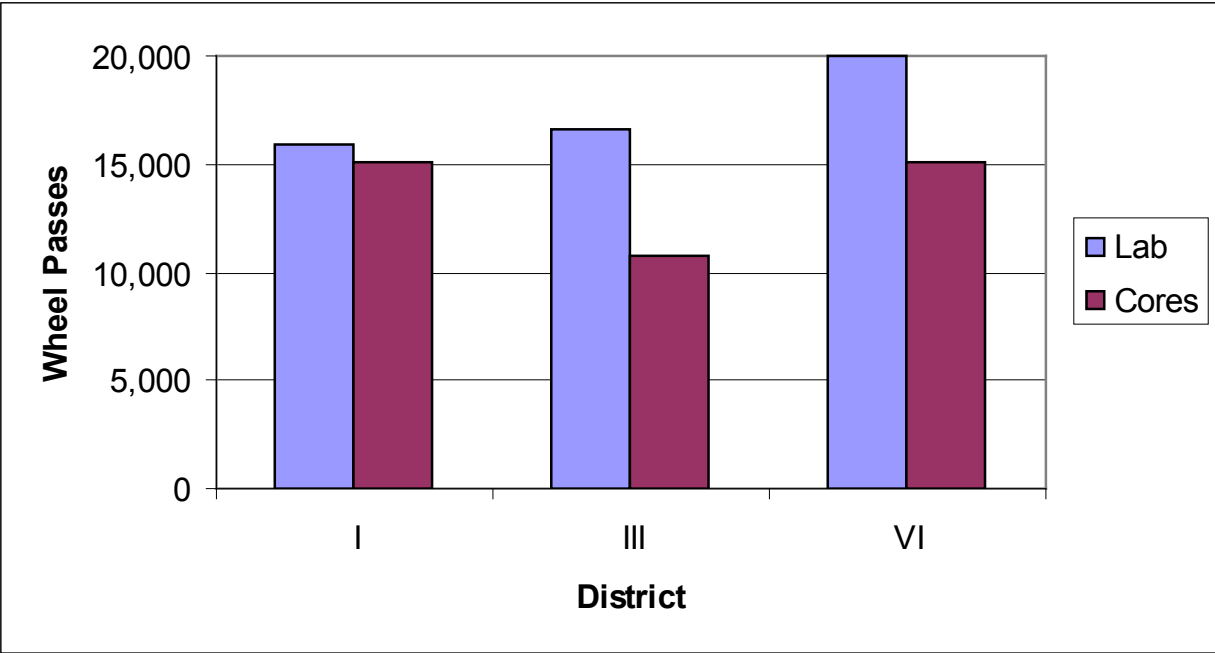


Figure 4.41 Comparison of HWTD Test Results of Laboratory Samples with Field Cores for 795 N Load at 50°C

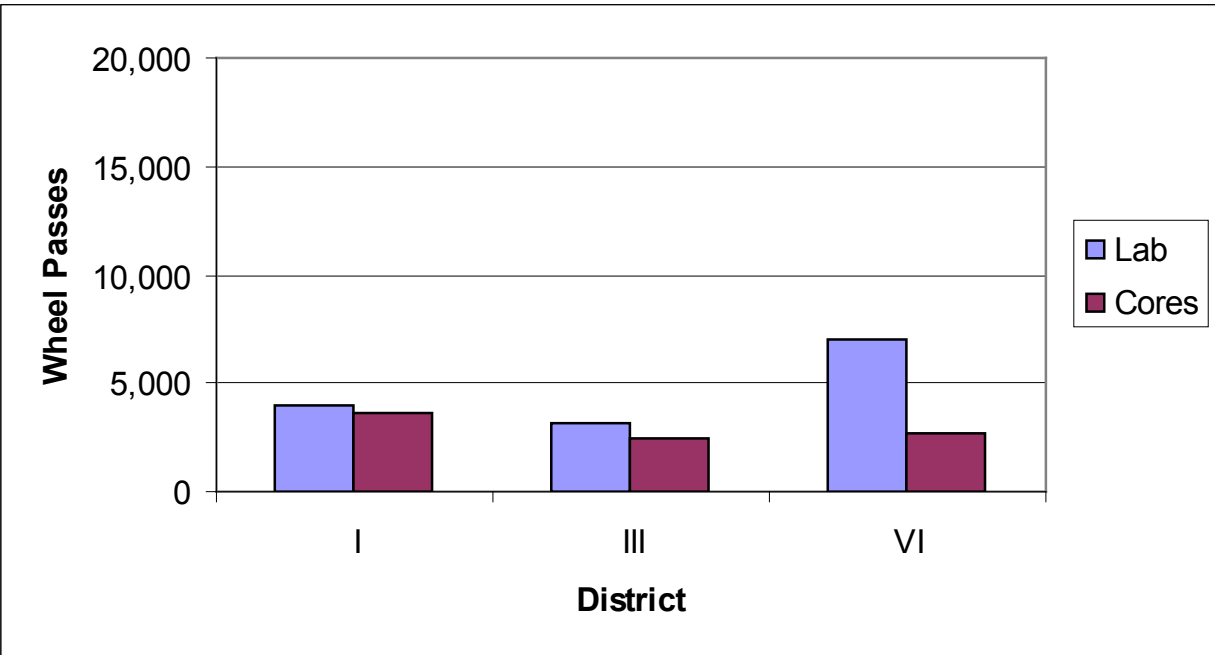


Figure 4.42 Comparison of HWTD Test Results of Laboratory Samples with Field Cores for 795 N Load at 60°C

Table 4.13 shows the predicted number of wheel passes from Equation (4.4) and the observed number of wheel passes for the field-core samples. Figure 4.43 shows the comparison of HWTB results of the overall model predicted without interaction between temperature and load levels with those for the field cores. The observed number of wheel passes are less than the model predicted values. The pattern of field cores and the predicted data are similar with certain deviations, which indicated good fit for the field verification of the model.

$$WP = e^{(22.8407 - 0.1315T - 0.0078L)} \quad (4.4)$$

where T = temperature ($^{\circ}\text{C}$); and

L = load (N).

Table 4.13 Comparison of Model-Predicted with Observed in Field Cores Results

Temp. ($^{\circ}\text{C}$)	Load (N)	Predicted Wheel Passes	Average Number of Observed Wheel Passes of Field Cores					
			K-4		K-258		US-83	
			Wheel Passes	% Diff.	Wheel Passes	% Diff.	Wheel Passes	% Diff.
50	705	47,415	17,290	63.5	14,270	69.9	15,210	67.9
50	750	33,380	18,020	46.0	15,420	53.8	18,530	44.5
50	795	23,499	15,130	35.6	10,750	54.3	15,070	35.9
60	705	12,730	4,860	61.8	2,870	77.5	3,150	75.3
60	750	8,962	4,590	48.8	3,690	58.8	3,310	63.1
60	795	6,309	3,660	42.0	2,450	61.2	2,720	56.9

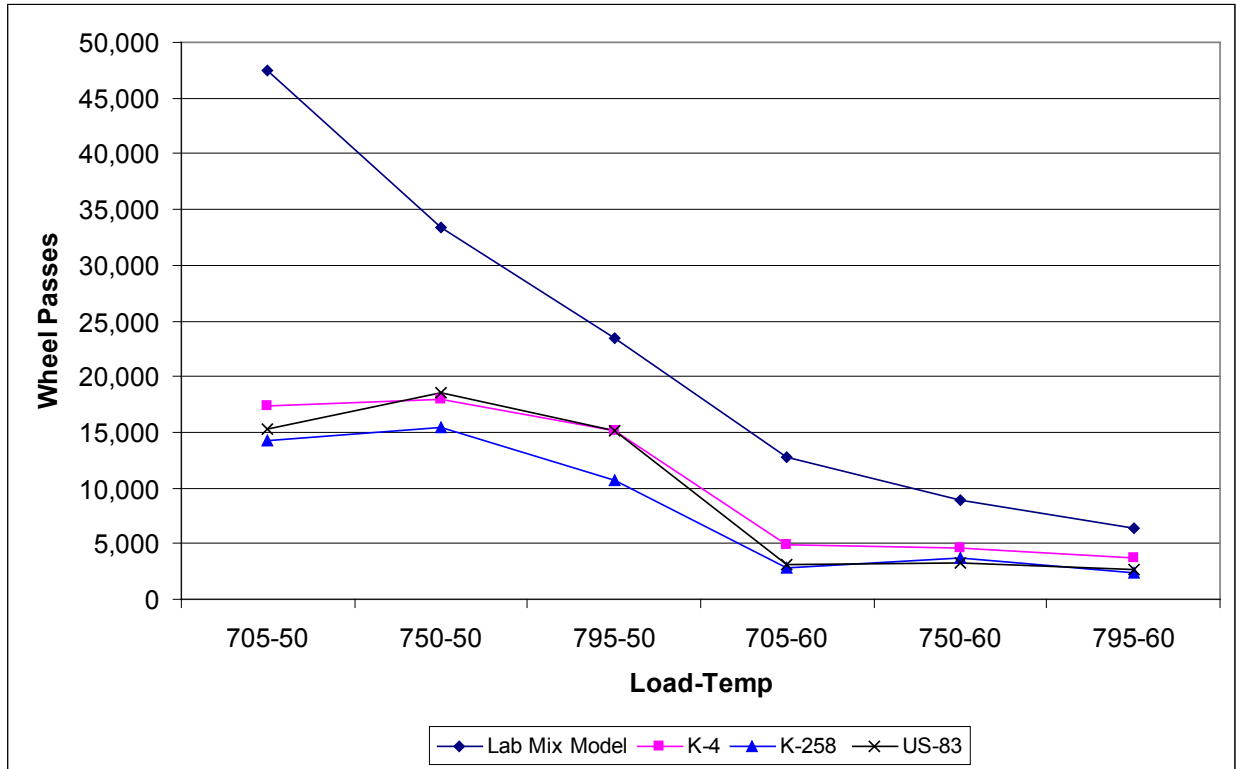


Figure 4.43 Comparison of HWTD Results of Statewide Model-Predicted with Observed in Field Cores

4.6.3 HWTD Test Results and Field Verification Considering Effects of Temperature, Load, and Air Voids

Equations (4.5), (4.6), and (4.7) were used for field verification purposes for K-4 project in District I, K-258 project in District III, and US-83 project in District VI, respectively.

For cores from the K-4 project in District I:

$$\text{Wheel Passes} = \exp (19.1588 - 0.1200 T - 0.004 L - 0.0504 A) \quad (4.5)$$

For cores from the K-258 project in District III:

$$\text{Wheel Passes} = \exp (19.9521 - 0.1618 T - 0.0021 L - 0.0836 A) \quad (4.6)$$

For cores from the US-83 project in District VI:

$$\text{Wheel Passes} = \exp (24.2580 - 0.1643 T - 0.0060 L - 0.1675 A) \quad (4.7)$$

Figures 4.44 to 4.46 show the comparison of predicted number of wheel passes using individual laboratory model with observed HWTD test results of field cores. The predicted number of wheel passes coincided or was very close to the observed number of wheel passes at the higher temperature level of 60 °C (140 °F).

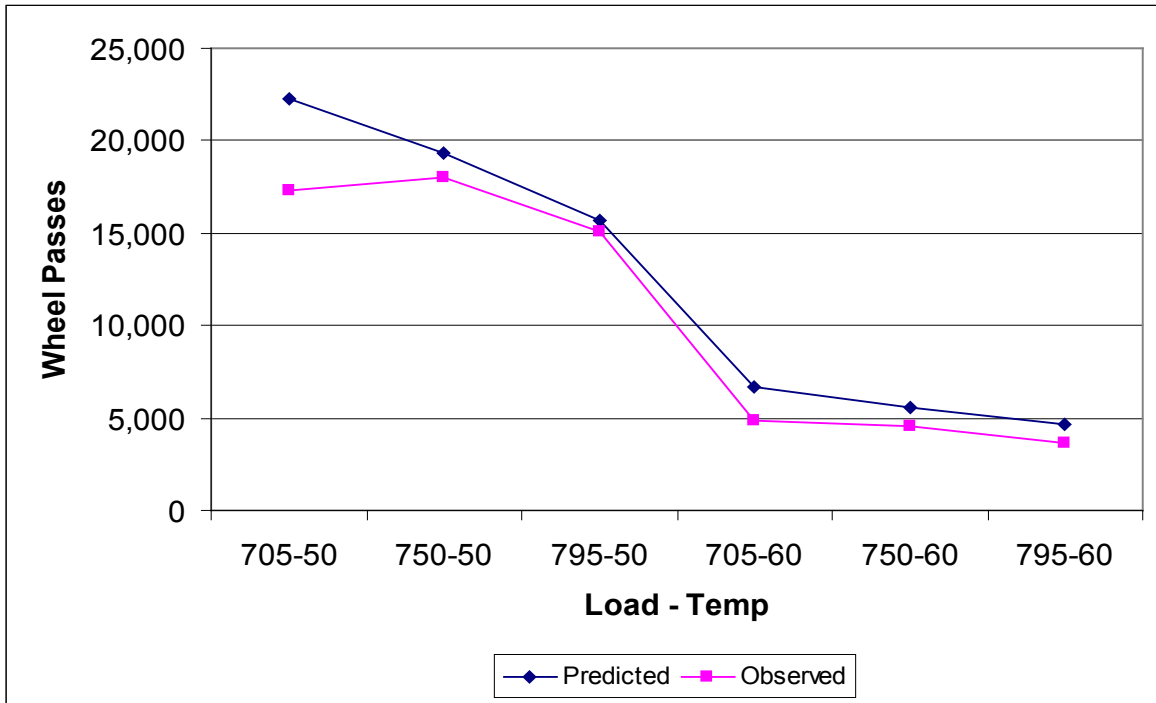


Figure 4.44 Comparison of Predicted with Observed Wheel Passes for K-4 Cores Without Interaction

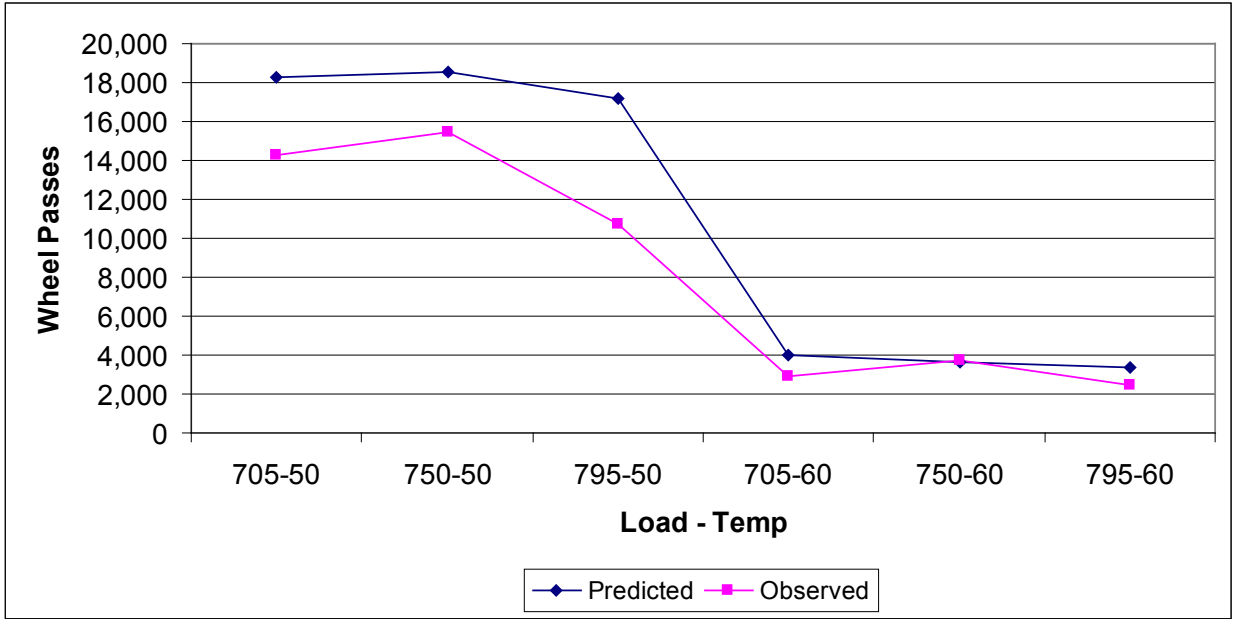


Figure 4.45 Comparison of Predicted with Observed Wheel Passes for US-24 Cores Without Interaction

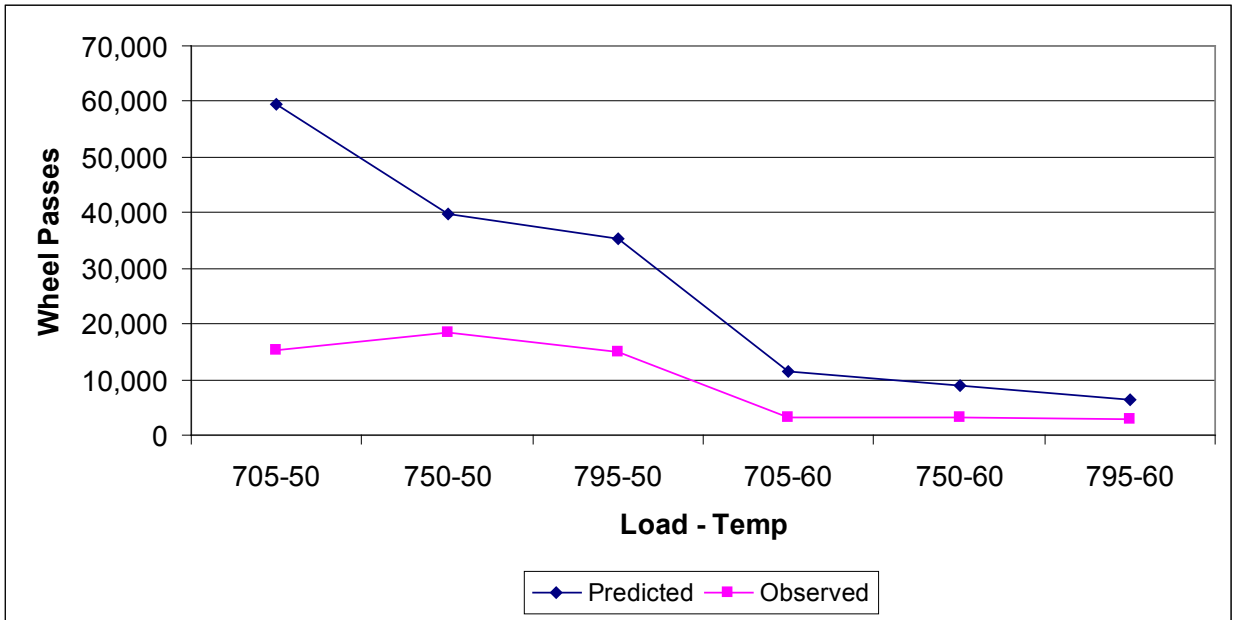


Figure 4.46 Comparison of Predicted with Observed Wheel Passes for US-83 Cores Without Interaction

CHAPTER 5 - CONCLUSIONS AND RECOMMENDATIONS

5.1 Conclusions

Based on this study, the following conclusions can be made for the Superpave mixes of 12.5-mm (0.5-in.) nominal maximum aggregate size (NMAS) using binder grade of PG 64-22.

1. In general, higher simulated in-place density, up to a certain limit of 91% to 93 %, results in better rutting and stripping performance of the Superpave mixtures in the Hamburg Wheel-Tracking Device (HWTD) tests.
2. Superpave mixtures with very low air voids @ N_{design} level (2%) perform very poorly in HWTD tests.
3. Statistical analysis of HWTD test results indicates that for most mixtures, air voids @ N_{design} and simulated in-place densities have significant effects on the average number of wheel passes to the failure condition. For most mixtures, interaction between air void @ N_{design} and density is not significant.
4. Good prediction of potential loss of pavement life can be made from the results of HWTD tests on the deficient mixtures in most cases. Thus, HWTD test results can be used for estimation of life of potentially deficient Superpave mixes.
5. HWTD results show good consistency between the accelerated mix testing models predicted and observed test results, when higher temperature and standard load level are used.
6. The test duration of HWTD can be reduced to two hours or less using accelerated mix testing (statistical) models.

5.2 Recommendations

Based on this study, the following recommendations are made:

1. Further study on estimating life of deficient Superpave pavement for various aggregate mixes with different binder grades is recommended. It should be noted that fabrication of the samples for the Hamburg test needs to be done carefully. Especially, mixing and compaction temperature must be within the specified range to achieve target air voids, and samples need to be made homogeneously mixed before compaction.
2. Further study on developing accelerated mix testing (statistical) models is recommended for various binder grades and aggregate mix types.
3. Study needs to be extended considering more load levels as well as temperature levels to capture performance trend more precisely.
4. Moisture sensitivity tests need to be done using different binder grades and aggregate mixes.

References

- AASHTO. (2001). *Standard Specifications for Transportation Materials and Methods of Sampling and Testing*. Twenty-fourth Edition. AASHTO, Washington, D.C.
- AASHTO. (2004). *2004 AASHTO Provisional Standards*. AASHTO, Washington, D.C.
- Aguiar-Moya, J.P., Prozzi, J. A., and Tahmoressi, M. (2007). “Optimum Number of Superpave Gyration Based on Project Requirements.” Paper presented at *the 86th Annual Meeting of the Transportation Research Board*, National Research Council, Washington, D. C.
- Allison, P. D. (1995). *Survival Analysis Using SAS; A Practical Guide*. SAS Institute, Inc., Cary, North Carolina.
- Al-Swailmi, S. and Terrel, R. L. (1994). “Water Sensitivity of Asphalt-Aggregate Mixtures: Test Selection.” *SHRP-A-403*. Strategic Highway Research Program, National Research Council, Washington, D.C.
- Archilla, A. R. (2000). “Development of Rutting Progression Models by Combining Data from Multiple Sources.” Doctoral dissertation, University of California, Berkeley, California.
- Aschenbrener, T. (1995). “Evaluation of Hamburg Wheel-Tracking Device to Predict Moisture Damage in Hot-Mix Asphalt.” *Transportation Research Record 1492*, TRB, National Research Council, Washington, D.C.,193-201.
- Aschenbrener, T. (1994). “Influence of Refining Processes and Crude Oil Sources Used in Colorado on Results from the Hamburg Wheel-Tracking Device.” Final Report No. CDOT-DTD-R-94-7. Colorado Department of Transportation, Denver, Colorado.

- Aschenbrener, T., and Far, N. (1994). "Influence of Compaction Temperature and Anti-Stripping Treatment on the Results from the Hamburg Wheel-Tracking Device." Report No. CDOT-DTD-R-94-9. Colorado Department of Transportation, Denver, Colorado.
- Aschenbrener, T., and McGennis, R. B. (1994). "Investigation of AASHTO T283 to Predict the Stripping Performance of Pavements in Colorado." *Transportation Research Record 1469*, TRB, National Research Council, Washington, D.C., pp. 26-33.
- Aschenbrener, T., Terrel, R. L., and Zamora, R. A. (1994). "Comparison of the Hamburg Wheel-Tracking Device and the Environmental Conditioning System to Pavements of Known Stripping Performance." Report No. CDOT-DTD-R-94-1. Colorado Department of Transportation, Denver, Colorado.
- Brown, E.R., and Cross, S.A. (1992). "A National Study of Rutting in Hot-Mix Asphalt (HMA) Pavements." *Journal of the Assoc. of Asphalt Paving Technologists*, 61, 535-573.
- Brown, E.R., Cooley Jr., L. A., Hanson, D., Lynn, C., Powell, B., and Watson, D. (2002). "NCAT Test Track Design, Construction, and Performance." NCAT Report No. 02-12. National Center for Asphalt Technology, Auburn University, Auburn, Alabama.
- Button, J. W., Chowdhury, A., and Bhasin, A. (2004). "Design of TXDOT Asphalt Mixtures Using The Superpave Gyratory Compactor." Report No. FHWA/TX-05/0-4203-1. Texas Department of Transportation, Austin, Texas.
- Cheng, D., Little, D.N., Lytton, R.L., and Holste, J.C. (2002). "Use of Surface Free Energy Properties of Asphalt – Aggregate System to Predict Damage Potential." Presented at Annual Meeting of the Association of Asphalt Paving Technologists.
- Collins, R., Watson, D., and Campbell, B. (1995). Development and Use of Georgia Loaded Wheel Tester. In *Transportation Research Record 1492*, TRB, National Research Council, Washington, D.C., pp. 202-207.

- Curtis, C. W., Ensley, K., and Epps, J. (1993). "Fundamental Properties of Asphalt-Aggregate Interactions Including Adhesion and Absorption." SHRP-A-341. Strategic Highway Research Program, National Research Council, Washington, D.C.
- Epps, J., Berger, E., and Anagnos, J. N. (2003). *Moisture Sensitivity in Asphalt Pavements*. Topic 4, Treatments, Proc. of a National Seminar, Transportation Research Board, National Research Council, Washington D.C.
- European Asphalt Study Tour. (1991). *Report on the 1990 European Asphalt Study Tour*. AASHTO, Washington, D. C.
- FHWA. (2008). "Equipment Hamburg Wheel-Tracking Device." Bituminous Mixtures Laboratory, Asphalt Pavement Technology, FHWA, U.S. Department of Transportation. <www.fhwa.dot.gov/pavement/asphalt/labs/mixtures/hamburg.cfm> (Jan. 4, 2008).
- FHWA. (2008). "Highway Statistics 2008." FHWA, U.S. Department of Transportation, <<http://www.fhwa.dot.gov/policyinformation/statistics/2008/index.cfm>> (Apr. 30, 2010).
- Gogula, A., Hossain, M., Boyer, J. and Romanoschi, S. (2003). "Effect of PG Binder Grade and Source on Performance of Superpave Mixtures under Hamburg Wheel Tester." *Proceedings of the 2003 Mid-Continent Transportation Research Symposium*, Ames, Iowa.
- Goode, F. F. (1959). "Use of Immersion Compression Test in Evaluating and Designing Bituminous Paving Mixtures." In ASTM STP 252, 113-126.
- Hicks, R. G. (1991). *NCHRP Synthesis of Highway Practice 175: Moisture Damage in Asphalt Concrete*. TRB, National Research Council, Washington, D.C., 1991.

- Hicks, G. R., Santucci, L., and Aschenbrener, T. (2003). "Introduction and Seminar Objectives." *National Seminar in Moisture Sensitivity of Asphalt Pavements*, San Diego, California.
- Hossain, M., Fager, G., and Maag, R. G. (2008). *Superpave Volumetric Mixture Design and Analysis Handbook*. Kansas State University, Manhattan, Kansas.
- Hrdlicka, G. M., and Tandon, V. (2007). "Estimation of Hot-Mix Asphalt Concrete Rutting Potential from Repeated Creep Binder Tests." *Paper No. 07-2886* (CD-ROM), Paper presented at *the 86th Annual Meeting of the Transportation Research Board*, National Research Council, Washington, D. C.
- Huang, Y. H. (2004). *Pavement Analysis and Design*. Prentice-Hall, Inc., Englewood Cliffs, New Jersey.
- Izzo, R. P., and Tahmoressi, M. (1999). "Use of the Hamburg Wheel-Tracking Device for Evaluating Moisture Susceptibility of Hot-Mix Asphalt." *Transportation Research Record 1681*, TRB, National Research Council, Washington, D. C., 76-85.
- Johnson, D. L. (1969). *Debonding of Water-Saturated Asphaltic Concrete Caused by Thermally Induced Pore Pressure*. MSCE thesis. University of Idaho, Moscow.
- Kandhal, P. S. (1994). "Field and Laboratory Investigation of Stripping in Asphalt Pavements: State of the Art Report." *Transportation Research Record 1454*, TRB, National Research Council, Washington, D. C., 36-47.
- Kennedy, T. W., Roberts, F. L., and Lee, K. W. (1984). "Evaluating moisture susceptibility of asphalt mixtures using the Texas Boiling Test". *Transportation Research Record 968*, TRB, National Research Council, Washington, D.C., 45-54.

- Klein, J. P., and Moeschberger, M. L. (2003). *Survival Analysis Techniques for Censored and Truncated Data*, Second Edition. Springer Science and Business Media Inc., New York.
- Kuehl, R. O. (2000). *Design of Experiments, Statistical Principles of Research Design and Analysis*, Second Edition. Brooks/Cole, Pacific Grove, California.
- Lai, J. S. and Lee, T. M. (1990). "Use of Loaded-Wheel Testing Machine to Evaluate Rutting of Asphalt Mixtures." *Transportation Research Record 1269*, TRB, National Research Council, Washington, D. C., 116-124.
- Lee, E. T., and Wang, J. W. (2003). *Statistical Methods for Survival Data Analysis*, Third Edition. John Wiley and Sons, Inc., Hoboken, New Jersey.
- Liddle, G., and Choi, Y. (2007). "Case Study and Test Method Review on Moisture Damage." *Austrroads Project No. TT1135*. Austrroads Incorporated, Sydney, NSW, Australia.
- Little, D. N. and Jones, D. R. IV (2003). *Moisture Sensitivity in Asphalt Pavements*. Topic 2, Chemical and Mechanical Processes of Moisture Damage in Hot-Mix Asphalt Pavements. Proc. of a National Seminar, Transportation Research Board, National Research Council, Washington D.C.
- Lottman, R. P. (1978). *NCHRP Report 192: Predicting Moisture-Induced Damage to Asphaltic Concrete*. TRB, National Research Council, Washington, D.C.
- Lottman, R. P. (1982). *NCHRP Report 246: Predicting Moisture-Induced Damage to Asphaltic Concrete: Field Evaluation*. TRB, National Research Council, Washington, D.C.
- Lu, Q. (2005). "Investigation of Conditions for Moisture Damage in Asphalt Concrete and Appropriate Laboratory Test Methods." Doctoral dissertation, University of California, Berkeley, California.

- Lu, Q., and Harvey, J. T. (2006). Long-Term Effectiveness of Antistripping Additives. *Transportation Research Record 1970*, TRB, National Research Council, Washington, D.C., 14-24.
- Lu, Q., and Harvey, J. T. (2006). Evaluation of Hamburg Wheel-Tracking Device Test with Laboratory and Field Performance Data. *Transportation Research Record 1970*, TRB, National Research Council, Washington, D.C., 25-44.
- Manandhar, C., Hossain, M., Nelson, P., and Hobson, C. (2008). “Estimation of Lives of Deficient Superpave Pavements.” *Transportation Research Record 2081*, Transportation Research Board of the National Academies, Washington, D. C., 83-91.
- Mohammad, L. N., Saadeh, S., Cooper Jr., S., and Obulareddy, S. (2007). “Characterization of Louisiana Asphalt Mixtures Using Simple Performance Tests.” *Paper No. 07-2597*, (CD-ROM). Paper presented at *the 86th Annual Meeting of the Transportation Research Board*, National Research Council, Washington, D. C.
- Nelson, W. (1990). *Accelerated Testing: Statistical Models, Test Plans, and Data Analysis*. John Wiley and Sons, Inc., New York.
- Novak, M. E. (2007). *Creation of a Laboratory Testing Device to Evaluate Instability Rutting in Asphalt Pavements*. Ph.D. Dissertation, University of Florida, Gainesville, FL.
- Roberts, F. L., Mohammad, L. N., and Wang, L. B. (2002). “History of Hot-Mix Asphalt Mixture Design in the United States.” *Journal of Materials in Civil Engineering*, ASCE, 14 (4) 279-293.
- Roberts, F. L., Kandhal, P. S., Brown, E. R., Lee, D. Y., and Kennedy, T. M. (1996). *Hot-Mix Asphalt Materials, Mixture Design, and Construction*. Second Edition, NAPA Research and Education Foundation, Lanham, Maryland.

- SAS User's Guide. (1982). *SAS User's Guide: Statistics*. SAS Institute, Inc. Cary, North Carolina.
- SAS Online Document. (2008). Version 9.1.3. SAS Institute Inc., Cary, North Carolina. <<http://support.sas.com/onlinedoc/913/docMainpage.jsp>> (Jul. 28, 2008).
- Schmidt, R. J., and Graf, P. E. (1972). The Effect of Water on the Resilient Modulus of Asphalt Treated Mixes. *Proc., Association of Asphalt Paving Technologists*, Vol. 41, pp. 118–162.
- Shiwakoti, H. (2007). “Development of a Rapid Test to Determine Moisture Sensitivity of HMA (Superpave) Mixtures.” M.S. thesis, The University of Kansas, Lawrence, Kansas.
- Solaimanian, M., Banaquist, R. F., and Tandon, V. (2007). *NCHRP Report 589: Improved Conditioning and Testing Procedures for HMA Moisture Susceptibility*. TRB, National Research Council, Washington, D.C.
- Taylor, M. A., and Khosla, N. P. (1983). “Stripping of Asphalt Pavements: State of the Art.” *Transportation Research Record 911*, TRB, National Research Council, Washington, D.C., 150-158.
- Thompson, M. R., and Nauman, D. (1993). “Rutting Rate Analyses of the AASHO Road Test Flexible Pavements.” *Transportation Research Record 1384*, TRB, National Research Council, Washington, D.C., 37-48.
- Tunicliff, D. G., and Root, R. E. (1984). *NCHRP Report 274: Use of Anti-stripping Additives in Asphaltic Concrete Mixtures*. TRB, National Research Council, Washington, D.C.
- Williams, R. C., and Prowell, B. D. (1999). “Comparison of Laboratory Wheel-Tracking Test Results with WesTrack Performance.” *Transportation Research Record 1681*, TRB, National Research Council, Washington, D. C., 121-128.

Williams, S. G. (2001). "Development of Wheel-Tracking Test Method and Performance Criteria for Asphalt Pavements." Doctoral dissertation, The University of Arkansas, Fayetteville, Arkansas.

Yildirim, Y., and Kennedy, T. W. (2001). "Correlation of Field Performance to Hamburg Wheel-Tracking Device Results." Report No. FHWA/TX-04/0-4185-1, FHWA, U.S. Department of Transportation, Austin, Texas.

Yildirim, Y., and Kennedy, T. W. (2002). "Hamburg Wheel-Tracking Device Results on Plant and Field Cores Produced Mixtures." Report No. FHWA/TX-04/0-4185-2, FHWA, U.S. Department of Transportation, Austin, Texas.

**Appendix A - HWTD, G_{mm} , and G_{mb} Test Results for Development
of Criteria for Out-of-Specification Pavements**

HWTD Test Results for Development of Criteria for Out-of-Specification Pavements

Table A.1 Hamburg Wheel-Tracking Device Test Results (Number of Wheel Passes)

Route	KDOT District	Wheel Path	% Target Air Voids											
			2				4				7			
			% Target Simulated In-Place Density				% Target Simulated In-Place Density				% Target Simulated In-Place Density			
			87	89	91	93	87	89	91	93	87	89	91	93
K-4	I	Left	6,010	14,210	11,350	13,500	9,210	8,300	20,000	14,000	9,610	11,500	18,000	17,290
		Right	7,100	7,260	9,350	11,160	8,500	7,700	20,000	13,400	8,710	10,010	17,800	12,960
K-9	II	Left	N/A	6,100	3,170	4,620	N/A	7,200	10,240	4,010	N/A	8,920	9,060	11,470
		Right	N/A	3,700	4,650	5,210	N/A	6,460	8,630	6,450	N/A	6,580	7,120	8,510
US-24	III	Left	N/A	8,480	11,970	13,260	N/A	6,880	16,220	19,330	N/A	10,000	11,720	10,090
		Right	N/A	5,950	12,350	12,870	N/A	6,720	18,720	15,920	N/A	10,540	13,600	17,540
K-152	IV	Left	N/A	4,720	5,790	5,650	N/A	3,930	7,000	14,850	N/A	8,880	18,160	16,060
		Right	N/A	5,020	8,260	10,430	N/A	3,560	9,600	8,280	N/A	6,430	11,420	8,860
K-15	V	Left	5,100	8,100	5,960	13,810	5,600	10,710	10,400	20,000	11,600	20,000	20,000	20,000
		Right	6,600	9,560	8,050	9,360	6,550	10,910	5,850	19,510	7,760	16,560	20,000	20,000
US-83	VI	Left	N/A	5,620	5,400	12,500	N/A	10,470	18,400	20,000	N/A	20,000	20,000	20,000
		Right	N/A	9,340	7,670	10,940	N/A	20,000	20,000	20,000	N/A	17,760	17,120	12,670
K-246	I	Left	N/A	10,330	4,100	3,740	N/A	10,860	13,240	6,700	N/A	19,950	13,280	16,400
		Right	N/A	11,710	5,850	4,050	N/A	12,060	14,900	7,590	N/A	15,870	13,120	16,100
US-56	II	Left	N/A	3,170	4,450	7,560	N/A	6,550	8,610	11,700	N/A	10,200	17,850	17,410
		Right	N/A	3,950	3,920	7,060	N/A	6,920	20,000	9,100	N/A	8,100	12,790	20,000
US-50	V	Left	N/A	7,920	7,720	20,000	N/A	11,060	15,490	20,000	N/A	14,190	20,000	20,000
		Right	N/A	6,620	10,550	20,000	N/A	11,300	15,310	20,000	N/A	16,000	20,000	20,000

NOTE: N/A – not available.

G_{mm} , G_{mb} , Simulated In-Place Densities, and Air Voids Results for Development of Criteria for Out-of-Specification Pavements

Table A.2 Simulated In-Place Densities and Air Voids for K-4 Project in District I

Sample ID	Target Simulated In-Place Density	Target Air Voids @ N_{design}	G_{mb}	G_{mm}	Simulated In-Place Density (% G_{mm})	% Air Voids @ N_{final}	Average Simulated In-place Density	Standard Deviation (σ)	Coefficient of Variation	% Air Voids @ N_{design}	Average % Air Voids @ N_{design}	Air Voids @ N_{design} (Trial Mix)
T43-1	93	2	2.315	2.425	95.5	4.5	95.2	0.20	0.21	0.8	0.9	3.4
T43-2			2.310		95.3	4.7				0.9		
T43-3			2.308		95.2	4.8				0.5		
T43-4			2.302		94.9	5.1				1.1		
T43-5			2.305		95.1	4.9				1.3		
T32-1	93	4	2.302	2.467	93.3	6.7	93.6	0.18	0.19	3.1	3.4	4.6
T32-2			2.306		93.5	6.5				2.9		
T32-3			2.313		93.8	6.2				3.4		
T32-4			2.315		93.8	6.2				4.1		
T32-5			2.311		93.7	6.3				3.5		
T28-1	93	7	2.326	2.480	93.8	6.2	93.6	0.23	0.25	3.8	3.6	7.5
T28-2			2.319		93.5	6.5				3.9		
T28-3			2.329		93.9	6.1				2.9		
T28-4			2.316		93.4	6.6				3.5		
T28-5			2.317		93.4	6.6				4.1		
T44-1	91	2	2.298	2.451	93.8	6.2	93.4	0.30	0.32	2.8	3.2	4.6
T44-2			2.292		93.5	6.5				3.4		
T44-3			2.278		92.9	7.1				4.2		
T44-4			2.290		93.4	6.6				2.9		
T44-5			2.293		93.6	6.4				2.7		
T36-1	91	4	2.267	2.459	92.2	7.8	92.4	0.29	0.31	2.5	2.8	4.7
T36-2			2.267		92.2	7.8				2.6		
T36-3			2.271		92.4	7.6				2.4		
T36-4			2.284		92.9	7.1				2.8		
T36-5			2.275		92.5	7.5				3.6		
T41-1	91	7	2.286	2.486	92.0	8.0	92.1	0.20	0.22	5.1	4.7	7.8
T41-2			2.283		91.8	8.2				4.9		
T41-3			2.293		92.2	7.8				3.8		
T41-4			2.288		92.0	8.0				4.5		
T41-5			2.295		92.3	7.7				5.0		
T51-1	89	2	2.212	2.450	90.3	9.7	90.9	0.38	0.42	3.1	2.5	4.6
T51-2			2.229		91.0	9.0				2.6		
T51-3			2.238		91.3	8.7				1.2		
T51-4			2.227		90.9	9.1				2.8		
T51-5			2.226		90.9	9.1				2.8		
T40-1	89	4	2.229	2.456	90.8	9.2	90.8	0.17	0.19	3.6	3.4	6.3
T40-2			2.227		90.7	9.3				3.5		
T40-3			2.228		90.7	9.3				2.6		
T40-4			2.227		90.7	9.3				3.9		

T40-5			2.237		91.1	8.9				3.3		
T42-1	89	7	2.230	2.480	89.9	10.1	90.0	0.27	0.30	6.0	5.5	6.9
T42-2			2.243		90.4	9.6				5.7		
T42-3			2.224		89.7	10.3				5.8		
T42-4			2.232		90.0	10.0				5.3		
T42-5			2.242		90.4	9.6				4.9		
T52-1	87	2	2.207	2.447	90.2	9.8	90.2	0.20	0.22	2.6	2.9	2.6
T52-2			2.215		90.5	9.5				2.6		
T52-3			2.202		90.0	10.0				2.9		
T52-4			2.200		89.9	10.1				3.0		
T52-5			2.201		89.9	10.1				3.3		
T53-1	87	4	2.199	2.457	89.5	10.5	89.4	0.20	0.22	4.1	4.4	4.6
T53-2			2.202		89.6	10.4				3.7		
T53-3			2.188		89.1	10.9				5.1		
T53-4			2.194		89.3	10.7				4.5		
T53-5			2.202		89.6	10.4				4.8		
T54-1	87	7	2.185	2.485	87.9	12.1	88.6	0.40	0.46	7.3	7.3	6.3
T54-2			2.200		88.5	11.5				7.0		
T54-3			2.199		88.5	11.5				7.1		
T54-4			2.199		88.5	11.5				7.6		
T54-5			2.186		88.0	12.0				7.6		

Table A.3 Simulated In-Place Densities and Air Voids for K-9 Project in District II

Sample ID	Target Simulated In-Place Density	Target Air Voids @ N_{design}	G_{mb}	G_{mm}	Simulated In-Place Density (% G_{mm})	% Air Voids @ N_{final}	Average Simulated In-Place Density	Standard Deviation (σ)	Coefficient of Variation	% Air Voids @ N_{design}	Average % Air Voids @ N_{design}	Air Voids @ N_{design} (Trial Mix)
T163-1	93	2	2.219	2.374	93.5	6.5	93.7	0.15	0.16	1.5	1.3	3.8
T163-2			2.224		93.7	6.3				1.2		
T163-3			2.223		93.6	6.4				1.4		
T163-4			2.223		93.6	6.4				1.3		
T163-5			2.229		93.9	6.1				1.0		
T152-1	93	4	2.232	2.381	93.7	6.3	93.7	0.30	0.32	3.1	3.1	5.2
T152-2			2.230		93.7	6.3				3.5		
T152-3			2.236		93.9	6.1				2.9		
T152-4			2.230		93.7	6.3				3.1		
T152-5			2.254		94.7	5.3				3.1		
T160-1	93	7	2.241	2.402	93.3	6.7	93.3	0.27	0.29	5.7	6.2	7.2
T160-2			2.231		92.9	7.1				5.4		
T160-3			2.242		93.3	6.7				6.7		
T160-4			2.249		93.6	6.4				6.6		
T160-5			2.241		93.3	6.7				6.5		
T162-1	91	2	2.186	2.362	92.5	7.5	92.8	0.22	0.24	1.9	1.7	3.5
T162-2			2.187		92.6	7.4				2.1		
T162-3			2.196		93.0	7.0				1.6		
T162-4			2.195		92.9	7.1				1.3		
T162-5			2.193		92.8	7.2				2.0		
T148-1	91	4	2.238	2.405	93.1	6.9	92.9	0.11	0.11	3.5	4.0	6.8
T148-2			2.232		92.8	7.2				4.0		
T148-3			2.233		92.8	7.2				4.0		
T148-4			2.235		92.9	7.1				4.2		
T148-5			2.232		92.8	7.2				4.1		
T158-1	91	7	2.211	2.427	91.1	8.9	91.0	0.10	0.11	6.4	6.7	6.0
T158-2			2.209		91.0	9.0				6.3		
T158-3			2.210		91.1	8.9				6.7		
T158-4			2.210		91.1	8.9				7.1		
T158-5			2.205		90.9	9.1				7.0		
T161-1	89	2	2.185	2.375	92.0	8.0	92.1	0.29	0.32	1.9	1.9	2.9
T161-2			2.184		92.0	8.0				1.9		
T161-3			2.196		92.5	7.5				2.2		
T161-4			2.189		92.2	7.8				2.0		
T161-5			2.177		91.7	8.3				1.6		
T150-1	89	4	2.197	2.403	91.4	8.6	91.6	0.45	0.50	3.6	3.6	6.3
T150-2			2.191		91.2	8.8				3.9		
T150-3			2.219		92.3	7.7				3.2		
T150-4			2.195		91.3	8.7				3.8		
T150-5			2.200		91.6	8.4				3.5		
T155-1	89	7	2.177	2.419	90.0	10.0	90.2	0.13	0.14	5.6	5.8	8.2
T155-2			2.182		90.2	9.8				5.4		
T155-3			2.189		90.5	9.5				6.0		
T155-4			2.179		90.1	9.9				5.8		
T155-5			2.181		90.2	9.8				6.0		

Table A.4 Simulated In-Place Densities and Air Voids for US-24 Project in District III

Sample ID	Target Simulated In-Place Density	Target Air Voids @ N_{design}	G_{mb}	G_{mm}	Simulated In-Place Density (% G_{mm})	% Air Voids @ N_{final}	Average Simulated In-Place Density	Standard Deviation (σ)	Coefficient of Variation	% Air Voids @ N_{design}	Average % Air Voids @ N_{design}	Air Voids @ N_{design} (Trial Mix)
T86-1	93	2	2.271	2.448	92.8	7.2	92.7	0.22	0.24	3.3	3.1	5.2
T86-2			2.269		92.7	7.3				3.4		
T86-3			2.263		92.4	7.6				3.0		
T86-4			2.265		92.5	7.5				3.3		
T86-5			2.277		93.0	7.0				2.7		
T88-1	93	4	2.282	2.444	93.4	6.6	93.3	0.19	0.20	4.0	3.6	4.7
T88-2			2.284		93.5	6.5				3.7		
T88-3			2.277		93.2	6.8				3.2		
T88-4			2.274		93.0	7.0				3.4		
T88-5			2.289		93.7	6.3				3.8		
T89-1	93	7	2.276	2.463	92.4	7.6	91.7	0.51	0.55	6.0	6.8	4.7
T89-2			2.268		92.1	7.9				6.1		
T89-3			2.255		91.6	8.4				8.1		
T89-4			2.254		91.5	8.5				6.1		
T89-5			2.244		91.1	8.9				7.8		
T84-1	91	2	2.280	2.415	94.4	5.6	93.9	0.40	0.42	1.6	2.7	5.4
T84-2			2.271		94.0	6.0				2.3		
T84-3			2.258		93.5	6.5				3.0		
T84-4			2.257		93.5	6.5				3.3		
T84-5			2.267		93.9	6.1				3.4		
T76-1	91	4	2.210	2.439	90.6	9.4	90.9	0.30	0.33	3.5	3.0	5.3
T76-2			2.214		90.8	9.2				3.0		
T76-3			2.229		91.4	8.6				2.2		
T76-4			2.215		90.8	9.2				3.5		
T76-5			2.215		90.8	9.2				3.0		
T80-1	91	7	2.238	2.479	90.3	9.7	90.4	0.12	0.13	7.0	6.8	8.3
T80-2			2.240		90.4	9.6				7.0		
T80-3			2.241		90.4	9.6				6.5		
T80-4			2.240		90.4	9.6				6.6		
T80-5			2.246		90.6	9.4				6.9		
T82-1	89	2	2.186	2.416	90.5	9.5	90.7	0.31	0.34	2.7	2.3	4.2
T82-2			2.186		90.5	9.5				2.7		
T82-3			2.204		91.2	8.8				1.4		
T82-4			2.189		90.6	9.4				2.1		
T82-5			2.190		90.6	9.4				2.6		
T74-1	89	4	2.190	2.428	90.2	9.8	89.9	0.68	0.76	3.1	3.7	5.6
T74-2			2.209		91.0	9.0				2.2		
T74-3			2.173		89.5	10.5				4.4		
T74-4			2.178		89.7	10.3				4.1		
T74-5			2.167		89.3	10.7				4.8		
T78-1	89	7	2.201	2.475	88.9	11.1	88.9	0.08	0.09	6.3	6.5	7.6
T78-2			2.199		88.8	11.2				7.2		
T78-3			2.204		89.1	10.9				6.1		
T78-4			2.199		88.8	11.2				6.4		
T78-5			2.204		89.1	10.9				6.6		

Table A.5 Simulated In-Place Densities and Air Voids for K-152 Project in District IV

Sample ID	Target Simulated In-Place Density	Target Air Voids @ N_{design}	G_{mb}	G_{mm}	Simulated In-Place Density (% G_{mm})	% Air Voids @ N_{final}	Average Simulated In-Place Density	Standard Deviation (σ)	Coefficient of Variation	% Air Voids @ N_{design}	Average % Air Voids @ N_{design}	Air Voids @ N_{design} (Trial Mix)
T61-1	93	2	2.252	2.376	94.8	5.2	93.8	0.83	0.88	3.5	2.2	4.1
T61-2			2.217		93.3	6.7				0.4		
T61-3			2.203		92.7	7.3				1.0		
T61-4			2.231		93.9	6.1				2.5		
T61-5			2.243		94.4	5.6				3.5		
T63-1	93	4	2.265	2.393	94.7	5.3	94.0	0.46	0.49	3.4	2.9	4.8
T63-2			2.241		93.6	6.4				2.6		
T63-3			2.259		94.4	5.6				3.9		
T63-4			2.234		93.4	6.6				0.4		
T63-5			2.257		94.3	5.7				4.3		
T59-1	93	7	2.268	2.434	93.2	6.8	92.2	0.57	0.62	5.8	2.4	5.7
T59-2			2.243		92.2	7.8				1.6		
T59-3			2.231		91.7	8.3				1.5		
T59-4			2.238		92.0	8.0				0.8		
T59-5			2.243		92.2	7.8				2.1		
T67-1	91	2	2.234	2.392	93.4	6.6	92.6	1.04	1.12	1.3	1.1	4.0
T67-2			2.247		93.9	6.1				2.9		
T67-3			2.194		91.7	8.3				0.3		
T67-4			2.195		91.8	8.2				0.4		
T67-5			2.199		91.9	8.1				0.5		
T57-1	91	4	2.236	2.401	93.1	6.9	92.9	0.51	0.55	2.3	1.7	2.2
T57-2			2.238		93.2	6.8				3.3		
T57-3			2.221		92.5	7.5				1.2		
T57-4			2.213		92.2	7.8				1.6		
T57-5			2.241		93.3	6.7				0.0		
T65-1	91	7	2.257	2.439	92.5	7.5	92.4	0.27	0.29	2.2	2.8	4.4
T65-2			2.264		92.8	7.2				3.0		
T65-3			2.247		92.1	7.9				3.2		
T65-4			2.250		92.3	7.7				2.8		
T65-5			2.255		92.5	7.5				2.6		
T71-1	89	2	2.220	2.412	92.0	8.0	92.1	0.36	0.39	0.6	0.3	6.0
T71-2			2.210		91.6	8.4				0.5		
T71-3			2.227		92.3	7.7				0.0		
T71-4			2.220		92.0	8.0				0.0		
T71-5			2.233		92.6	7.4				0.5		
T70-1	89	4	2.245	2.399	93.6	6.4	92.7	0.69	0.74	0.0	0.0	3.8
T70-2			2.223		92.7	7.3				0.0		
T70-3			2.215		92.3	7.7				0.0		
T70-4			2.233		93.1	6.9				0.0		
T70-5			2.202		91.8	8.2				0.0		
T69-1	89	7	2.202	2.450	89.9	10.1	90.3	0.60	0.67	2.9	2.3	6.0
T69-2			2.201		89.8	10.2				3.0		
T69-3			2.217		90.5	9.5				1.1		
T69-4			2.233		91.1	8.9				1.7		
T69-5			2.242		91.5	8.5				2.6		

Table A.6 Simulated In-Place Densities and Air Voids for K-15 Project in District V

Sample ID	Target Simulated In-Place Density	Target Air Voids @ N_{design}	G_{mb}	G_{mm}	Simulated In-Place Density (% G_{mm})	% Air Voids @ N_{final}	Average Simulated In-Place Density	Standard Deviation (σ)	Coefficient of Variation	% Air Voids @ N_{design}	Average % Air Voids @ N_{design}	Air Voids @ N_{design} (Trial Mix)
T8-1	93	2	2.274	2.361	93.2	3.7	96.0	0.42	0.44	0.0	0.1	1.8
T8-2			2.267		96.0	4.0				0.0		
T8-3			2.255		95.5	4.5				0.5		
T8-4			2.279		96.5	3.5				0.0		
T8-5			2.259		95.7	4.3				0.0		
T3-1	93	4	2.265	2.418	93.7	6.3	93.6	0.15	0.16	1.9	1.5	5.5
T3-2			2.270		93.9	6.1				1.5		
T3-3			2.261		93.5	6.5				1.3		
T3-4			2.257		93.3	6.7				1.0		
T3-5			2.264		93.6	6.4				1.9		
T4-1	93	7	2.260	2.466	91.6	8.4	91.7	0.20	0.22	3.9	3.9	5.2
T4-2			2.261		91.7	8.3				4.0		
T4-3			2.267		91.9	8.1				3.8		
T4-4			2.262		91.7	8.3				3.9		
T4-5			2.253		91.4	8.6				3.8		
T10-1	91	2	2.254	2.466	91.4	8.6	91.2	0.48	0.53	0.0	0.1	2.6
T10-2			2.253		91.4	8.6				0.0		
T10-3			2.259		91.6	8.4				0.0		
T10-4			2.232		90.5	9.5				0.5		
T10-5			2.239		90.8	9.2				0.0		
T12-1	91	4	2.238	2.424	92.3	7.7	91.7	0.52	0.57	4.9	4.6	4.2
T12-2			2.211		91.2	8.8				4.4		
T12-3			2.209		91.1	8.9				4.1		
T12-4			2.232		92.1	7.9				5.0		
T12-5			2.222		91.7	8.3				4.7		
T15-1	91	7	2.222	2.450	90.7	9.3	91.2	0.48	0.52	5.7	6.0	8.3
T15-2			2.231		91.0	9.0				7.9		
T15-3			2.224		90.8	9.2				5.4		
T15-4			2.247		91.7	8.3				5.4		
T15-5			2.245		91.6	8.4				5.7		
T21-1	89	2	2.202	2.392	92.0	8.0	92.4	0.46	0.50	1.6	1.1	3.6
T21-2			2.196		91.8	8.2				2.3		
T21-3			2.220		92.8	7.2				0.4		
T21-4			2.216		92.6	7.4				0.6		
T21-5			2.220		92.8	7.2				0.8		
T19-1	89	4	2.203	2.406	91.6	8.4	91.8	0.40	0.44	2.0	2.0	5.9
T19-2			2.197		91.3	8.7				2.6		
T19-3			2.210		91.9	8.1				2.2		
T19-4			2.216		92.1	7.9				1.7		
T19-5			2.221		92.3	7.7				1.7		
T17-1	89	7	2.196	2.443	89.9	10.1	90.3	0.35	0.39	4.5	4.8	8.7
T17-2			2.207		90.3	9.7				4.8		
T17-3			2.218		90.8	9.2				4.3		
T17-4			2.203		90.2	9.8				5.1		
T17-5			2.222		91.0	9.0				5.2		
T25-1	87	2	2.176	2.454	88.7	11.3	89.1	0.29	0.33	6.9	6.3	2.4
T25-2			2.192		89.3	10.7				6.2		

T25-3			2.197		89.5	10.5				5.4		
T25-4			2.178		88.8	11.2				6.3		
T25-5			2.185		89.0	11.0				6.5		
T27-1	87	4	2.188	2.424	90.3	9.7	90.3	0.34	0.38	3.9	3.9	6.6
T27-2			2.188		90.3	9.7				3.9		
T27-3			2.177		89.8	10.2				3.9		
T27-4			2.197		90.6	9.4				3.9		
T27-5			2.197		90.6	9.4				3.8		
T24-1	87	7	2.173	2.394	90.8	9.2	91.6	0.46	0.50	3.0	1.9	8.2
T24-2			2.193		91.6	8.4				1.9		
T24-3			2.197		91.8	8.2				1.5		
T24-4			2.208		92.2	7.8				1.2		
T24-5			2.212		92.4	7.6				1.9		

Table A.7 Simulated In-Place Densities and Air Voids for US-83 Project in District VI

Sample ID	Target Simulated In-Place Density	Target Air Voids @ N_{design}	G_{mb}	G_{mm}	Simulated In-Place Density (% G_{mm})	% Air Voids @ N_{final}	Average Simulated In-Place Density	Standard Deviation (σ)	Coefficient of Variation	% Air Voids @ N_{design}	Average % Air Voids @ N_{design}	Air Voids @ N_{design} (Trial Mix)
T106-1	93	2	2.247	2.413	93.1	6.9	94.1	0.66	0.70	0.0	0.0	1.5
T106-2			2.274		94.2	5.8				0.0		
T106-3			2.261		93.7	6.3				0.0		
T106-4			2.284		94.7	5.3				0.0		
T106-5			2.284		94.7	5.3				0.0		
T108-1	93	4	2.275	2.426	93.8	6.2	94.0	0.14	0.14	1.3	1.7	1.0
T108-2			2.282		94.1	5.9				1.4		
T108-3			2.279		93.9	6.1				2.2		
T108-4			2.287		94.3	5.7				1.6		
T108-5			2.279		93.9	6.1				2.2		
T109-1	93	7	2.286	2.456	93.1	6.9	92.6	0.29	0.31	4.1	4.3	4.3
T109-2			2.269		92.4	7.6				4.2		
T109-3			2.275		92.6	7.4				4.7		
T109-4			2.278		92.8	7.2				4.1		
T109-5			2.269		92.4	7.6				4.5		
T104-1	91	2	2.292	2.411	95.1	4.9	94.9	0.33	0.35	0.0	0.0	1.0
T104-2			2.278		94.5	5.5				0.0		
T104-3			2.289		94.9	5.1				0.0		
T104-4			2.297		95.3	4.7				0.0		
T104-5			2.289		94.9	5.1				0.0		
T107-1	91	4	2.325	2.389	97.3	2.7	95.1	1.52	1.59	2.4	0.8	1.2
T107-2			2.288		95.8	4.2				1.6		
T107-3			2.235		93.6	6.4				0.0		
T107-4			2.260		94.6	5.4				0.0		
T107-5			2.246		94.0	6.0				0.0		
T98-1	91	7	2.290	2.459	93.1	6.9	93.2	0.43	0.46	0.3	0.3	4.4
T98-2			2.277		92.6	7.4				0.4		
T98-3			2.301		93.6	6.4				0.0		
T98-4			2.304		93.7	6.3				0.0		
T98-5			2.293		93.2	6.8				0.6		
T100-1	89	2	2.317	2.405	96.3	3.7	94.7	1.49	1.58	5.1	1.9	3.9
T100-2			2.266		94.2	5.8				0.0		
T100-3			2.308		96.0	4.0				4.6		
T100-4			2.268		94.3	5.7				0.0		
T100-5			2.228		92.6	7.4				0.0		
T102-1	89	4	2.270	2.418	93.9	6.1	93.6	0.45	0.48	0.0	0.0	2.5
T102-2			2.273		94.0	6.0				0.0		
T102-3			2.249		93.0	7.0				0.0		
T102-4			2.256		93.3	6.7				0.0		
T102-5			2.272		94.0	6.0				0.0		
T96-1	89	7	2.255	2.465	91.5	8.5	91.5	0.27	0.29	4.2	4.2	5.8
T96-2			2.248		91.2	8.8				3.7		
T96-3			2.248		91.2	8.8				5.6		
T96-4			2.268		92.0	8.0				2.6		
T96-5			2.260		91.7	8.3				4.8		

Table A.8 Simulated In-Place Densities and Air Voids for K-246 Project in District I

Sample ID	Target Simulated In-Place Density	Target Air Voids @ N_{design}	G_{mb}	G_{mm}	Simulated In-Place Density (% G_{mm})	% Air Voids @ N_{final}	Average Simulated In-Place Density	Standard Deviation (σ)	Coefficient of Variation	% Air Voids @ N_{design}	Average % Air Voids @ N_{design}	Air Voids @ N_{design} (Trial Mix)
T125-1	93	2	2.234	2.415	92.5	7.5	92.1	0.30	0.33	0.9	1.2	3.3
T125-2			2.216		91.8	8.2				1.4		
T125-3			2.225		92.1	7.9				0.4		
T125-4			2.230		92.3	7.7				1.1		
T125-5			2.230		91.9	8.1				2.2		
T127-1	93	4	2.274	2.435	93.4	6.6	92.9	0.31	0.33	4.5	3.5	7.9
T127-2			2.264		93.0	7.0				3.3		
T127-3			2.247		92.3	7.7				2.7		
T127-4			2.257		92.7	7.3				3.4		
T127-5			2.265		93.0	7.0				3.6		
T126-1	93	7	2.266	2.472	91.7	8.3	91.4	0.30	0.33	7.4	7.5	5.4
T126-2			2.262		91.5	8.5				7.6		
T126-3			2.261		91.5	8.5				7.3		
T126-4			2.247		90.9	9.1				7.1		
T126-5			2.264		91.6	8.4				8.1		
T120-1	91	2	2.211	2.387	92.6	7.4	92.6	0.20	0.21	0.0	0.0	2.3
T120-2			2.210		92.6	7.4				0.0		
T120-3			2.207		92.5	7.5				0.0		
T120-4			2.218		92.9	7.1				0.0		
T120-5			2.219		92.6	7.4				0.0		
T122-1	91	4	2.214	2.449	90.4	9.6	90.7	0.22	0.24	3.5	3.6	4.6
T122-2			2.220		90.6	9.4				3.9		
T122-3			2.222		90.7	9.3				4.0		
T122-4			2.227		90.9	9.1				3.6		
T122-5			2.227		90.9	9.1				2.9		
T124-1	91	7	2.216	2.475	89.5	10.5	89.7	0.25	0.28	6.4	6.4	7.1
T124-2			2.216		89.5	10.5				6.3		
T124-3			2.215		89.5	10.5				6.2		
T124-4			2.220		89.7	10.3				6.3		
T124-5			2.230		90.1	9.9				6.6		
T116-1	89	2	2.200	2.419	90.9	9.1	91.4	0.47	0.52	0.8	0.6	1.0
T116-2			2.202		91.0	9.0				0.4		
T116-3			2.212		91.4	8.6				0.8		
T116-4			2.231		92.2	7.8				0.8		
T116-5			2.226		92.0	8.0				0.4		
T114-1	89	4	2.193	2.416	90.8	9.2	90.8	0.15	0.17	2.6	2.7	2.2
T114-2			2.200		91.1	8.9				2.5		
T114-3			2.194		90.8	9.2				2.6		
T114-4			2.190		90.6	9.4				3.3		
T114-5			2.195		90.9	9.1				2.6		
T118-1	89	7	2.192	2.468	88.8	11.2	89.4	0.52	0.58	5.9	5.5	7.9
T118-2			2.202		89.2	10.8				5.6		
T118-3			2.197		89.0	11.0				5.5		
T118-4			2.215		89.8	10.2				5.3		
T118-5			2.223		90.1	9.9				5.2		

Table A.9 Simulated In-Place Densities and Air Voids for US-56 Project in District II

Sample ID	Target Simulated In-Place Density	Target Air Voids @ N_{design}	G_{mb}	G_{mm}	Simulated In-Place Density (% G_{mm})	% Air Voids @ N_{final}	Average Simulated In-Place Density	Standard Deviation (σ)	Coefficient of Variation	% Air Voids @ N_{design}	Average % Air Voids @ N_{design}	Air Voids @ N_{design} (Trial Mix)
T195-1	93	2	2.248	2.401	93.6	6.4	93.5	0.35	0.37	0.2	0.4	4.0
T195-2			2.243		93.4	6.6				0.5		
T195-3			2.256		94.0	6.0				0.0		
T195-4			2.236		93.1	6.9				1.2		
T195-5			2.255		93.9	6.1				0.3		
T191-1	93	4	2.262	2.404	94.1	5.9	94.2	0.26	0.28	3.3	2.0	4.7
T191-2			2.283		95.0	5.0				0.2		
T191-3			2.262		94.1	5.9				2.9		
T191-4			2.264		94.2	5.8				0.5		
T191-5			2.266		94.3	5.7				3.3		
T193-1	93	7	2.290	2.461	93.1	6.9	92.4	0.62	0.68	5.7	6.4	8.2
T193-2			2.257		91.7	8.3				6.4		
T193-3			2.270		92.2	7.8				6.3		
T193-4			2.259		91.8	8.2				7.7		
T193-5			2.287		92.9	7.1				5.9		
T204-1	91	2	2.211	2.398	92.2	7.8	92.0	0.17	0.19	0.5	0.8	4.0
T204-2			2.213		92.3	7.7				0.9		
T204-3			2.205		92.0	8.0				0.6		
T204-4			2.205		92.0	8.0				1.0		
T204-5			2.208		92.1	7.9				0.9		
T197-1	91	4	2.231	2.425	92.0	8.0	92.1	0.36	0.39	1.2	1.4	5.9
T197-2			2.230		92.0	8.0				0.7		
T197-3			2.230		92.0	8.0				1.7		
T197-4			2.242		92.5	7.5				1.9		
T197-5			2.249		92.7	7.3				1.4		
T203-1	91	7	2.247	2.475	90.8	9.2	90.6	0.24	0.27	5.8	6.1	8.0
T203-2			2.234		90.3	9.7				6.1		
T203-3			2.243		90.6	9.4				5.9		
T203-4			2.233		90.2	9.8				6.4		
T203-5			2.241		90.5	9.5				6.1		
T205-1	89	2	2.202	2.390	92.1	7.9	91.8	0.35	0.38	0.4	0.4	2.8
T205-2			2.184		91.4	8.6				1.1		
T205-3			2.206		92.3	7.7				0.0		
T205-4			2.194		91.8	8.2				0.0		
T205-5			2.198		92.0	8.0				0.7		
T202-1	89	4	2.211	2.443	90.5	9.5	90.1	0.24	0.27	4.3	4.6	4.6
T202-2			2.206		90.3	9.7				4.2		
T202-3			2.197		89.9	10.1				4.6		
T202-4			2.198		90.0	10.0				5.0		
T202-5			2.200		90.1	9.9				5.0		
T201-1	89	7	2.225	2.465	90.3	9.7	90.0	0.27	0.30	5.4	5.8	8.5
T201-2			2.221		90.1	9.9				6.0		
T201-3			2.215		89.9	10.1				5.6		
T201-4			2.210		89.7	10.3				5.9		
T201-5			2.233		90.6	9.4				6.2		

Table A.10 Simulated In-Place Densities and Air Voids for US-50 Project in District V

Sample ID	Target Simulated In-Place Density	Target Air Voids @ N_{design}	G_{mb}	G_{mm}	Simulated In-Place Density (% G_{mm})	% Air Voids @ N_{final}	Average Simulated In-Place Density	Standard Deviation (σ)	Coefficient of Variation	% Air Voids @ N_{design}	Average % Air Voids @ N_{design}	Air Voids @ N_{design} (Trial Mix)
T143-1	93	2	2.235	2.417	92.5	7.5	92.6	0.36	0.39	4.3	4.6	4.2
T143-2			2.245		92.9	7.1				3.4		
T143-3			2.236		92.5	7.5				4.7		
T143-4			2.224		92.0	8.0				5.6		
T143-5			2.245		92.9	7.1				5.1		
T144-1	93	4	2.253	2.435	92.5	7.5	92.5	0.16	0.17	6.3	7.0	6.0
T144-2			2.248		92.3	7.7				7.6		
T144-3			2.249		92.4	7.6				6.7		
T144-4			2.256		92.6	7.4				7.1		
T144-5			2.260		92.8	7.2				7.2		
T145-1	93	7	2.279	2.466	92.4	7.6	91.9	0.56	0.61	8.0	8.5	9.9
T145-2			2.273		92.2	7.8				8.6		
T145-3			2.273		92.2	7.8				9.3		
T145-4			2.248		91.2	8.8				8.5		
T145-5			2.253		91.4	8.6				8.3		
T138-1	91	2	2.195	2.410	91.1	8.9	91.4	0.35	0.38	3.5	3.4	5.4
T138-2			2.196		91.1	8.9				3.5		
T138-3			2.213		91.8	8.2				3.5		
T138-4			2.204		91.5	8.5				3.1		
T138-5			2.204		91.4	8.6				3.6		
T132-1	91	4	2.206	2.432	90.7	9.3	91.1	0.25	0.28	6.2	5.9	5.9
T132-2			2.220		91.3	8.7				5.6		
T132-3			2.213		91.0	9.0				5.7		
T132-4			2.212		91.0	9.0				5.6		
T132-5			2.221		91.3	8.7				6.2		
T142-1	91	7	2.242	2.481	90.4	9.6	90.1	0.51	0.56	8.6	8.7	8.8
T142-2			2.249		90.6	9.4				8.5		
T142-3			2.234		90.0	10.0				8.1		
T142-4			2.230		89.9	10.1				8.8		
T142-5			2.216		89.3	10.7				9.3		
T136-1	89	2	2.167	2.399	90.3	9.7	91.0	0.43	0.47	4.3	3.6	4.5
T136-2			2.178		90.8	9.2				3.5		
T136-3			2.189		91.2	8.8				3.2		
T136-4			2.190		91.3	8.7				3.4		
T136-5			2.191		91.3	8.7				3.6		
T134-1	89	4	2.190	2.444	89.6	10.4	89.5	0.15	0.17	5.2	5.2	5.9
T134-2			2.185		89.4	10.6				5.4		
T134-3			2.185		89.4	10.6				5.3		
T134-4			2.182		89.3	10.7				5.3		
T134-5			2.191		89.6	10.4				4.7		
T140-1	89	7	2.187	2.463	88.8	11.2	88.7	0.07	0.08	7.3	7.4	7.2
T140-2			2.183		88.6	11.4				7.4		
T140-3			2.182		88.6	11.4				7.2		
T140-4			2.185		88.7	11.3				7.4		
T140-5			2.182		88.6	11.4				7.5		

Appendix B - Histogram of HWTD Test Results with Simulated In-Place Densities and Air Voids for Development of Criteria for Out-of-Specification Pavements

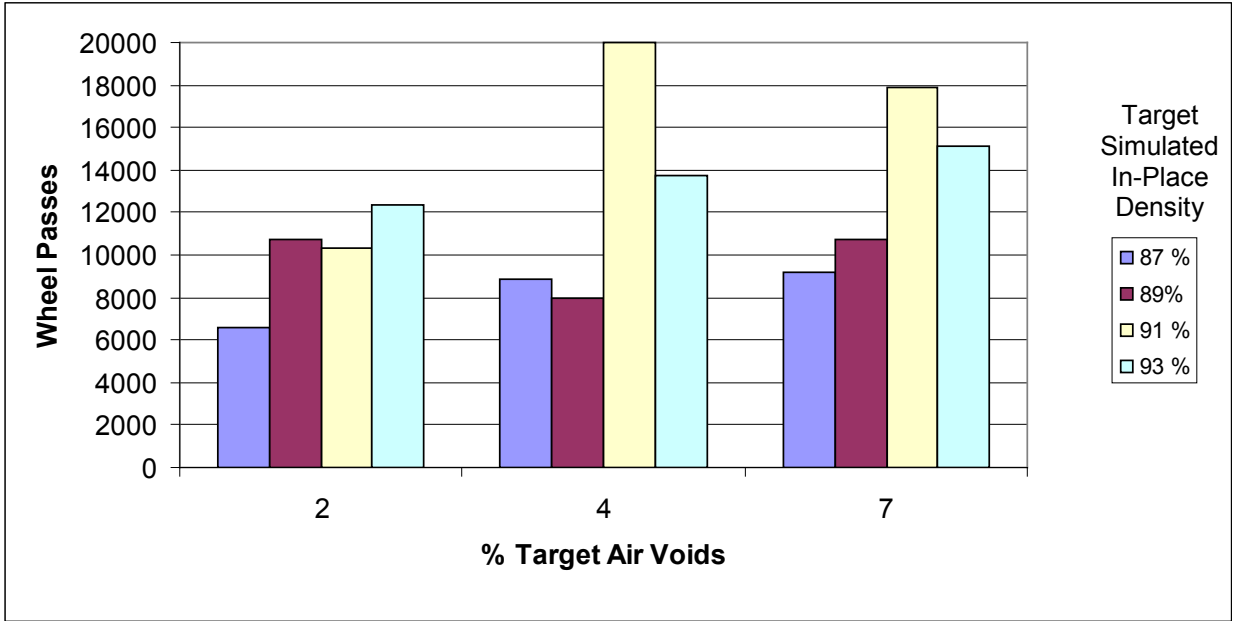


Figure B.1 HWTD Wheel Passes Results for K-4 Project with Target Simulated In-Place Densities and Target Air Voids @ N_{design}

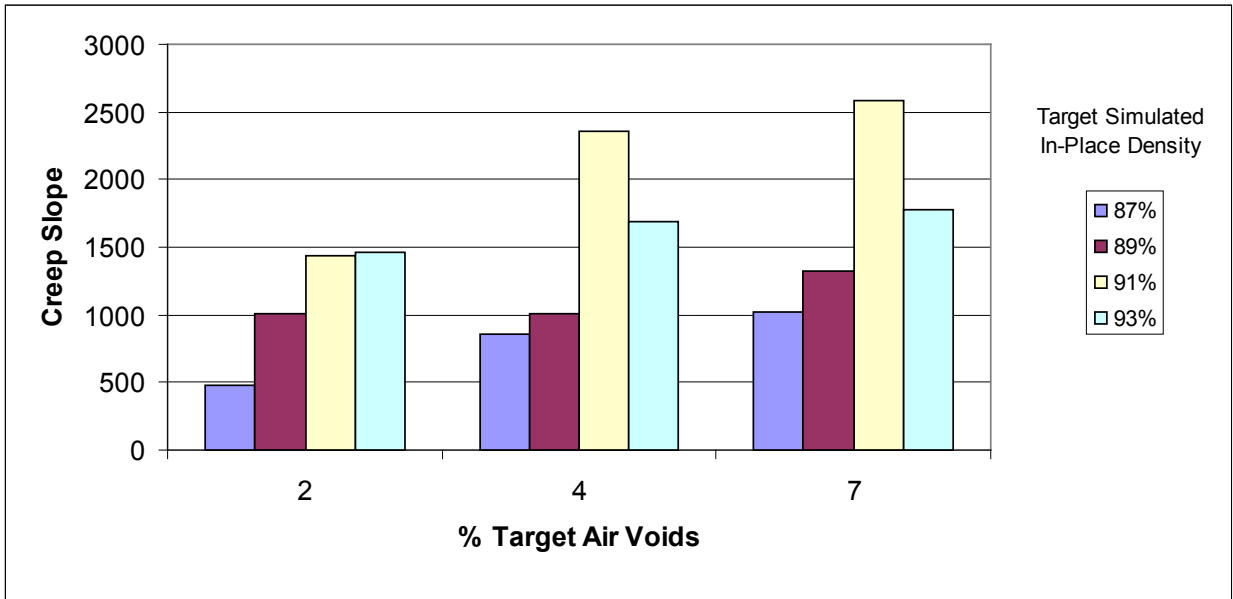


Figure B.2 HWTD Creep Slope Results for K-4 Project with Target Simulated In-Place Densities and Target Air Voids @ N_{design}

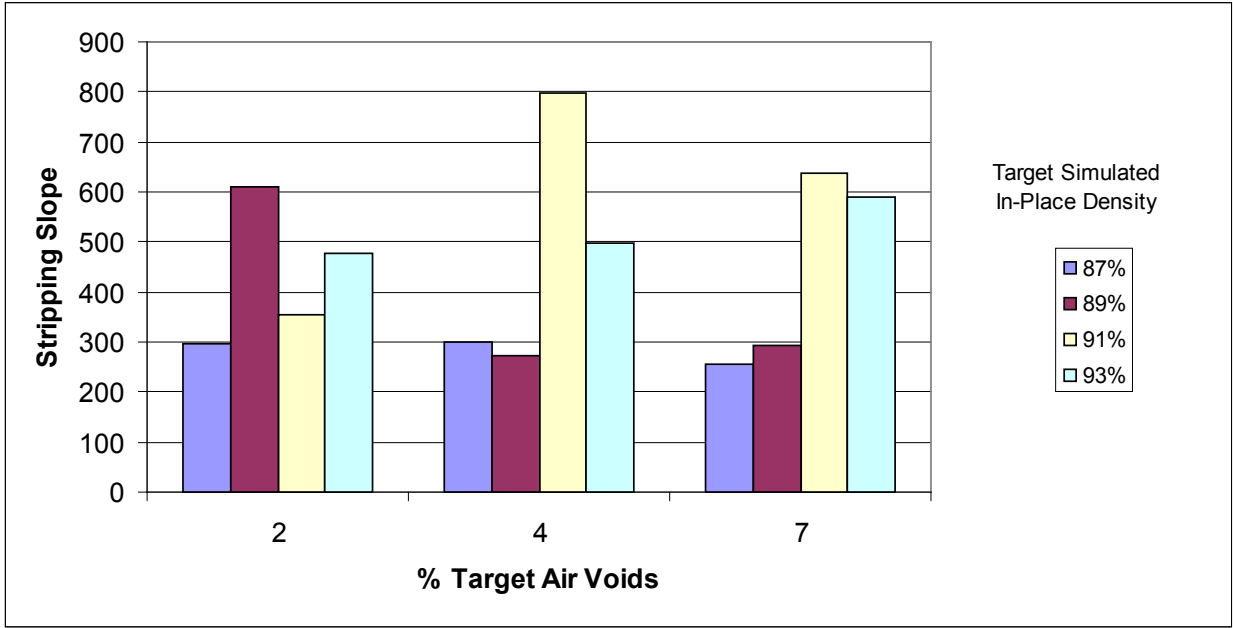


Figure B.3 HWTD Stripping Slope Results for K-4 Project with Target Simulated In-Place Densities and Target Air Voids @ N_{design}

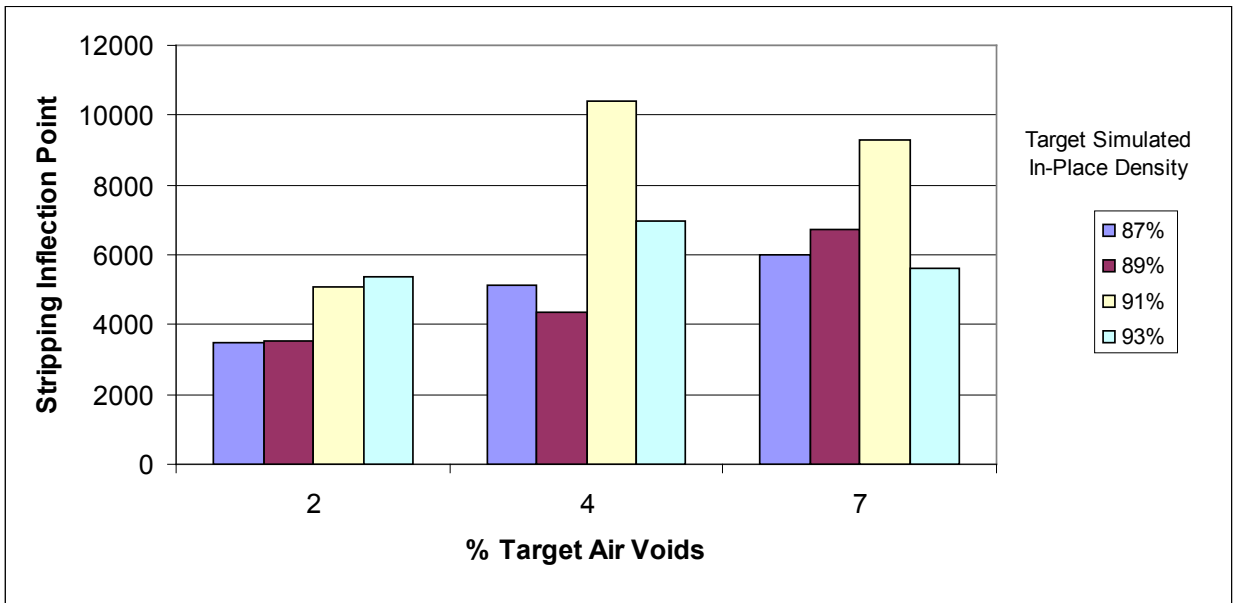


Figure B.4 HWTD Stripping Inflection Points Results for K-4 Project with Target Simulated In-Place Densities and Target Air Voids @ N_{design}

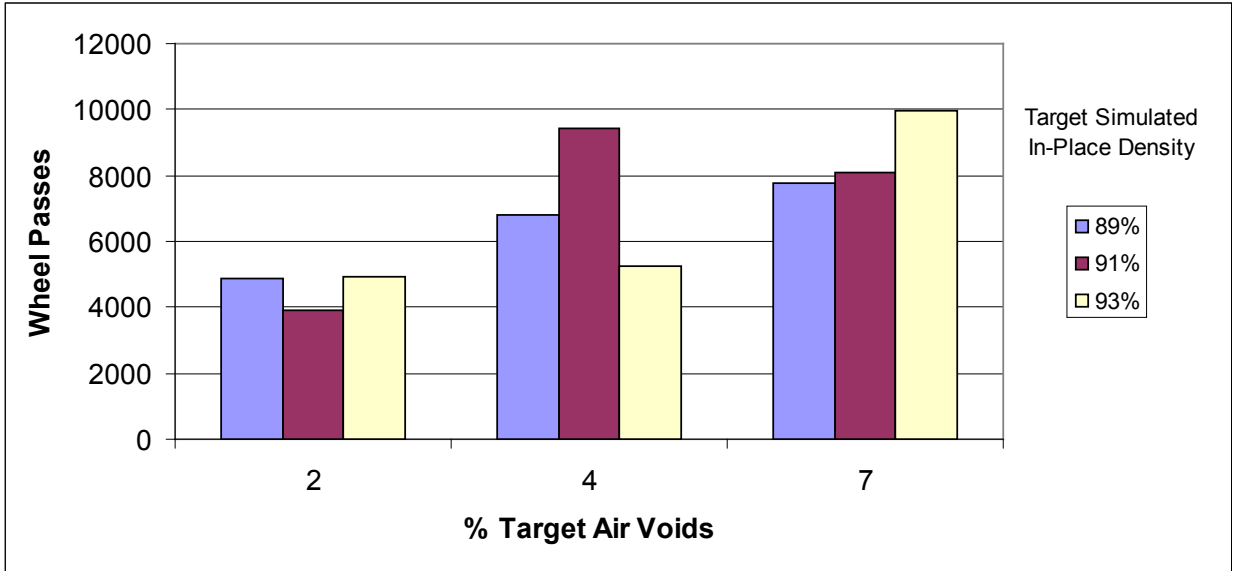


Figure B.5 HWTD Wheel Passes Results for K-9 Project with Target Simulated In-Place Densities and Target Air Voids @ N_{design}

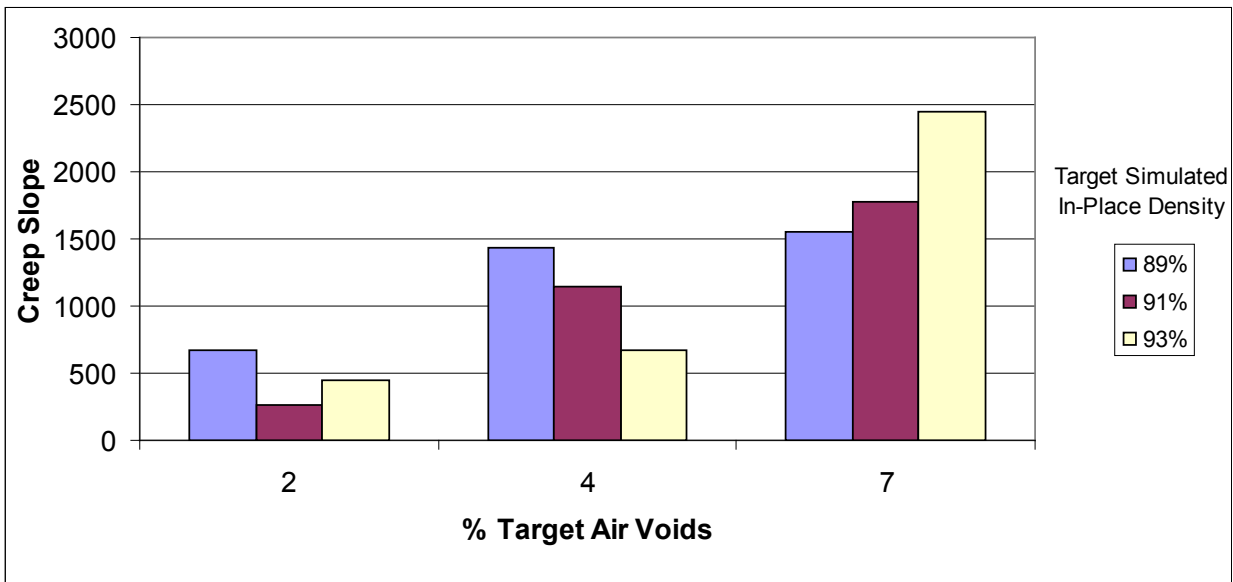


Figure B.6 HWTD Creep Slope Results for K-9 Project with Target Simulated In-Place Densities and Target Air Voids @ N_{design}

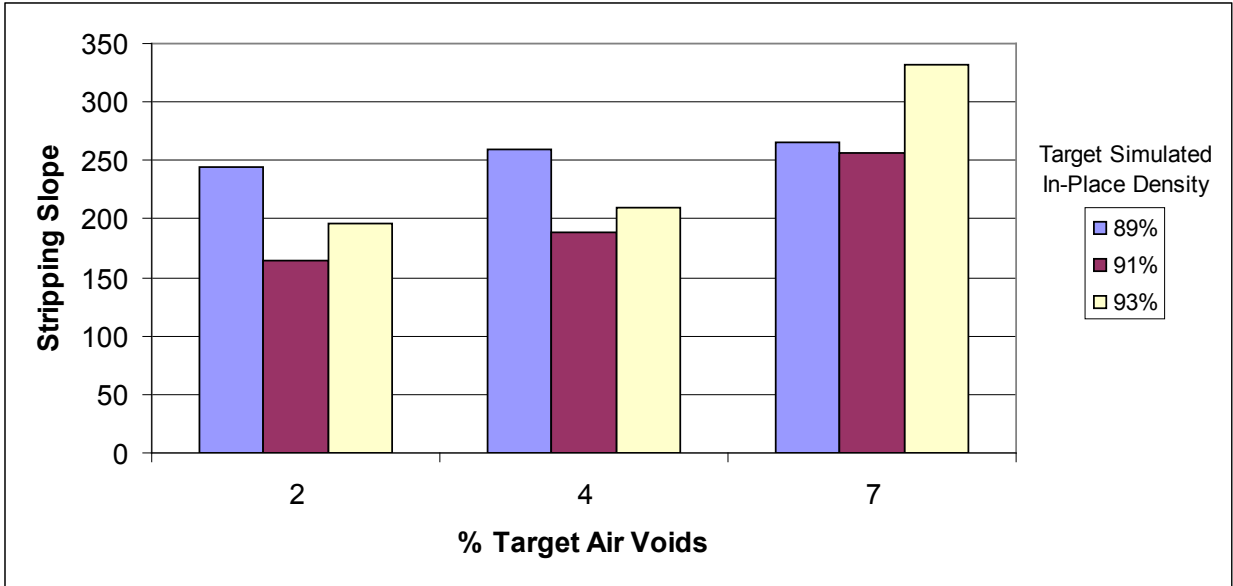


Figure B.7 HWTD Stripping Slope Results for K-9 Project with Target Simulated In-Place Densities and Target Air Voids @ N_{design}

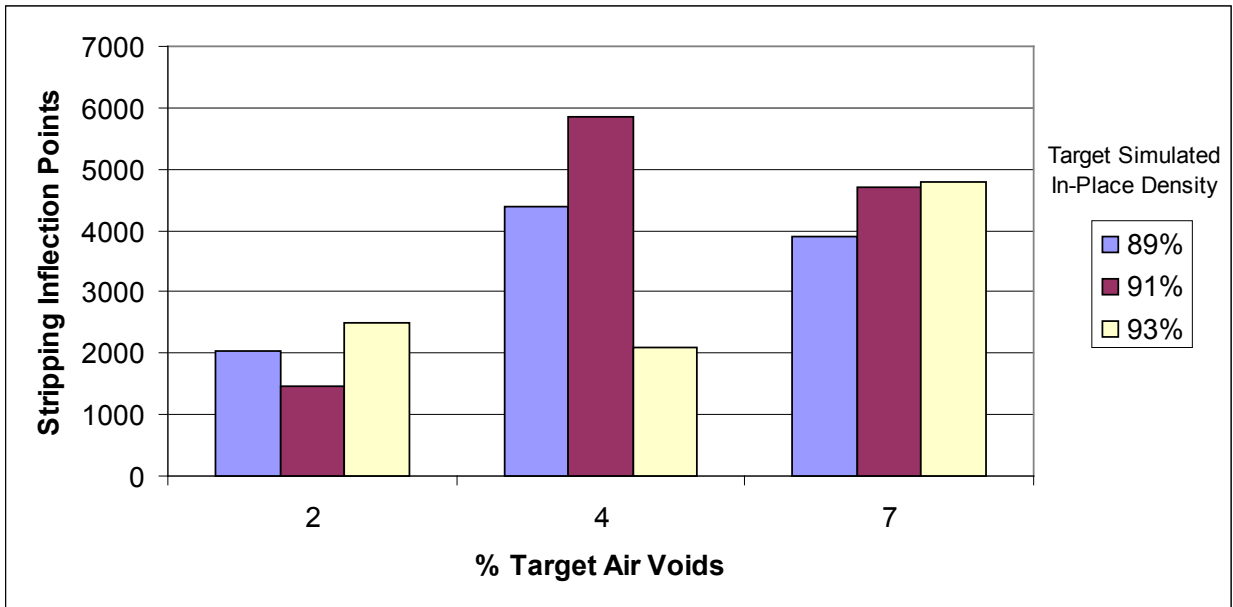


Figure B.8 HWTD Stripping Inflection Points Results for K-9 Project with Target Simulated In-Place Densities and Target Air Voids @ N_{design}

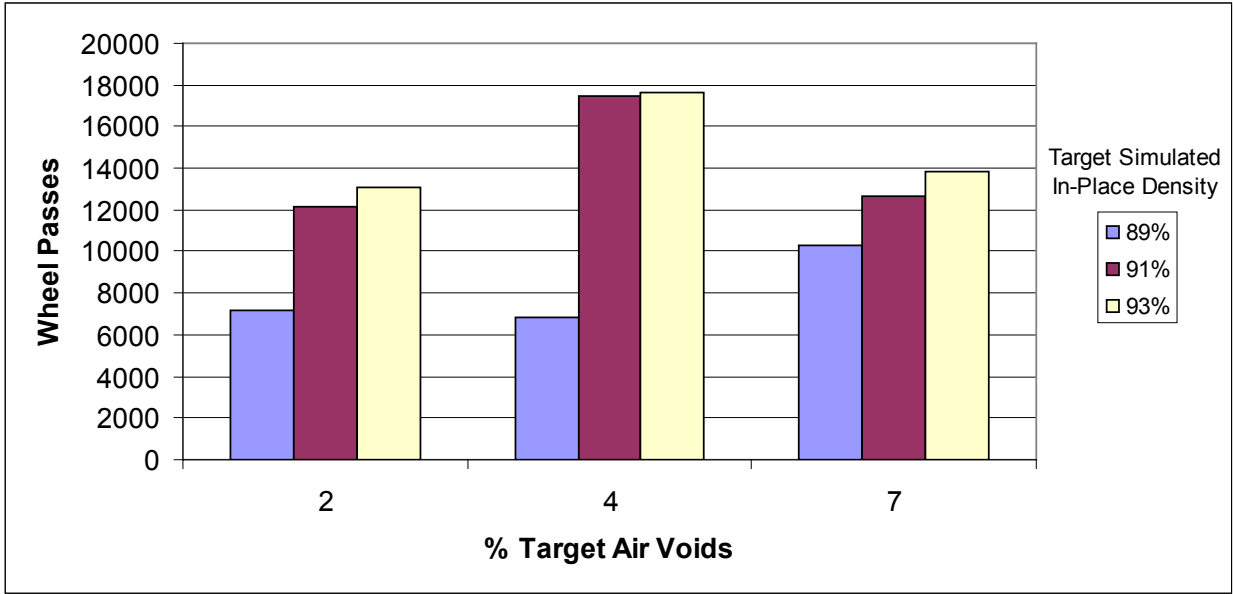


Figure B.9 HWTD Wheel Passes Results for US-24 Project with Target Simulated In-Place Densities and Target Air Voids @ N_{design}

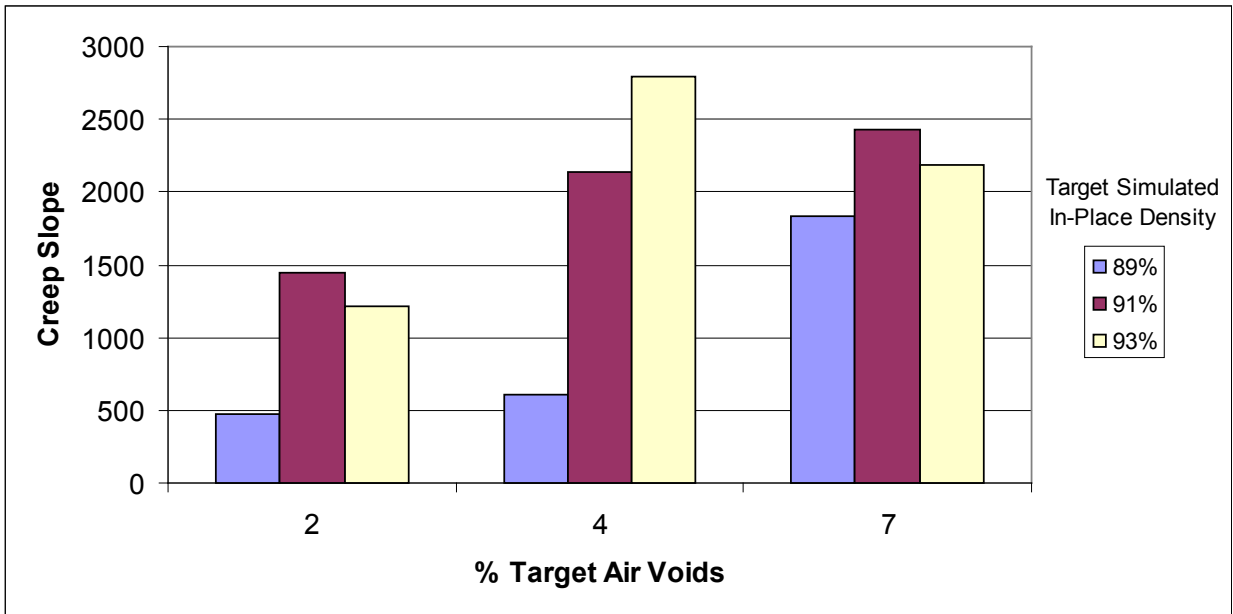


Figure B.10 HWTD Creep Slope Results for US-24 Project with Target Simulated In-Place Densities and Target Air Voids @ N_{design}

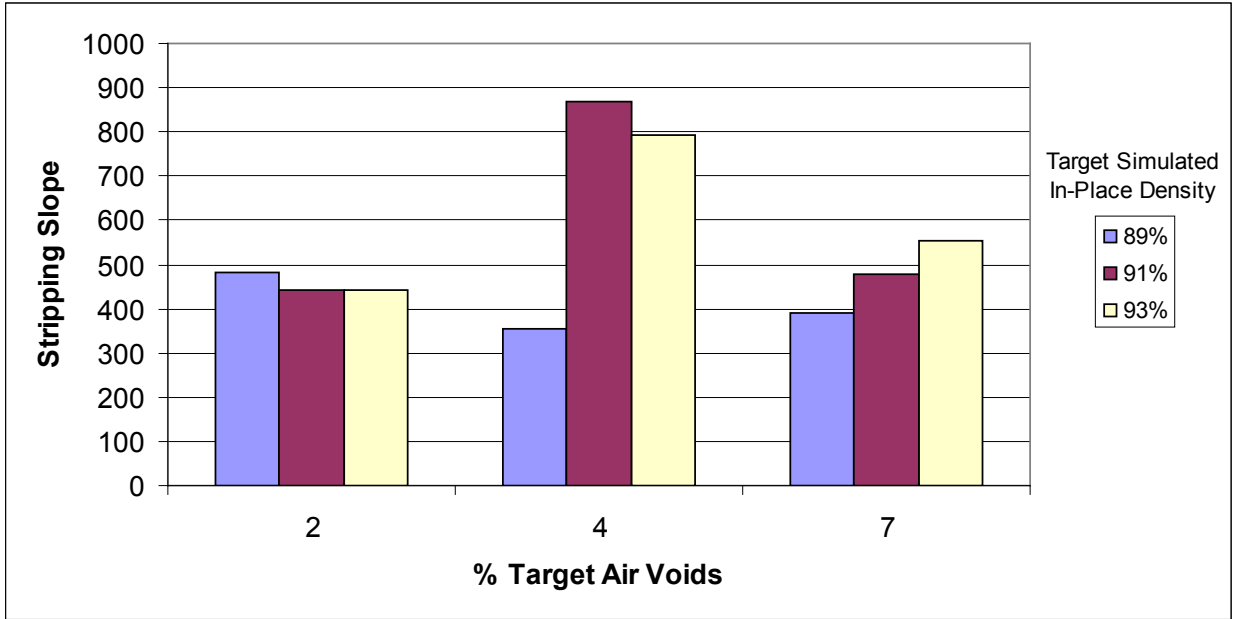


Figure B.11 HWTD Stripping Slope Results for US-24 Project with Target Simulated In-Place Densities and Target Air Voids @ N_{design}

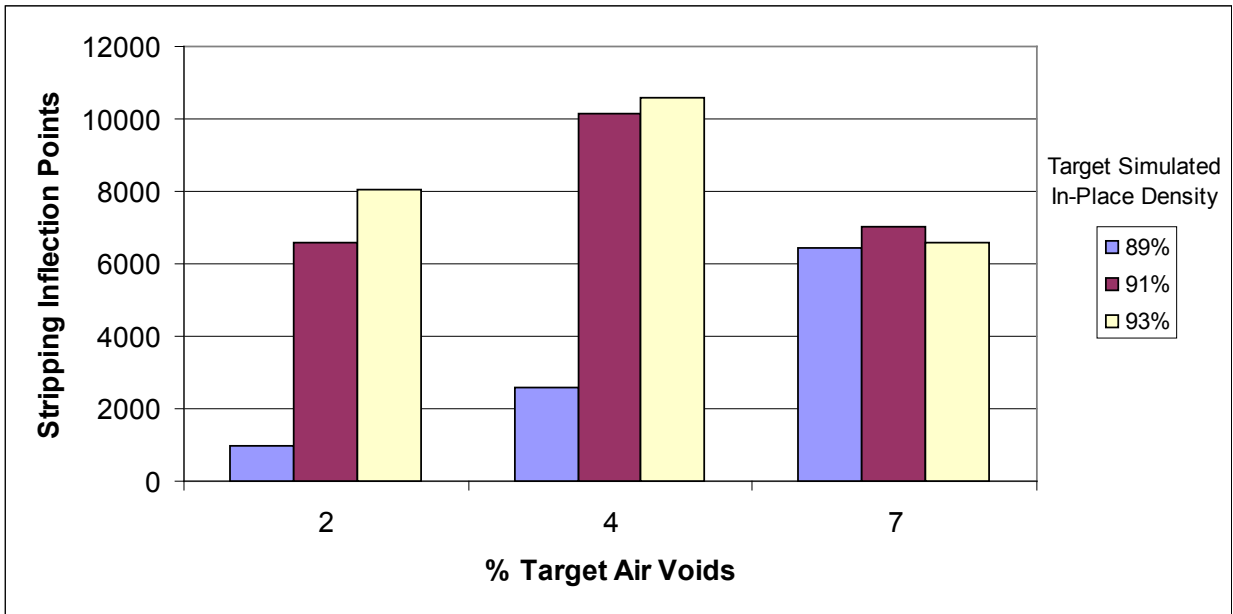


Figure B.12 HWTD Stripping Inflection Points Results for US-24 Project with Target Simulated In-Place Densities and Target Air Voids @ N_{design}

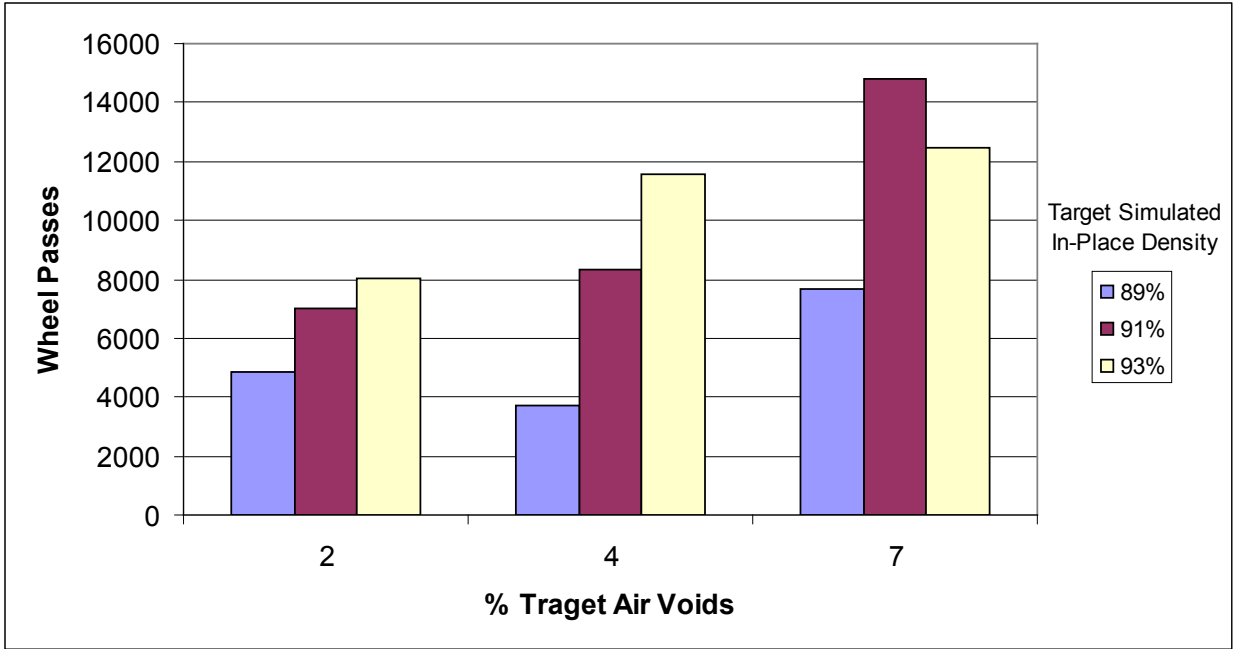


Figure B.13 HWTD Wheel Passes Results for K-152 Project with Target Simulated In-Place Densities and Target Air Voids @ N_{design}

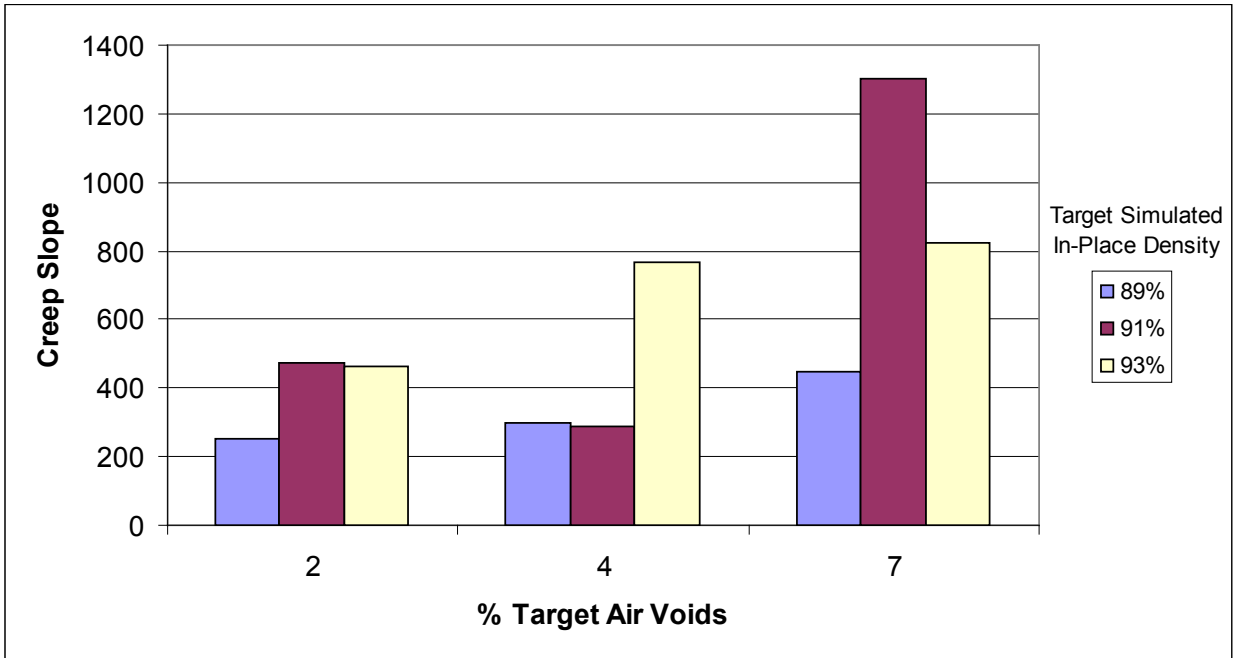


Figure B.14 HWTD Creep Slope Results for K-152 Project with Target Simulated In-Place Densities and Target Air Voids @ N_{design}

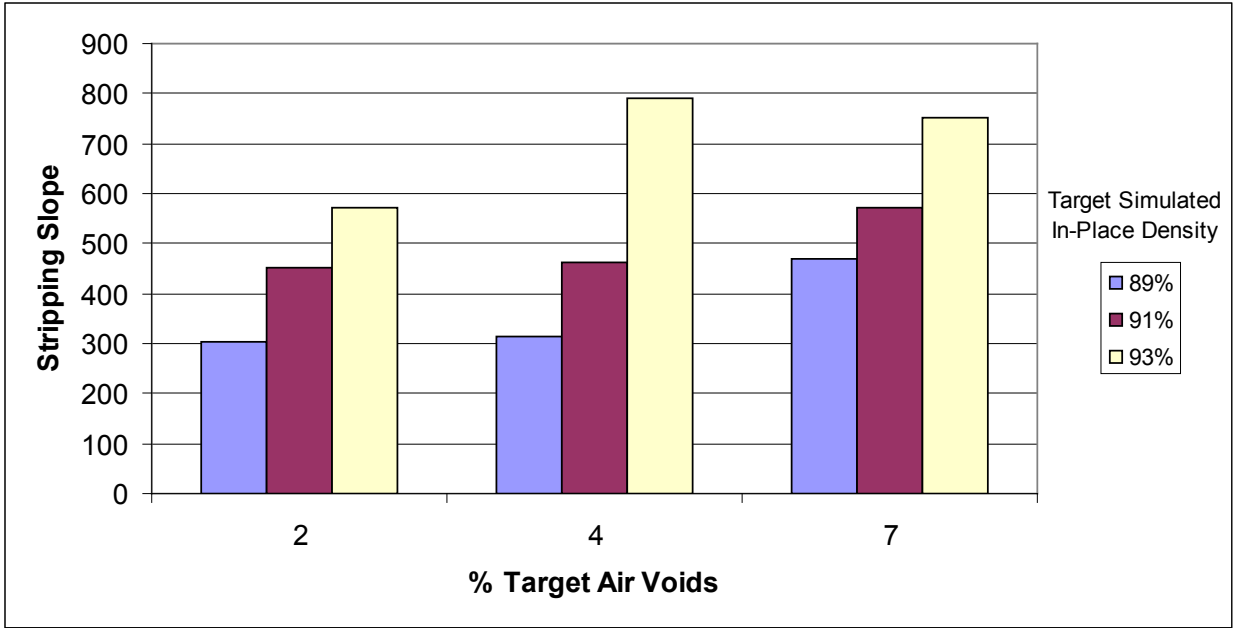


Figure B.15 HWTD Stripping Slope Results for K-152 Project with Target Simulated In-Place Densities and Target Air Voids @ N_{design}

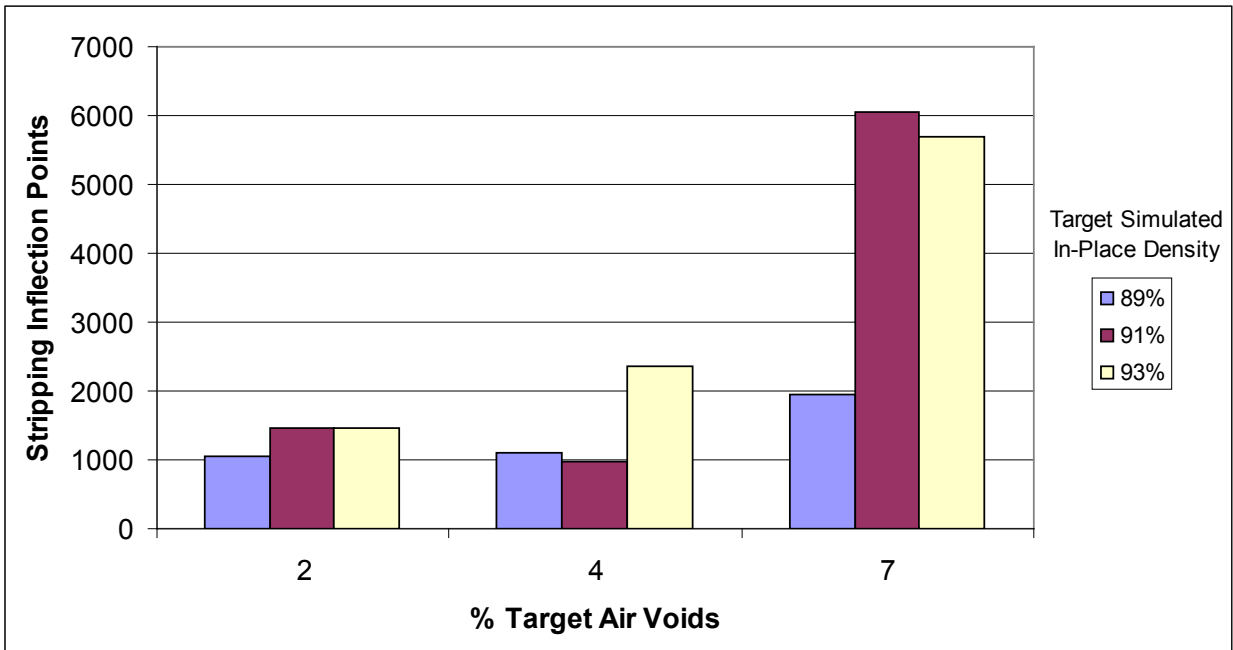


Figure B.16 HWTD Stripping Inflection Points Results for K-152 Project with Target Simulated In-Place Densities and Target Air Voids @ N_{design}

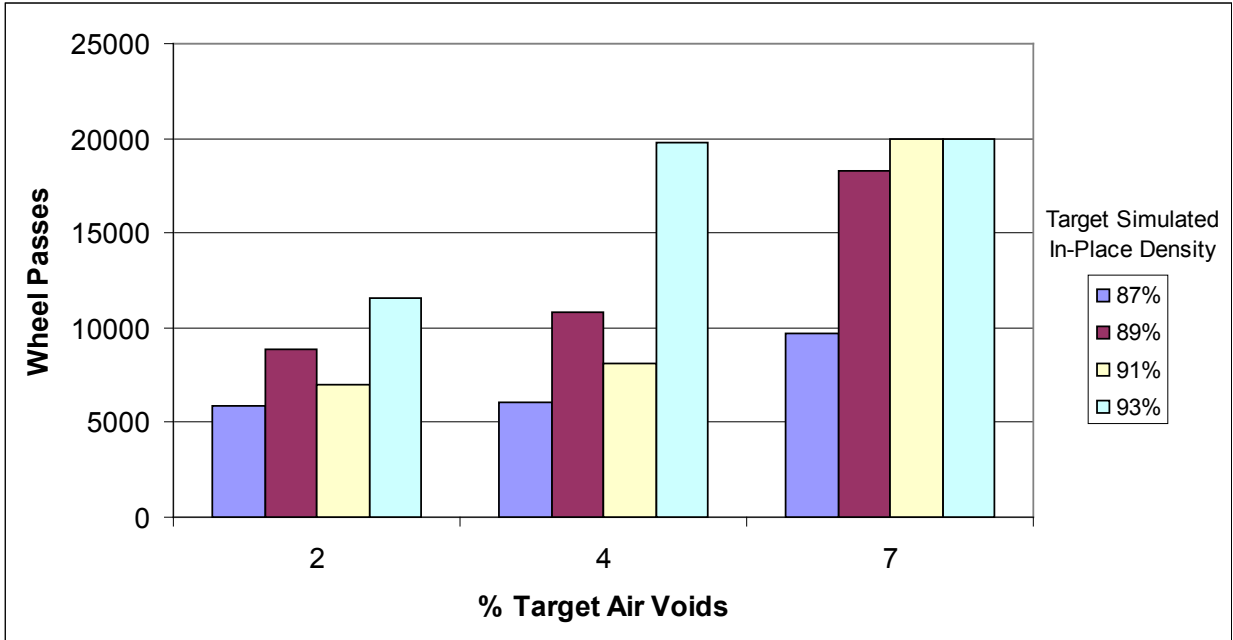


Figure B.17 HWTD Wheel Passes Results for K-15 Project with Target Simulated In-Place Densities and Target Air Voids @ N_{design}

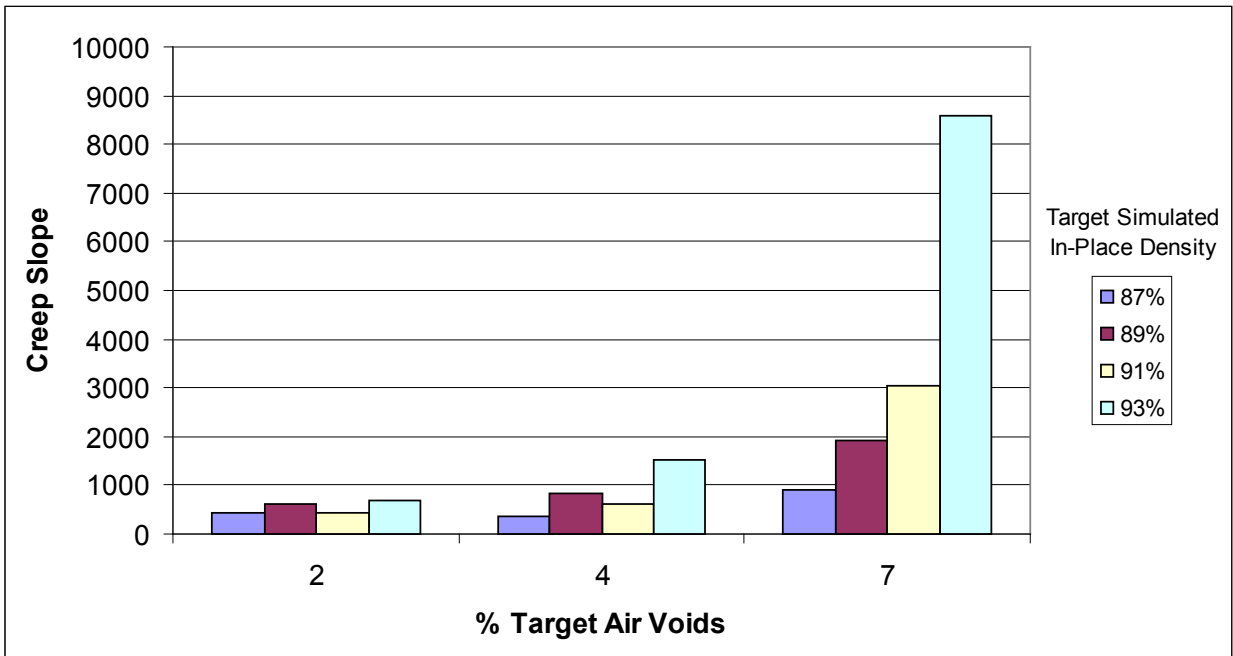


Figure B.18 HWTD Creep Slope Results for K-15 Project with Target Simulated In-Place Densities and Target Air Voids @ N_{design}

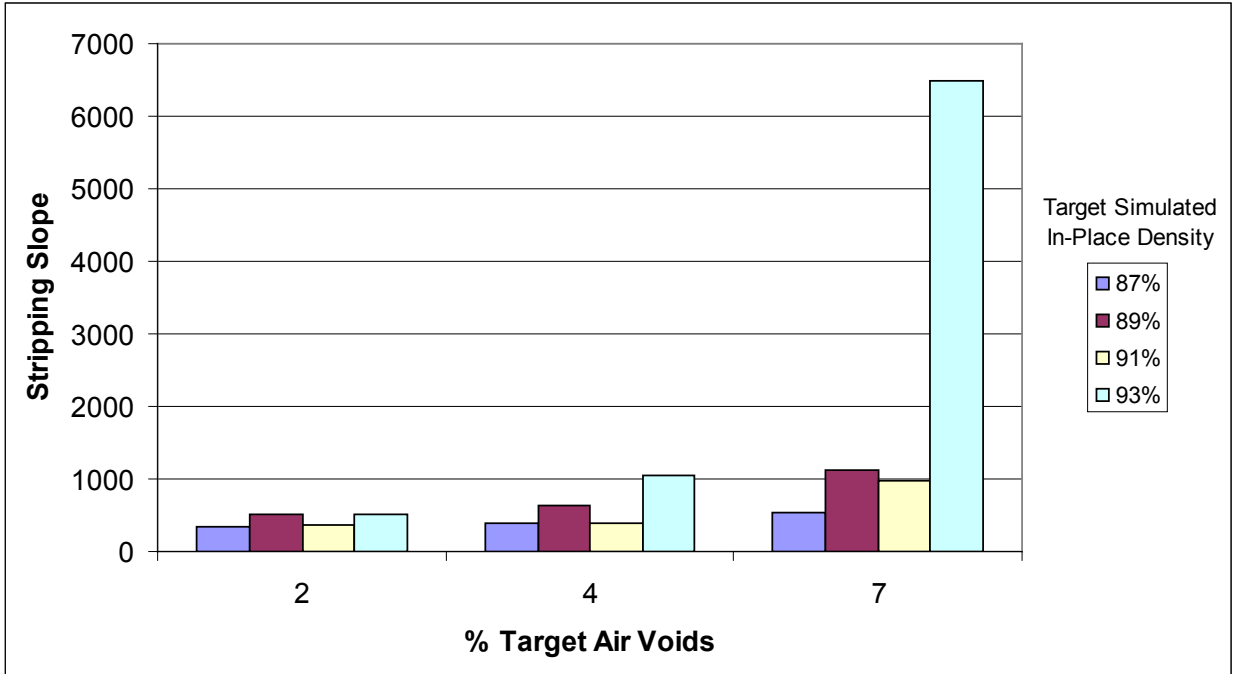


Figure B.19 HWTD Stripping Slope Results for K-15 Project with Target Simulated In-Place Densities and Target Air Voids @ N_{design}

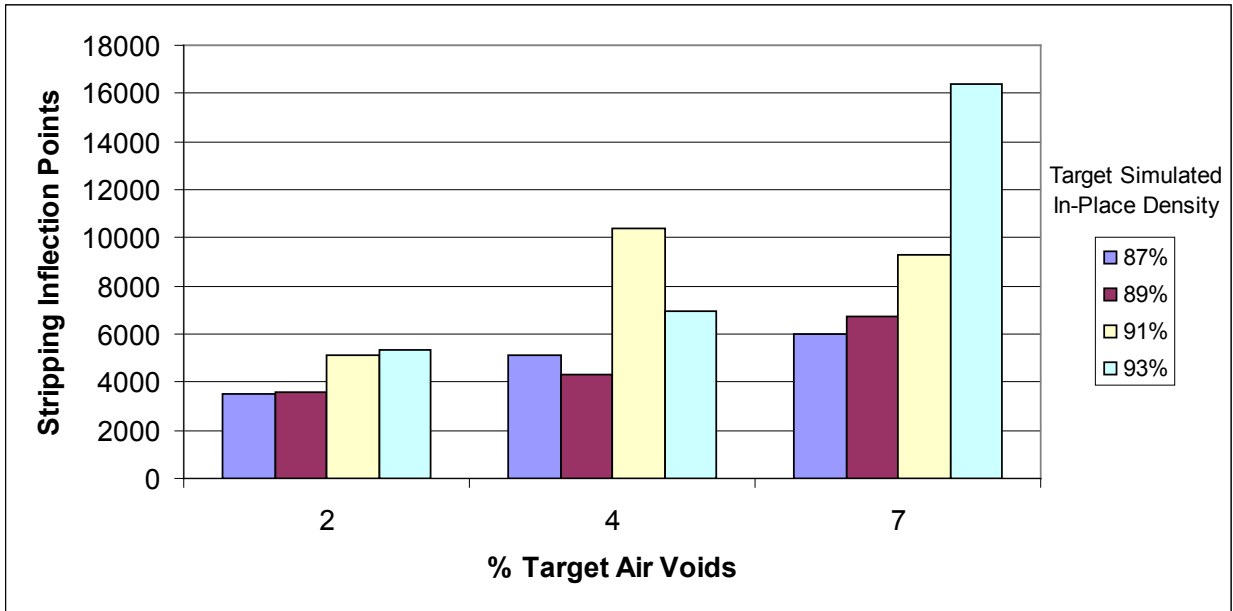


Figure B.20 HWTD Stripping Inflection Points Results for K-15 Project with Target Simulated In-Place Densities and Target Air Voids @ N_{design}

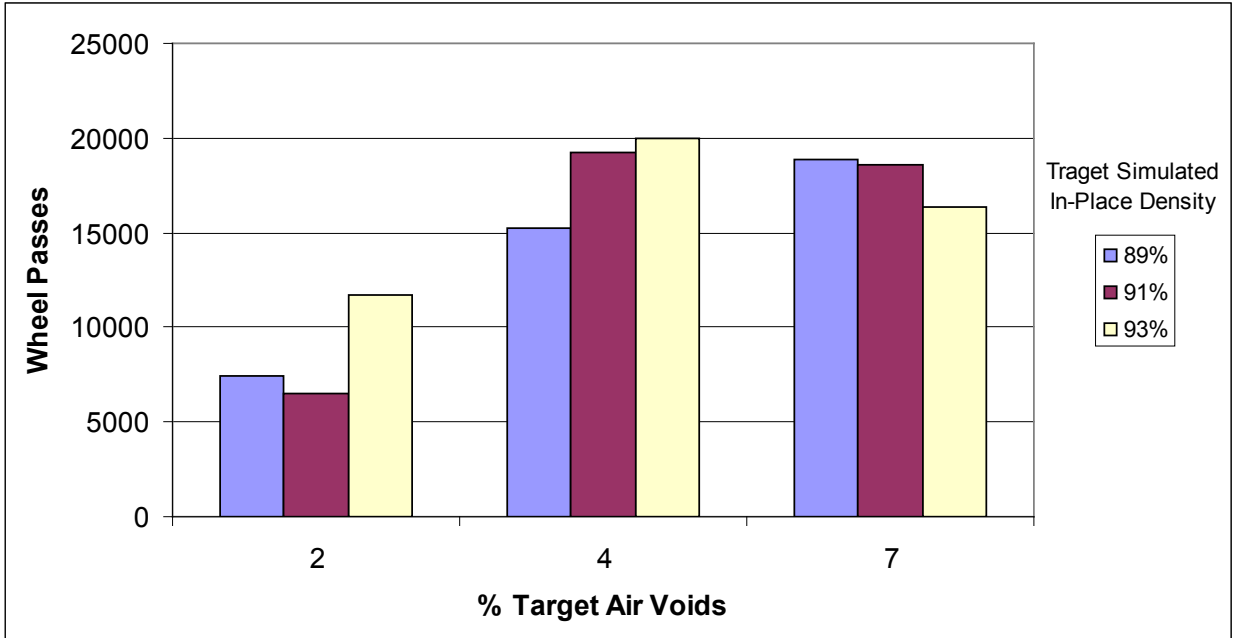


Figure B.21 HWTD Wheel Passes Results for US-83 Project with Target Simulated In-Place Densities and Target Air Voids @ N_{design}

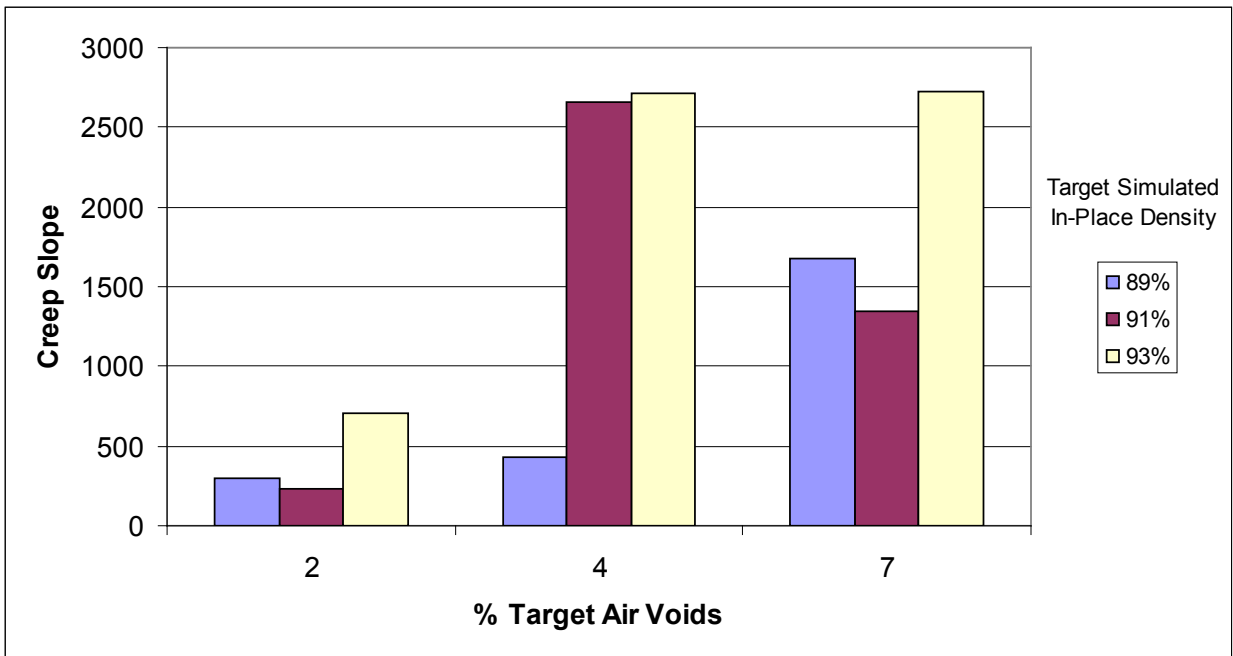


Figure B.22 HWTD Creep Slope Results for US-83 Project with Target Simulated In-Place Densities and Target Air Voids @ N_{design}

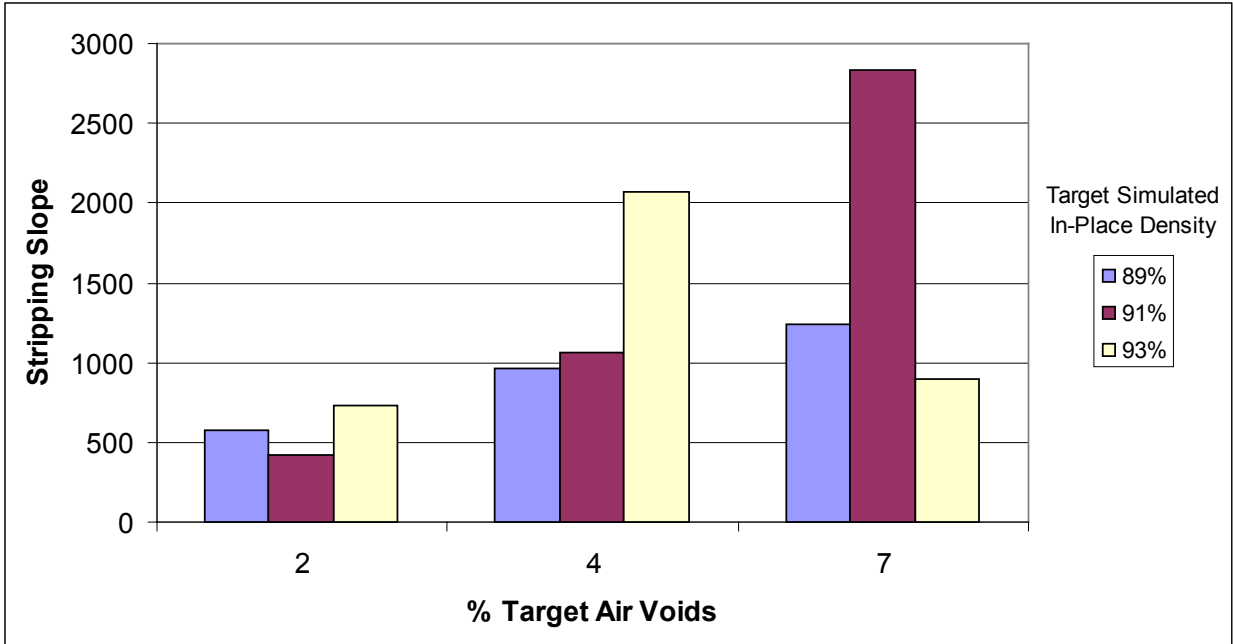


Figure B.23 HWTD Stripping Slope Results for US-83 Project with Target Simulated In-Place Densities and Target Air Voids @ N_{design}

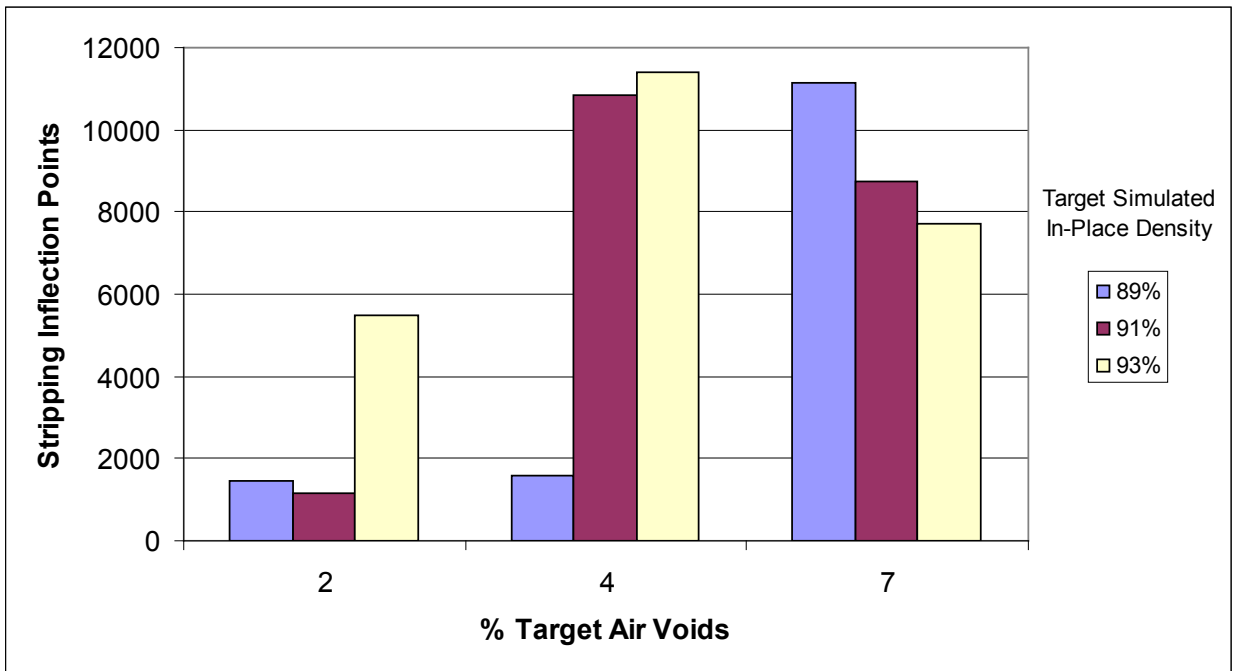


Figure B.24 HWTD Stripping Inflection Points Results for US-83 Project with Target Simulated In-Place Densities and Target Air Voids @ N_{design}

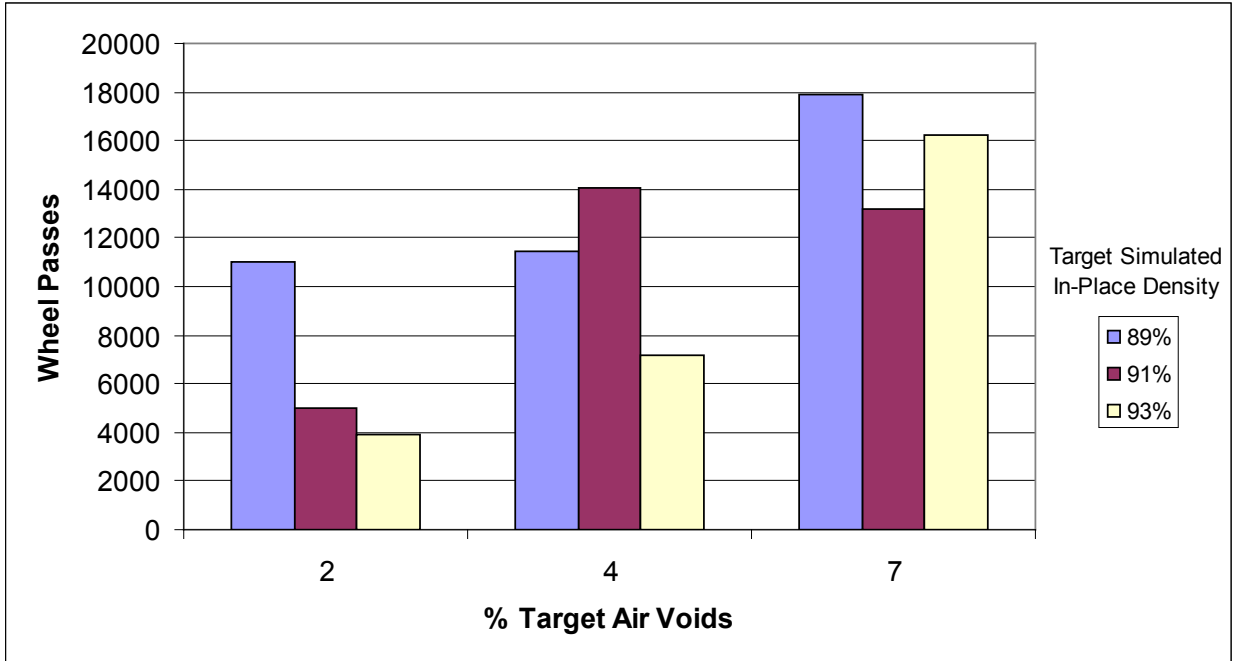


Figure B.25 HWTD Wheel Passes Results for K-246 Project with Target Simulated In-Place Densities and Target Air Voids @ N_{design}

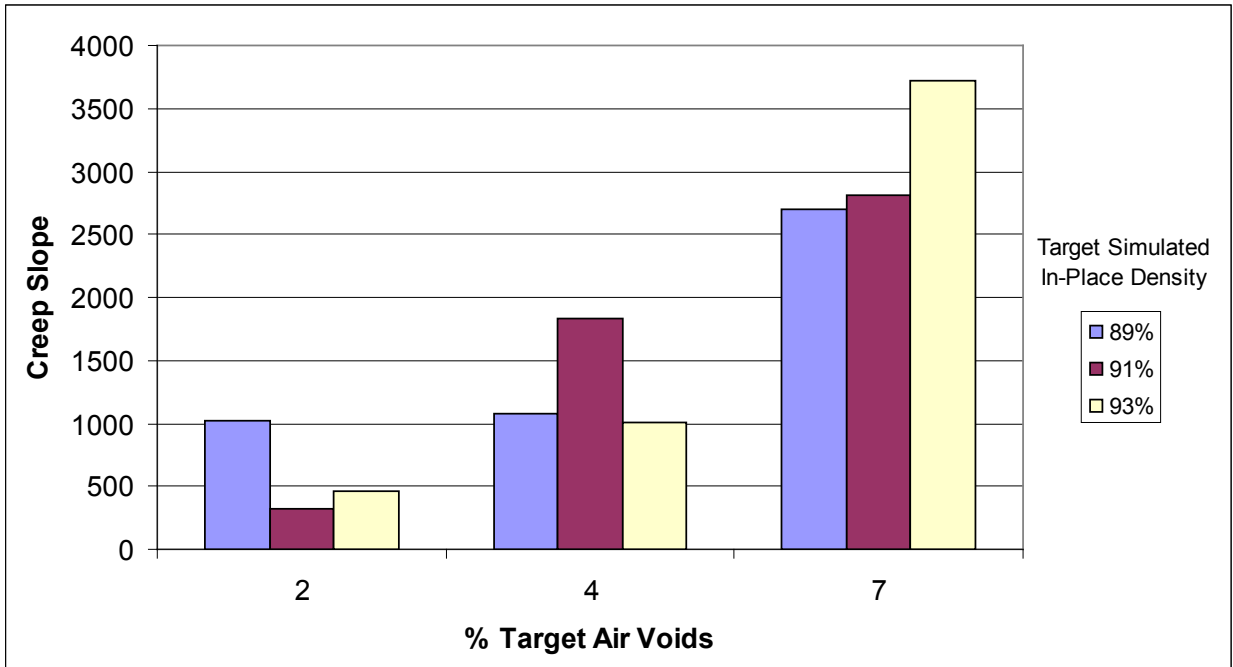


Figure B.26 HWTD Creep Slope Results for K-246 Project with Target Simulated In-Place Densities and Target Air Voids @ N_{design}

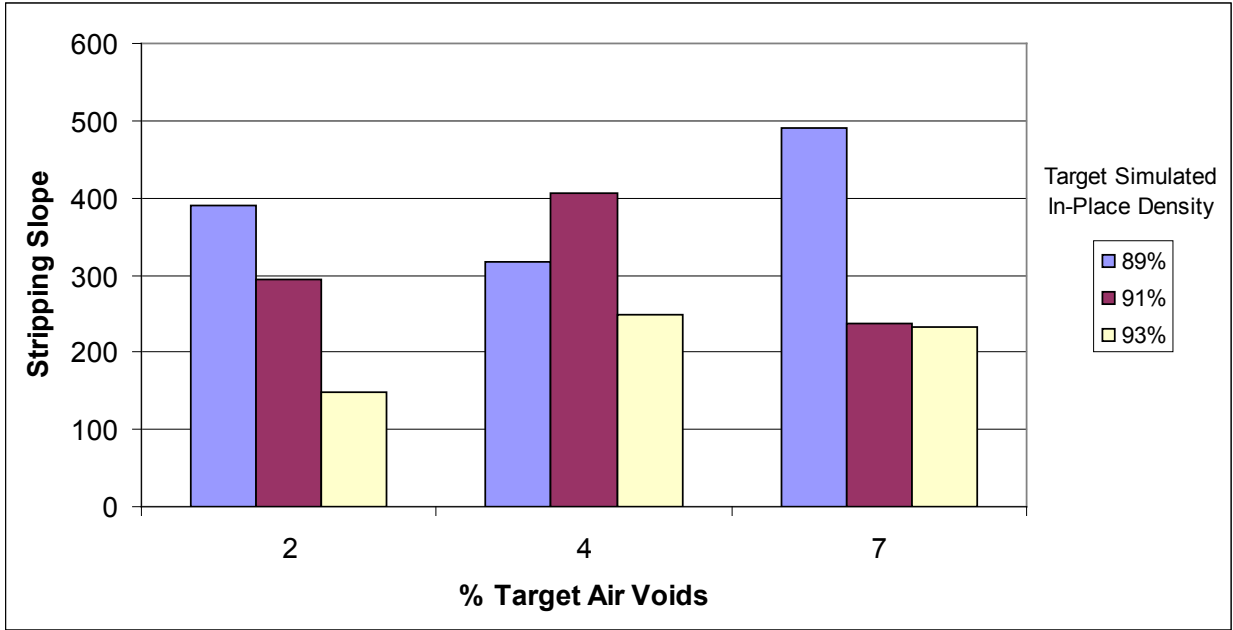


Figure B.27 HWTD Stripping Slope Results for K-246 Project with Target Simulated In-Place Densities and Target Air Voids @ N_{design}

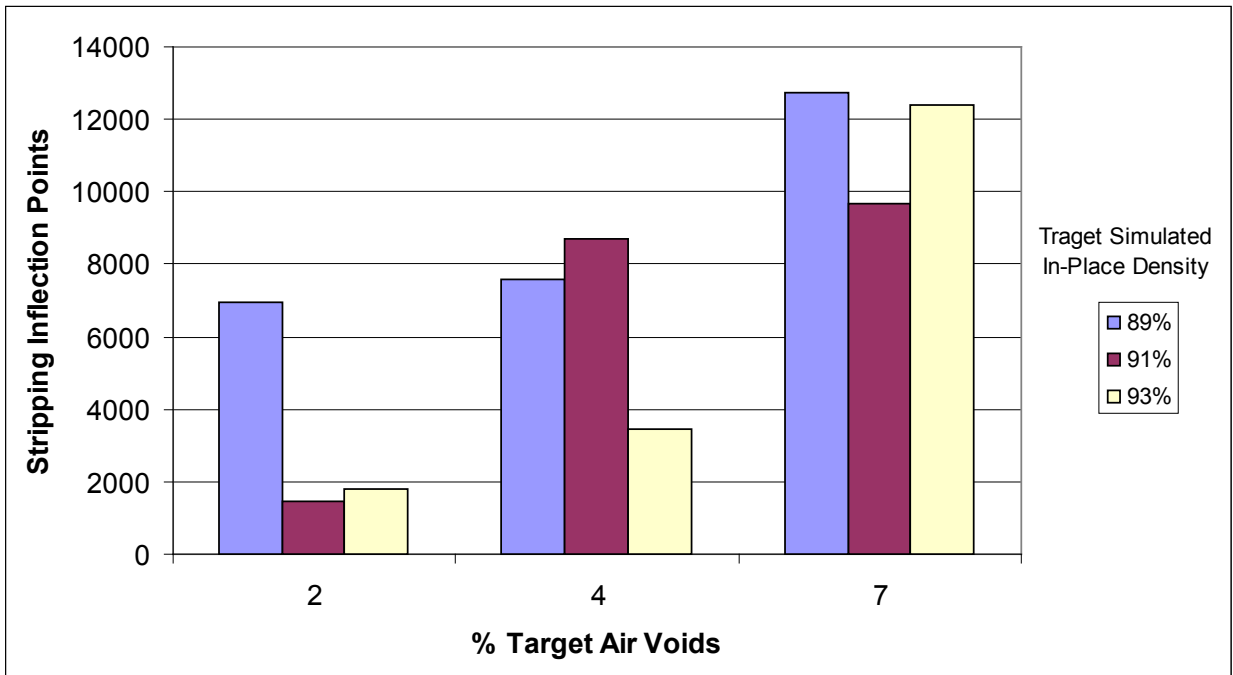


Figure B.28 HWTD Stripping Inflection Points Results for K-246 Project with Target Simulated In-Place Densities and Target Air Voids @ N_{design}

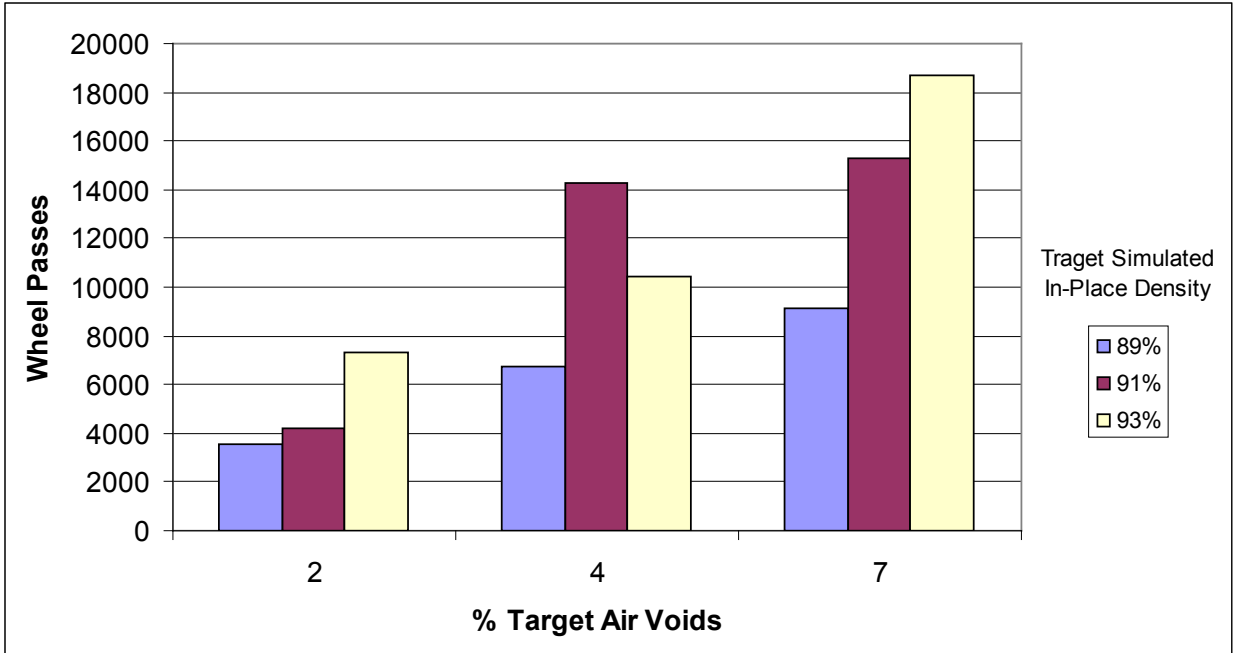


Figure B.29 HWTD Wheel Passes Results for US-56 Project with Target Simulated In-Place Densities and Target Air Voids @ N_{design}

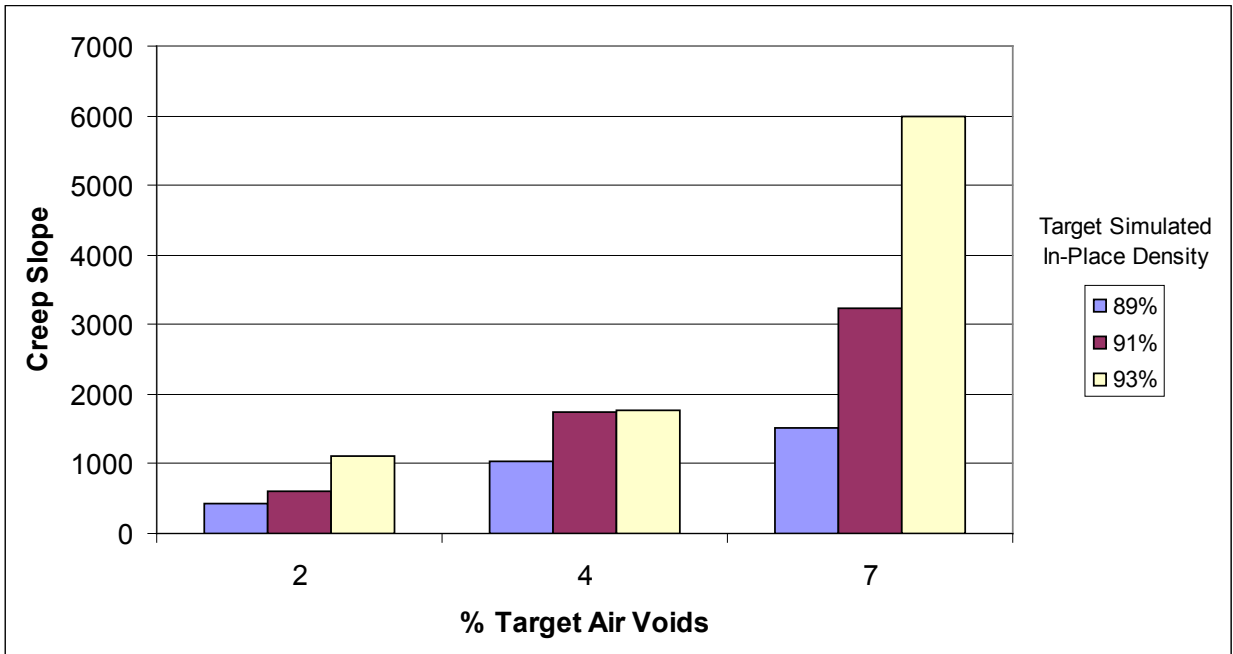


Figure B.30 HWTD Creep Slope Results for US-56 Project with Target Simulated In-Place Densities and Target Air Voids @ N_{design}

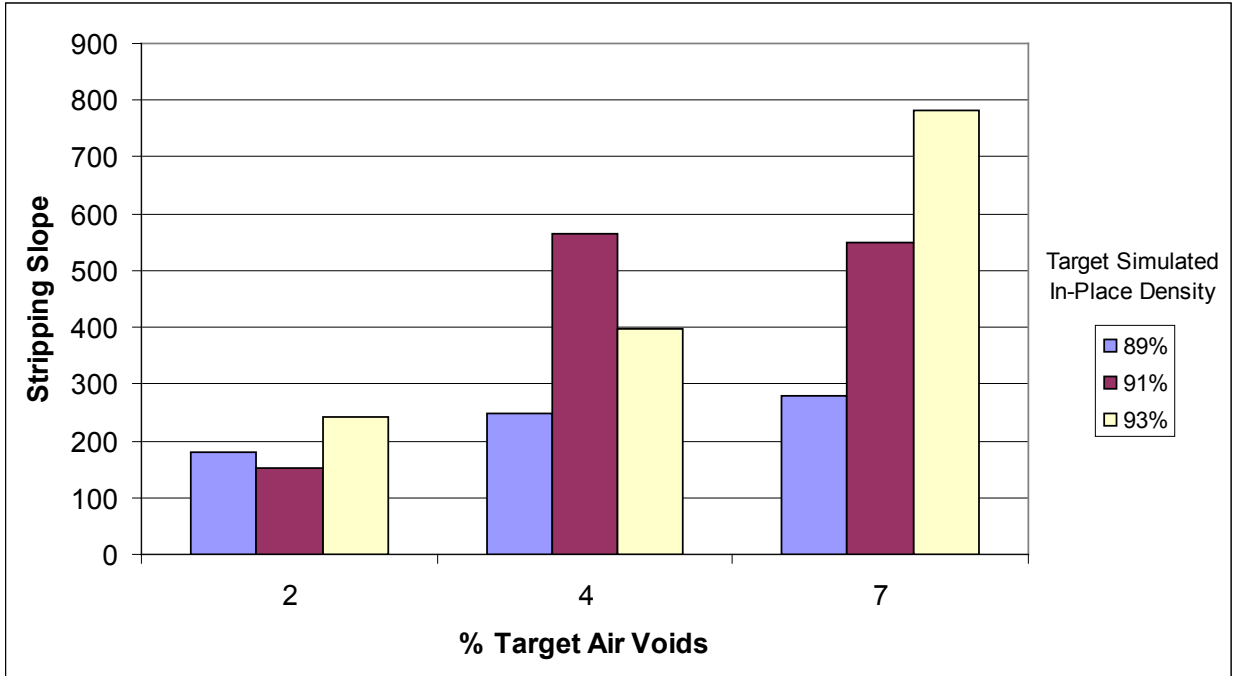


Figure B.31 HWTD Stripping Slope Results for US-56 Project with Target Simulated In-Place Densities and Target Air Voids @ N_{design}

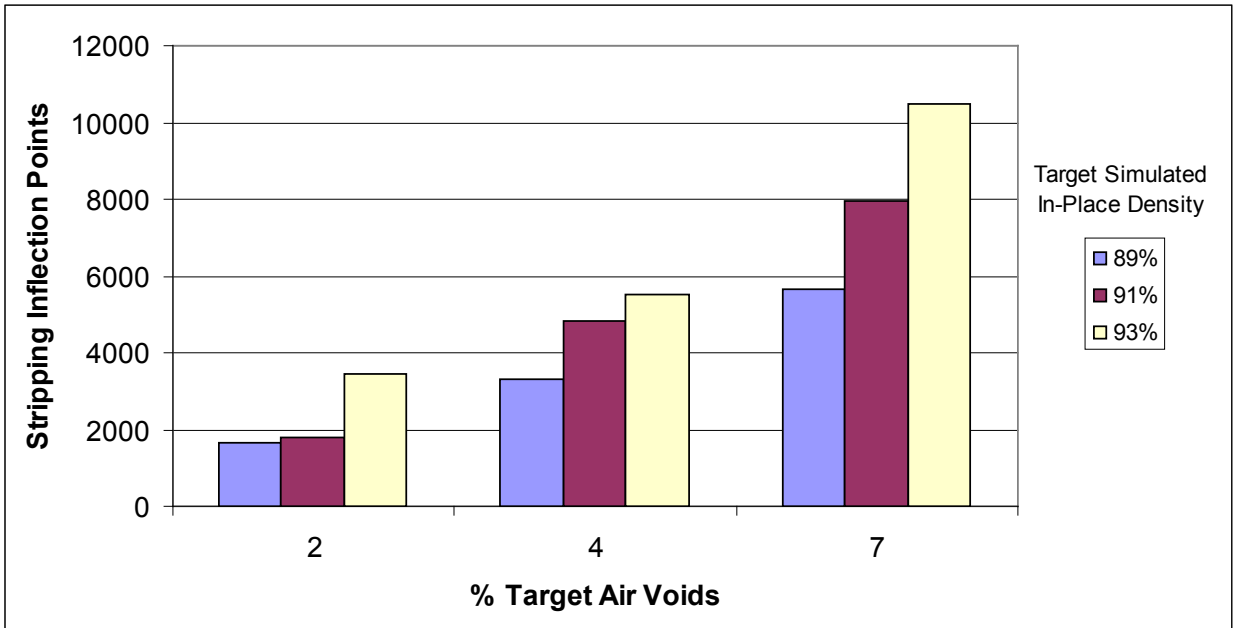


Figure B.32 HWTD Stripping Inflection Points Results for US-56 Project with Target Simulated In-Place Densities and Target Air Voids @ N_{design}

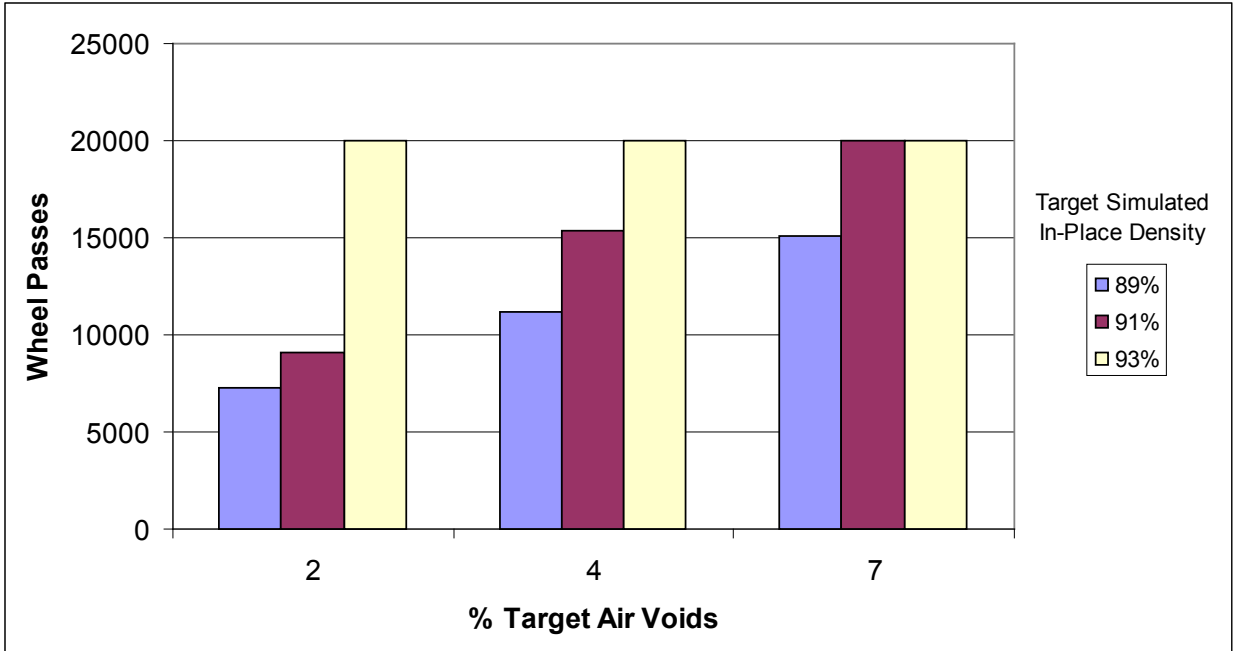


Figure B.33 HWTD Wheel Passes Results for US-50 Project with Simulated In-Place Densities and Target Air Voids @ N_{design}

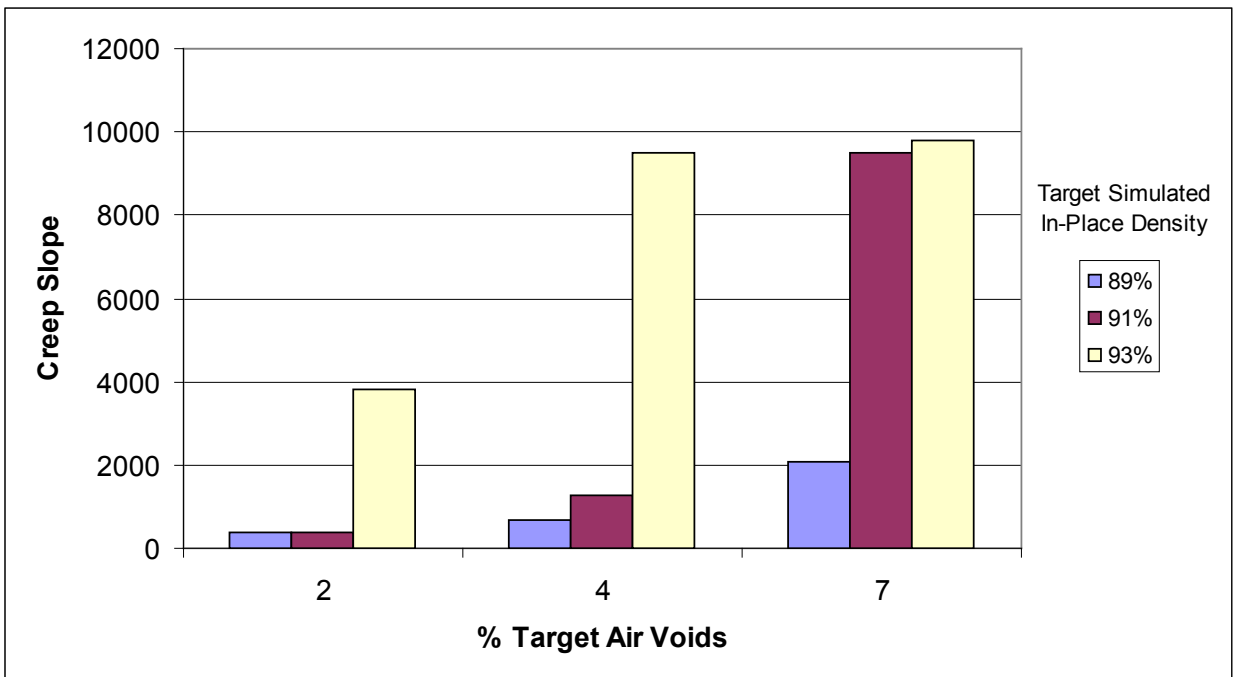


Figure B.34 HWTD Creep Slope Results for US-50 Project with Target Simulated In-Place Densities and Target Air Voids @ N_{design}

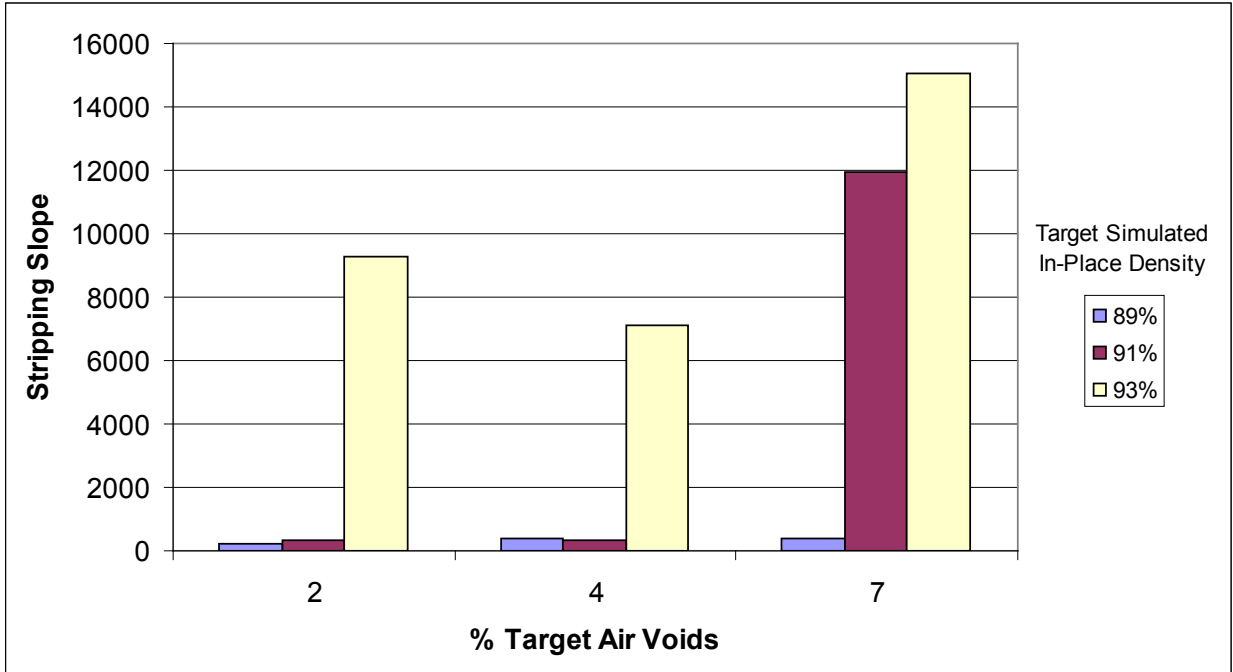


Figure B.35 HWTD Stripping Slope Results for US-50 Project with Target Simulated In-Place Densities and Target Air Voids @ N_{design}

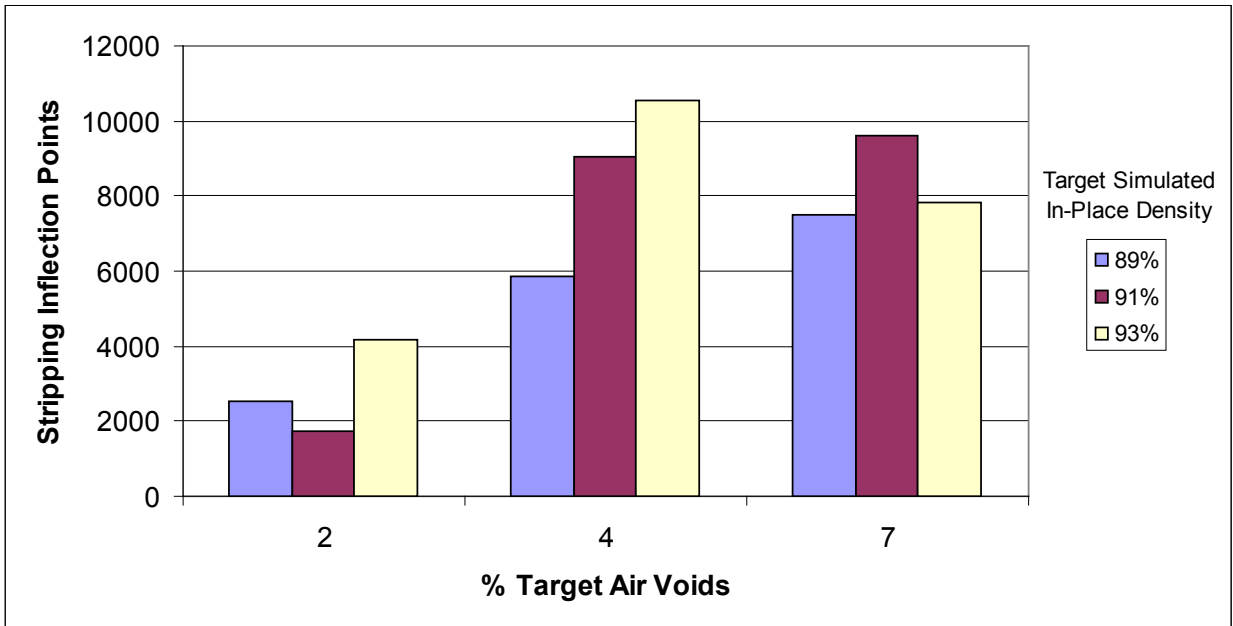


Figure B.36 HWTD Stripping Inflection Points Results for US-50 Project with Target Simulated In-Place Densities and Target Air Voids @ N_{design}

**Appendix C - Comparative Plots of HWTD Test Results for
Development of Criteria for Out-of-Specification Pavements**

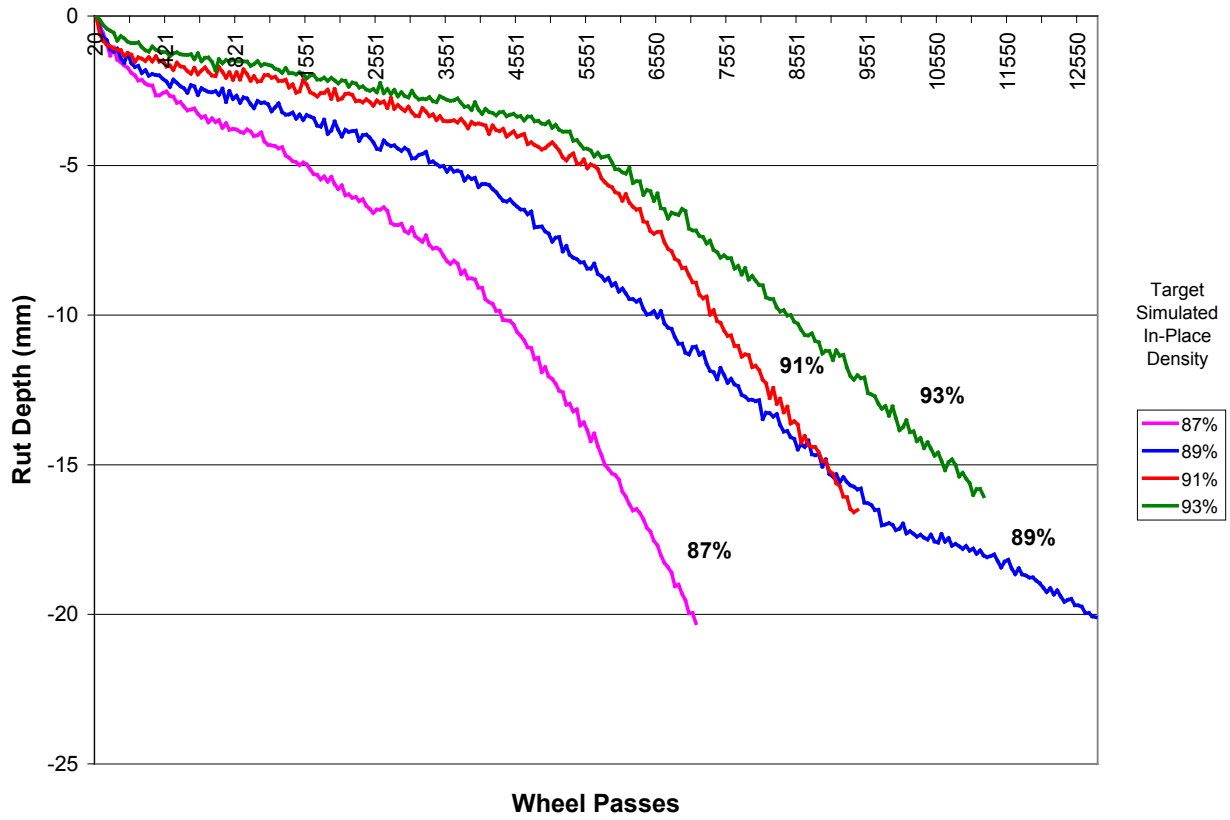


Figure C.1 Comparative HWTD Test Results of K-4 Project at 2% Target Air Voids @ N_{design}

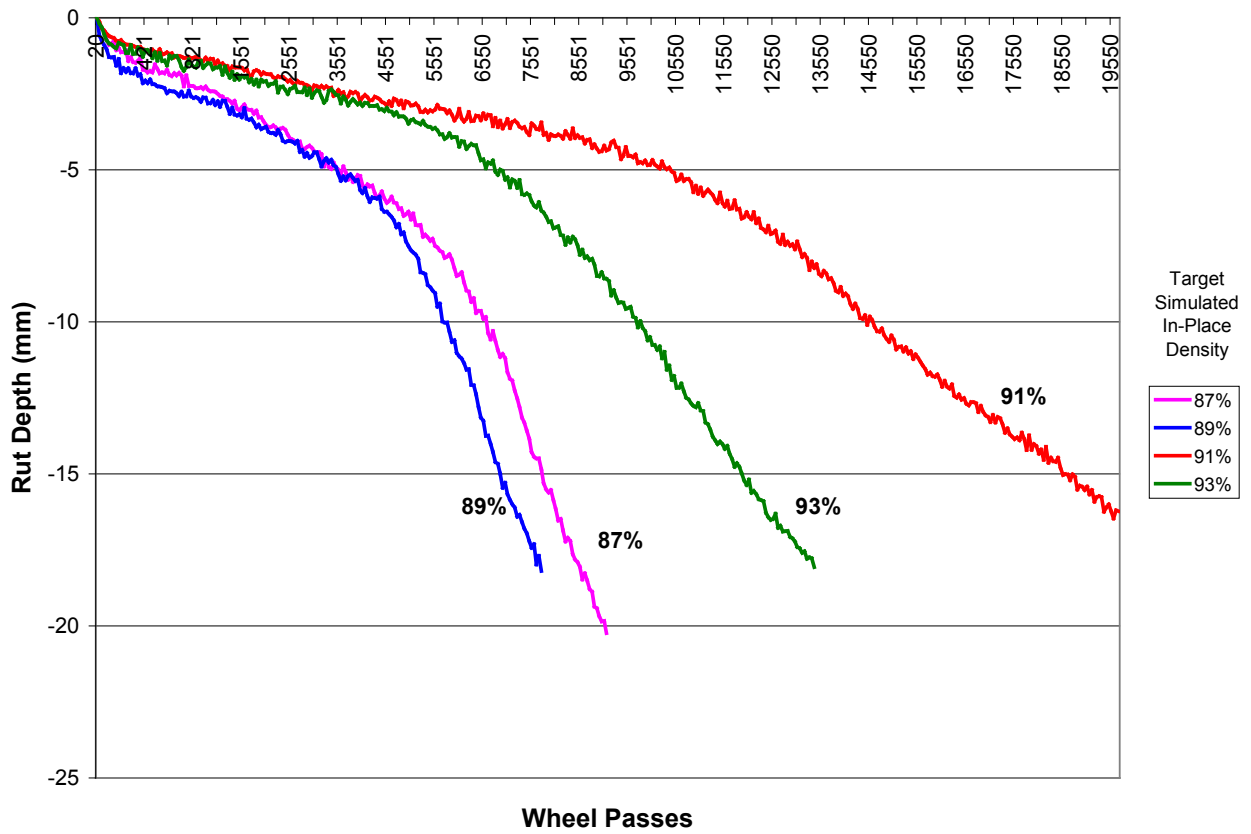


Figure C.2 Comparative HWTD Test Results of K-4 Project at 4% Target Air Voids @ N_{design}

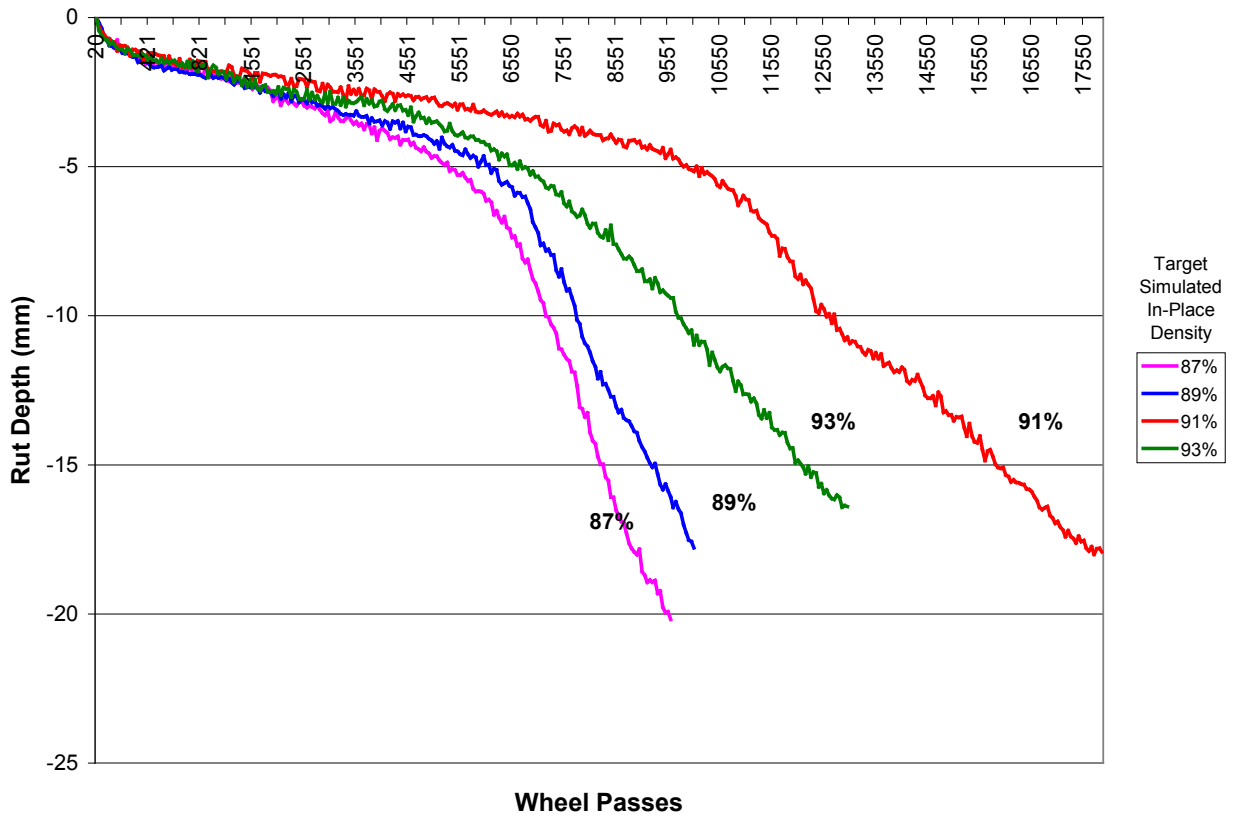


Figure C.3 Comparative HWTD Test Results of K-4 Project at 7% Target Air Voids @ N_{design}

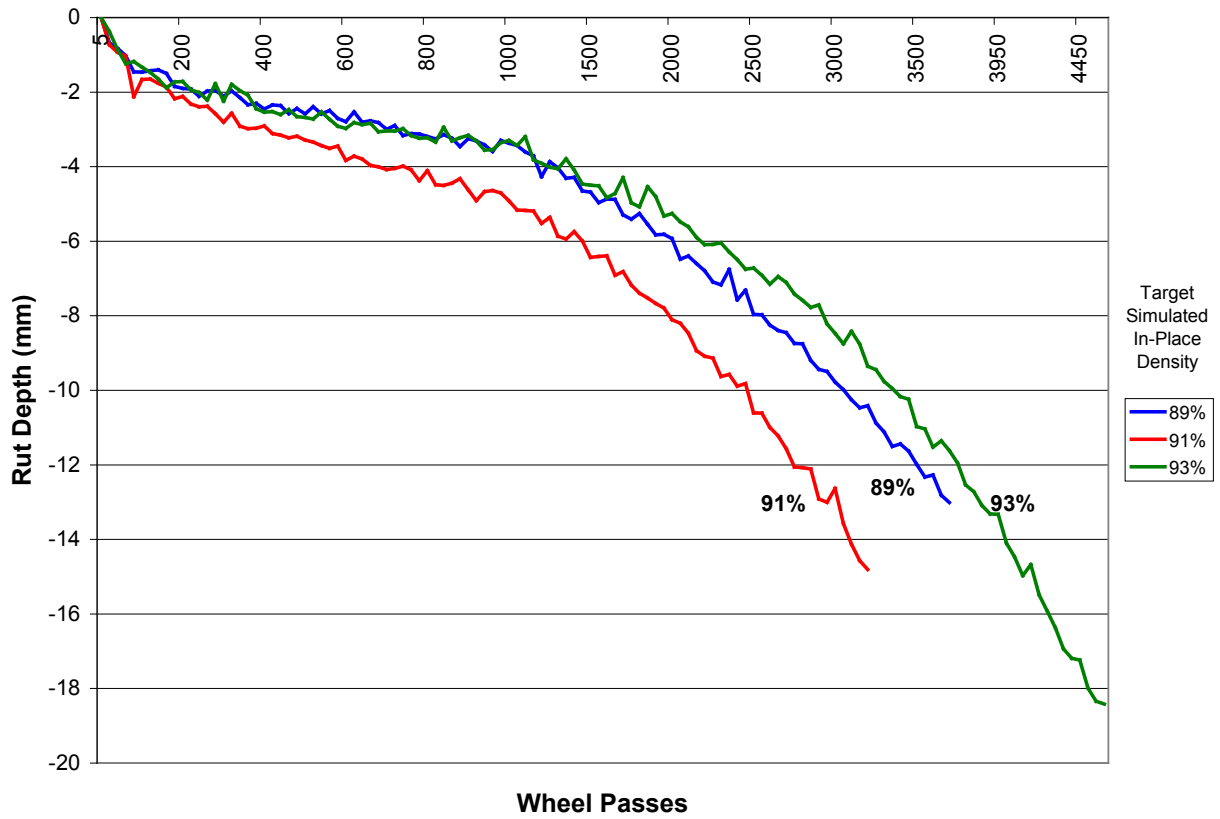


Figure C.4 Comparative HWTD Test Results of K-9 Project at 2% Target Air Voids @ N_{design}

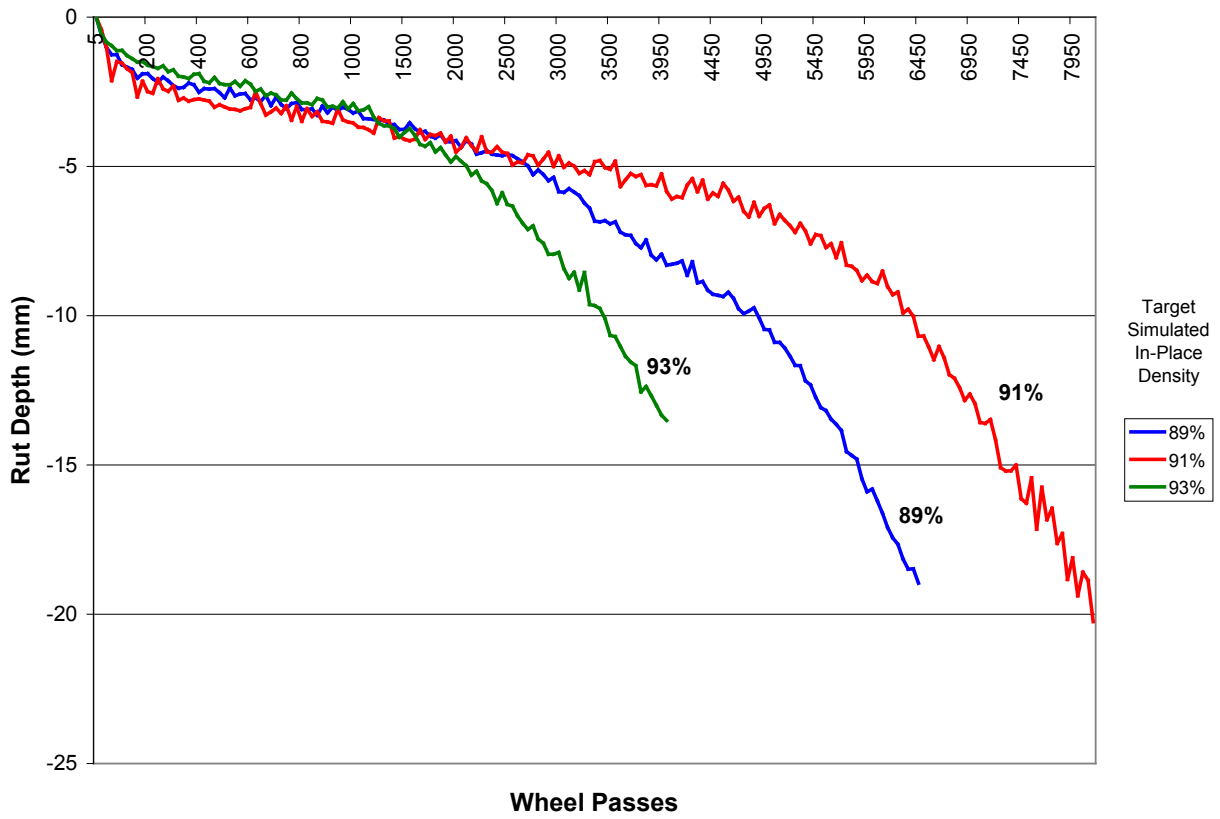


Figure C.5 Comparative HWTD Test Results of K-9 Project at 4% Target Air Voids @ N_{design}

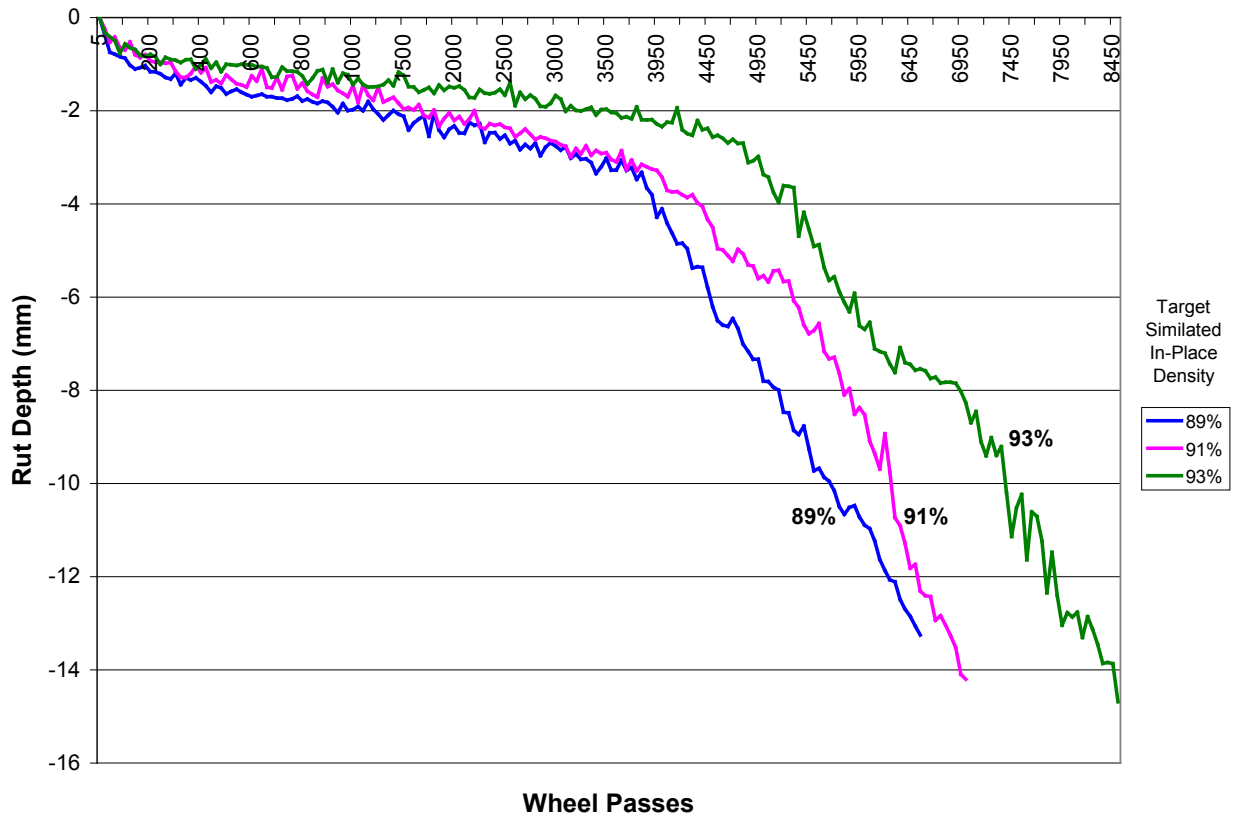


Figure C.6 Comparative HWTD Test Results of K-9 Project at 7% Target Air Voids @ N_{design}

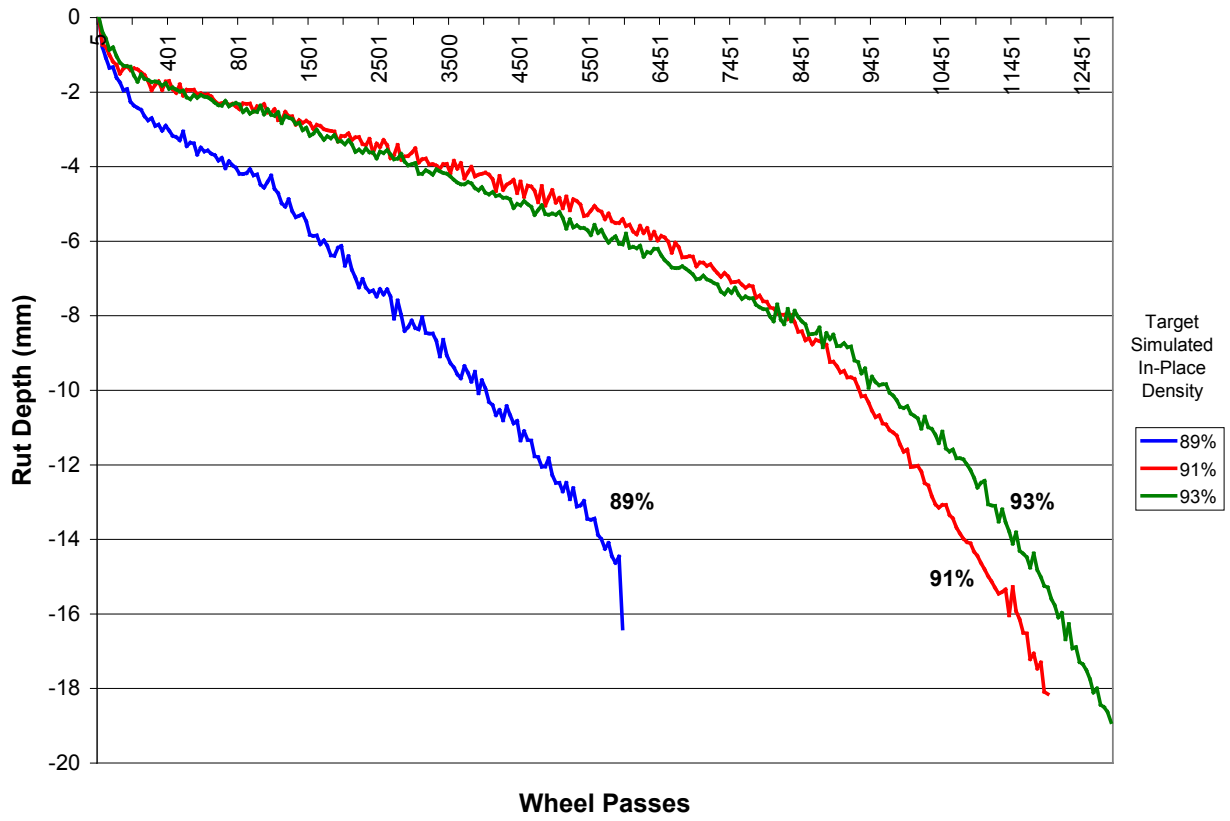


Figure C.7 Comparative HWTD Test Results of US-24 Project at 2% Target Air Voids @ N_{design}

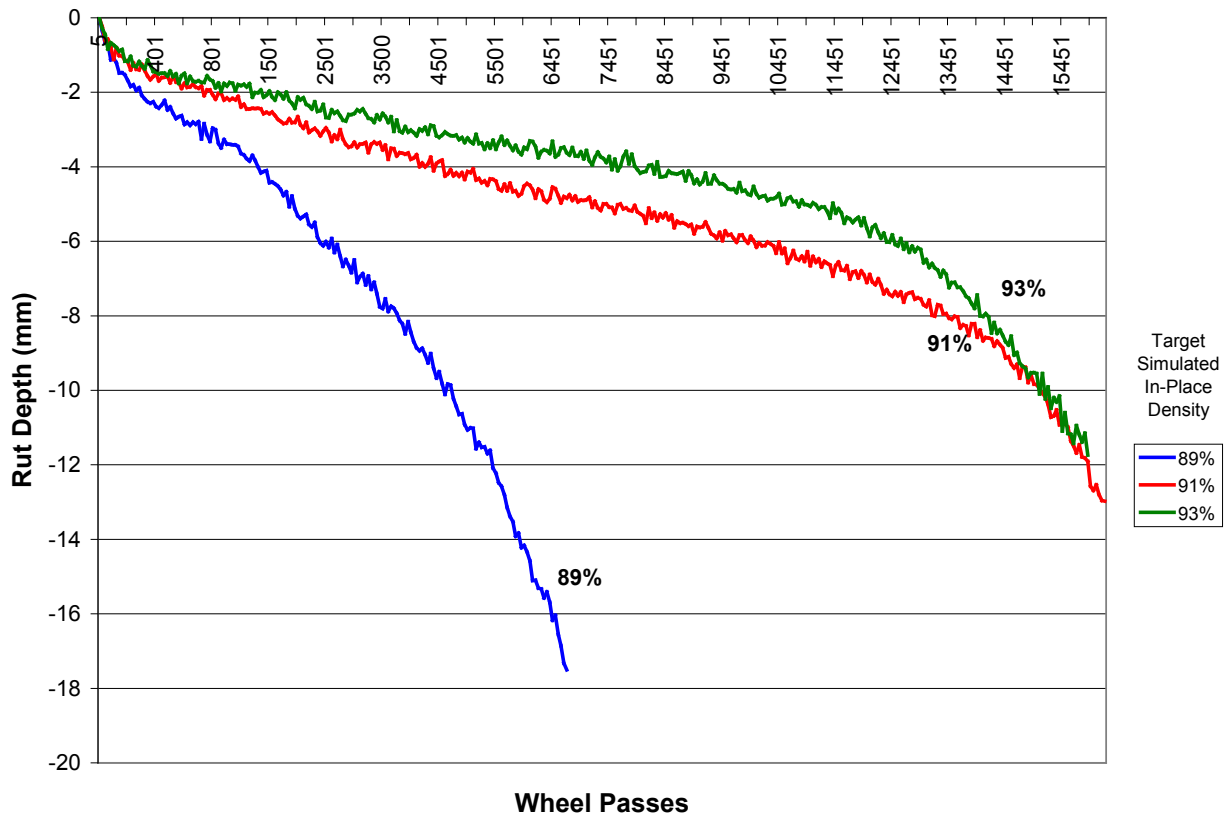


Figure C.8 Comparative HWTD Test Results of US-24 Project at 4% Target Air Voids @ N_{design}

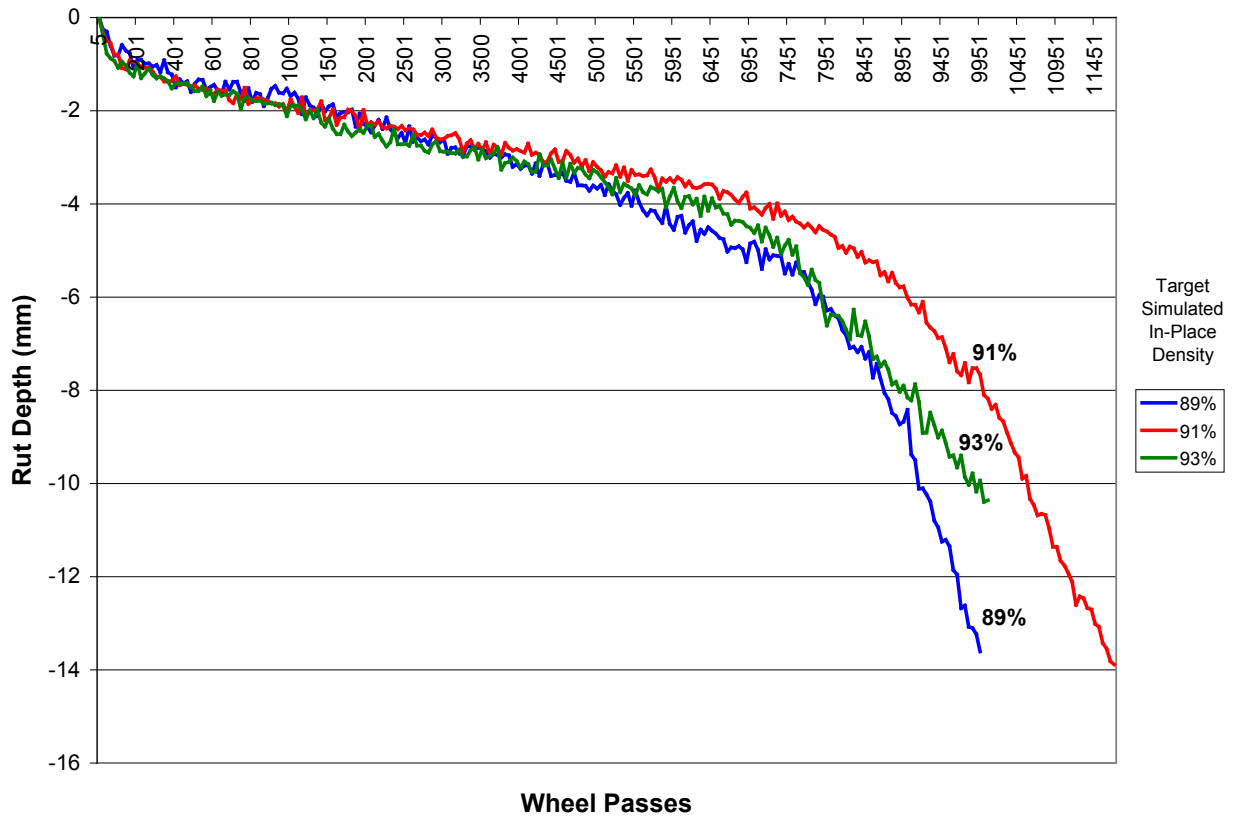


Figure C.9 Comparative HWTD Test Results of US-24 Project at 7% Target Air Voids @ N_{design}

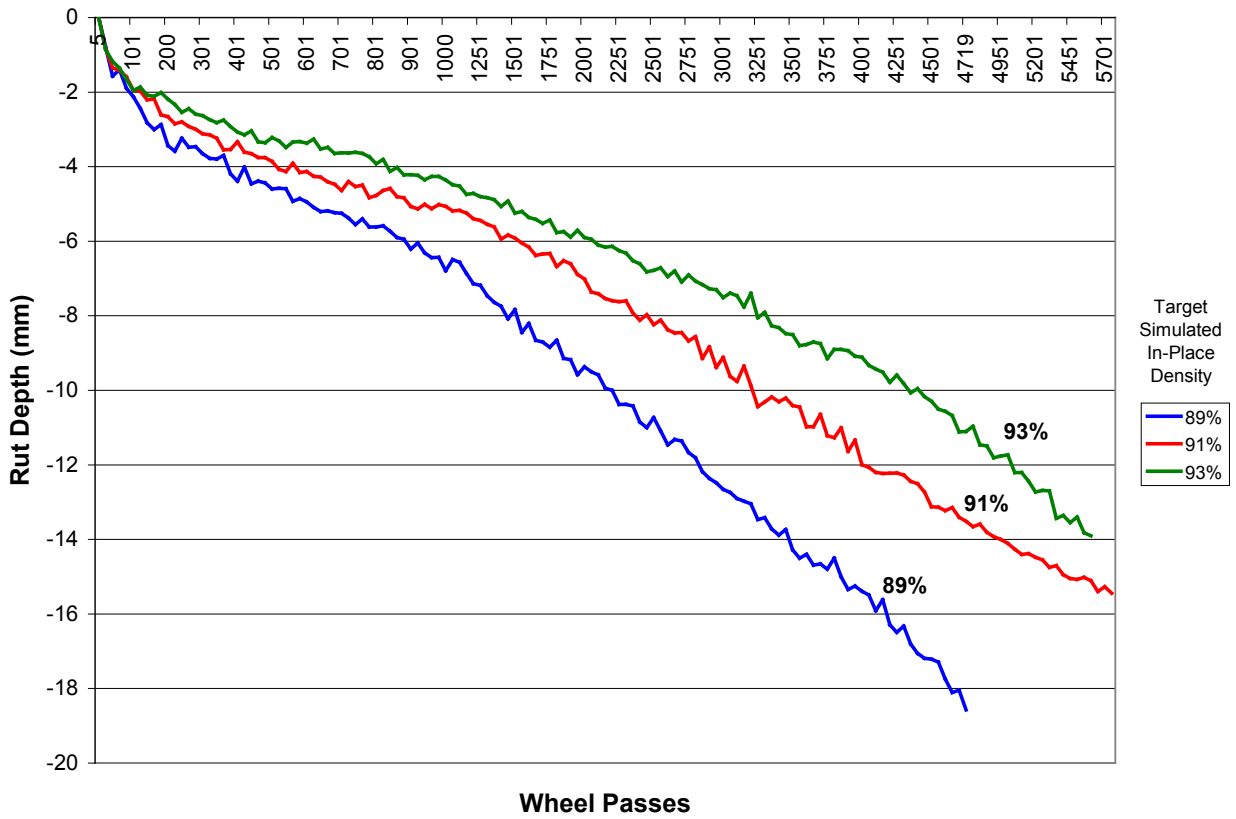


Figure C.10 Comparative HWTD Test Results of K-152 Project at 2% Target Air Voids @ N_{design}

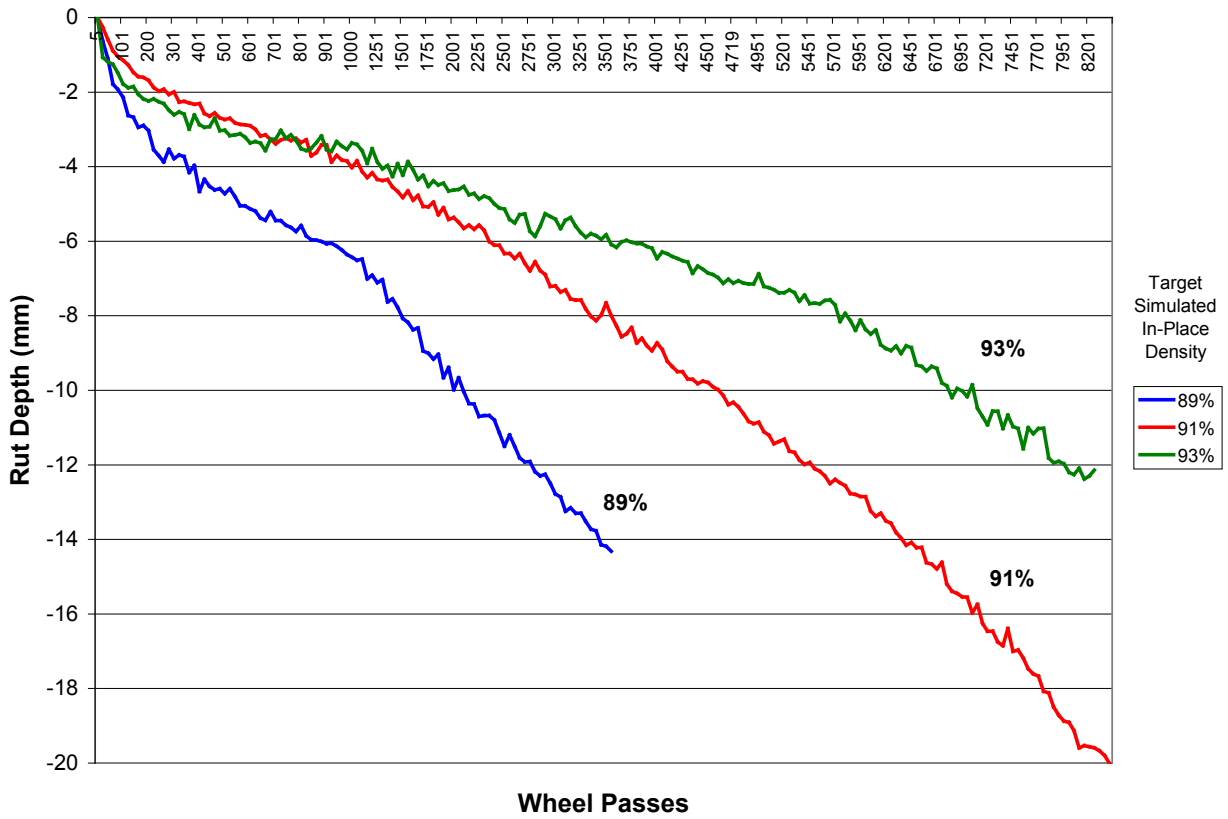


Figure C.11 Comparative HWTD Test Results of K-152 Project at 4% Target Air Voids @ N_{design}

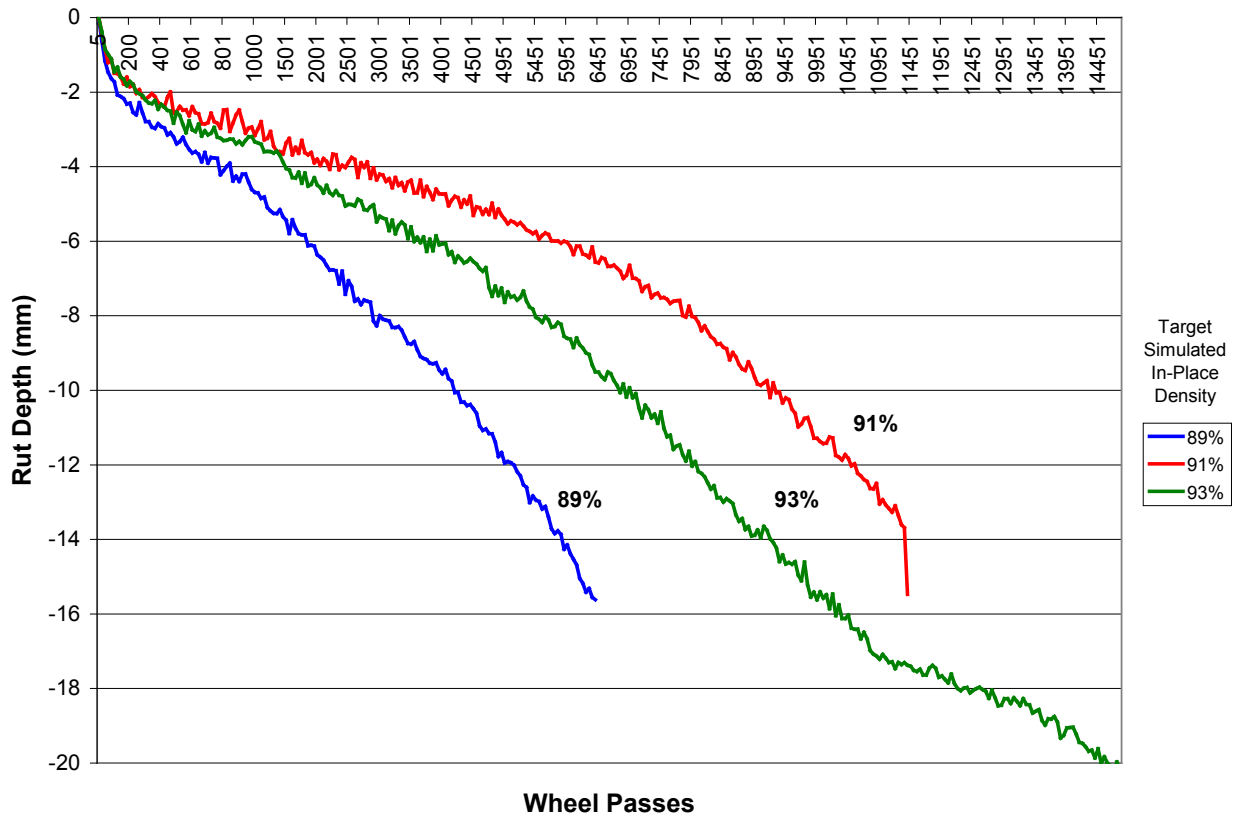


Figure C.12 Comparative HWTD Test Results of K-152 Project at 7% Target Air Voids @ N_{design}

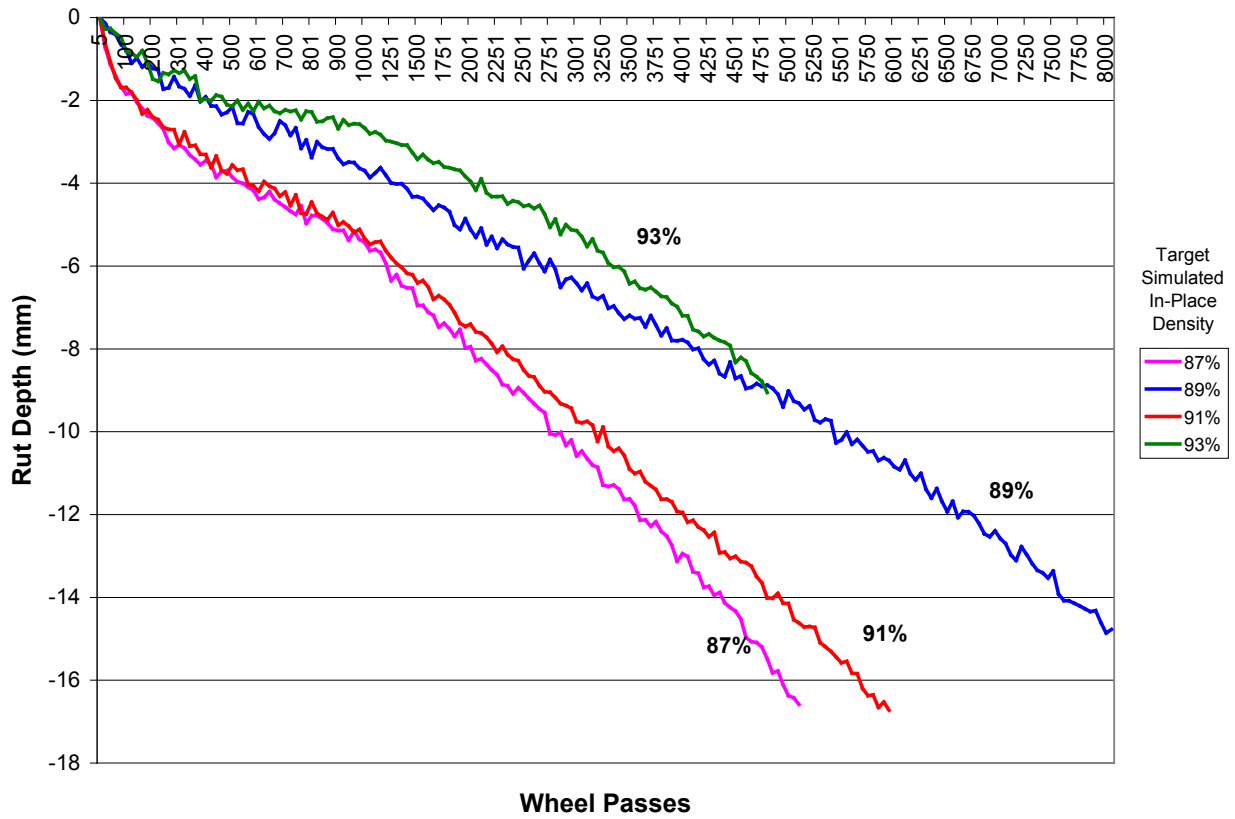


Figure C.13 Comparative HWTD Test Results of K-15 Project at 2% Target Air Voids @ N_{design}

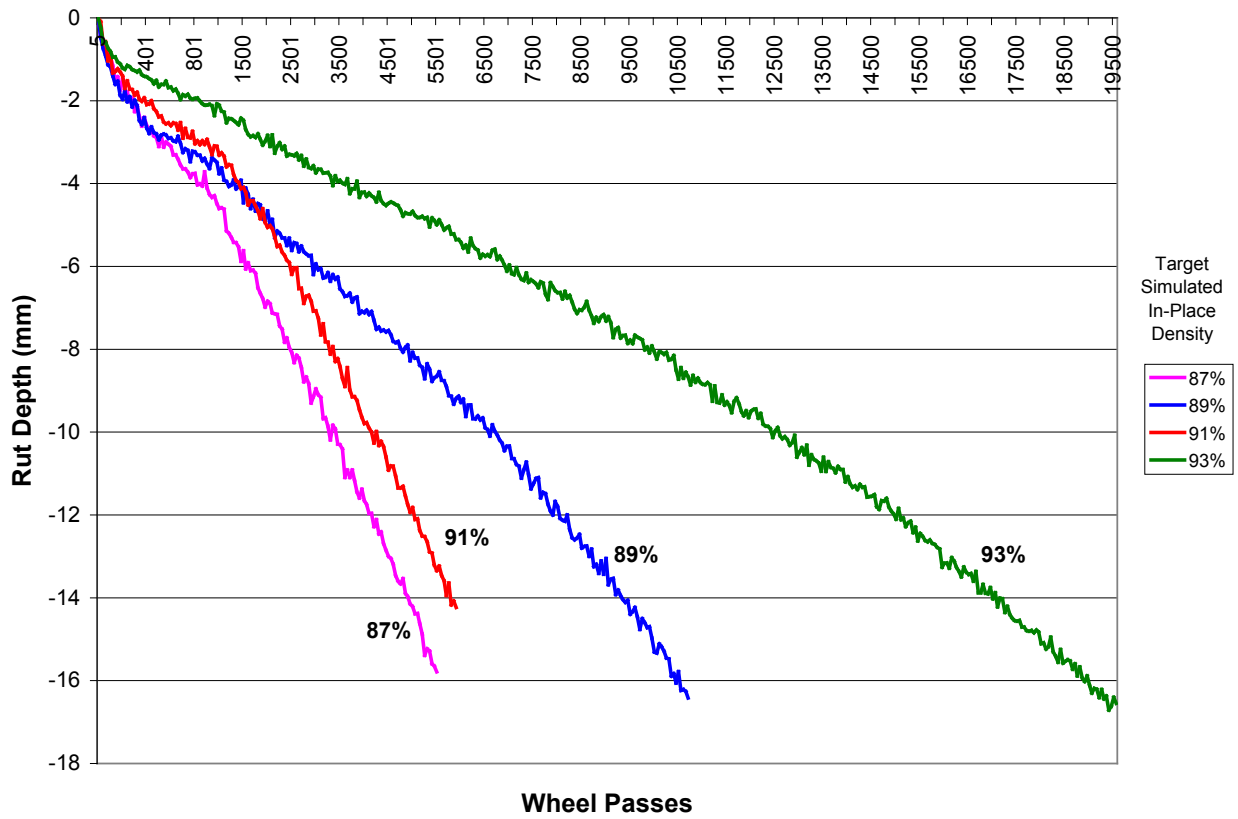


Figure C.14 Comparative HWTD Test Results of K-15 Project at 4% Target Air Voids @ N_{design}

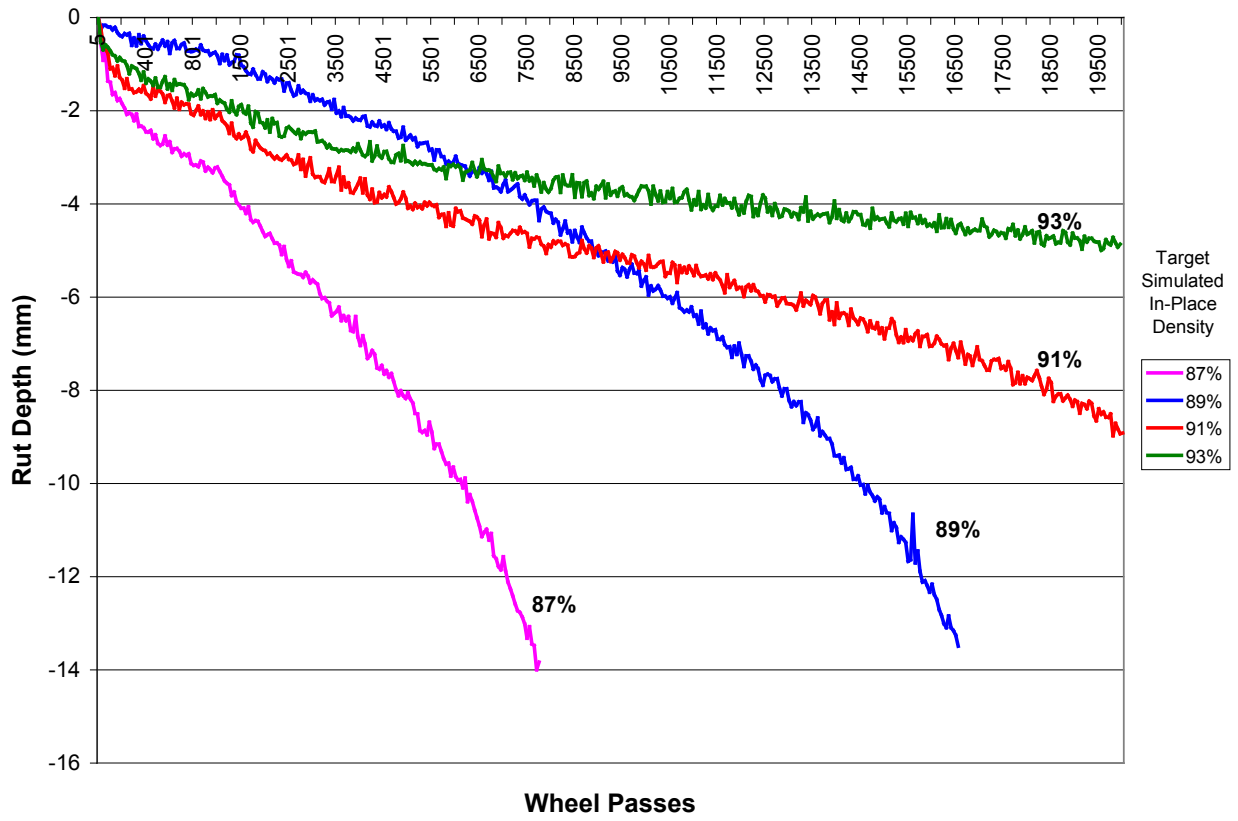


Figure C.15 Comparative HWTD Test Results of K-15 Project at 7% Target Air Voids @ N_{design}

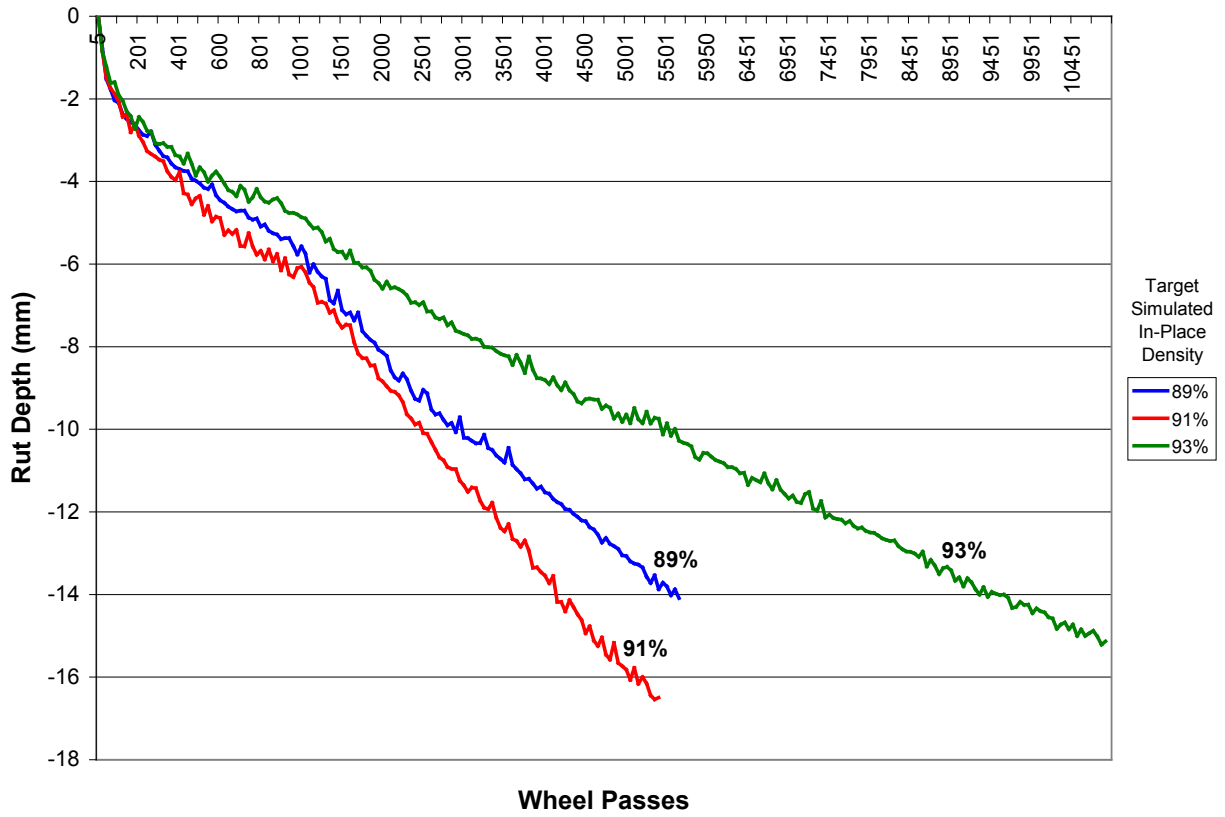


Figure C.16 Comparative HWTD Test Results of US-83 Project at 2% Target Air Voids @ N_{design}

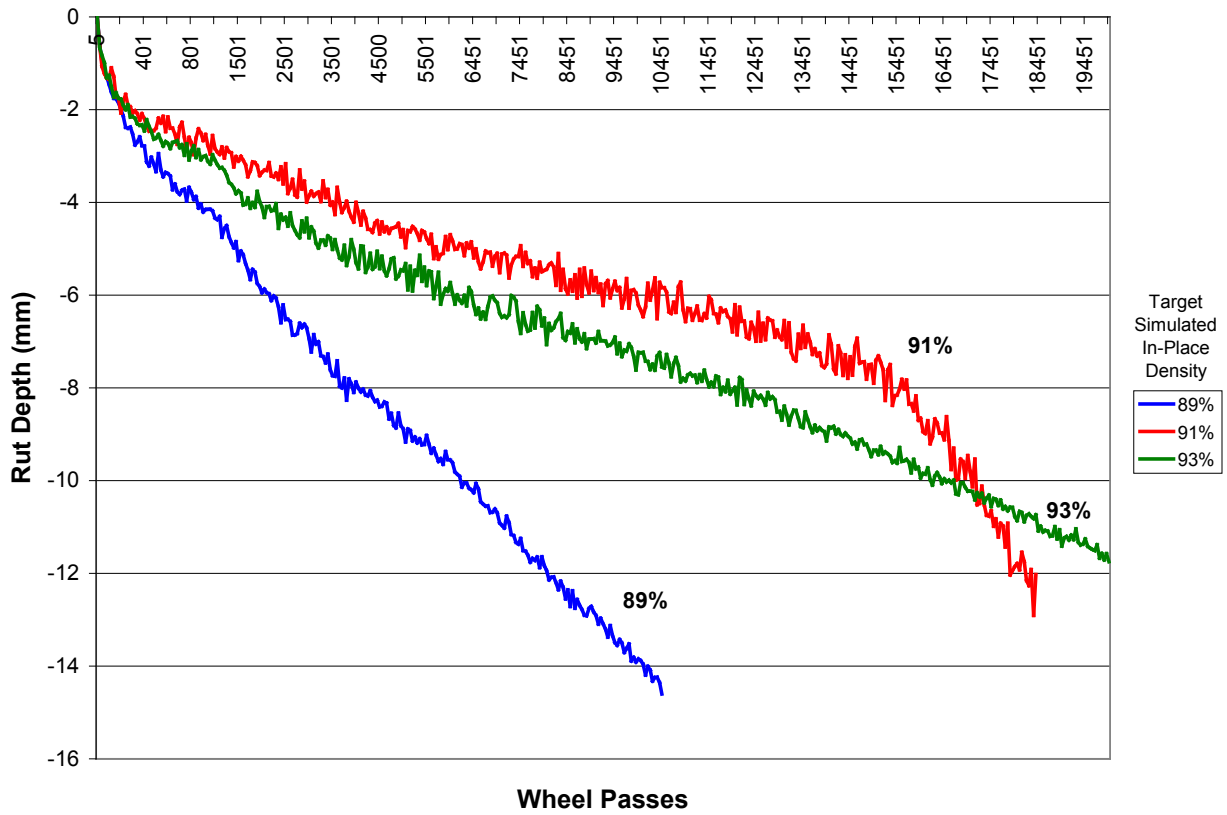


Figure C.17 Comparative HWTD Test Results of US-83 Project at 4% Target Air Voids @ N_{design}

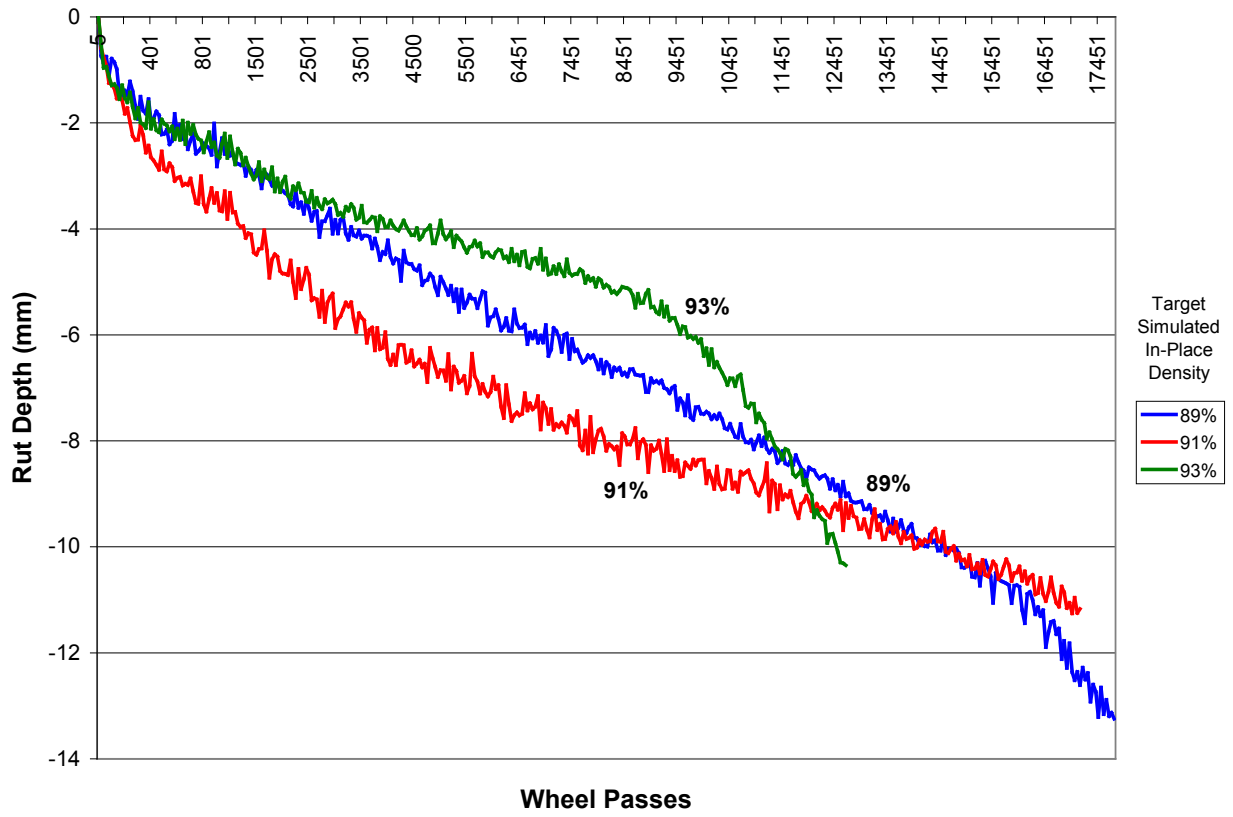


Figure C.18 Comparative HWTD Test Results of US-83 Project at 7% Target Air Voids @ N_{design}

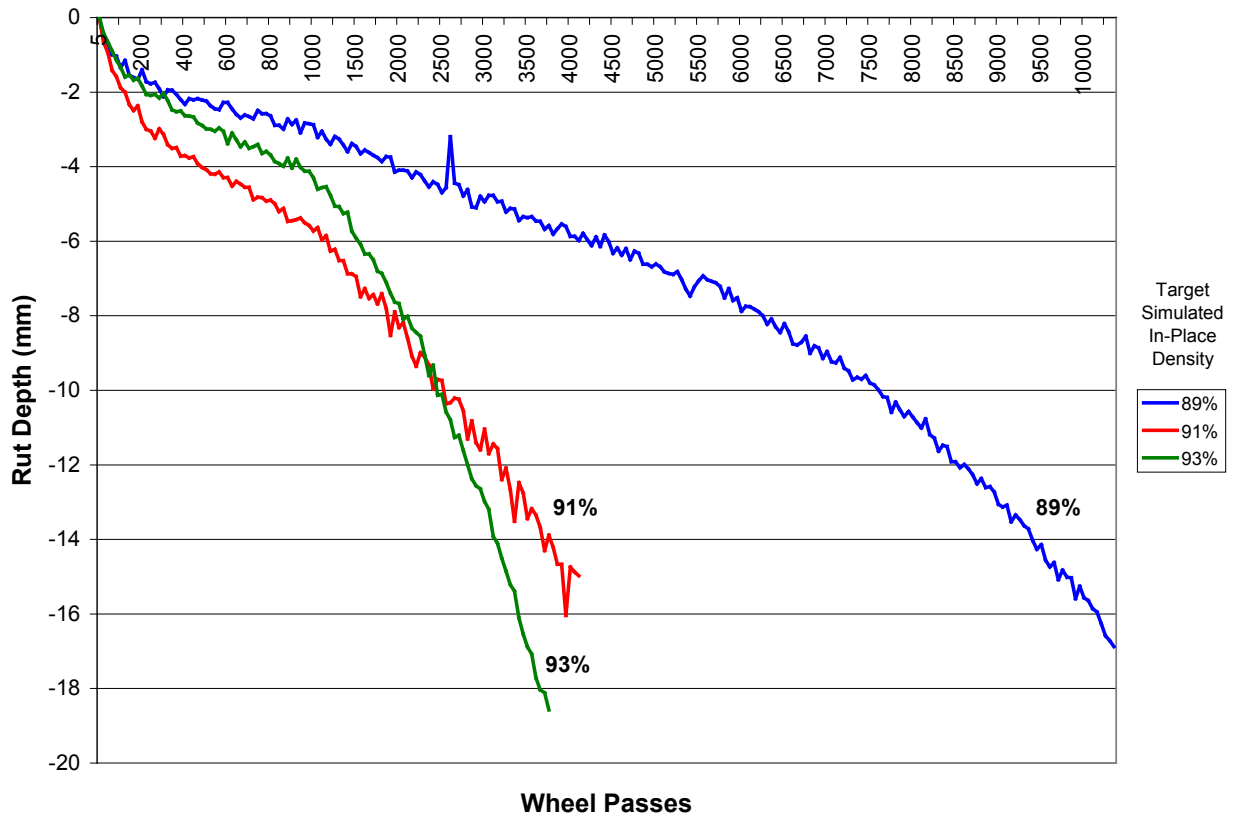


Figure C.19 Comparative HWTD Test Results of K-246 Project at 2% Target Air Voids @ N_{design}

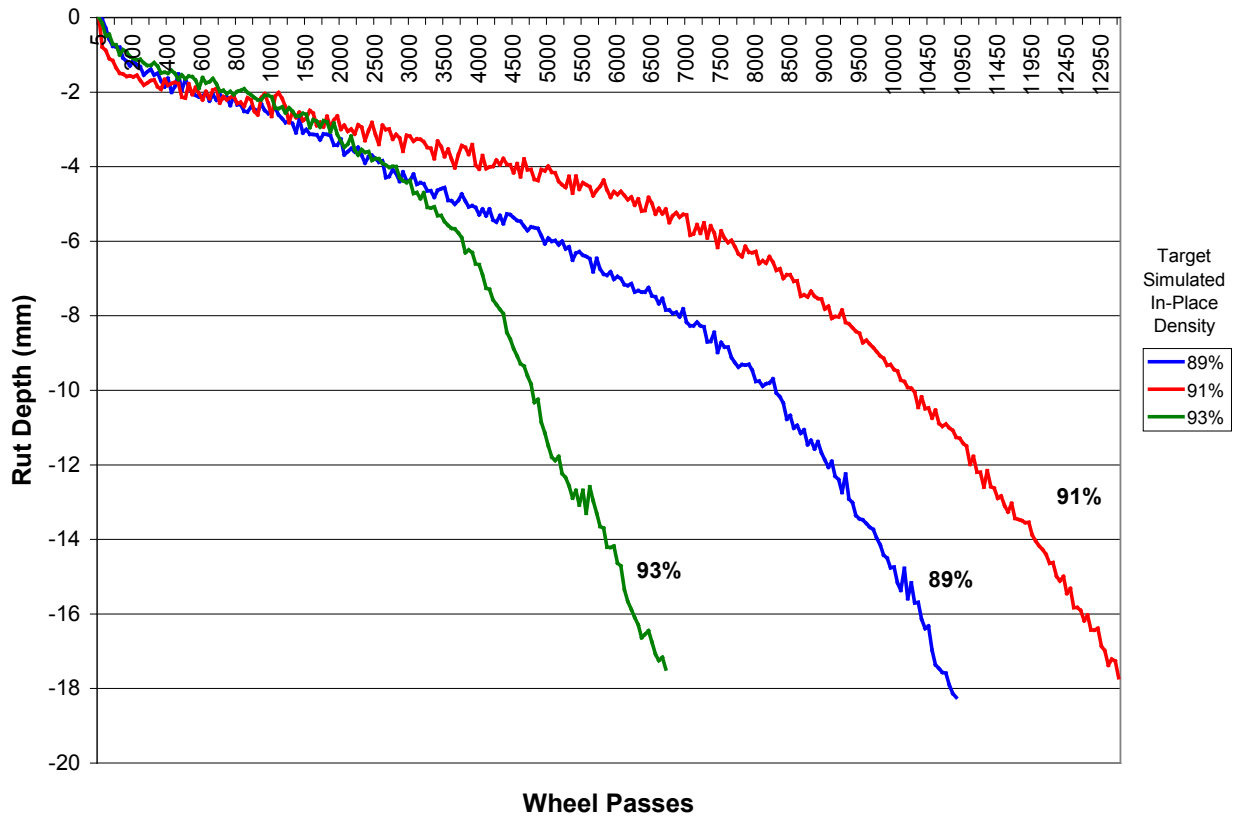


Figure C.20 Comparative HWTD Test Results of K-246 Project at 4% Target Air Voids @ N_{design}

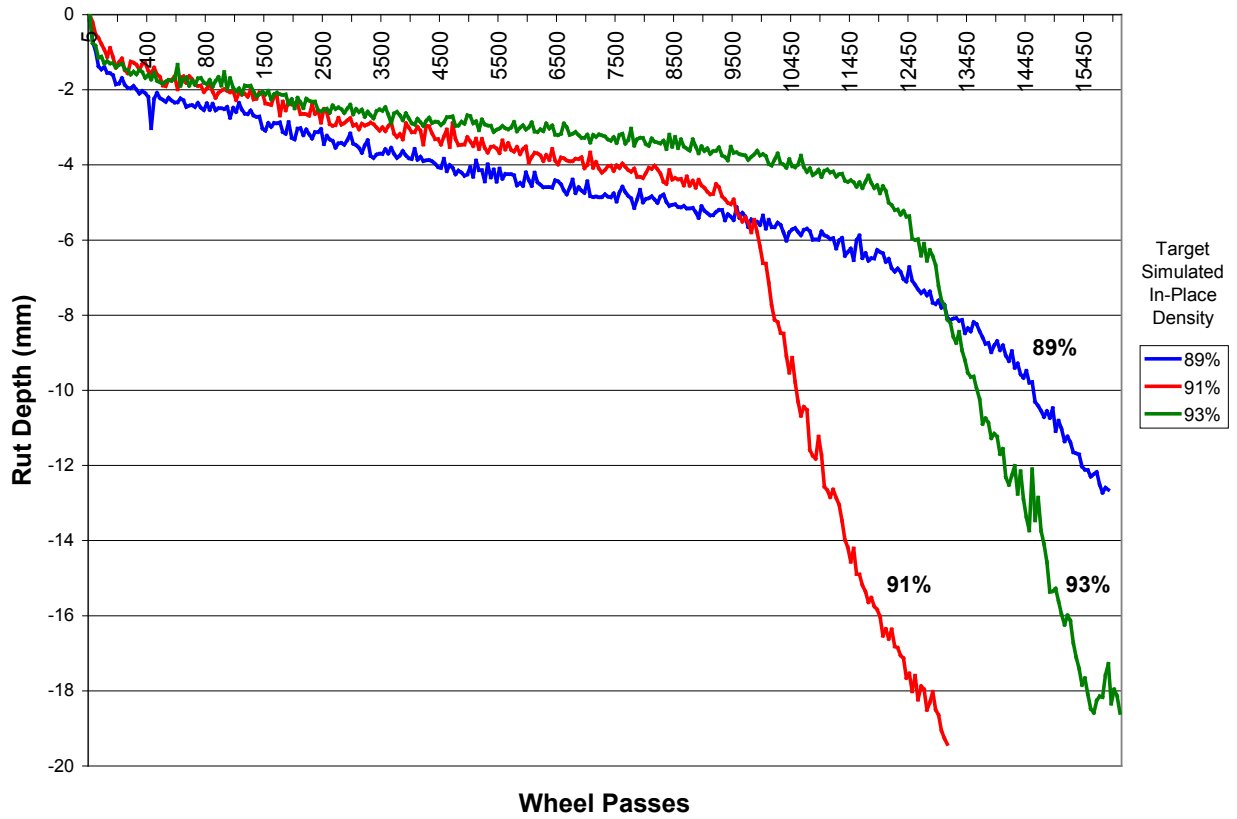


Figure C.21 Comparative HWTD Test Results of K-246 Project at 7% Target Air Voids @ N_{design}

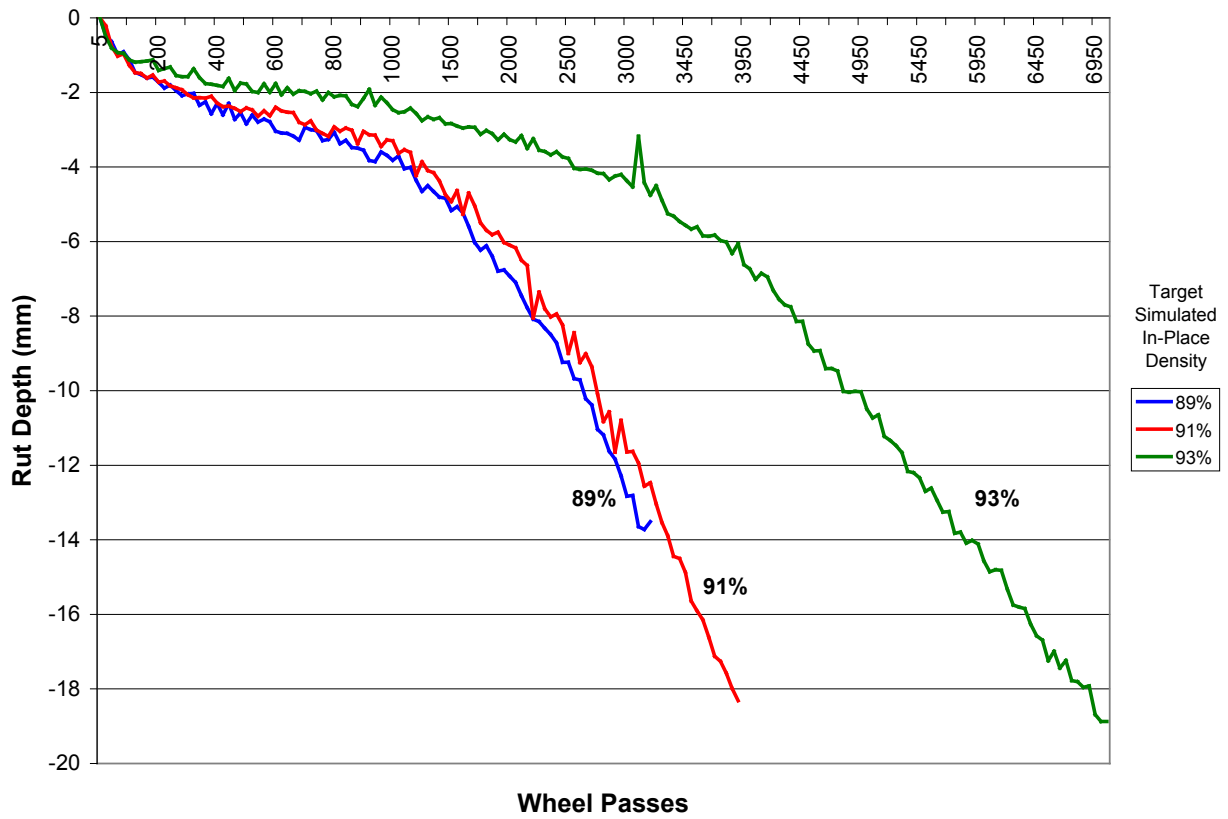


Figure C.22 Comparative HWTD Test Results of US-56 Project at 2% Target Air Voids @ N_{design}

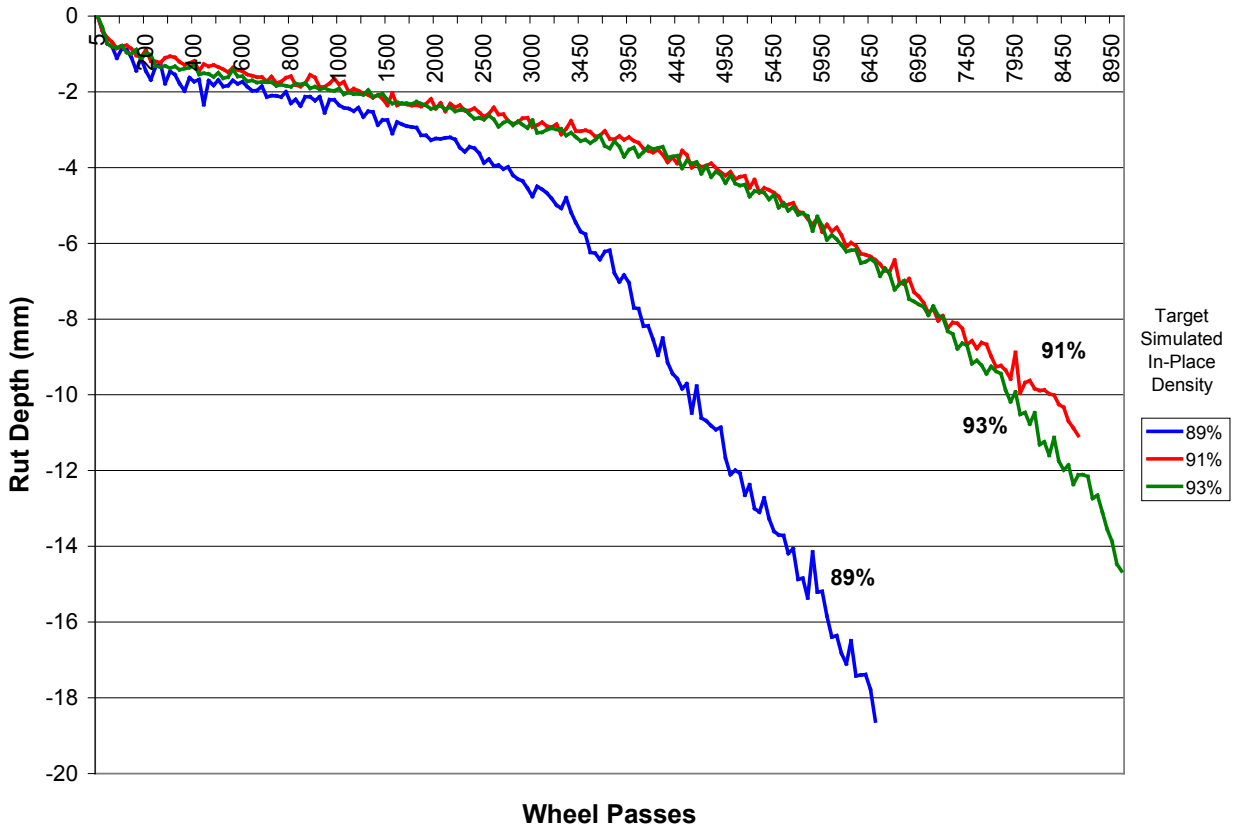


Figure C.23 Comparative HWTD Test Results of US-56 Project at 4% Target Air Voids @ N_{design}

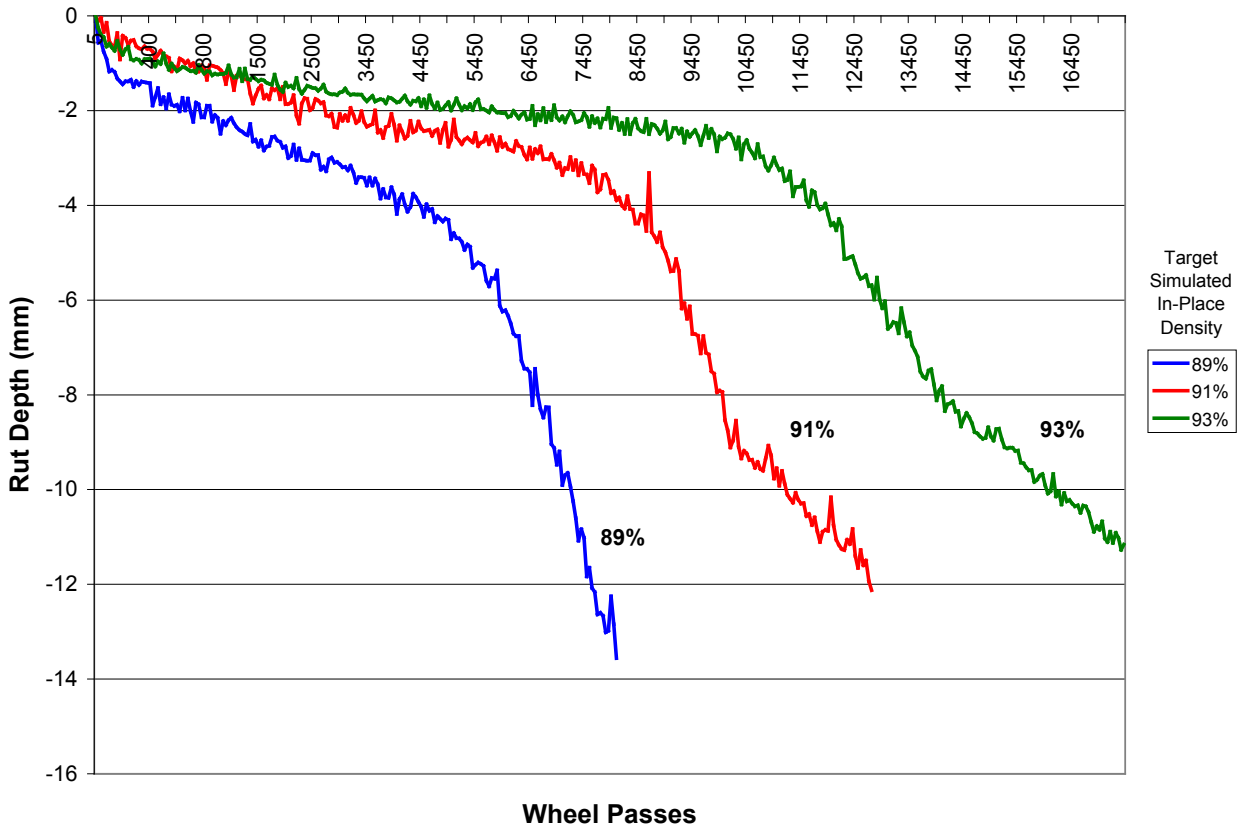


Figure C.24 Comparative HWTD Test Results of US-56 Project at 7% Target Air Voids @ N_{design}

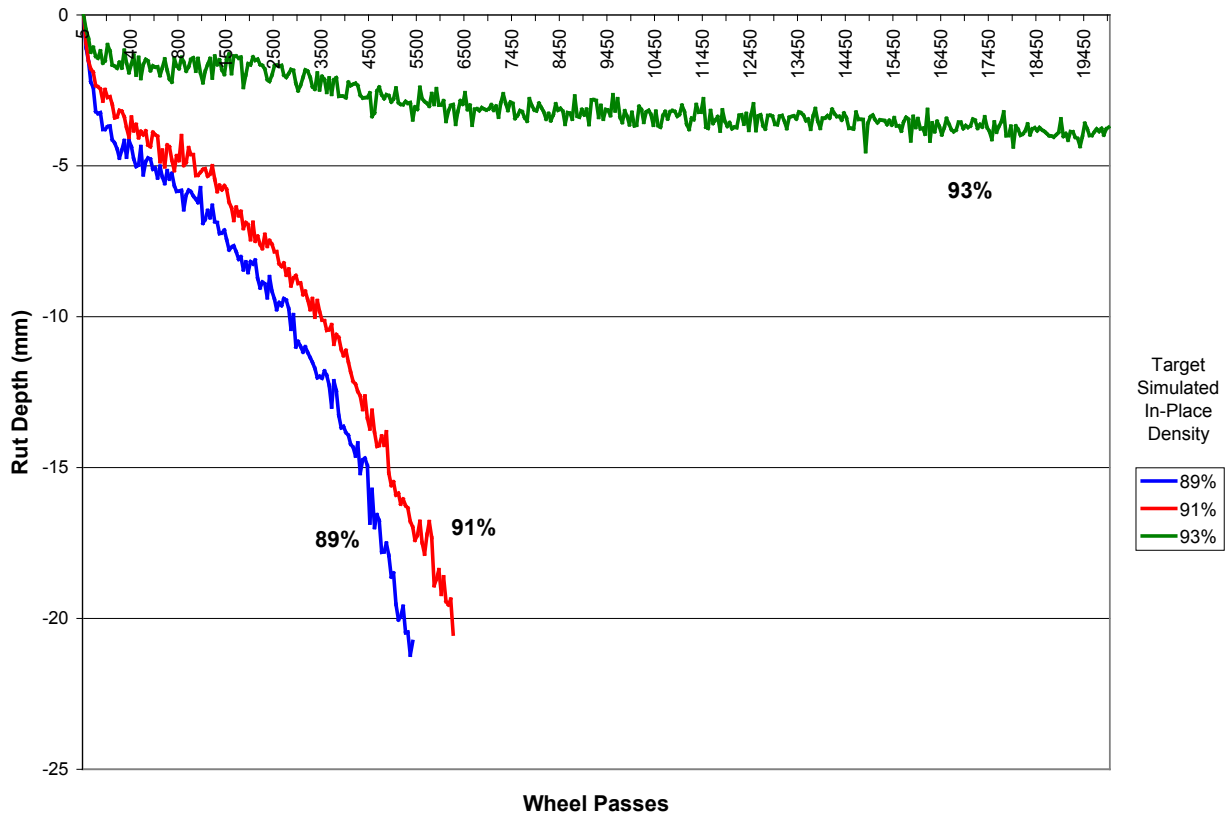


Figure C.25 Comparative HWTD Test Results of US-50 Project at 2% Target Air Voids @ N_{design}

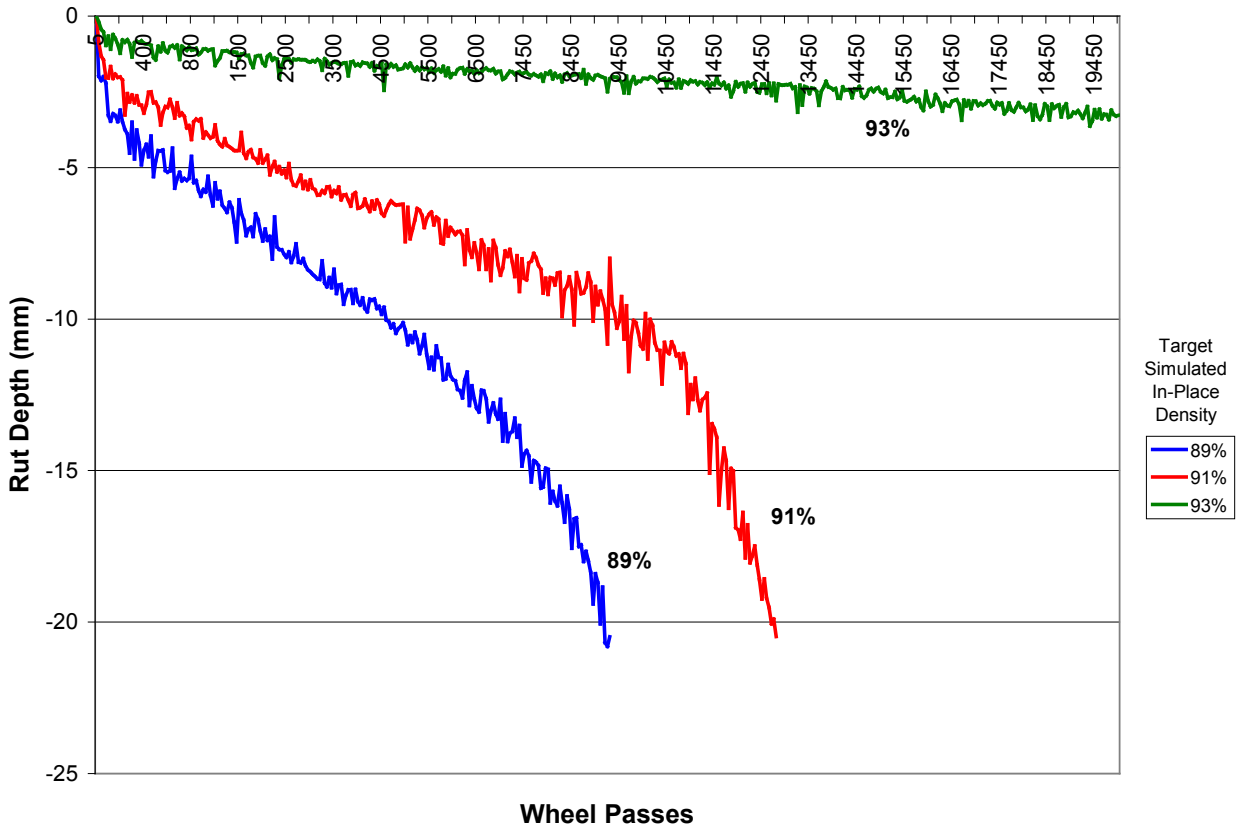


Figure C.26 Comparative HWTD Test Results of US-50 Project at 4% Target Air Voids @ N_{design}

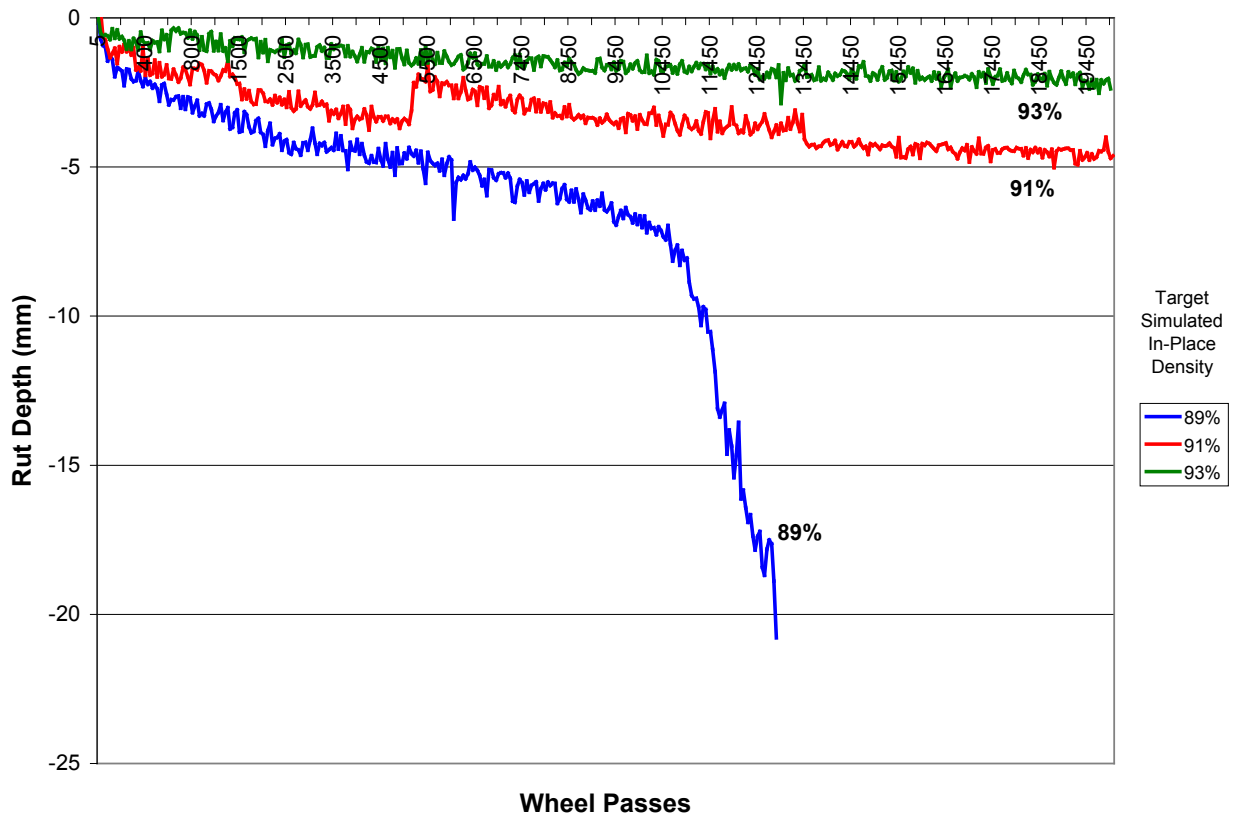


Figure C.27 Comparative HWTD Test Results of US-50 Project at 7% Target Air Voids @ N_{design}

Appendix D - Calculation of Lives of Deficient Superpave Pavements

Tables below show the calculation of lives of defective pavements for various projects and statewide, based on the parameters developed, based on the statistical analysis.

Table D.1 Lives of Deficient Superpave Pavements for Route K-4

Route	Parameter	Description	Estimate	R ²
K-4	Intercept	Vertical Intercept	-52,172.1	0.48
	A	Target Air Voids @ N _{design}	-13,496.0	
	D	Target Simulated In-Place Density	655.6	
	A×D	Air Voids × Density	157.7	
Wheel Passes = -52,172.1 - 13,496.0 A + 655.6 D + 157.7 A×D				
D	A	Wheel Passes	% Life	% Life Lost
88	2	6,284	52	48
88	4	7,047	58	42
88	7	8,192	67	33
89	2	7,255	60	40
89	4	8,333	68	32
89	7	9,951	82	18
90	2	8,226	67	33
90	4	9,620	79	21
90	7	11,711	96	4
91	2	9,197	75	25
91	4	10,906	89	11
91	7	13,470	100	0
92	2	10,168	83	17
92	4	12,193	100	0
92	7	15,230	100	0
93	2	11,139	91	9
93	4	13,479	100	0
93	7	16,989	100	0

Table D.2 Lives of Deficient Superpave Pavements for Route K-9

Route	Parameter	Description	Estimate	R ²
K-9	Intercept	Vertical Intercept	94,518.2	0.57
	A	Target Air Voids @ N _{design}	-21,800.3	
	D	Target Simulated In-Place Density	-987.4	
	A×D	Air Voids × Density	245.4	
Wheel Passes = 94,518.2 – 21,800.3 A – 987.4 D + 245.4 A×D				
D	A	Wheel Passes	% Life	% Life Lost
88	2	7,217	100	0
88	4	6,807	100	0
88	7	6,191	91	9
89	2	6,720	99	1
89	4	6,801	100	0
89	7	6,922	100	0
90	2	6,224	92	8
90	4	6,795	100	0
90	7	7,652	100	0
91	2	5,727	84	16
91	4	6,789	100	0
91	7	8,383	100	0
92	2	5,230	77	23
92	4	6,783	100	0
92	7	9,113	100	0
93	2	4,734	70	30
93	4	6,778	100	0
93	7	9,843	100	0

Table D.3 Lives of Deficient Superpave Pavements for Route US-24

Route	Parameter	Description	Estimate	R ²
US-24	Intercept	Vertical Intercept	-33,376.7	0.10
	A	Target Air Voids @ N _{design}	-7,156.1	
	D	Target Simulated In-Place Density	480.6	
	A×D	Air Voids × Density	83.6	
Wheel Passes = -33,376.7 - 7,156.1 A + 480.6 D + 83.6 A×D				
D	A	Wheel Passes	% Life	% Life Lost
88	2	9,318	72	28
88	4	9,719	75	25
88	7	10,321	80	20
89	2	9,956	77	23
89	4	10,534	81	19
89	7	11,387	88	12
90	2	10,613	82	18
90	4	11,349	87	13
90	7	12,453	96	4
91	2	11,261	87	13
91	4	12,164	94	6
91	7	13,518	100	0
92	2	11,909	92	8
92	4	12,979	100	0
92	7	14,584	100	0
93	2	12,557	97	3
93	4	13,794	100	0
93	7	15,650	100	0

Table D.4 Lives of Deficient Superpave Pavements for Route K-152

Route	Parameter	Description	Estimate	R ²
K-152	Intercept	Vertical Intercept	-153,923.6	0.48
	A	Target Air Voids @ N _{design}	-9,611.4	
	D	Target Simulated In-Place Density	1,683.4	
	A×D	Air Voids × Density	120.9	
Wheel Passes = -153,923.6 - 9,611.4 A + 1,683.4 D + 120.9 A×D				
D	A	Wheel Passes	% Life	% Life Lost
88	2	0	0	100
88	4	0	0	100
88	7	1,410	30	70
89	2	0	0	100
89	4	494	19	81
89	7	3,940	62	38
90	2	122	14	86
90	4	2,661	46	54
90	7	6,470	100	0
91	2	2,047	38	62
91	4	4,828	73	27
91	7	8,999	100	0
92	2	3,972	62	38
92	4	6,995	100	0
92	7	11,529	100	0
93	2	5,897	86	14
93	4	9,162	100	0
93	7	14,059	100	0

Table D.5 Lives of Deficient Superpave Pavements for Route K-15

Route	Parameter	Description	Estimate	R ²
K-15	Intercept	Vertical Intercept	-29,365.7	0.80
	A	Target Air Voids @ N _{design}	-51,472.9	
	D	Target Simulated In-Place Density	299.0	
	A×D	Air Voids × Density	598.2	
Wheel Passes = -29,365.7 – 51,472.9 A + 299.0 D + 598.2 A×D				
D	A	Wheel Passes	% Life	% Life Lost
88	2	0	0	100
88	4	1,621	13	87
88	7	5,127	41	59
89	2	779	6	94
89	4	4,313	35	65
89	7	9,614	78	22
90	2	2,275	18	82
90	4	7,005	57	43
90	7	14,100	100	0
91	2	3,770	30	70
91	4	9,697	78	22
91	7	18,586	100	0
92	2	5,265	43	57
92	4	12,388	100	0
92	7	23,073	100	0
93	2	6,761	55	45
93	4	15,080	100	0
93	7	27,559	100	0

Table D.6 Lives of Deficient Superpave Pavements for Route US-83

Route	Parameter	Description	Estimate	R ²
US-83	Intercept	Vertical Intercept	618,386.4	0.59
	A	Target Air Voids @ N _{design}	-127,505.7	
	D	Target Simulated In-Place Density	-6,503.3	
	A×D	Air Voids × Density	1,381.6	
Wheel Passes = 618,386.4 - 127,505.7 A - 6,503.3 D + 1,381.6 A×D				
D	A	Wheel Passes	% Life	% Life Lost
88	2	34,246	100	0
88	4	22,396	100	0
88	7	4,622	25	75
89	2	30,506	100	0
89	4	21,419	100	0
89	7	7,790	42	58
90	2	26,766	100	0
90	4	20,443	100	0
90	7	10,957	59	41
91	2	23,026	100	0
91	4	19,466	100	0
91	7	14,125	76	24
92	2	19,286	100	0
92	4	18,489	100	0
92	7	17,293	94	6
93	2	15,546	84	16
93	4	17,512	95	5
93	7	20,461	100	0

Table D.7 Lives of Deficient Superpave Pavements for Route K-246

Route	Parameter	Description	Estimate	R ²
K-246	Intercept	Vertical Intercept	563,197.6	0.84
	A	Target Air Voids @ N _{design}	-75,241.0	
	D	Target Simulated In-Place Density	-6,089.2	
	A×D	Air Voids × Density	836.7	
Wheel Passes = 563,197.6 - 75,241.0 A - 6,089.2 D + 836.7 A×D				
D	A	Wheel Passes	% Life	% Life Lost
88	2	24,125	100	0
88	4	20,902	100	0
88	7	16,068	100	0
89	2	19,709	100	0
89	4	18,160	100	0
89	7	15,836	100	0
90	2	15,294	100	0
90	4	15,418	100	0
90	7	15,604	100	0
91	2	10,878	100	0
91	4	12,675	100	0
91	7	15,371	100	0
92	2	6,462	65	35
92	4	9,933	100	0
92	7	15,139	100	0
93	2	2,046	21	79
93	4	7,190	72	28
93	7	14,907	100	0

Table D.8 Lives of Deficient Superpave Pavements for Route US-56

Route	Parameter	Description	Estimate	R ²
US-56	Intercept	Vertical Intercept	45,013.6	0.70
	A	Target Air Voids @ N _{design}	-42,919.3	
	D	Target Simulated In-Place Density	-489.7	
	A×D	Air Voids × Density	493.8	
Wheel Passes = 45,013.6 - 42,919.3 A - 489.7 D + 493.8 A×D				
D	A	Wheel Passes	% Life	% Life Lost
88	2	2,990	30	70
88	4	4,060	41	59
88	7	5,666	57	43
89	2	3,488	35	65
89	4	5,546	55	45
89	7	8,633	86	14
90	2	3,986	40	60
90	4	7,031	70	30
90	7	11,600	100	0
91	2	4,484	45	55
91	4	8,517	85	15
91	7	14,566	100	0
92	2	4,982	50	50
92	4	10,002	100	0
92	7	17,533	100	0
93	2	5,480	55	45
93	4	11,488	100	0
93	7	20,500	100	0

Table D.9 Lives of Deficient Superpave Pavements for Route US-50

Route	Parameter	Description	Estimate	R ²
US-50	Intercept	Vertical Intercept	-614,106.5	0.83
	A	Target Air Voids @ N _{design}	71,479.5	
	D	Target Simulated In-Place Density	6,807.2	
	A×D	Air Voids × Density	-762.3	
Wheel Passes = -614,106.5 + 71,479.5 A + 6,807.2 D - 762.3 A×D				
D	A	Wheel Passes	% Life	% Life Lost
88	2	0	0	100
88	4	2,516	14	86
88	7	15,707	90	10
89	2	0	0	100
89	4	6,273	36	64
89	7	17,178	98	2
90	2	4,287	24	76
90	4	10,032	57	43
90	7	18,649	100	0
91	2	9,569	55	45
91	4	13,789	79	21
91	7	10,120	100	0
92	2	14,852	85	15
92	4	17,548	100	0
92	7	21,591	100	0
93	2	20,134	100	0
93	4	21,306	100	0
93	7	23,062	100	0

Table D.10 Lives of Deficient Superpave Pavements for Statewide Project

Route	Parameter	Description	Estimate	R ²
Statewide	Intercept	Vertical Intercept	-15,475.1	0.28
	A	Target Air Voids @ N _{design}	-11,000.2	
	D	Target Simulated In-Place Density	223.9	
	A×D	Air Voids × Density	136.2	
Wheel Passes = -15,475.1 - 11,000.2 A + 223.9 D + 136.2 A×D				
D	A	Wheel Passes	% Life	% Life Lost
88	2	6,199	55	45
88	4	8,170	73	27
88	7	11,126	99	1
89	2	6,695	60	40
89	4	8,938	79	21
89	7	12,303	100	0
90	2	7,192	64	36
90	4	9,707	86	14
90	7	13,481	100	0
91	2	7,688	68	32
91	4	10,476	93	7
91	7	14,658	100	0
92	2	8,184	73	27
92	4	11,245	100	0
92	7	15,835	100	0
93	2	8,680	77	23
93	4	12,013	100	0
93	7	17,012	100	0

**Appendix E - HWTD, G_{mm} , G_{mb} , Simulated In-Place Densities and
Air Voids Test Results for Development of Laboratory - Based
Accelerated Mix Testing Models and Field Cores**

HWTD Test Results and Air Voids for Development of Laboratory - Based Accelerated Mix Testing Models

Table E.1 Summary of Hamburg Wheel Test Results for Accelerated Mix Testing Models (Number of wheel passes at left and right wheel paths)

Route	District	Temp. (°C)	Wheel Passes at									
			Load (705 N)		Load (750 N)		Load (795 N)		Load (840 N)		Load (885 N)	
			Left	Right	Left	Right	Left	Right	Left	Right	Left	Right
K-4	I	50	14,000	13,400	20,000	17,460	16,900	15,000	N/A	N/A	N/A	N/A
		60	6,300	8,160	3,700	4,450	3,360	4,630	N/A	N/A	N/A	N/A
US-24	III	50	19,330	15,920	17,400	17,380	13,300	20,000	10,750	11,670	12,800	13,970
		60	4,660	2,410	1,770	3,360	2,630	3,730	3,670	3,000	1,310	1,490
US-50	V	50	20,000	20,000	20,000	20,000	20,000	20,000	8,700	8,140	8,480	6,420
		60	5,990	4,720	12,550	5,750	3,170	5,420	2,780	2,500	2,500	1,840
US-83	VI	50	20,000	20,000	20,000	20,000	20,000	20,000	10,360	12,160	20,000	11,540
		60	5,780	8,510	1,510	6,430	8,110	5,940	3,620	3,380	1,850	3,840
CISL-A	I	50	20,000	20,000	17,220	18,920	15,810	14,300	N/A	N/A	N/A	N/A
		60	2,740	8,040	4,760	3,280	5,670	3,580	N/A	N/A	N/A	N/A
CISL-B	N/A	50	20,000	20,000	20,000	20,000	20,000	20,000	N/A	N/A	N/A	N/A
		60	20,000	20,000	20,000	20,000	20,000	20,000	N/A	N/A	N/A	N/A

Table E.2 Air Voids and Asphalt Content of Hamburg Test Samples for Accelerated Mix Testing Models

Route	District	% Asphalt Content	Temp. (°C)	Air Voids @ N _{final}									
				Load (705 N)		Load (750 N)		Load (795 N)		Load (840 N)		Load (885 N)	
				Left	Right	Left	Right	Left	Right	Left	Right	Left	Right
K-4	I	4.9	50	6.5	6.4	5.9	5.5	6.6	6.0	N/A	N/A	N/A	N/A
			60	6.8	6.5	6.3	7.2	6.0	7.0	N/A	N/A	N/A	N/A
US-24	III	5.0	50	6.7	6.8	5.4	5.5	5.3	5.3	6.2	6.1	6.2	6.3
			60	5.6	5.6	5.3	5.7	5.5	5.5	6.3	6.5	6.2	6.4
US-50	V	5.4	50	7.5	7.4	6.9	6.7	7.2	7.4	7.3	7.4	7.3	7.5
			60	7.9	7.8	7.5	6.6	7.3	7.3	7.1	6.1	6.1	5.7
US-83	VI	4.9	50	6.1	6.0	6.9	6.8	6.5	5.5	5.4	6.1	4.7	6.3
			60	6.1	6.4	5.8	5.9	6.4	6.2	6.0	6.0	7.2	5.7
CISL-A	I	4.9	50	7.1	7.1	7.8	7.6	7.3	7.5	N/A	N/A	N/A	N/A
			60	7.9	7.9	7.3	7.8	7.1	7.3	N/A	N/A	N/A	N/A
CISL-B	N/A	5.4	50	7.4	7.4	7.4	7.5	7.3	7.5	N/A	N/A	N/A	N/A
			60	7.1	7.3	7.3	7.5	7.3	7.0	N/A	N/A	N/A	N/A

**Gmm, Gmb, Simulated In-Place Densities, and Air Voids Test
Results for Development of Laboratory - Based Accelerated Mix
Testing Models**

Table E.3 Simulated In-Place Densities and Air Voids for K-4 Project in District I

Sample ID	G _{mb}	G _{mm}	% Simulated In-place Density	% Air Voids @ N _{final}
1-1	2.309	2.451	94.2	5.8
1-2	2.309		94.2	5.8
1-3	2.303		94.0	6.0
1-4	2.325		94.9	5.1
1-5	2.302		93.9	6.1
1-6	2.302		93.9	6.1
1-7	2.279		93.0	7.0
1-8	2.327		95.0	5.0
1-9	2.257		92.1	7.9
1-10	2.308		94.2	5.8
1-11	2.307		94.1	5.9
1-12	2.289		93.4	6.6
1-13	2.267		92.5	7.5
1-14	2.281		93.1	6.9
1-15	2.291		93.5	6.5
1-16	2.308		94.2	5.8
1-17	2.298		93.8	6.2
1-18	2.299		93.8	6.2
1-19	2.273		92.7	7.3
1-20	2.286		93.3	6.7

Table E.4 Simulated In-Place Densities and Air Voids for US-24 Project in District III

Sample ID	G_{mb}	G_{mm}	% Simulated In-place Density	% Air Voids @ N_{final}
2-1	2.239	2.397	93.4	6.6
2-2	2.262		94.4	5.6
2-3	2.279		95.1	4.9
2-4	2.283		95.3	4.7
2-5	2.261		94.3	5.7
2-6	2.278		95.0	5.0
2-7	2.262		94.4	5.6
2-8	2.284		95.3	4.7
2-9	2.276		94.9	5.1
2-10	2.260		94.3	5.7
2-11	2.261		94.4	5.6
2-12	2.267		94.6	5.4
2-13	2.265		94.5	5.5
2-14	2.265		94.5	5.5
2-15	2.267		94.6	5.4
2-16	2.264		94.5	5.5
2-17	2.255		94.1	5.9
2-18	2.275		94.9	5.1
2-19	2.265		94.5	5.5
2-20	2.266		94.6	5.4

Table E.5 Simulated In-Place Densities and Air Voids for US-24 Project in District III

Sample ID	G_{mb}	G_{mm}	% Simulated In-place Density	% Air Voids @ N_{final}
2-21	2.264	2.413	93.8	6.2
2-22	2.265		93.9	6.1
2-23	2.270		94.1	5.9
2-24	2.262		93.7	6.3
2-25	2.271		94.1	5.9
2-26	2.257		93.5	6.5
2-27	2.251		93.3	6.7
2-28	2.256		93.5	6.5
2-29	2.254		93.4	6.6
2-30	2.263		93.8	6.2
2-31	2.270		94.0	6.0
2-32	2.261		93.7	6.3
2-33	2.265		93.9	6.1
2-34	2.250		93.2	6.8
2-35	2.259		93.6	6.4
2-36	2.259		93.6	6.4

Table E.6 Simulated In-Place Densities and Air Voids for US-50 Project in District V

Sample ID	G_{mb}	G_{mm}	% Simulated In-place Density	% Air Voids @ N_{final}
3-1	2.265	2.439	92.9	7.1
3-2	2.255		92.5	7.5
3-3	2.262		92.8	7.2
3-4	2.261		92.7	7.3
3-5	2.278		93.4	6.6
3-6	2.265		92.9	7.1
3-7	2.262		92.8	7.2
3-8	2.286		93.7	6.3
3-9	2.259		92.6	7.4
3-10	2.255		92.5	7.5
3-11	2.265		92.9	7.1
3-12	2.265		92.9	7.1
3-13	2.256		92.5	7.5
3-14	2.279		93.5	6.5
3-15	2.259		92.6	7.4
3-16	2.266		92.9	7.1
3-17	2.263		92.8	7.2
3-18	2.255		92.5	7.5
3-19	2.260		92.7	7.3
3-20	2.267		93.0	7.0

Table E.7 Simulated In-Place Densities and Air Voids for US-50 Project in District V

Sample ID	G_{mb}	G_{mm}	% Simulated In-place Density	% Air Voids @ N_{final}
3-21	2.256	2.430	92.8	7.2
3-22	2.249		92.6	7.4
3-23	2.267		93.3	6.7
3-24	2.259		93.0	7.0
3-25	2.262		93.1	6.9
3-26	2.249		92.6	7.4
3-27	2.244		92.4	7.6
3-28	2.254		92.8	7.2
3-29	2.252		92.7	7.3
3-30	2.251		92.6	7.4
3-31	2.251		92.7	7.3
3-32	2.308		95.0	5.0
3-33	2.255		92.8	7.2
3-34	2.302		94.7	5.3
3-35	2.248		92.5	7.5
3-36	2.246		92.4	7.6

Table E.8 Simulated In-Place Densities and Air Voids for US-83 Project in District VI

Sample ID	G_{mb}	G_{mm}	% Simulated In-place Density	% Air Voids @ N_{final}
4-1	2.263	2.427	93.2	6.8
4-2	2.257		93.0	7.0
4-3	2.261		93.1	6.9
4-4	2.266		93.4	6.6
4-5	2.274		93.7	6.3
4-6	2.292		94.4	5.6
4-7	2.284		94.1	5.9
4-8	2.295		94.5	5.5
4-9	2.273		93.6	6.4
4-10	2.285		94.2	5.8
4-11	2.268		93.4	6.6
4-12	2.274		93.7	6.3
4-13	2.275		93.7	6.3
4-14	2.269		93.5	6.5
4-15	2.293		94.5	5.5
4-16	2.293		94.5	5.5
4-17	2.270		93.5	6.5
4-18	2.270		93.5	6.5
4-19	2.280		93.9	6.1
4-20	2.274		93.7	6.3

Table E.9 Simulated In-Place Densities and Air Voids for US-83 Project in District VI

Sample ID	G_{mb}	G_{mm}	% Simulated In-place Density	% Air Voids @ N_{final}
4-21	2.284	2.416	94.5	5.5
4-22	2.268		93.9	6.1
4-23	2.269		93.9	6.1
4-24	2.268		93.9	6.1
4-25	2.308		95.5	4.5
4-26	2.284		94.6	5.4
4-27	2.268		93.9	6.1
4-28	2.274		94.2	5.8
4-29	2.256		93.4	6.6
4-30	2.298		95.1	4.9
4-31	2.289		94.8	5.2
4-32	2.266		93.8	6.2
4-33	2.268		93.9	6.1
4-34	2.237		92.6	7.4
4-35	2.268		93.9	6.1
4-36	2.259		93.5	6.5

Table E.10 Simulated In-Place Densities and Air Voids for CISL-A Project

Sample ID	G_{mb}	G_{mm}	% Simulated In-place Density	% Air Voids @ N_{final}
5-1	2.282	2.469	92.4	7.6
5-2	2.275		92.1	7.9
5-3	2.279		92.3	7.7
5-4	2.275		92.1	7.9
5-5	2.277		92.2	7.8
5-6	2.288		92.7	7.3
5-7	2.282		92.4	7.6
5-8	2.294		92.9	7.1
5-9	2.285		92.6	7.4
5-10	2.282		92.4	7.6
5-11	2.280		92.3	7.7
5-12	2.277		92.2	7.8
5-13	2.285		92.6	7.4
5-14	2.282		92.4	7.6
5-15	2.290		92.8	7.2
5-16	2.297		93.0	7.0
5-17	2.287		92.6	7.4
5-18	2.293		92.9	7.1
5-19	2.296		93.0	7.0
5-20	2.291		92.8	7.2
5-21	2.298		93.1	6.9
5-22	2.297		93.0	7.0
5-23	2.313		93.7	6.3
5-24	2.289		92.7	7.3

Table E.11 Simulated In-Place Densities and Air Voids for CISL-B Project

Sample ID	G_{mb}	G_{mm}	% Simulated In-place Density	% Air Voids @ N_{final}
6-1	2.293	2.472	92.8	7.2
6-2	2.287		92.5	7.5
6-3	2.290		92.6	7.4
6-4	2.301		93.1	6.9
6-5	2.287		92.5	7.5
6-6	2.285		92.4	7.6
6-7	2.288		92.6	7.4
6-8	2.294		92.8	7.2
6-9	2.291		92.7	7.3
6-10	2.290		92.7	7.3
6-11	2.287		92.5	7.5
6-12	2.301		93.1	6.9
6-13	2.286		92.5	7.5
6-14	2.296		92.9	7.1
6-15	2.296		92.9	7.1
6-16	2.289		92.6	7.4
6-17	2.293		92.8	7.2
6-18	2.300		93.0	7.0
6-19	2.289		92.6	7.4
6-20	2.285		92.4	7.6
6-21	2.299		93.0	7.0
6-22	2.291		92.7	7.3
6-23	2.291		92.7	7.3
6-24	2.290		92.6	7.4

HWTD Test Results and Air Voids of Field Cores

Table E.12 Summary of Hamburg Wheel Test Results of Field Cores for Accelerated Mix Testing Models (Number of wheel passes at left and right wheel paths)

Route	District	Temp. (°C)	% Asphalt Content	Wheel Passes					
				Load (705 N)		Load (750 N)		Load (795 N)	
				Left	Right	Left	Right	Left	Right
K-4	I	50	4.9	17,750	16,830	20,000	16,030	15,310	14,950
		60		4,340	5,370	4,890	4,280	3,560	3,750
K-258	III	50	5.0	13,650	14,890	13,530	17,310	9,870	11,620
		60		2,840	2,900	4,070	3,300	2,610	2,280
US-83	VI	50	4.9	13,500	16,920	17,050	20,000	14,640	15,490
		60		3,350	2,940	3,430	3,190	2,160	3,270

Table E.13 Air Voids of Hamburg Test Samples of Field Cores

Route	District	Temp. (°C)	% Asphalt Content	Air Voids @ N_{final}					
				Load (705 N)		Load (750 N)		Load (795 N)	
				Left	Right	Left	Right	Left	Right
K-4	I	50	4.9	9.5	9.8	9.2	9.4	9.2	9.3
		60		9.3	9.6	9.6	9.3	9.7	9.5
K-258	III	50	5.0	8.1	7.6	6.9	6.8	8.3	6.6
		60		7.6	6.4	8.9	9.7	7.0	10.0
US-83	VI	50	4.9	9.3	8.9	7.8	7.6	8.6	7.9
		60		9.0	9.3	7.6	7.6	8.9	9.0

Gmm, Gmb, Simulated In-Place Densities, and Air Voids Test Results of Field Cores

Table E.14 Simulated In-Place Densities and Air Voids for K-4 Field Cores

Sample ID	G_{mb}	G_{mm}	% Simulated In-place Density	% Air Voids @ N_{final}
1-1	2.227	2.464	90.4	9.6
1-2	2.220		90.1	9.9
2-1	2.226		90.4	9.6
2-2	2.253		91.4	8.6
3-1	2.201		89.3	10.7
3-2	2.247		91.2	8.8
4-1	2.228		90.4	9.6
4-2	2.232		90.6	9.4
5-1	2.223		90.2	9.8
5-2	2.231		90.5	9.5
6-1	2.241		91.0	9.0
6-2	2.220		90.1	9.9
7-1	2.241		91.0	9.0
7-2	2.234		90.7	9.3
8-1	2.243		91.0	9.0
8-2	2.227		90.4	9.6
9-1	2.237		90.8	9.2
9-2	2.237		90.8	9.2
10-1	2.235		90.7	9.3
10-2	2.221		90.2	9.8
11-1	2.237		90.8	9.2
11-2	2.230		90.5	9.5
12-1	2.236		90.8	9.2
12-2	2.198		89.2	10.8

Table E.15 Simulated In-Place Densities and Air Voids for K-258 Field Cores

Sample ID	G_{mb}	G_{mm}	% Simulated In-place Density	% Air Voids @ N_{final}
1-1	2.252	2.447	92.0	8.0
1-2	2.247		91.8	8.2
2-1	2.281		93.2	6.8
2-2	2.242		91.6	8.4
3-1	2.297		93.8	6.2
3-2	2.297		93.7	6.3
4-1	2.240		91.5	8.5
4-2	2.229		91.1	8.9
5-1	2.244		91.7	8.3
5-2	2.202		90.0	10.0
6-1	2.287		93.4	6.6
6-2	2.289		93.5	6.5
7-1	2.264		92.5	7.5
7-2	2.289		93.5	6.5
8-1	2.266		92.6	7.4
8-2	2.290		93.6	6.4
9-1	2.263		92.5	7.5
9-2	2.288		93.5	6.5
10-1	2.235		91.3	8.7
10-2	2.228		91.0	9.0
11-1	2.264		92.5	7.5
11-2	2.299		94.0	6.0
12-1	2.175		88.9	11.1
12-2	2.244		91.7	8.3

Table E.16 Simulated In-Place Densities and Air Voids for US-83 Field Cores

Sample ID	G_{mb}	G_{mm}	% Simulated In-place Density	% Air Voids @ N_{final}
1-1	2.233	2.445	91.3	8.7
1-2	2.223		90.9	9.1
2-1	2.213		90.5	9.5
2-2	2.224		91.0	9.0
3-1	2.227		91.1	8.9
3-2	2.223		90.9	9.1
4-1	2.247		91.9	8.1
4-2	2.190		89.6	10.4
5-1	2.241		91.7	8.3
5-2	2.212		90.5	9.5
6-1	2.241		91.7	8.3
6-2	2.211		90.4	9.6
7-1	2.248		91.9	8.1
7-2	2.226		91.0	9.0
8-1	2.248		92.0	8.0
8-2	2.255		92.2	7.8
9-1	2.255		92.2	7.8
9-2	2.253		92.2	7.8
10-1	2.257		92.3	7.7
10-2	2.263		92.6	7.4
11-1	2.221		90.8	9.2
11-2	2.251		92.1	7.9
12-1	2.259		92.4	7.6
12-2	2.262		92.5	7.5
13-1	2.263		92.6	7.4
13-2	2.253		92.2	7.8

**Appendix F - Comparison of Models Predicted with Observed
Wheel Passes**

Comparison Tables Considering Effects of Temperature and Load with Interaction

Table F.1 Comparison of Model Predicted with Observed Wheel Passes for K-4 Project Considering Temperature and Load with Interaction

Route	Parameter	Description	Estimate	p-value
K-4	Intercept	Intercept	-16.3237	0.2520
	T	Temperature	0.4951	0.0440
	L	Load	0.0426	0.0248
	T × L	Temp. × Load	-0.0008	0.0126
Wheel Passes = exp (-16.3237 + 0.4951 T + 0.0426 L - 0.0008 T×L)				
Temp. (°C)	Load (N)	Predicted	Observed	% Diff.
50	705	28,690	13,700	52.2
50	750	32,251	18,730	41.9
50	795	36,254	15,950	56.0
60	705	14,405	7,230	49.8
60	750	11,297	4,075	63.9
60	795	8,860	3,995	54.9

Table F.2 Comparison of Model Predicted With Observed Wheel Passes for US-24 Project Considering Temperature and Load with Interaction

Route	Parameter	Description	Estimate	p-value
US-24	Intercept	Intercept	17.1197	0.0356
	T	Temperature	-0.1159	0.4353
	L	Load	0.0009	0.9322
	T × L	Temp. × Load	-0.0001	0.7534
Wheel Passes = exp (17.1197 - 0.1159 T + 0.0009 L - 0.0001 T×L)				
Temp. (°C)	Load (N)	Predicted	Observed	% Diff.
50	705	4,602	17,625	-283.0
50	750	3,826	17,390	-354.5
50	795	3,182	16,650	-423.3
50	840	2,646	11,210	-323.7
50	885	2,200	13,385	-508.4
60	705	714	3,535	-395.4
60	750	567	2,565	-352.2
60	795	451	3,180	-605.3
60	840	358	3,335	-830.5
60	885	285	1,400	-391.4

**Table F.3 Comparison of Model Predicted With Observed Wheel Passes for US-50 Project
Considering Temperature and Load with Interaction**

Route	Parameter	Description	Estimate	p-value
US-50	Intercept	Intercept	59.8241	0.0230
	T	Temperature	-0.7323	0.1032
	L	Load	-0.0512	0.0950
	T × L	Temp. × Load	0.0007	0.1835
Wheel Passes = exp (59.8241 - 0.7323 T - 0.0512 L + 0.0007 T×L)				
Temp. (°C)	Load (N)	Predicted	Observed	% Diff.
50	705	131,676	20,000	84.8
50	750	63,519	20,000	68.5
50	795	30,641	20,000	34.7
50	840	14,781	8,420	43.0
50	885	7,130	7,450	-4.5
60	705	12,090	5,355	55.7
60	750	7,991	9,150	-14.5
60	795	5,282	4,295	18.7
60	840	3,492	2,640	24.4
60	885	2,308	2,170	6.0

**Table F.4 Comparison of Model Predicted With Observed Wheel Passes for US-83 Project
Considering Temperature and Load with Interaction**

Route	Parameter	Description	Estimate	p-value
US-83	Intercept	Intercept	39.0583	0.1266
	T	Temperature	-0.4465	0.3063
	L	Load	-0.0243	0.4180
	T × L	Temp. × Load	0.0003	0.5240
Wheel Passes = exp (39.0583 - 0.4465 T - 0.0243 L + 0.0003 T×L)				
Temp. (°C)	Load (N)	Predicted	Observed	% Diff.
50	705	26,286	20,000	23.9
50	750	17,297	20,000	-15.6
50	795	11,382	20,000	-75.7
50	840	7,490	11,260	-50.3
50	885	4,929	15,770	-220.0
60	705	2,507	7,145	-185.0
60	750	1,888	3,970	-110.3
60	795	1,422	7,025	-394.0
60	840	1,071	3,500	-226.8
60	885	807	2,845	-252.7

Table F.5 Comparison of Model Predicted With Observed Wheel Passes for CISL-A Project Considering Temperature and Load with Interaction

Route	Parameter	Description	Estimate	p-value
CISL-A	Intercept	Intercept	36.5642	0.0630
	T	Temperature	-0.4207	0.2162
	L	Load	-0.0268	0.2925
	T × L	Temp. × Load	0.0004	0.3808
Wheel Passes = exp (36.5642 - 0.4207 T - 0.0268 L + 0.0004 T×L)				
Temp. (°C)	Load (N)	Predicted	Observed	% Diff.
50	705	45,945	20,000	56.5
50	750	33,833	18,070	46.6
50	795	24,914	15,055	39.6
60	705	11,478	5,390	53.0
60	750	10,119	4,020	60.3
60	795	8,921	4,625	48.2

Table F.6 Comparison of Model-Predicted with Observed Wheel Passes for All Projects Without CISL Projects Considering Temperature and Load with Interaction

Route	Parameter	Description	Estimate	p-value			
All Without CISL Projects	Intercept	Intercept	15.1836	0.0728			
	T	Temperature	-0.0355	0.8138			
	L	Load	0.0027	0.7961			
	T × L	Temp. × Load	-0.0001	0.4469			
Wheel Passes = exp (15.1836 - 0.0355 T + 0.0027 L - 0.0001 T×L)							
Temp. (°C)	Load (N)	Predicted	Observed Wheel Passes				
			K-4	US-24	US-50	US-83	
50	705	131,544	13,700	17,625	20,000	20,000	
50	750	118,610	18,730	17,390	20,000	20,000	
50	795	106,948	15,950	16,650	20,000	20,000	
50	840	96,433	N/A	11,210	8,420	11,260	
50	885	86,951	N/A	13,385	7,450	15,770	
60	705	45,574	7,230	3,535	5,355	7,145	
60	750	39,285	4,075	2,565	9,150	3,970	
60	795	33,864	3,995	3,180	4,295	7,025	
60	840	29,191	N/A	3,335	2,640	3,500	
60	885	25,162	N/A	1,400	2,170	2,845	

Table F.7 Comparison of Model-Predicted with Observed Wheel Passes for All Projects Without CISL-B Considering Temperature and Load with Interaction

Route	Parameter	Description	Estimate	p-value			
All without CISL-B	Intercept	Intercept	16.1005	0.0329			
	T	Temperature	-0.0551	0.6829			
	L	Load	0.0014	0.8827			
	T × L	Temp. × Load	-0.0001	0.4952			
Wheel Passes = exp (16.1005 - 0.0551 T + 0.0014 L - 0.0001 T×L)							
Temp. (°C)	Load (N)	Predicted	Observed Wheel Passes				
			K-4	US-24	US-50	US-83	CISL-A
50	705	49,390	13,700	17,625	20,000	20,000	20,000
50	750	42,003	18,730	17,390	20,000	20,000	18,070
50	795	35,721	15,950	16,650	20,000	20,000	15,055
50	840	30,379	N/A	11,210	8,420	11,260	N/A
50	885	25,835	N/A	13,385	7,450	15,770	N/A
60	705	14,066	7,230	3,535	5,355	7,145	5,390
60	750	11,436	4,075	2,565	9,150	3,970	4,020
60	795	9,297	3,995	3,180	4,295	7,025	4,625
60	840	7,559	N/A	3,335	2,640	3,500	N/A
60	885	6,146	N/A	1,400	2,170	2,845	N/A

Table F.8 Comparison of Model Predicted With Observed Wheel Passes for All Projects Considering Temperature and Load with Interaction

Route	Parameter	Description	Estimate	p-value				
All Projects	Intercept	Intercept	16.6737	0.2164				
	T	Temperature	-0.0205	0.9325				
	L	Load	0.0000	0.9983				
	T × L	Temp. × Load	-0.0001	0.6455				
Wheel Passes = exp (16.6737 - 0.0205 T - 0.0000 L - 0.0001 T×L)								
Temp. (°C)	Load (N)	Predicted	Observed Wheel Passes					
			K-4	US-24	US-50	US-83	CISL-A	CISL-B
50	705	184,186	13,700	17,625	20,000	20,000	20,000	20,000
50	750	147,075	18,730	17,390	20,000	20,000	18,070	20,000
50	795	117,442	15,950	16,650	20,000	20,000	15,055	20,000
50	840	93,779		11,210	8,420	11,260		
50	885	74,884		13,385	7,450	15,770		
60	705	74,139	7,230	3,535	5,355	7,145	5,390	20,000
60	750	56,596	4,075	2,565	9,150	3,970	4,020	20,000
60	795	43,205	3,995	3,180	4,295	7,025	4,625	20,000
60	840	32,981		3,335	2,640	3,500		
60	885	25,177		1,400	2,170	2,845		

Comparison Tables Considering Effects of Temperature and Load Without Interaction

**Table F.9 Comparison of Model Predicted with Observed Wheel Passes for K-4 Project
Considering Temperature and Load Without Interaction**

Route	Parameter	Description	Estimate	p-value
K-4	Intercept	Intercept	19.2288	< 0.0001
	T	Temperature	-0.1237	< 0.0001
	L	Load	-0.0043	0.0197
Wheel Passes = exp (19.2288 - 0.1237 T - 0.0043 L)				
Temp. (°C)	Load (N)	Predicted	Observed	% Diff.
50	705	22,299	13,700	38.6
50	750	18,376	18,730	-1.9
50	795	15,143	15,950	-5.3
60	705	6,472	7,230	-11.7
60	750	5,334	4,075	23.6
60	795	4,395	3,995	9.1

**Table F.10 Comparison of Model Predicted With Observed Wheel Passes for US-24 Project
Considering Temperature and Load without Interaction**

Route	Parameter	Description	Estimate	p-value
US-24	Intercept	Intercept	19.6673	< 0.0001
	T	Temperature	-0.1623	< 0.0001
	L	Load	-0.0023	0.0111
Wheel Passes = exp (19.6673 - 0.1623 T - 0.0023 L)				
Temp. (°C)	Load (N)	Predicted	Observed	% Diff.
50	705	20,554	17,625	14.2
50	750	18,533	17,390	6.2
50	795	16,711	16,650	0.4
50	840	15,068	11,210	25.6
50	885	13,586	13,385	1.5
60	705	4,055	3,535	12.8
60	750	3,657	2,565	29.9
60	795	3,297	3,180	3.6
60	840	2,973	3,335	-12.2
60	885	2,681	1,400	47.8

**Table F.11 Comparison of Model Predicted With Observed Wheel Passes for US-50 Project
Considering Temperature and Load without Interaction**

Route	Parameter	Description	Estimate	p-value
US-50	Intercept	Intercept	25.7294	< 0.0001
	T	Temperature	-0.1451	< 0.0001
	L	Load	-0.0107	< 0.0001
Wheel Passes = exp (25.7294 - 0.1451 T - 0.0107 L)				
Temp. (°C)	Load (N)	Predicted	Observed	% Diff.
50	705	55,877	20,000	64.2
50	750	34,524	20,000	42.1
50	795	21,331	20,000	6.2
50	840	13,179	8,420	36.1
50	885	8,143	7,450	8.5
60	705	13,094	5,355	59.1
60	750	8,090	9,150	-13.1
60	795	4,999	4,295	14.1
60	840	3,088	2,640	14.5
60	885	1,908	2,170	-13.7

**Table F.12 Comparison of Model Predicted With Observed Wheel Passes for US-83 Project
Considering Temperature and Load without Interaction**

Route	Parameter	Description	Estimate	p-value
US-83	Intercept	Intercept	23.1491	< 0.0001
	T	Temperature	-0.1721	< 0.0001
	L	Load	-0.0053	0.0031
Wheel Passes = exp (23.1491 - 0.1721 T - 0.0053 L)				
Temp. (°C)	Load (N)	Predicted	Observed	% Diff.
50	705	49,395	20,000	59.5
50	750	38,914	20,000	48.6
50	795	30,657	20,000	34.8
50	840	24,151	11,260	53.4
50	885	19,027	15,770	17.1
60	705	8,836	7,145	19.1
60	750	6,961	3,970	43.0
60	795	5,484	7,025	-28.1
60	840	4,320	3,500	19.0
60	885	3,404	2,845	16.4

Table F.13 Comparison of Model Predicted With Observed Wheel Passes for CISL-A Project Considering Temperature and Load without Interaction

Route	Parameter	Description	Estimate	p-value
CISL-A	Intercept	Intercept	19.6677	< 0.0001
	T	Temperature	-0.1254	< 0.0001
	L	Load	-0.0047	0.0078
Wheel Passes = exp (19.6677 - 0.1254 T - 0.0047 L)				
Temp. (°C)	Load (N)	Predicted	Observed	% Diff.
50	705	23,961	20,000	16.5
50	750	19,394	18,070	6.8
50	795	15,697	15,055	4.1
60	705	6,838	5,390	21.2
60	750	5,534	4,020	27.4
60	795	4,479	4,625	-3.3

Table F.14 Comparison of Model-Predicted with Observed Wheel Passes for All Without CISL Projects Considering Temperature and Load Without Interaction

Route	Parameter	Description	Estimate	p-value			
Overall without CISL	Intercept	Intercept	21.5924	< 0.0001			
	T	Temperature	-0.1501	< 0.0001			
	L	Load	-0.0052	< 0.0001			
Wheel Passes = exp (21.5924 - 0.1501 T - 0.0052 L)							
Temp. (°C)	Load (N)	Predicted	Observed Wheel Passes				
			K-4	US-24	US-50	US-83	
50	705	33,570	13,700	17,625	20,000	20,000	
50	750	26,566	18,730	17,390	20,000	20,000	
50	795	21,024	15,950	16,650	20,000	20,000	
50	840	16,637	N/A	11,210	8,420	11,260	
50	885	13,166	N/A	13,385	7,450	15,770	
60	705	7,483	7,230	3,535	5,355	7,145	
60	750	5,922	4,075	2,565	9,150	3,970	
60	795	4,686	3,995	3,180	4,295	7,025	
60	840	3,709	N/A	3,335	2,640	3,500	
60	885	2,935	N/A	1,400	2,170	2,845	

Table F.15 Comparison of Model-Predicted with Observed Wheel Passes for All Projects Without CISL-B Considering Temperature and Load Without Interaction

Route	Parameter	Description	Estimate	p-value			
All without CISL-B	Intercept	Intercept	21.2212	< 0.0001			
	T	Temperature	-0.1470	< 0.0001			
	L	Load	-0.0050	< 0.0001			
Wheel Passes = exp (21.2212 - 0.1470 T - 0.0050 L)							
Temp. (°C)	Load (N)	Predicted	Observed Wheel Passes				
			K-4	US-24	US-50	US-83	CISL-A
50	705	31,138	13,700	17,625	20,000	20,000	20,000
50	750	24,865	18,730	17,390	20,000	20,000	18,070
50	795	19,855	15,950	16,650	20,000	20,000	15,055
50	840	15,854	N/A	11,210	8,420	11,260	N/A
50	885	12,660	N/A	13,385	7,450	15,770	N/A
60	705	7,160	7,230	3,535	5,355	7,145	5,390
60	750	5,717	4,075	2,565	9,150	3,970	4,020
60	795	4,565	3,995	3,180	4,295	7,025	4,625
60	840	3,645	N/A	3,335	2,640	3,500	N/A
60	885	2,911	N/A	1,400	2,170	2,845	N/A

Table F.16 Comparison of Model Predicted With Observed Wheel Passes for All Projects Considering Temperature and Load without Interaction

Route	Parameter	Description	Estimate	p-value				
All Projects	Intercept	Intercept	22.8407	< 0.0001				
	T	Temperature	-0.1315	< 0.0001				
	L	Load	-0.0078	< 0.0001				
Wheel Passes = exp (22.8407 - 0.1315 T - 0.0078 L)								
Temp. (°C)	Load (N)	Predicted	Observed Wheel Passes					
			K-4	US-24	US-50	US-83	CISL-A	CISL-B
50	705	47,415	13,700	17,625	20,000	20,000	20,000	20,000
50	750	33,380	18,730	17,390	20,000	20,000	18,070	20,000
50	795	23,499	15,950	16,650	20,000	20,000	15,055	20,000
50	840	16,543		11,210	8,420	11,260		
50	885	11,646		13,385	7,450	15,770		
60	705	12,730	7,230	3,535	5,355	7,145	5,390	20,000
60	750	8,962	4,075	2,565	9,150	3,970	4,020	20,000
60	795	6,309	3,995	3,180	4,295	7,025	4,625	20,000
60	840	4,441		3,335	2,640	3,500		
60	885	3,127		1,400	2,170	2,845		

Comparison Tables Considering Effects of Temperature, Load, and Air Voids Without Interaction

Table F.17 Comparison of Model Predicted With Observed Wheel Passes for K-4 Project

Route	Parameter	Description	Estimate	p-value	Significant
K-4	Intercept	Intercept	19.1588	< 0.0001	*
	T	Temperature	-0.1200	< 0.0001	*
	L	Load	-0.0040	0.0562	*
	A	Air Voids	-0.0504	0.8084	
Wheel Passes = exp (19.1588 - 0.1200 T - 0.0040 L - 0.0504 A)					
Temp. (°C)	Load (N)	Air Voids	Predicted	Observed	% Diff.
50	705	6.5	22,275	13,700	38.5
50	750	5.7	19,371	18,730	3.3
50	795	6.3	15,698	15,950	-1.6
60	705	6.7	6,642	7,230	-8.9
60	750	6.8	5,520	4,075	26.2
60	795	6.5	4,681	3,995	14.6

Table F.18 Comparison of Model Predicted With Observed Wheel Passes for US-24 Project

Route	Parameter	Description	Estimate	p-value	Significant
US-24	Intercept	Intercept	19.9521	< 0.0001	*
	T	Temperature	-0.1618	< 0.0001	*
	L	Load	-0.0021	0.0180	*
	A	Air Voids	-0.0836	0.4521	
Wheel Passes = exp (19.9521 - 0.1618 T - 0.0021 L - 0.0836 A)					
Temp. (°C)	Load (N)	% Air Voids	Predicted	Observed	% Diff.
50	705	6.8	18,272	17,625	3.5
50	750	5.5	18,533	17,390	6.2
50	795	5.3	17,146	16,650	2.9
50	840	6.2	14,469	11,210	22.5
50	885	6.3	13,055	13,385	-2.5
60	705	5.6	4,006	3,535	11.7
60	750	5.5	3,675	2,565	30.2
60	795	5.5	3,344	3,180	4.9
60	840	6.4	2,822	3,335	-18.2
60	885	6.3	2,589	1,400	45.9

Table F.19 Comparison of Model Predicted With Observed Wheel Passes for US-50 Project

Route	Parameter	Description	Estimate	p-value	Significant
US-50	Intercept	Intercept	28.8328	< 0.0001	*
	T	Temperature	-0.1560	< 0.0001	*
	L	Load	-0.0120	< 0.0001	*
	A	Air Voids	-0.1995	0.4941	
Wheel Passes = exp (28.8328 - 0.1560 T - 0.00120 L - 0.1995 A)					
Temp. (°C)	Load (N)	% Air Voids	Predicted	Observed	% Diff.
50	705	7.5	64,637	20,000	69.1
50	750	6.8	43,313	20,000	53.8
50	795	7.3	22,844	20,000	12.5
50	840	7.4	13,049	8,420	35.5
50	885	7.4	7,605	7,450	2.0
60	705	7.9	12,541	5,355	57.3
60	750	7.1	8,573	9,150	-6.7
60	795	7.3	4,800	4,295	10.5
60	840	6.6	3,217	2,640	17.9
60	885	5.9	2,155	2,170	-0.7

Table F.20 Comparison of Model Predicted With Observed Wheel Passes for US-83 Project

Route	Parameter	Description	Estimate	p-value	Significant
US-83	Intercept	Intercept	24.4580	< 0.0001	*
	T	Temperature	-0.1643	< 0.0001	*
	L	Load	-0.0060	0.0023	*
	A	Air Voids	-0.1675	0.4409	
Wheel Passes = exp (24.458 - 0.1643 T - 0.0060 L - 0.1675 A)					
Temp. (°C)	Load (N)	% Air Voids	Predicted	Observed	% Diff.
50	705	6.1	59,353	20,000	66.3
50	750	6.9	39,626	20,000	49.5
50	795	6.0	35,172	20,000	43.1
50	840	5.8	27,764	11,260	59.4
50	885	5.5	22,287	15,770	29.2
60	705	6.1	11,479	7,145	37.8
60	750	5.9	9,061	3,970	56.2
60	795	6.3	6,469	7,025	-8.6
60	840	6.0	5,193	3,500	32.6
60	885	6.5	3,646	2,845	22.0

Table F.21 Comparison of Model Predicted With Observed Wheel Passes for CISL-A Project

Route	Parameter	Description	Estimate	p-value	Significant
CISL-A	Intercept	Intercept	33.8756	0.0005	*
	T	Temperature	-0.1406	< 0.0001	*
	L	Load	-0.0122	0.0246	*
	A	Air Voids	-1.0209	0.1076	**
Wheel Passes = exp (33.8756 - 0.1406 T - 0.0122 L - 1.0209 A)					
Temp. (°C)	Load (N)	Air Voids	Predicted	Observed	% Diff.
50	705	7.1	59,648	20,000	66.5
50	750	7.7	18,670	18,070	3.2
50	795	7.4	14,646	15,055	-2.8
60	705	7.9	6,461	5,390	16.6
60	750	7.6	5,068	4,020	20.7
60	795	7.2	4,403	4,625	-5.0

Table F.22 Comparison of Model Predicted With Observed Wheel Passes for All Projects

Route	Parameter	Description	Estimate	p-value	Note: Air Voids are taken from US-24 Project					
All Projects	Intercept	Intercept	20.0357	< 0.0001						
	T	Temperature	-0.1417	< 0.0001						
	L	Load	-0.0060	0.0001						
	A	Air Voids	0.2968	0.0094						
Wheel Passes = exp (20.0357 - 0.1417 T - 0.006 L + 0.2968 A)										
Temp. (°C)	Load (N)	Air Voids	Predicted	Observed Wheel Passes						
				K-4	US-24	US-50	US-83	CISL-A	CISL-B	
50	705	6.8	46,117	13,700	17,625	20,000	20,000	20,000	20,000	
50	750	5.5	23,935	18,730	17,390	20,000	20,000	18,070	20,000	
50	795	5.3	17,219	15,950	16,650	20,000	20,000	15,055	20,000	
50	840	6.2	17,169	N/A	11,210	8,420	11,260	N/A	N/A	
50	885	6.3	13,501	N/A	13,385	7,450	15,770	N/A	N/A	
60	705	5.1	6,751	7,230	3,535	5,355	7,145	5,390	20,000	
60	750	5.0	5,003	4,075	2,565	9,150	3,970	4,020	20,000	
60	795	5.5	4,430	3,995	3,180	4,295	7,025	4,625	20,000	
60	840	6.4	4,417	N/A	3,335	2,640	3,500	N/A	N/A	
60	885	6.3	3,273	N/A	1,400	2,170	2,845	N/A	N/A	

**Table F.23 Comparison of Model Predicted With Observed Wheel Passes for All Projects
Model Compared With US-24 Project**

Route	Parameter	Description	Estimate	p-value	Significant
All Projects	Intercept	Intercept	20.0357	< 0.0001	*
	T	Temperature	-0.1417	< 0.0001	*
	L	Load	-0.0060	0.0001	*
	A	Air Voids	0.2968	0.0094	*
Wheel Passes = exp (20.0357 - 0.1417 T - 0.006 L + 0.2968 A)					
Temp. (°C)	Load (N)	Air Voids	Predicted	Observed Wheel Passes	
				US-24	% Diff.
50	705	6.8	46,117	17,625	61.8
50	750	5.5	23,935	17,390	27.3
50	795	5.3	17,219	16,650	3.3
50	840	6.2	17,169	11,210	34.7
50	885	6.3	13,501	13,385	0.9
60	705	5.1	6,751	3,535	47.6
60	750	5.0	5,003	2,565	48.7
60	795	5.5	4,430	3,180	28.2
60	840	6.4	4,417	3,335	24.5
60	885	6.3	3,273	1,400	57.2

Comparison Tables Considering Effects of Temperature, Load, and Air Voids Without Interaction for Field Cores

Table F.24 Comparison of Model-Predicted with Observed Wheel Passes for K-4 Model Compared with K-4 Cores

Route	Parameter	Description	Estimate	p-value	Significant
K-4 Cores	Intercept	Intercept	19.1588	< 0.0001	*
	T	Temperature	-0.1200	< 0.0001	*
	L	Load	-0.004	0.0562	*
	A	Air Voids	-0.0504	0.8084	
Wheel Passes = exp (19.1588 - 0.1200 T - 0.004 L - 0.0504 A)					
Temp. (°C)	Load (N)	Air Voids	Predicted	Observed	% Diff.
50	705	9.6	19,053	17,290	9.3
50	750	9.3	16,157	18,020	-11.5
50	795	9.2	13,563	15,130	-11.6
60	705	9.4	5,797	4,860	16.2
60	750	9.4	4,842	4,590	5.2
60	795	9.6	4,004	3,660	8.6

Table F.25 Comparison of Model-Predicted with Observed Wheel Passes for US-24 Model Compared with K-258 Cores

Route	Parameter	Description	Estimate	p-value	Significant
K-258 Cores	Intercept	Intercept	19.9521	< 0.0001	*
	T	Temperature	-0.1618	< 0.0001	*
	L	Load	-0.0021	0.0180	*
	A	Air Voids	-0.0836	0.4521	
Wheel Passes = exp (19.9521 - 0.1618 T - 0.0021 L - 0.0836 A)					
Temp. (°C)	Load (N)	% Air Voids	Predicted	Observed	% Diff.
50	705	7.9	16,667	14,270	14.4
50	750	6.8	16,624	15,420	7.2
50	795	7.4	14,385	10,750	25.3
60	705	7.0	3,563	2,870	19.5
60	750	9.3	2,675	3,690	-38.0
60	795	8.5	2,602	2,450	5.8

Table F.26 Comparison of Model-Predicted with Observed Wheel Passes for US-83 Model Compared with US-83 Cores

Route	Parameter	Description	Estimate	p-value	Significant
US-83 Cores	Intercept	Intercept	24.2580	< 0.0001	*
	T	Temperature	-0.1643	< 0.0001	*
	L	Load	-0.0060	0.0023	*
	A	Air Voids	-0.1675	0.4409	
Wheel Passes = exp (24.2580 - 0.1643 T - 0.006 L - 0.1675 A)					
Temp. (°C)	Load (lbs)	% Air Voids	Predicted	Observed	% Diff.
50	705	9.1	29,400	15,210	48.3
50	750	7.7	28,375	18,530	34.7
50	795	8.2	19,920	15,070	24.3
60	705	9.1	5,686	3,150	44.6
60	750	7.6	5,580	3,310	40.7
60	795	8.9	3,426	2,720	20.6

Appendix G - Typical SAS Input Files

(1) Developing Criteria for Out-Of-Specification Pavements for K-4 Project in District I

```
TITLE 'PROJECT 1 GLM_WHEEL';
OPTIONS LS = 75;
DATA;
INPUT X A D Y DELTA;
Z = 1;
CARDS;
1 2 90.2 7100 1
1 2 90.2 6010 1
1 2 90.9 7260 1
1 2 90.9 14210 1
1 2 93.4 9350 1
1 2 93.4 11350 1
1 2 95.2 11160 1
1 2 95.2 13500 1
1 4 89.4 8500 1
1 4 89.4 9210 1
1 4 90.8 7700 1
1 4 90.8 8300 1
1 4 92.4 20000 0
1 4 92.4 20000 0
1 4 93.6 13400 1
1 4 93.6 14000 1
1 7 88.6 8710 1
1 7 88.6 9610 1
1 7 90.0 10010 1
1 7 90.0 11500 1
1 7 92.1 17800 1
1 7 92.1 18000 1
1 7 93.6 12960 1
1 7 93.6 17290 1
```

```
PROC PRINT;
RUN;
```

```
PROC GLM;
TITLE 'GLM';
MODEL Y = A D A*D;
RUN;
```

```
PROC GLM;
TITLE 'GLM WO INTERATION';
MODEL Y = A D;
RUN;
```

(2) Developing Accelerated Mix Testing Models for K-4 Project in District I

```
Title 'AMT K-4 Route Project-Wheel with air voids';
options ls = 80;
data one;
input route $ dist $ temp load wp censor air;
cards;
k4 1 50 705 14000 1 7.0
k4 1 50 705 13400 1 7.0
k4 1 50 750 20000 0 5.9
k4 1 50 750 17460 1 5.5
k4 1 50 795 16900 1 5.3
k4 1 50 795 15000 1 6.0
k4 1 60 705 6300 1 6.8
k4 1 60 705 8160 1 6.5
k4 1 60 750 3700 1 6.3
k4 1 60 750 4450 1 7.2
k4 1 60 795 3360 1 6.0
k4 1 60 795 4630 1 7.0
run;
proc print;
run;

proc lifereg;
model wp*censor(0) = temp load air temp*load;
run;

proc lifereg;
model wp*censor(0) = temp load air;
run;
```

(3) For Residual Plots for Developing Accelerated Mix Testing Models for Five Projects Without CISL-B

```
Title 'AMT Overall five Projects with plots';
options ls = 80;
data one;
input route $ dist $ temp load wp censor;
cards;
k4 1 50 705 14000 1
k4 1 50 705 13400 1
k4 1 50 750 20000 0
k4 1 50 750 17460 1
k4 1 50 795 16900 1
k4 1 50 795 15000 1
k4 1 60 705 6300 1
k4 1 60 705 8160 1
k4 1 60 750 3700 1
k4 1 60 750 4450 1
k4 1 60 795 3360 1
k4 1 60 795 4630 1
us24 3 50 705 19330 1
us24 3 50 705 15920 1
us24 3 50 750 17400 1
us24 3 50 750 17380 1
us24 3 50 795 13300 1
us24 3 50 795 20000 0
us24 3 50 840 10750 1
us24 3 50 840 11670 1
us24 3 50 885 12800 1
us24 3 50 885 13970 1
us24 3 60 705 4660 1
us24 3 60 705 2410 1
us24 3 60 750 1770 1
us24 3 60 750 3360 1
us24 3 60 795 2630 1
us24 3 60 795 3730 1
us24 3 60 840 3670 1
us24 3 60 840 3000 1
us24 3 60 885 1310 1
us24 3 60 885 1490 1
us50 5 50 705 20000 0
us50 5 50 705 20000 0
us50 5 50 750 20000 0
us50 5 50 750 20000 0
us50 5 50 795 20000 0
us50 5 50 795 20000 0
us50 5 50 840 8700 1
us50 5 50 840 8140 1
us50 5 50 885 8480 1
us50 5 50 885 6420 1
us50 5 60 705 5990 1
us50 5 60 705 4720 1
us50 5 60 750 12550 1
us50 5 60 750 5750 1
us50 5 60 795 3170 1
```

```

us50 5 60 795 5420 1
us50 5 60 840 2780 1
us50 5 60 840 2500 1
us50 5 60 885 2500 1
us50 5 60 885 1840 1
us83 6 50 705 20000 0
us83 6 50 705 20000 0
us83 6 50 750 20000 0
us83 6 50 750 20000 0
us83 6 50 795 20000 0
us83 6 50 795 20000 0
us83 6 50 840 10360 1
us83 6 50 840 12160 1
us83 6 50 885 20000 0
us83 6 50 885 11540 1
us83 6 60 705 5780 1
us83 6 60 705 8510 1
us83 6 60 750 1510 1
us83 6 60 750 6430 1
us83 6 60 795 8110 1
us83 6 60 795 5940 1
us83 6 60 840 3620 1
us83 6 60 840 3380 1
us83 6 60 885 1850 1
us83 6 60 885 3840 1
cisl 1 50 705 20000 0
cisl 1 50 705 20000 0
cisl 1 50 750 17220 1
cisl 1 50 750 18920 1
cisl 1 50 795 15810 1
cisl 1 50 795 14300 1
cisl 1 60 705 2740 1
cisl 1 60 705 8040 1
cisl 1 60 750 4760 1
cisl 1 60 750 3280 1
cisl 1 60 795 5670 1
cisl 1 60 795 3580 1

run;
proc print;
run;

title' Weibull Regression With Interaction';
proc lifereg;
model wp*censor(0) = temp load temp*load;
output out = results xbeta = reg;
run;

title' Weibull Regression No Interaction';
proc lifereg;
model wp*censor(0) = temp load;
output out = results xbeta = reg;
run;

title 'Residual Analysis Weibull with Interaction';
data residual;

```

```
set results;
c_nres = wp**(1/.3753)*exp(-reg/.3753);
run;

proc lifetest plots = (lls) data=residual;
time c_nres*censor(0);
run;
title 'Weibull Regression Without Interaction';
proc lifereg data = one;
model wp*censor(0) = temp load ;
output out = results xbeta = reg;
run;
title 'Residual Analysis Weibull Without Interaction';
data residual_2;
set results;
c_nres = wp**(1/.3808)*exp(-reg/.3808);
run;
```